The role of the clock in lipid metabolism

A thesis submitted to the University of Manchester for the degree of **Doctor of Philosophy** in the Faculty of Biology, Medicine and Health

2016

Siobhán Anne Ahern

School of Medical Sciences

Contents

List of figures

Chapter 5

Chapter 6

List of tables

Chapter 2

Abstract

The University of Manchester

Submitted by Siobhán Anne Ahern for the degree of Doctor of Philosophy and entitled: **The role of the clock in lipid metabolism**. September 2016.

In mammals, the circadian clock coordinates multiple behavioural and physical processes, including energy homeostasis. At the centre of these rhythms lies the circadian clock machinery, a precisely coordinated transcription-translation feedback system required to maintain the correct time. Metabolic homeostasis requires accurate and coordinated circadian timing within individual cells and tissues of the body. Moreover, recent evidence has shown that the coupling of circadian and metabolic circuits involves reciprocal regulatory feedback. In line with this, mounting evidence suggests that disruption of the clock contributes to the development of obesity and its comorbidities. This is particularly concerning given that modern lifestyles often undermine our bodies' clock. However, the casual mechanisms which link circadian disruption to metabolic disease are not well defined. This work aims to gain a further understanding of clock control of metabolic homeostasis and especially regulation of lipid metabolism.

This work uses dietary challenge to determine which peripheral clocks and downstream metabolic pathways are particularly susceptible to diet induced obesity (DIO). We demonstrate that although behavioural rhythmicity was maintained in DIO, gene expression profiling revealed tissue-specific alteration to the phase and amplitude of the molecular clockwork. Clock function was most significantly attenuated in visceral white adipose tissue (WAT) of DIO mice, and was coincident with elevated tissue inflammation, and dysregulation of clock-coupled metabolic regulators PPARα/γ.

The rhythmic expression of *Rev-erbα*, a nuclear receptor involved in the circadian clock, was particularly affected in DIO mice. This study uses the *Rev-erbα*$^{-/-}$ mouse to explore clock-metabolic coupling, specifically lipid metabolism. In line with published work, *Rev-erbα*$^{-/-}$ mice exhibit an obese phenotype with associated upregulation in gWAT of lipogenic (*Dgat2, Fasn*) and fatty acid liberation (*Lpl)* genes. Differences in fat mobilization are observed as *Rev-erbα*$^{-/-}$ mice show a heightened insulin stimulated lipogenic drive and an attenuation of the lipolytic drive in the fasted state, suggesting an increased propensity for fat accumulation. The role of the clock was further investigated in adipose tissue by deletion of *Bmal1* (clock ablation) or *Rev-erb*α (clock manipulation) specifically in adipocytes using Cre-Lox methodology. *Adipo*^{CRE}*Bmal1*$^{flox/flox}$ mice showed attenuated feeding rhythms, indicating a direct effect of the adipocyte circadian clock on hypothalamic feeding centres and severe dysregulation of metabolic genes. However, *Adipo*^{CRE}*Rev-erbα*$^{flox/flox}$ displayed very little phenotypic difference compared to control littermates, suggesting that global loss of *Rev-erbα* may have reinforcing metabolic consequences.

This work suggests a key role of the clock in lipid handling and the pathogenesis of obesity. Insights into this link may lead to novel targets for treating both obesity and metabolic complications.

Declaration of copyright statement

DECLARATION

No portion of the work referred to in this thesis has been submitted in support of an application for another degree or qualification of this or any other university or other institute of learning

Abbreviations

$^{-/-}$ - knockout

~ - approximately

≤ - less than or equal to

5HT – serotonin

ACAT – acyl-CoA cholesterol acetyletransferases

ACC – acetyl-CoA carboxylase

ACTH – adrenocorticotrophic hormone

Adipo - Adiponectin

AEE – activity energy expenditure

AKT – Protein kinase B

ALAS1 – delta-aminolevulinate synthase 1

AMPK - 5' adenosine monophosphate-activated protein kinase

ANP – Atrial natriuretic peptide

AP – area postrema

Apo – apolipoproteins

ARC – arcuate nucleus

Atgl – adipose triglyceride lipase

ATP – adenosine triphosphate

BAT – brown adipose tissue

bHLH – basic helix loop helix

Bmal1 – aryl hydrocarbon receptor nuclear translocator-like protein 1

BMI – body mass index

BMR – basal metabolic rate

BNP – brain natriuretic peptide

C – Carbon

cAMP – adenosine 3'5' Cyclic Monophosphate

CART - amphetamine-regulated transcript

CCK – cholecystokinin

CD36/FAT – fatty acid translocase

cGMP – cyclic guanosine monophosphate

CK – casein kinase

CLAMS – Comprehensive Lab Animal Monitoring System

Clock – Circadian Locomotor Output Cycles Kaput

COX – carbohydrate oxidation

CPT-1 - carnitine palmitoyltransferase I

CREBP – cAMP Response Element-*Binding* Protein

CRH – corticotrophin releasing hormone

Cry – cryptochrome

CV – calorific value

DA – dopamine

Dbp – D site of albumin promoter

DD – constant darkness

DEC – deleted in oesophageal cancer

Dgat2 – diacylglycerol O-acyltransferase 2

DHAP – dihydroxyacetone phosphate

DIO – Diet Induced Obesity

DMEM – Dulbecco's Modified Eagles Medium

DMN – default mode network

DRN – dorsal raphe nucleus

ER - endoplasmic reticulum

ERK – extracellular signal related kinases

F1,6P – fructose 1,6, bisphosphate

FA – fatty acids

Fabp4 – fatty acid binding protein 4

FAO – fatty acid β-oxidation

Fasn – fatty acid synthase

FATP – fatty acid transport protein

FBPase - fructose 1,6, bisphosphatase

FFA – free fatty acids

FOX – fatty acid oxidation

FSP27/Cidec – fat specific protein 27

g - Gravitational field

G3PDH – glycerol-3-phosphate dehydrogenase

G6P – glucose-6-phosphate

G6Pase – glucose-6-phosphatase

GABA – γ-aminobutyric acid

GHT - geniculohypothalamic tract

GK – glucokinase

GLP-1 – glucagon-like peptide 1

Glut2/4 – glucose transporter 2/4

GSK-3 – glycogen synthase 3

GTT – glucose tolerance test

GWAS – genome wide associate studies

gWAT – gonadal white adipose tissue

Gys2 – glycogen synthase 2

H – Hydrogen

HAT – histone acetyltransferase

HBSS – Hank's buffered salt solution

HDAC-1 - *Histone deacetylase 1*

HDL – high density lipoprotein

HFD – high fat diet

HK -hexokinase

HLF – hepatic leukaemia factor

HMG-CoA - 3-hydroxy-3-methyl-glutaryl-coenzyme A

HNF – hepatic nuclear factor

HPA – hypothalamic-pituitary-adrenal axis

Hsl – hormone sensitive lipase

HSPG – heparin sulphate proteoglycans

I.P – intraperitoneal

IDL – intermediate density lipoprotein

IL-6 - interleukin 6

iNOS – inducible nitric oxide synthase

ITT – insulin tolerance test

JNK – c-Jun amino-terminal kinase

KO - knockout

LCFA – long chain fatty acids

LCFA-CoA - long chain fatty acyl-*CoA*

LD - 12:12 light dark

LDL – low density lipoprotein

LH – lateral hypothalamus

Lpl – lipoprotein lipase

LPS – lipopolysaccharide

MAG – monoglyceride

MBH - mediobasal hypothalamus

MC – melanocortin

MCP-1 – monocyte chemoattractant protein-1

mPFC – medio prefrontal cortex

MRN – median raphe nucleus

NAc – nucleus accumbens

NAMPT – Nicotinamide phosphoribosyltransferase

NC – normal chow

NCoR1 - Nuclear Receptor Corepressor 1

NEAT – non exercise activity thermogenesis

NEFA – non-esterified fatty acid

NK – natural killer

Npas2 – neuronal PAS domain containing protein 2

NPY - Neuropeptide Y

NR - nuclear receptor

NST – non-shivering thermogenesis

NTS – nucleus of the solitary tract

O – Oxygen

^{o}C – degrees Celsius

OFC – orbitofrontal cortex

P13K – phosphoinositide-3-kinase

PAI-1 – plasminogen activator inhibitor 1

PC – pyruvate carboxylase

PDE – phosphodiesterase

PDH – pyruvate dehydrogenase

PEPCK - phosphoenolpyruvate carboxykinase

Per – Period

PGC-1α - peroxisome proliferator-activated receptor gamma coactivator 1-alpha

PKA – protein kinase A

POMC - pro-opiomelanocortin

PP1 – phosphoprotein phosphatase-1

Ppar – peroxisome proliferator-activated receptor

PVN – paraventricular nucleus

PYY – Peptide YY

qPCR - real-time PCR

RBP – retinol binding protein

REE – resting energy expenditure

RER – respiratory exchange ratio

RF – restricted feeding

RHT – retinohypothalamic tract

RMR – resting metabolic rate

ROR – retinoic acid-related orphan nuclear receptor

ROS – reactive oxygen species

RQ – relative quantification

RRE – ROR response element

SCN – suprachiasmatic nucleus

scWAT – subcutaneous white adipose tissue

SEM – standard error of the mean

SIRT1 – histone deacetylase sirtuin 1

SREBP – *sterol regulatory element-binding protein*

SSD – sterol sensing domain

T2DM – Type 2 Diabetes Mellitus

TAG – triglyceride

TCA – tricarboxyclic acid

TEF – thermic effect of food

TNFα - tumour necrosis factor α

Treg – T regulator cell

TZD – Thiazolidinedione

UCP1 – uncoupling protein 1

UTR – untranslated region

V_{CO2} – carbon dioxide consumption

VLDL – very low density lipoproteins

VMH –ventromedial nucleus of the hypothalamus

V_{O2} – oxygen consumption

VTA – ventral tegmental area

WHO – World Health Organisation

WT -wild type

α - alpha

β –beta

γ – gamma

Δ – delta/change

Acknowledgements

I would like to thank my supervisors, Dr. David Bechtold, Professor David Ray and Professor Garth Cooper for the opportunity to undertake this project and for their encouragement during my PhD. I would also like to thank my advisor, Professor Simon Luckman for his guidance and help over the past few years. I would also like to acknowledge the financial support provided by the Biotechnology and Biological Sciences Research council for funding my studies.

I would particularly like to express my sincere gratitude to all members of the Bechtold lab who have made for an enjoyable 4 years. This project was made possible by the unwavering support and mentorship from Dr. David Bechtold. I will be eternally grateful to Dr. Peter Cunningham for introducing me a huge variety of laboratory techniques and his assistance with experiments. He always went above and beyond his duty to lend me a helping hand whenever it was required and his support, advice and guidance have been immeasurable. I would also like to thank Dr. Alex West for his support and continued interest in the project as well as for his comments, advice and discussions throughout my PhD. Not only were they both amazing mentors, but great friends. My sincere gratitude must also be extended to Laura Smith, not only for her vast technical support throughout the project, but for being a best friend. She has been my rock throughout the past four years, during both the good and bad times. Our infamous summer holidays have helped maintain my sanity and I hope they continue for many years to come.

Finally, I would like to thank my parents and brother, whose undying love and support made me believe that I could do anything I put my mind to. I am eternally indebted to you and extremely grateful for the opportunities that you have enabled to me have in life. I hope I have made you proud.

Contributions

Other members of the lab contributed to some studies. Specifically, Dr. Peter Cunningham and Laura Smith contributed to the collection and the processing of tissue from the Diet Induced Obesity trial described in Chapter 3. Dr. Peter Cunningham also performed the wheel running studies described in both Chapter 3 and Chapter 4.

Chapter 1: Introduction

1.1 Introduction

Obesity is a heritable disease, and is rapidly becoming one of the most serious health problems throughout the world. Obesity is defined as an abnormal or excessive accumulation of white adipose tissue (WAT), which may impair health. Body Mass Index (BMI) is a commonly used and simple calculation [weight (kg) / height^2 (m^2)] to characterise the appropriateness of a persons' body weight. BMI is often used to classify subjects as overweight (BMI ≥25) and obese (BMI ≥ 30). Worldwide, obesity has nearly doubled since 1980, and the World Health Organisation (WHO) estimates indicate that in 2014 1.9 billion adults over the age of 18 (39% of the population) were overweight and of these, 600 million (13% of the population) were obese (WHO, 2016). Further cause for concern is that obesity is now not simply a problem that affects the adult population. WHO data also shows that in 2014, 42 million children under the age of 5 were obese. Obesity is a major risk factor to a range of comorbidities such as cardiovascular disease, cancer and type 2 diabetes mellitus (T2DM), with 90% of adults aged 16-54 years with T2DM being overweight or obese (National Health Service, 2012). This epidemic has begun to, and will increasingly pressurise the healthcare systems of the world. It is therefore important to elucidate the pathophysiological mechanisms involved in the development of obesity, and its progression to metabolic and cardiovascular disease.

The increased prevalence of obesity in our society has been clearly linked to shifting lifestyle and diet, with over consumption of energy rich foods and decreased physical activity prevalent among the population. A U.S Department of Agriculture Economic Research Service study showed that adults in the US consumed 363 more calories per day in 2009 than they did in 1960. Ultimately, obesity reflects energy imbalance, and to further compound the problem of increased energy intake, energy expenditure through physical activity has decreased. Lifestyle clearly plays a role in the development of obesity; however, it has recently come to light that it is not simply about how much we eat and how much physical activity we partake in, but also about when we consume energy and when we are active. Our behaviour and physiology follows a pronounced 24 hour rhythm. This is underpinned by clocks found in almost every tissue and cell throughout our body (Yoo *et al*., 2004). These clocks allow for the anticipation of temporal changes in the environment, optimising biological processes so that they occur at the correct time of the day. For example, food intake in animals occurs during the active phase, which results in higher circulating glucose concentrations. Fatty acid synthesis is increased and triglyceride storage in adipose tissue is enhanced. However, during the inactive phase, food intake is reduced and therefore fat stores must be mobilized from adipose tissue

and energy usage switches from glucose to fatty acids. The clock mechanism ensures tissues are poised to anticipate diurnal variations in feeding/fasting cycles in order to deal with changing energy supply.

The modern lifestyle has dramatically altered the way in which we live our daily lives. The ever increasing work demands facing the industrialised population, alongside the increasing popularity of the 24-hour lifestyle has resulted in an increased prevalence of shift work, sleep deprivation and light exposure at night which undermines our natural timing system. It has also been suggested that the light emitted from electronic devices can suppress nocturnal melatonin, a hormone responsible for the anticipation of night-time, and therefore cause sleep disruption (Czeisler, 2013). One area of research receiving much attention is how the chronic misalignment of the internal body clock with the environment contributes to the pathogenesis of obesity (Karlsson *et al.,* 2001; Di Lorenzo *et al.,* 2003; Zhao *et al*., 2011).

Epidemiological evidence available suggests that disruption of the circadian clock is associated with metabolic complications and obesity (Maury *et al*., 2010; Eckel-Mahan and Sassone Corsi, 2013). A number of studies have now established that shift work, in which the normal synchrony between the light/dark phase, sleeping and eating is significantly disturbed, is an independent risk factor for obesity and diabetes (Pan *et al*., 2011). Shift work has become increasingly necessary over the past century, and in 2014 it was reported that 33% of men and 22% of women in the United Kingdom partook in such activity (Health and Social Care Information Centre, 2015). In 2003, Karlsson *et al*. showed that night shift workers had higher circulating triglycerides, lower low density lipoproteins and were more likely to be obese in comparison to day workers. In another study, duration of shift work was positively associated with both BMI and waist/hip ratio in both men and women, independent of age and sex (Van Amelsvoort *et al*., 1999). Further studies have supported these observations of altered plasma lipid metabolism and adiposity among night-shift workers (Karlsson *et al*., 2001; Di Lorenzo *et al*., 2002). A more recent cross-sectional study also supported the notion that rotating shift work is an independent risk factor for obesity, regardless of dietary habits and physical activity levels (Barbadoro *et al*., 2013) and prospective studies of healthy volunteers undergoing a 6-day simulated shift work protocol show a reduction of energy expenditure in response to the shift work (Mchill et al., 2014). On top of this, human desynchrony has been shown to compromise metabolic homeostasis, leading to obesogenic physiology, hypertension and decreased insulin sensitivity (Morris *et al*., 2012).

Both animal and human studies have revealed a strong link between eating at the 'wrong' time and development of obesity. When humans display nocturnal feeding patterns, such as in night-eating disorder, the risk of metabolic disease is greatly increased (Allison *et al*., 2007). Similarly, mouse studies have shown that as mice become obese their feeding becomes shifted toward the day (normally an inactive period) (Kohsaka *et al.,* 2007), and diet-induced obesity in mice is exacerbated when food availability is restricted to the daytime (Arble *et al*., 2009). Importantly, if mice are fed high fat diet at the 'correct' time (i.e. food is only accessible in the dark phase of the day), they do not increase in body weight, become obese, or exhibit a loss in insulin sensitivity (Hatori *et al*., 2012).

The modern lifestyle has also led to a decrease in the number of hours the adult population spend sleeping. Over the past century, nightly sleep duration has been reduced by ~1.5 hours, and this has been accompanied by an increase in the prevalence of obesity (Bonnet and Arand, 1995). Sleep restriction and circadian dysfunction alters eating behaviour, glucose homeostasis, and energy handling. For example, it has been shown that the neuroendocrine control of appetite and glucose tolerance is dramatically affected by sleep restriction in humans, with an 18% decrease in leptin (an anorexigenic hormone) and 24% increase in ghrelin (an orexigenic hormone) (Spiegal *et al.,* 2004). In addition, sleep restriction to 4 hours/night for 6 successive nights in healthy individuals resulted not only in impaired glucose tolerance but also a decline in the response to insulin after glucose challenge (Van Cauter and Knutson, 2008). Another prospective study of sleep deprivation shows an increase in body weight after 5 days of insufficient sleep (5 hours per night), which was characterised by an increased in food intake at night (Markwald *et al*., 2013).

The evidence for clock/metabolic coupling is clear and it originates from a complex system involving behavioural and metabolic pathways. My work will examine how specific components of the clock contribute to this coupling, focusing on lipid metabolism and white adipose tissue (WAT), and how it is altered during metabolic disturbance during obesity. This will be done firstly by examining how obesity impacts on the clock and then specifically focussing on *Rev-erbα*, a nuclear hormone receptor, which is a key interface.

1.2 Energy Balance

Energy balance is the balance of calories consumed through eating and drinking compared to calories burned through physical activity. Alterations in body weight and body composition occur when energy intake is not equal to energy expenditure over an extended period of time.

Energy is expended through resting metabolism rate (RMR), the energetic cost of absorbing and metabolising food consumed, and the energy expanded through physical activity. Energy intake depends on the digestible energy available from food intake, and generally reflects protein, carbohydrate, fat content of the food. Not all the energy present in food is metabolically available, with the net absorption of the major macronutrients (carbohydrate, protein and fat) generally incomplete and therefore faecal loss accounts for between 2-10% of gross intake (Hall *et al*., 2012). The magnitude of these losses is influenced by factors such as macronutrient composition (Southgate and Durnin, 1970), fibre and resistant starch intake (Behall and Howe, 1995) and gut microbiota (Jumpertz *et al*., 2011). Metabolically available energy varies between macronutrients (e.g. 4 kcal/g for carbohydrate and protein and 9 kcal/g for fat) (Hall *et al*., 2012).

When energy intake exceeds energy expenditure, a state of positive energy balance occurs which leads to excess energy storage and ultimately increased body mass. On the other hand, when energy expenditure exceeds energy intake, a state of negative energy balance is created with consequential loss of body mass. A complex physiological control system is responsible for achieving and maintaining an energy balance in the body. Signals and hormones are produced by peripheral organ systems, for example the liver and adipose tissue, and food-derived nutrient signals reflect both acute and chronic changes in energy status and energy demand. Based on these signals, feeding and metabolic control centres of the brain dictate proper behavioural (e.g. food seeking/eating) and physiological (increased storage/liberation of energy) responses to maintain energy homeostasis.

Substrate storage and mobilization naturally fluctuate across the day and night and from day to day, with nutrients being stored during periods of high energy intake and mobilized during the fasting period. Fat and carbohydrate are the primary dynamic energy storage depots within the body, but the relative contributions of both macronutrients are vastly different. Dynamic carbohydrate storage occurs primarily in the form of intracellular glycogen stored within skeletal muscle and liver. Glycogen turnover can be rapid; maximal amounts are present in the post-prandial state (Wasserman, 2009) and after a 24-hour fast in rats, liver glycogen was shown to be entirely depleted, whereas muscle glycogen was significantly decreased (Dohm *et* al., 1993). The glucose from glycogen is therefore a good source of energy for sudden, strenuous activity. Unlike fatty acids, the released glucose can provide energy in the absence of oxygen and can thus supply energy for anaerobic activity (Berg *et al*., 2002).

Of course, the other principle form of energy storage in the body is triglyceride (TAG) storage in adipose and non-adipose (e.g. liver) tissues. TAGs are esters derived from glycerol and three fatty acids. Lipids stored in adipose tissue can originate from exogenous (dietary) lipids or from non-lipid precursors, such as carbohydrates. Due to the limited nature of carbohydrate storage within the body, carbohydrates undergo a process called *de novo* lipogenesis and can therefore be stored as lipids in adipocytes (Schutz, 2004). In a state of chronic positive energy balance, adipose tissue expands due to excess energy storage, and ultimately leads to obesity. Increased adiposity is brought about by both hyperplasia (increased number of adipocytes) and hypertrophy (increased amount of lipid stored within the adipocyte) (Jo *et al*., 2009).

1.3 Homeostatic control of feeding

Humans, like most mammals, consume food in discrete bouts (meals); therefore, total daily energy intake is a function of the size, frequency and composition of meals. The perception of hunger and the decision to initiate a meal involves complex interactions between genetic, social, learned, environmental, circadian and humoral cues (Cummings *et al*., 2001; Woods *et al*., 1998). However, at its most basic, food seeking behaviour and meal initiation is based on a homeostatic response to reduced energy supply and increased secretion of orexigenic (food intake promoting) signals. For example, ghrelin is a peptide secreted from the gastric mucosa that stimulates feeding and is implicated in meal initiation (Cummings *et al*., 2001). It is unique in that it is the only known orexigenic hormone. Peripheral ghrelin administration stimulates food intake in both rats (Wren *et al*, 2000; Tschop *et al*., 2000) and humans (Wren *et al*., 2001, Druce *et al*., 2005, Druce *et al*., 2006).

Once feeding commences, the amount consumed is determined by factors involved in satiety perception. The term 'satiation' refers to the perception of fullness that leads to meal termination, whereas 'satiety' describes the reduced interest in food after a meal. These processes are strongly influenced by gastric distention and the release of peptide signals from enteroendocrine cells lining the gastrointestinal tract (Cummings and Overduin, 2007). Gastric distension is sensed by mechanoreceptor neurons in the stomach and relayed to the hindbrain via vagal afferent and spinal sensory nerves (Ritter, 2004). Some satiation-inducing gut peptides enter the brain from the circulation and can exert their effects directly, such as Peptide YY (PYY) which activates Neuropeptide Y (NPY) type 2 (Y2) receptors in the arcuate nucleus (Chee and Colmers, 2008) (Figure 1.1). However, the majority of satiation-inducing gut peptides also mediate their effects via vagal afferent fibres, for example cholecystokinin (CCK) and glucagon-like peptide-1 and (GLP-1) (Cummings and Overduin, 2007). CCK is a prototypic

satiation peptide that is secreted by the duodenal and jejunal mucosa primarily in response to fat and protein ingestion, and it decreases food intake rapidly but transiently via the activation of vagal afferents (Cummings and Overduin, 2007). Exogenous administration of CCK reduces food intake in humans (Kissileff *et al*., 1981; Stacher *et al.*, 1982; Lieverse *et al*., 1995) and rodents (Gibbs *et al*., 1973; Antin *et al*., 1975; Bado *et al*., 1998;). Further supporting its role in satiation, meal size is increased by interventions that disrupt CCK signalling (Moran *et al*., 2002).

Afferent signals involved in satiety are processed initially in the hindbrain. The nucleus of the solitary tract (NTS) plays an important role in the processing of satiety-related input from vagal sensory fibres, and the adjacent circumventricular organ the area postrema (AP) responds to circulating peptides due to its altered blood brain barrier (Cummings and Overduin, 2007). Evidence that hindbrain circuitry is itself sufficient to regulate meal size stems from experiments in 'decerebrate' rats, in which the hindbrain and forebrain are surgically disconnected. These animals are incapable of spontaneously initiating meals and rely on liquid food delivered directly into the mouth, but nonetheless they terminate meals normally in response to gastric distention or satiation peptides such as CCK (Grill and Norgen, 1978; Grill and Smith, 1988). However, it was shown by Kaplan *et al*., (1993) that decerebrate rats fail to adjust meal size to compensate for changes in energy balance and therefore communication between forebrain and hindbrain appears necessary for adaptive changes in meal size to occur in response to energy needs.

The mediobasal hypothalamus (MBH) is a major hub for integrating nutritionally relevant information originating from all peripheral organs and mediated through circulating hormones and metabolites and/or neural pathways from mainly the brainstem. Within the MBH there are numerous important regulatory sites such as the arcuate nucleus (ARC), ventromedial nucleus of the hypothalamus (VMH), lateral hypothalamus (LH), paraventricular nucleus (PVN) and default mode network (DMN). These sites sense peripheral energy signals, integrate these with higher cognitive and contextual information and then regulate the appropriate behaviour and physiological response. The ARC is a major site for sensing and integrating peripheral energy balance signals, including hormones such as leptin, insulin, and ghrelin and nutrients (fatty acids, amino acids, and glucose) (Yu and Kim, 2012). These effects are mediated by at least two distinct leptin-sensitive neuron subpopulations in the ARC. Neurons that express pro-opiomelanocortin (POMC) synthesize and release melanocortin peptides such as α-MSH that are potently anorexigenic, and are stimulated by both leptin and insulin (Morton *et* al., 2006).

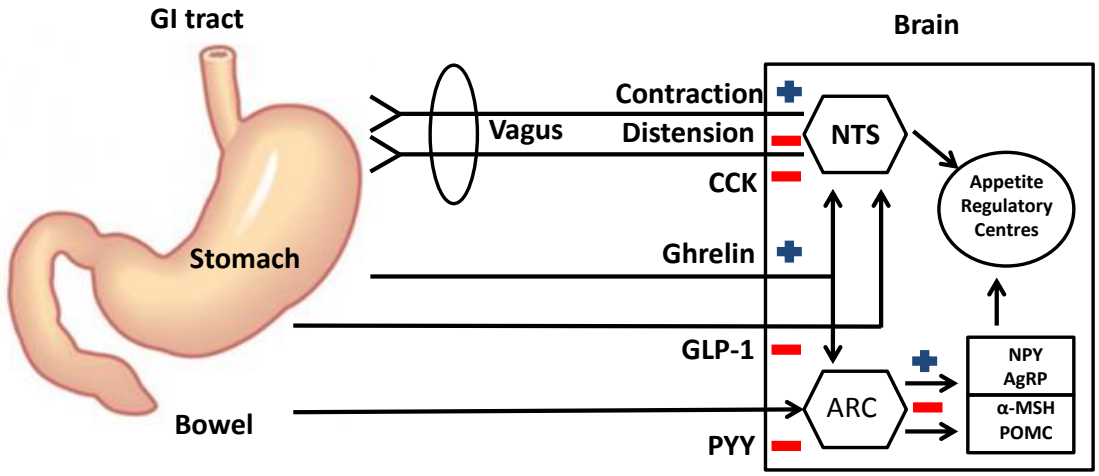

Figure 1.1 - Afferent gastrointestinal signals controlling food intake.
The brain receives hormonal, neural, and metabolic signals regarding body-energy status and, in response to these inputs alters energy intake and expenditure. To regulate food intake, the brain must modulate appetite, and the core of appetite regulation lies in the gut-brain axis. The vagus nerve is the primary neuroanatomic substrate in the gut-brain axis, transmitting meal-related signals caused by food intake in the gastrointestinal tract to sites in the central nervous system that mediate ingestive behaviour. Neuroendocrine regulation of food intake by the gastrointestinal system consists of gastric distention, intestinal and pancreatic satiation peptides, and the orexigenic gastric hormone ghrelin. Abbreviations: CCK, cholecystokinin; GLP-1, glucagon-like peptide-1; PYY, peptide YY; NPY, neuropeptide Y; AgRP, Agouti gene-related peptide; α -MSH, α -melanocyte stimulating hormone; POMC, pro-opiomelanocortin; NTS, nucleus tractus solitarius; ARC, arcuate nucleus.

Melanocortin signalling plays a key role in defending against excess fat gain, particularly during exposure to energy-dense, highly palatable foods. Actions of α-MSH in the hypothalamus are mediated through melanocortin-3 (MC3) and melanocortin-4 (MC4) receptors. In response to moderately increased dietary fat content, MC4 receptor-null mutant ($MC4R^{-/-}$) mice exhibit hyperphagia and accelerated weight gain compared to wild-type mice and mutations in the MC4R represent the commonest monogenic cause of human obesity (Butler *et al*., 2001; Hinney *et* al., 1999; Krude *et al*., 1998). Located adjacent to POMC cells are a population of orexigenic neurons that express the neuropeptides NPY and AgRP (Aponte *et* al., 2010). Agrp is an endogenous antagonist of the MC4R, and therefore acts as a counterbalance to αMSH signalling. Both cell types regulate energy balance via projections to brain regions that influence motivation/reward, energy expenditure, hunger, and ingestive behaviours (Cowley *et al*., 2001). In addition, NPY/AgRP neurons synapse onto and inhibit POMC neurons. The adaptive response to energy depletion induced by fasting or calorie-restricted diets illustrates how coordinated regulation of ARC neurons participates in energy homeostasis. Negative energy balance and loss of body fat lowers plasma levels of adiposity negative feedback signals (e.g. leptin and insulin) while also raising ghrelin levels. In response, NPY/AgRP neurons are activated, whereas POMC cells are inhibited, a combination that potently promotes hyperphagia, positive energy balance, and the recovery of lost fat (Flier, 2004).

The function of the ARC must be placed in a wider context and other hypothalamic nuclei, such as the DMH, LH, PVN and VMH, play important roles in the regulation of energy balance via neuroendocrine and autonomic pathways to the body. For example, NPY/AgRP neurons from the ARC communicate with PVN neurons. The PVN acts as a primary endocrine control centre for the brain, as neurons from this nucleus send their axons into the posterior pituitary causing the release of vasopressin or oxytocin. Neurons from the PVN also project widely throughout the brain stem and therefore WAT, pancreas and liver are linked multi-synaptically with the PVN. Through these connections, the PVN directs autonomic systems controlling pancreatic secretion and adipose storage (Stanely *et al*., 2010). On top of this, the PVN, along with the DMH and VMH feed out onto BAT to regulate thermogenesis, therefore also implicating them in energy expenditure (Zhang and Bi, 2015).

One of the key hormones involved in long term regulation of food intake and energy balance is leptin. Originally identified and characterised by Zhang *et al*. (1994), leptin is secreted by adipocytes in WAT in proportion to adipose tissue mass. Leptin deficient humans display hyperphagia and early onset obesity (Montague *et* al., 1997). Leptin acts in the brain as a

negative feedback regulator of adiposity, regulating fat mass by limiting energy intake and supporting energy expenditure. Decreased leptin signalling promotes increased food intake, positive energy balance, and fat accumulation (Morton *et* al., 2006). Although plasma leptin levels reliably reflect body fat mass under steady-state body weight conditions, they also fluctuate in response to short-term alterations of energy balance (i.e. feeding/fasting period), well before significant changes of fat mass have occurred (Chin-Chiance *et al*., 2000). Leptin's effects on energy balance are mainly mediated via leptin receptors in hypothalamic areas such as the ARC, PVN, VHN, and LHA (Morton *et* al., 2006). Many extra-hypothalamic regions are also leptin-sensitive, including the NTS and midbrain regions central to reward and motivation (Figlewicz and Sipols, 2010).

Not only is insulin a prominent positive regulator of leptin expression in the fat cell, but the mild obesity in mice with neuron-specific deletion of the insulin receptor or the insulin receptor substrate IRS-2 support the idea that insulin and leptin may cooperate in central pathway regulation (Bruning *et al*., 2000; Burks *et al*., 2000). Insulin concentrations are positively correlated with adiposity and act on similar neuronal populations within the brain as leptin (Wynne *et al*., 2005). Administration of insulin has been found to decrease food intake and body weight in mice, rats and humans (Brown *et al*., 2006; Chavez *et al*., 1995; Hallschmid *et al*., 2004), although the effects on reducing food intake are less potent than leptin (Belgardt and Bruning, 2010).

Several nutrient-related signals are also implicated in the homeostatic control of feeding. Among these are free fatty acids (FFAs), which provide a signal of nutrient abundance to key brain areas responsible for energy homeostasis regulation. This likely occurs by favouring intracellular accumulation of long-chain fatty acyl-CoA (LCFA-CoA) which in turn activates a neuronal pathway designed to promote a switch in fuel sources from carbohydrates to lipids (Obici *et al*., 2002; Loftus *et al*., 2000). When LCFA-CoA is selectively reduced in the ARC of rats, the animals become obese, demonstrating the critical role of hypothalamic LCFA-CoA signalling in energy homeostasis (He *et al*., 2006). The enzyme AMP-activated protein kinase (AMPK) is a sensor of nutrient insufficiency. When cells experience a critical drop of fuel availability (as reflected by an increased AMP/ATP ratio), AMPK activation increases substrate oxidation to replenish depleted ATP levels. In the MBH, activation of AMPK increases food intake and body weight whereas inhibition of AMPK has the opposite effect (Minokoshi *et al*., 2004). Changes in hypothalamic AMPK activity drives alterations of neuropeptide expression, for example, expression of constitutively active AMPK in the MBH results in increased mRNA

expression of orexigenic neuropeptides NPY and AgRP in the ARC (Minokoshi *et al*., 2008). In turn, this results in increased food intake. Because hypothalamic AMPK activity is inhibited by leptin and insulin (Minokoshi *et al*., 2004) but stimulated by ghrelin (Andersson *et al*., 2004), altered AMPK signalling may contribute to the feeding effects of these hormones.

1.4 Drive to eat

The control of feeding depends not only on homeostatic signals but also on the hedonic drive to eat. Whereas homeostatic regulatory signals are regulated in large part by hormones and nutrients impacting on brainstem and hypothalamic nuclei, the hedonic drive to eat is controlled by the activity of the mesolimbic dopaminergic system as well as non-dopaminergic systems such as the serotoninergic system (Bertrand, 2011; Saper *et al*., 2002; Volkow *et al.,* 2011). Dopamine (DA), produced by ventral tegmental neurons (VTA) and released in the nucleus accumbens (NAc), plays an important role in motivated behaviour (Salmone and Correa, 2012). DA signalling is utilised by brain areas specialized in food selection and decision-making: the medial prefrontal cortex (mPFC) and the orbitofrontal cortex (OFC). These areas attribute reward value to food cues to inform us on food availability and attractiveness. The DA system is also regulated by internal homeostatic signals such as hormones and nutrients, which can act directly on neurons of the DA system, but also indirectly through hypothalamic or brainstem neurons. Satiety signals such as leptin, insulin and GLP-1 inhibit dopamine neuronal activity and/or reduce dopamine levels in the NAc (Hamel *et al*., 2006; Alhadeff *et al*., 2012; Mebel *et al*., 2012, Labouebe *et al*., 2013). By contrast, hunger signals such as ghrelin and orexins or NPY enhance dopaminergic signalling to increase food reward (Borgland *et al*., 2009; Sorensen *et al*., 2009; Skibicka *et al*., 2011). Nutrients, in particular those rich in glucose and fat, have a high reward effect that leads to DA release in the NAc in proportion to their calorie contents (Bassareo and Di Chiara, 1999; Hajnal *et* al., 2004). Interestingly, recent data showed hyper-dompaminergic activity in *Rev-erbα* mutant mice (Chung *et al*., 2014). REV-ERBα is a nuclear receptor protein expressed rhythmically in the superchiasmatic nucleus and peripheral organs (Preitner *et al.* 2002). The hyper-dopaminergic activity observed in these mutant animals is evidence that *Rev-erbα* has a repressive action on the dopaminergic system, involved in the regulation of hedonic feeding behaviour, therefore linking circadian rhythms to metabolism and behaviour (discussed in detail in section 1.36).

1.5 Energy Expenditure

The other key factor in energy balance is energy expenditure. Energy expenditure is comprised of three components – resting energy expenditure (REE), diet induced thermogenesis and activity energy expenditure (AEE). The body also expends energy to support growth, stay warm in cold environments and metabolise drugs/toxins. REE reflects energetic costs of maintaining cardiac function, respiration, nervous function, muscle tone and body temperature. Energy expenditure at rest accounts for 60-75% of total energy expenditure (Carpenter *et al*., 1995) and this is therefore the greatest single contributor to overall energy expenditure. The rate of energy expended at rest (as kcal/h) is typically reported as either basal metabolic rate (BMR) or RMR, whereas REE refers to energy expended over a 24 hr period. BMR is measured after no physical activity has taken place for >12hours, whereas RMR is measured 3-4 hours after a person eats or does significant physical work. Muscle and organ mass (lean mass) accounts for much of the individual differences observed in RMR because they have a much greater metabolic capacity compared to adipose tissue (Ravussin *et al*., 1982; Johnstone *et al*., 2005; Javed *et al*., 2010). Differences in lean body mass account for 60-80% of the total variation in RMR amongst individuals. AEE is split into two main components, non-exercise activity thermogenesis (NEAT) and exercise energy expenditure (Levine et al., 1999). NEAT is defined as the energy expended for everything we do that is not sleeping, eating or sports-like exercise (Levine et al., 1999). These two components combined can be referred to as physical activity (Caspersen et al., 1985). Physical activity energy expenditure is the most modifiable of the components of energy expenditure (Westerterp, 2003), and the factor that is most under voluntary control for the majority of individuals. During physical activity, mechanical work associated with muscle contraction requires energy. Exercise can also affect RMR due to excess post exercise oxygen consumption (Laforgia *et al*., 1997). The thermic effect of food (TEF) is the increase in RMR after ingestion of a meal and represents the increase in energy expenditure associated with the body's processing of food, including work associated with the digestion, absorption, transport, metabolism and storage of energy from ingested food. The percentage increase in energy expenditure over BMR caused by the thermic effect of food has been estimated to range from 5-30% and is macronutrient dependent, with protein having the highest thermic effect (Bray *et al*., 1974). Converting excess protein and carbohydrate to energy stores (fat and glycogen) requires more energy than the efficient process of simply storing excess dietary fat as body fat. A rise in metabolism following food consumption reaches a maximum about 1 hour after eating and is generally absent by 4 hours postprandium (Halton and Hu, 2004).

Energy expenditure is measured by direct or indirect calorimetry. Direct calorimetry is the determination of energy use by measuring the heat released from an organism enclosed in a small insulated chamber surrounded by water (calorimeter). The rise in temperature of the water is directly related to the energy used by the organism (Jequier, 1985). Direct calorimetry is expensive and complex, whereas indirect calorimetry is easier and less expensive. Indirect calorimetry is the quantification of energy expenditure based on the non-invasive measurement of oxygen consumption (V_{O2}) and carbon dioxide production (V_{CO2}). O_2 and CO_2 are measured in source air and expired air to give V_{O2} and V_{CO2} in ml/min/kg. Correcting energy expenditure for the metabolically active mass of a subject is important if one wants to compare data from animals of different body weights as expansion of adipose tissue happens during obesity, but adipose tissue has relatively low metabolic activity. One of the most common ways of correcting for this using the Brody-Kleiber allometric equation, which works on the basis that basal energy expenditure is proportional to body-weight raised at the ¾ power in order to normalize between species (Brody, 1945; Kleiber, 1947). However, using straight body weight is also common. Once corrected, V_{O2} and V_{CO2} can be converted into a value for REE in kcal (or kJ)/day (Branson and Johannigman, 2004). An evaluation of substrate oxidation from calorimetry is also possible. The respiratory quotient is a unitless value calculated from V_{CO2}/V_{O2}. Many metabolised substances only contain the elements carbon, hydrogen and oxygen, e.g. fatty acids and carbohydrates. The major source of energy in these compounds is stored in the Carbon (C)- Hydrogen (H) bond and during oxidative metabolism these C-H bonds are converted to CO_2 and H_2O (Even *et al*., 1993). The following equation describes complete oxidation of carbohydrates, lipids and proteins: $C_xH_yO_z + (x + y/4 - z/2)\ O_2 \rightarrow x\ CO_2 + (y/2)\ H_2O$. When 1 mole of each of the three main fuels is burnt up in a calorimetric bomb, the volumes of O_2 used and CO_2 released and the amount of energy liberated as heat can be used to determine respiratory quotient and therefore metabolism of these compounds gives an respiratory quotient of $x/(x + y/4 - z/2)$. respiratory quotients of organisms in metabolic balance usually ranges from 1.0 (pure carbohydrate oxidation) to ~0.7 (pure fat oxidation) (Westenskow *et al*., 1988). Other metabolic processes, such as lipogenesis, the formation of lipid from non-lipid precursors, result in an respiratory quotient greater than 1. Under normal circumstances protein oxidation contributes very little to overall energy metabolism, and thus protein oxidation is generally ignored in the determination of respiratory quotient. If appropriate, respiratory quotient is corrected for protein oxidation by measuring urinary nitrogen excretion (Branson and Johannigman, 2004). Energy expenditure (kcal/hr) can also be determined using the respiratory quotient value. Firstly, a calorific value (CV) is determined

using the following equation, CV = 3.815 + 1.232 * respiratory quotient. The rate of energy expenditure can then be calculated using the following equation: Heat = CV * VO_2. Carbohydrate and fatty acid oxidation (COX and FOX) can also be derived using the following equations: COX: 4.55 * VCO_2 – 3.21 * VO_2; FOX: 1.67 * VO_2 – 1.67 * VCO_2 (Frayn, 1983).

1.6 BAT thermogenesis

In endothermic animals maintenance of stable body temperature represents a major energetic cost. Mammals, including humans, depend on both shivering and non-shivering thermogenesis (NST) mechanisms for temperature homoeostasis (Block, 1994; Silva, 2011). Although muscle shivering is an immediate response to cold stress, continuous muscle shivering leads to exhaustion and muscle damage. NST mechanisms are activated in order to adapt to minor or gradual shifts in temperature acclimation to stable temperature changes. Brown adipose tissue (BAT) is an important site of NST in many mammals (Enerback *et al*., 1997; Cannon and Nedergaard, 2010). BAT is only found in mammals and is especially prominent in mammalian new-borns. BAT mitochondria are unique in that they express a high level of uncoupling protein 1 (UCP1) on the inner membrane. During oxidation of fatty acids, protons are pumped out by the respiratory chain. In BAT mitochondria the protons may then re-enter through ATP-synthetase, as in normal mitochondria, or through UCP1. In the latter case, all chemical energy released by oxidation and temporarily stored in the mitochondrial proton electrochemical gradient is released in the form of heat. The activity of BAT is controlled from the hypothalamic area, via the sympathetic nervous system and norepinephrine release. Norepinephrine signalling at adrenergic receptors (AR), and especially the β_3–AR receptor, stimulates BAT activity and increases the expression of UCP1. During acute thermogenic stimulation (e.g. acute cold exposure) β_3–AR receptor signalling enhances hormone sensitive lipase activity, which in turn leads to the release of free fatty acids from triglyceride stores in the brown adipocytes, and increased β–oxidation within the mitochondria. Cold exposure directly activates thermogenesis in BAT – cold is sensed through sensory nerves in peripheral tissues and activates central sympathetic outflow and catecholamine secretion. Contrary to what happens in cold acclimation, starvation in rodents leads to atrophy of BAT and a marked decrease in NST, which has been related to a decrease in UCP1 protein and mRNA levels (Champigny and Ricquier, 1990; Matamala *et al.,* 1996). Early physiological studies have also shown that caloric excess itself can stimulate BAT expansion and thermogenesis, mediated by UCP1 (Rothwell and Stock, 1997). This is referred to as diet-induced thermogenesis. Ablation of UCP1 in mice resulted in increased susceptibility to hypothermia but had no propensity to

develop obesity under normal ambient temperatures (Enerback *et al.,* 1997). It was later shown that UCP1 knockout mice shiver extensively, and that any loss of diet-induced thermogenesis was masked by the energetic cost of shivering. Indeed, when UCP1 knockout mice were raised under thermoneutral conditions (approx. 30°C in mice), the animals gained significantly more weight and adipose tissue than littermate controls (Feldmann et al. 2009).

It has been shown that peroxisome proliferator-activated receptor γ (PPARγ) participates in the activation of BAT genes, such as UCP1 (Sears *et al*., 1996). Synthetic PPARγ activators, especially those in the Thiazolidinedione (TZD) class are potent activators of mitochondrial biogenesis and BAT-selective genes. TZD treatment is associated with increased capacity of UCP1 mediated uncoupled respiration (Petrovic *et al*., 2010; Bartesaghi *et al*., 2015). Transcriptional activity of PPARγ on UCP1 expression is greatly increased by the PPARγ-coactivtor-1α (PGC-1α) (Puigserver *et al*., 1998). PGC-1α controls thermogenic gene activation in response to cold and β-adrenergic agonists (Lin *et al*., 2004; Uldry *et al.,* 2006). PGC-1α is phosphorylated and directly activated by p38 mitogen activated protein kinase following β_3 adrenergic stimulation of BAT cells (Cao *et al*., 2004). PGC-1α then binds to various transcription factors to induce the expression of thermogenic genes such as UCP1.

In addition to BAT, skeletal muscle has an important role in NST, especially in humans (van Marken Lichtenbelt and Schrauwen, 2011). Adult humans have no large deposits of brown adipose tissue. In adult humans, the contribution of BAT to adrenaline-induced thermogenesis has been estimated at <25%, whereas skeletal muscle accounts for up to 50% of adrenaline-induced thermogenesis (Astrup *et al.,* 1985; Simonsen *et al.,* 1993). Similar to the role of UCP1 in BAT, UCP3 is the principle uncoupling protein in skeletal muscle. UCP3 is specifically expressed in skeletal muscle and brown adipose tissue. Like UCP1, UCP3 also reduces the proton gradient across the inner mitochondrial membrane when expressed in yeast (Gong et al., 1997; Boss et al., 1998). UCP3 mRNA expression is upregulated after thyroid hormone treatment, which is known to increase thermogenesis in rodents (Gong et al., 1997) and in humans (Barbe et al., 2001). Furthermore, like UCP1 in BAT, UCP3 is upregulated after the consumption of a high-fat diet in rodents (Gong et al., 1999) and humans (Schrauwen et al., 2001).

1.7 Digestion and Absorption

The gastrointestinal system is the portal through which nutritive substances, vitamins, minerals and fluids enter the body. Proteins, fats and complex carbohydrates are broken down into absorbable units (digested) and along with vitamins, minerals and water, cross the mucosa of the small intestine and enter the lymph or blood (absorption) (Johansson, 1972). Digestion of the major foodstuffs is an orderly process involving the action of a large number of digestive enzymes. Digestive enzymes are found in the secretions of the salivary glands, the stomach and exocrine portion of the pancreas. Other enzymes are found in the luminal membranes and the cytoplasm of the cells that line the small intestine (Isenman *et al*., 1999). The action of digestive enzymes is aided by the hydrochloric acid secreted by the stomach and bile secreted by the liver. Here, we will concentrate on the digestion and absorption of carbohydrates and lipids.

The principal dietary carbohydrates are polysaccharides, disaccharides and monosaccharides. The enzyme α-amylase in saliva initiates the digestion of carbohydrates and in the small intestine, potent pancreatic α-amylase also acts on polysaccharides, resulting in oligosaccharides which are further acted on in the ileum by oligosaccharidases. Resulting sugar molecules either enter mucosal cells or are absorbed further along the GI tract (Ferraris, 2001). Ingested disaccharides are hydrolysed by lactase or sucrose on the luminal surface of mucosal cells. Hexoses and pentoses are rapidly absorbed across the wall of the small intestine via secondary active transport. This is dependent on Na^+ concentration in the lumen. Sugar molecules pass from mucosal cells to the blood in the capillaries draining into the portal vein (Dashty, 2013).

Depending on diet, on average 30 to 40% of total energy intake consists of dietary fats which mainly reflect long-chain fatty acids (LCFAs) esterified into TAGs (Glatz *et al*., 2010). TAGs can be hydrolysed by lingual lipases, but significant fat digestion begins in the duodenum, with pancreatic lipase being the most important enzyme involved. Principal products of its action are FFAs and 2-monoglycerides (Carey, 1983). Pancreatic lipase acts on fats that have been emulsified; however it cannot penetrate fat droplets covered by emulsifying agents without colipase, which is also secreted by the exocrine portion of the pancreas (Lowe, 1994). Most of the dietary cholesterol is in the form of cholesteryl esters and pancreatic esterase hydrolyses these esters in the intestinal lumen. Fats are emulsified in the small intestine by the detergent action of bile salts, lecithin and monoglycerides. Bile salts alone are relatively poor emulsifying

agents and require phospholipids and monoglycerides. As concentration of bile salts in the intestine rises, which is under both dietary and circadian control (Duez *et al*., 2008), lipids and bile salts form micelles, spherical aggregates containing fatty acids (FAs), monoglycerides and cholesterol. Micellar formation facilitates transport to the mucosal cells by passive diffusion. The subsequent fate of FAs depends on their size. FAs with less than 10-12 carbon atoms pass from the mucosal cells directly into the portal blood where they are transported as FFA. Cholesterol and FAs with more than 10-12 carbon atoms are re-esterified in mucosal cells. TAGs and cholesterol esters are then coated with a layer of protein, cholesterol and phospholipid to form chylomicrons, the largest of the lipoprotein particles, which leave the cell and enter the lymphatics (Jensen, 2003). In mucosal cells, most of the TAG is formed by the acylation of the absorbed 2-monoglycerides, primarily in smooth endoplasmic reticulum. However, TAG is also formed from glycerophosphate, which is a product of glucose catabolism. The acylation of glycerophosphate and the formation of very-low-density lipoproteins (VLDL) occurs in the rough endoplasmic reticulum of hepatocytes. Carbohydrate moieties are added to the protein in the golgi apparatus and the finished chylomicrons are extruded by exocytosis into the circulation (Mansbach and Siddiqi, 2016)

1.8 Liver as a metabolic regulator

All blood leaving the absorptive surfaces of the digestive tract enters the hepatic portal system and flows into the liver. Liver cells extract nutrients or toxins absorbed from blood before it reaches the systemic circulation through the hepatic veins. In the post-absorptive state, blood glucose levels increase and hepatocytes remove glucose from the blood stream and either store it as glycogen or use it to synthesise lipids that can be stored in the liver or other tissues (Rui, 2014). The liver stabilises blood glucose levels at about 90 mg/dl in humans. The liver also regulates circulating levels of TAGs, FAs and cholesterol. In the post-absorptive state, lipids are removed for storage. However, because most lipids absorbed by the digestive tract bypass the hepatic portal circulation as they are packaged into chylomicrons, the regulation occurs only after lipid levels have risen within the general circulation (Mansbach and Siddiqi, 2016).

1.9 Glucose regulation

Hepatocytes make up around 80% of the cells in the liver. Glucose enters hepatocytes principally via Glut2, a plasma membrane glucose transporter. Glut2 also mediates glucose release from the liver, with Glut1 and other transporters also playing a role in glucose release

from hepatocytes (Hosokawa and Thorens, 2002). Glucose is phosphorylated by glucokinase in hepatocytes to generate glucose-6-phosphate (G6P) leading to a reduction in intracellular glucose concentration which further increases glucose uptake. G6P is unable to be transported by GLUT transporters so it is retained within hepatocytes. In the fed state, G6P acts as a precursor for both glycogen synthesis (via glycogen synthase), and for metabolism through glycolysis to generate ATP and pyruvate. G6P is also an allosteric inhibitor of glycogen synthase, thus further increasing liver glycogen levels in times of glucose excess. In the fasted state, when generation of glucose is required, glycogen is hydrolysed by glycogen phosphorylase (glycerogenolysis), and G6P can be dephosphorylated by glucose-6-phosphatase (G6Pase) (Villar-Palasí and Guinovart, 1997).

Activity of both glycogen synthase and glycogen phosphorylase is also regulated by posttranslational modifications. Phosphorylation of glycogen synthase, mainly by glycogen synthase 3 (GSK-3) inhibits glycogen synthase activity and in contrast, phosphorylation of glycogen phosphorylase increases its activity (Fang *et al*., 2000). Both glycogen synthase and glycogen phosphorylase are able to be dephosphorylated by protein phosphatase 1. In the fed state, pancreatic β-cells secrete insulin in response to an increase in blood glucose, amino acids and fatty acids. Insulin stimulates glycogen synthase by activating Akt which phosphorylates and inactivates GSK-3, thus increasing glycogen synthesis (Figure 1.2). Insulin stimulates the expression of glucokinase which increases hepatocyte glucose uptake indirectly by phosphorylating glucose and generating 6GP (Cohen *et al*., 1978). Moreover, glucagon and catecholamines (epinephrine and norepinephrine), collectively called counter regulatory hormones, bind to their cognate G-protein coupled receptors and activate protein kinase A (PKA) by increasing intracellular cAMP levels. PKA phosphorylates and activates glycogen phosphorylase directly or indirectly by phosphorylating and inactivating phosphorylase kinases. Glucagon inhibits acetylation of glycogen phosphorylase, which decreases the ability of protein phosphatase 1 to bind to, dephosphorylate and inactivate glycogen phosphorylase (Jiang and Zhang, 2003). During short term fasting periods, the liver produces and releases glucose mainly through glycogenolysis (Lodish *et al*., 2007). During prolonged fasting in which glycogen stores become depleted, hepatocytes synthesise glucose through gluconeogenesis using lactate, pyruvate, glycerol or amino acids. These gluconeogenic substrates are either generated in the liver or delivered to the liver through circulation from extrahepatic tissues. Lactate is oxidised by lactate dehydrogenase to generate pyruvate. Pyruvate is transported into the mitochondria and converted to oxaloacetate by pyruvate carboxylase. Oxaloacetate is reduced to malate by mitochondrial malate dehydrogenase to regenerate oxaloacetate.

Cytoplasmic oxaloacetate is converted to phosphoenolpyruvate by cytoplasmic phosphoenolpyruvate carboxylase (PEPCK-C), a key step of gluconeogenesis. Phosphoenolpyruvate, after multiple biochemical reactions is converted into fructose 1,6-bisphosphate (F1,6P) which is then dephosphorylated by fructose 1,6 bisphosphatase (FBPase) to generate fructiose-6-phosphate. FGP is converted to 6GP, transported into the ER and dephosphorylated by G6Pase to generate glucose. Dephosphorylation of G6P is a rate limiting step common for both glycogenolysis and gluconeogenesis. Glycerol enters into hepatocytes via aquaporin-9 and is phosphorylated by glycerol kinase to generate glycerate-3-phosphate, a substrate for gluconeogenesis. Amino acids are converted to α-ketoacids through deamination reactions catalysed by glutaminase, glutamate dehydrogenase and/or amino transferase. The α-ketoacids are further converted to intermediates of the TCA cycle (e.g. pyruvate, oxaloacetate, fumarate, succinyl-CoA or α-ketoglutarate) which serve as precursors for gluconeogenesis (Landau *et al.,* 1996).

When carbohydrates are abundant, the liver not only utilises glucose as the main metabolic fuel but also converts glucose into fatty acids. Firstly, glucose in broken down in a process called glycolysis, which is a three step process The first step involves phosphorylation, isomerization and further phosphorylation of glucose to provide fructose 1,6 bisphosphate. The second stage involves the cleavage of the fructose 1,6-bisphosphate into two three-carbon fragments, resulting in three-carbon units that are readily interconvertible. In the final step, ATP is harvested when the three-carbon fragments are oxidized to pyruvate. Pyruvate is then channelled into the mitochondria and completely oxidised to generate ATP through the tricarboxylic acid (TCA) cycle and oxidative phosphorylation. Alternatively, pyruvate can be used to synthesise fatty acids through lipogenesis. G6P can also be metabolised via the pentose phosphate pathway to generate NADPH. NADPH is required for lipogenesis and biosynthesis of other bioactive molecules (Rui, 2014).

1.10 Lipid Metabolism

The term lipid describes a group of organic compounds, such as fats, waxes and sterols. Lipids have an array of important biological roles, ranging from energy storage to signalling. Lipids can be divided into eight classes (Fahy *et al*., 2005) and FAs are carboxylic acids with long aliphatic tails and fall into the fatty acyl group (Figure 1.3). They can either be saturated or unsaturated and their aliphatic tail is often made up of an even number of carbon atoms.

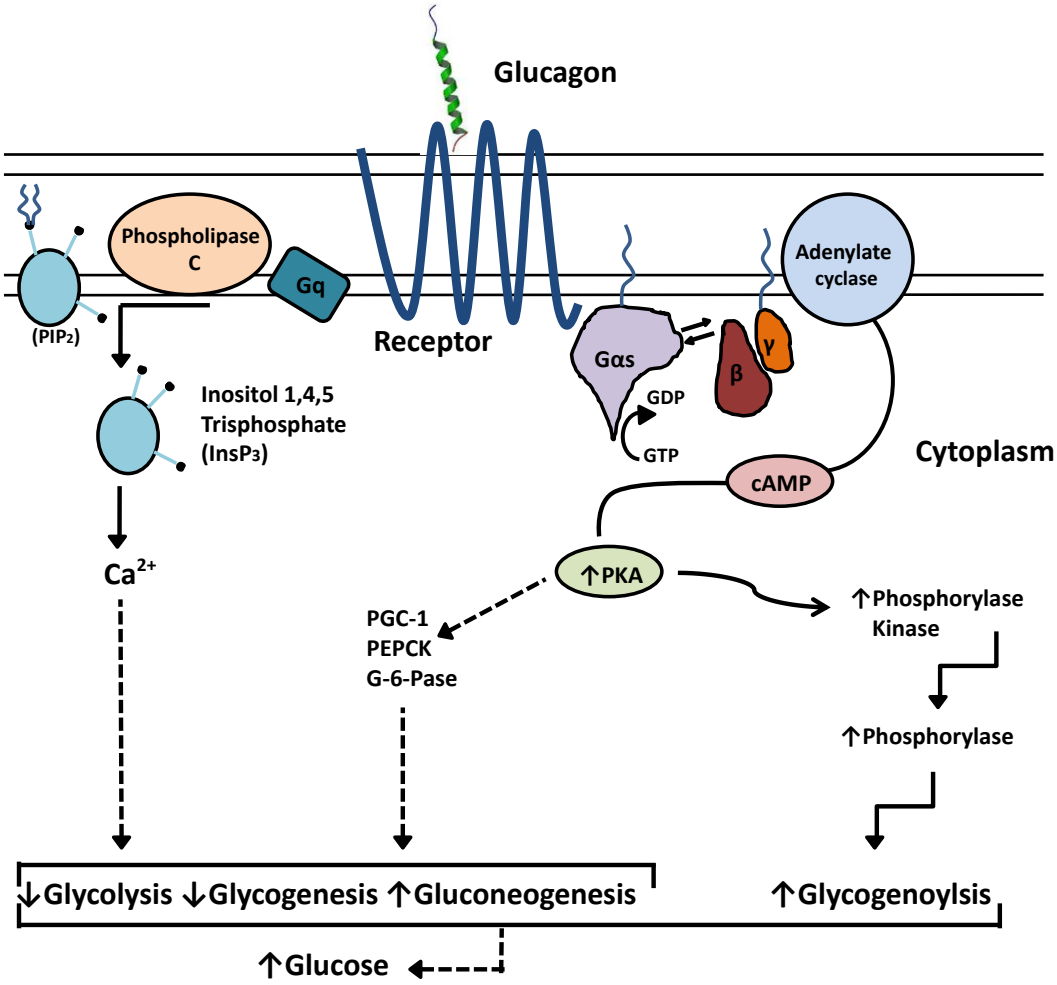

Figure 1.2 - Glucagon-signalling pathway.
Glucagon binds to the glucagon receptor, resulting in a conformational change activating G-proteins, subsequently resulting in activation of Adenylate Cyclase. cAMP is then formed, activating PKA. In turn, this modulates PGC-1/PEPCK and G-6-Pase activity to result in decreased glycolysis and glycogenesis and increased gluconeogenesis. PKA activates phosphorylase kinase, an enzyme responsible for the conversion of glycogen phosphorylase to the correct isoform (a) to increase glycogenolysis. Glucagon also results in the activation of phospholipase C, catalysing the hydrolysis of PIP2. This is further hydrolysed to InsP3, resulting in calcium release causing a cascade of intracellular changes and activity, again contributing to decreased glycolysis, decreased glycogenesis and increased gluconeogenesis. Taken together, this results in increased glucose availability. Abbreviations: PIP_2, phosphatidylinositol 4,5-biphosphate; PGC-1, peroxisome proliferator-activated receptor-γ coactivator-1; PEPCK, phospho*enol*pyruvate carboxykinase; G-6-Pase, glucose-6-phosphatase.

Triacylglycerols (TAGs) are esters made up of three fatty acids and a molecule of glycerol (Figure 1.3) (Glatz *et al*., 2010).

In humans, TAGs store unused calories (Roberts *et al.,* 1988). A variety of tissues, such as adipose tissue, skeletal muscle and liver, use fatty acids as an energy source (Frayn *et al.,* 2006). TAG stores in these tissues can be mobilised by hydrolysis to release energy in the form of fatty acids to fulfil metabolic requirements during periods of reduced energy consumption (Bernlohr *et al.*, 2002). Fatty acids in the body are derived from dietary consumption or through their endogenous synthesis during *de novo lipogenesis*, the majority of which takes place in the liver. Fatty acids can be divided into two groups: essential and non-essential. Essential fatty acids cannot be synthesised in the body and therefore are a dietary requirement (Thomasson, 1962).

As previously discussed, TAGs are transported around the body as lipoproteins. Lipoproteins consist of an amphipathic monolayer of lipids composed of an assembly of hydrophilic head groups of phospholipids and free (non-esterified) cholesterol together with apolipoproteins (Apo) that face the aqueous phase and cover the inner hydrophobic region containing TAGs and cholesterol esters (Hoofnagle and Heinecke, 2009). The polarity of the surface lipoproteins prevents their aggregation and allows them to be solubilized in the circulation (Tzen *et* al., 1992). The overall structure of lipoproteins is determined by apolipoproteins (Campos *et al*., 2001; Campos *et al*., 2005). Based on the density, which results from the percentage of the proteins and lipids in their structure, they are divided into major classes including high density lipoprotein (HDL), low density lipoprotein (LDL), intermediate density lipoprotein (IDL), VLDL and chylomicrons (Mahley *et al.,* 1984)

Chylomicrons and VLDL are involved in the transport of TAGs. Chylomicrons transport newly absorbed TAGs from the intestine to the skeletal muscle for consumption, to adipose tissue for storage, or to the liver for synthesis of VLDL. VLDL is secreted from the liver to the circulation for transport to other tissues, including adipose tissues. In the exogenous lipoprotein pathway, lipid components of the lipoproteins are synthesized by the intestine from dietary lipids while in the endogenous lipoprotein pathway the lipid components are newly synthesized within the liver. In the exogenous pathway the intestinal lipids are absorbed by the epithelium and assembled with apoB48, apoA-I, apoA-II and apoA-IV to make nascent chylomicrons which are secreted to the lymphatic vessels and released directly into the circulation by the subclavian vein. In the circulation, HDL delivers its apolipoproteins apoC-II and apo-E to the nascent chylomicron to make a mature chylomicron. These exchangeable apolipoproteins protect the

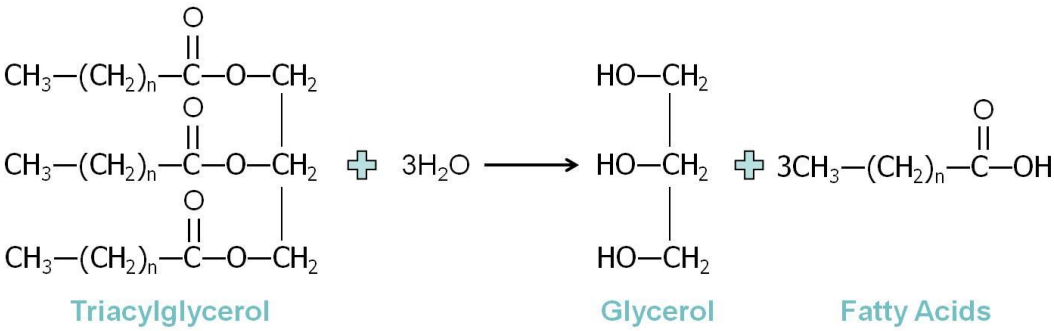

Figure 1.3 Biochemical representation of triglyceride breakdown.
One molecular of triacylglycerol is hydrolysed to give 1 molecule of glycerol and 3 molecules of fatty acid. 3 molecules of water are needed to add -H and -OH groups to break the ester bonds, an action which is catalysed by the enzyme lipase

TAG-rich lipoprotein particles (chylomicrons and VLDL) from non-specified interaction with the plasma and lead to their correct configuration for the action of lipoprotein lipase (LPL). In skeletal muscle and adipose tissue, TAG in mature chylomicrons, via activation of the endothelial LPL in the presence of phospholipids and its cofactor apo-CII, is hydrolysed to glycerol and FAs, and taken up by the tissue. Glycerol is returned to the liver and kidney to be converted to the glycolytic intermediates and the phospholipid and apoA and apoC of mature chylomicrons is transferred to HDL. The hydrolysed chylomicron, known as a remnant chylomicron, contains cholesterol esters, apoE and apoB48. Remnant chylomicrons are transferred to the liver through the circulation. Ultimately, remnant chylomicrons are degraded in the lysosome which results in release of FAs and glycerol (Wang *et al*., 1985).

In the endogenous pathway, liver is the main source of VLDL lipid constituent. Assembly of intracellular TAG and cholesterol in the liver is maintained by apoB100 and delivered to the circulation by lipid transporters (Rivellese *et al*., 2004; Frayn, 1998). Similar to chylomicrons, circulating HDL provides apoE and apoCII to VLDL (Murdoch and Breckenridge, 1995). VLDLs contain TAG, cholesterol, cholesteryl ester, apoB-100, apoC-I, apoC-II, apo-C-III and apoE. Thus, VLDL plays an important role in the delivery of FAs to adipose tissue to store energy as inactive fuel in the form of TAGs or to supply active energy for skeletal muscles and other tissues via FFA delivery (Frayn, 1998). LPL ensures release of FAs and glycerol via hydrolysation of TAGs and loss of apoCs from VLDL to transfer back to HDL. The VLDL is then converted to remnant VLDL or IDL, which contains apoB-100 and apoE (Mahley *et al*., 1984).The interaction of remnant VLDL or IDL with LDL receptors of the liver in the presence of apoB-100 and apoE ends in TAG hydrolysation and loss of apoE to constitute the remnant IDL or LDL lipoproteins. Fusion of endosomes with lysosomes leads to degradation of apolipoproteins and hydrolysation of cholesterol esters to free cholesterols which are incorporated into the plasma membranes. Excess intracellular cholesterol enhances activity of acyl-CoA cholesterol acyltransferases (ACAT) for re-esterification of cholesterol to the cholesterol esters for intracellular storage (Chang *et al*., 2009).

Lipoprotein (LPL), pancreatic, hepatic and endothelial lipases are soluble hydrolytic enzymes whose main function is the hydrolysis of TAGs of the circulatory TAG-rich chylomicrons and VLDL subsequently converting them to non-esterified FAs (NEFA) and 2-monoacylglycerol. They also increase the cellular uptake of remnant chylomicrons, cholesterol rich lipoproteins and FFAs. The apolipoproteins of lipoprotein particles have a role in targeting of the lipoproteins to the tissues. They also function as a cofactor, especially (apoC-II), for LPL,

although apoC-III is an inhibitor of LPL activity (Shachter, 2001; Yu and Ginsberg, 2005). On top of its enzymatic function, LPL plays an important role in lipid metabolism and transport. LPL acts as a linker between lipoproteins and cell surface receptors, including proteoglycans such as cell surface related LDL receptors and heparin sulphate proteoglycans (HSPG), and thus facilitates the uptake of lipoproteins by the tissues (Yu and Ginsberg, 2005). Expression of LPL is regulated through a complex interaction between sterol regulatory element-binding protein (SREBP), peroxisome proliferator-activated receptor-alpha (PPARα), cyclic adenosine 3',5'-monophosphate (cAMP) response element binding protein (CREBP) and activator protein-1-like factors (Sartippour and Renier, 2000; Mead *et* al., 2002). In addition, expression of LPL is influenced by nutritional factors, blood glucose levels, FA concentration, as well as insulin, catecholamines, thyroid hormone, growth hormone, and oestrogen (Mead *et* al., 2002). LPL is produced in parenchymal cells, heart, skeletal muscles as well as macrophages and is distributed along the vasculature (Mead *et* al., 2002). Thereafter, it is secreted and translocated to the functional HSPG-binding site on the luminal surface of the endothelium (Wang and Eckel, 2009).

LPL expression in adipose tissue and skeletal muscle reflects whether dietary lipids are mainly stored in the adipose tissue or are used for energy consumption in the skeletal muscle. In the fed state, the activity of LPL is high in adipose tissue and low in skeletal and cardiac muscle; thus extra energy is stored. In contrast, in a fasted state, LPL expression in adipose decreases, while increasing in muscle reflecting the metabolic demand for lipid fuels in those tissues (Frayn, 1998; Sakayama *et al*., 2008). Insulin is a major regulator of the LPL activity in adipose tissue. In the fed state, insulin upregulates LPL expression in adipose tissue (thereby increasing FA storage), but inhibits LPL expression in muscle. In the fasted state, insulin levels fall and LPL expression increases in the skeletal muscle. Of note, obesity-related insulin resistance is associated with a proinflammatory state of adipose tissue in which production of cytokines, such as interleukin-6 (IL-6) and tumour necrosis factor α (TNFα), reduces LPL expression (Frayn, 1998).

Once liberated from chylomicrons and lipoprotein particles, FAs enter tissues by facilitated diffusion. Numerous fatty acid transporters facilitate and regulate the movement of fatty acids through the plasma membrane. These include fatty acid translocase (CD36/FAT), fatty acid transport proteins (FATPs), and membrane fatty acid binding protein (Abumrad *et al*., 1993;

Schaffer and Lodish, 1994; Isola *et al*., 1995; Stahl *et al.,* 2001). Once inside the cell, the fatty acids are either used for metabolism via β-oxidation or storage as TAG.

1.11 Fatty acid oxidation

FA beta oxidation (FAO) is a mitochondrial (and peroxisomal for LCFAs) process in which the conserved energy of the FAs is released in a stepwise manner. FAs are long carbon chain molecules that in each step of FAO lose 2 carbon molecules to produce the activated intermediate, acetyl-CoA. FAO also results in the reduction of NAD^+ and FAD^+ cofactors to produces NADH and $FADH_2$. Oxidation of FAs happens in two stages, first in the cytoplasm then in the mitochondria. In the cytoplasmic stage, FAs are first activated via conversion to acyl-CoA via fatty acyl-CoA synthase (Schulz, 1991). Thereafter, acyl-CoA is complexed with carnitine by acyl-carnitine palmitoyltransferase transferase I (CPT-1) for transfer into the mitochondrial membrane. The liver isoform (CPT1A) is found throughout the body on the mitochondria of all cells except for skeletal muscle cells and brown adipose cells. The muscle isoform (CPT1B) is highly expressed in heart and skeletal muscle cells and brown adipose cells. In acyl-CoA with long chain hydrocarbons, acylcarnitine translocase enzyme transfers the acylcarnitine across the inner mitochondrial membrane. In the mitochondrial stage, carnitine is subsequently removed from the acyl-CoA via acyl-carnitine transferase II (Schreurs *et al*., 2009). Acyl-CoA is then degraded by a recurring sequence of four reactions (dehydrogenation, hydration, oxidation and thiolysis) until the long chain FA becomes completely degraded to acetyl-CoA (as described in figure 1.4). Acetyl-CoA then enters the TCA cycle to produce adenosine triphosphate (ATP). The reactions of the cycle are carried out by 8 enzymes that completely oxidise acetyl-CoA into two molecules each of carbon dioxide and water. For each acetyl group that enters the citric acid cycle, three molecules of NADH are produced, which are in turn required for ATP generation via oxidative phosphorylation. At the end of each cycle, the four-carbon oxaloacetate has been regenerated, and the cycle continues.

The level of acetyl-CoA is one of the main determinant parameters in the regulation of FAO. Acetyl-CoA is the product of glucose degradation during glycolysis and pyruvate dehydrogenase (PDH) reaction as well as FAO. Therefore, acetyl-CoA links the carbohydrate and lipid pathways. Acetyl-CoA is consumed in different pathways including the TCA cycle, gluconeogenesis using pyruvate carboxylase (PC), oxaloacetate production to store glucose in the liver as glycogen, FA biosynthesis and cholesterol synthesis (Dashty, 2013).

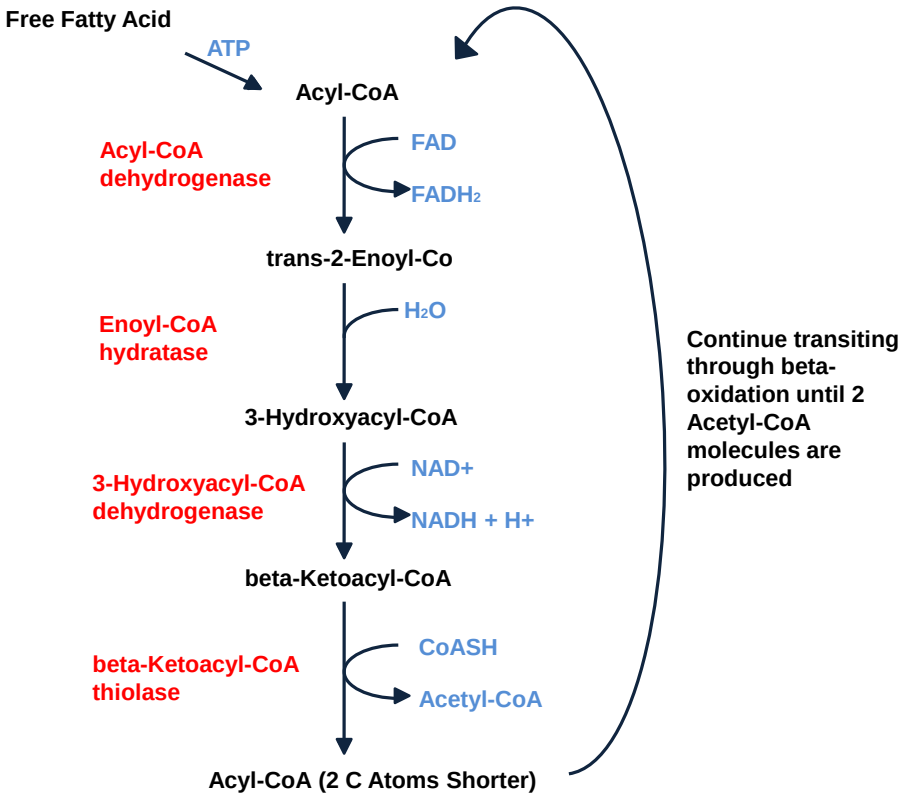

Figure 1.4 - Reactions of beta-oxidation.
During beta-oxidation in the mitochondria, fatty acid molecules are broken down by removing two-carbon units from the carboxyl end of a fatty acid molecule to produce acetyl-CoA. Abbreviations: CoA, Coenzyme A; CoASH, Coenzyme A with Sulfhydryl Functional Group; FAD, flavin adenine dinucleotide; NAD, nicotinamide adenine dinucleotide

1.12 Fatty Acid Synthesis

When the concentration of acetyl-CoA in the cytoplasm increases sufficiently pathways involved in FA synthesis are engaged. Most of the acetyl-CoA which is converted into fatty acids is derived from carbohydrates via the glycolytic pathway. Biosynthesis of long chain fatty acids occurs in two distinct steps – the first is the conversion of acetyl-CoA to malonyl-CoA, a reaction catalysed by the biotin containing multi enzyme system acetyl-CoA carboxylase (ACC). The second step is the conversion of acetyl-CoA and malonyl-CoA to palmitate in the presence of NADPH. This conversion to palmitate involves six recurring reactions catalysed by a single, homodimeric, multifunctional protein, FA synthase (FAS). Each FAS monomer contains three catalytic N-terminal domains and four C-terminal domains that are separated from each other by a structural core. The conserved acyl carrier protein acts as the mobile domain responsible for shuttling the intermediate fatty acid substrates to various catalytic sites (Smith *et* al., 2006). Palmitoyl-ACP is released from the enzymatic complex using deacylase and one molecule water to produce palmitate. ACC is the rate limiting enzyme of FA synthesis that is regulated in a variety of ways. Palmitoyl-CoA, a LCFA, is negative allosteric regulator of ACC (i.e. when the cell contains high levels of LCFAs, ACC, and thereby FA synthesis, is turned off). When intracellular energy is low, phosphorylation of ACC by AMPK decreases the level of malonyl-CoA and inhibits FA synthesis (Foster, 2012). Malonyl-CoA is a key allosteric inhibitor of CPT-1 (Xue and Kahn, 2006), and therefore as malonyl-CoA levels fall, FAO rates increase thereby increasing energy production. ACC is also subject to regulation by insulin and glucagon. For example, when blood glucose levels are low, glucagon results in decreased phosphorylation of ACC, therefore causing its activation. However, when blood glucose levels are high, insulin causes increased phosphorylation of ACC, causing its inhibition. In mammals, two main isoforms of ACC are expressed – ACC1 and ACC2 – and these are the principal regulators of FA synthesis and β-oxidation. ACC1 is found in the cytoplasm of all cells but enriched in lipogenic tissue such as adipose tissue, and the production of malonyl-CoA in these tissues drives FA synthesis. ACC2 is expressed at high levels in oxidative tissue such as muscle and high levels of malonyl-CoA in these tissues inhibits β-oxidation.

1.13 Triglyceride Synthesis

TAGs are synthesised from glycerol-3-phosphate (G3P) and fatty acyl co-As (Figure 1.5). G3P is produced by different mechanisms in the liver and adipose tissue. In the liver, G3P is made by

phosphorylation of glycerol using glycerol kinase and ATP. Glycerol is derived from degradation of adipocyte-TAGs and is transferred to the liver via circulation. In adipose tissue, G3P comes principally from the reduction of dihydroxyacetone phosphate (DHAP), a product of the glycolysis pathway, by glycerol-3-phosphate dehydrogenase (G3PDH). In the next step, two molecules of acyl-CoA join to G3P using phosphatidic synthetase or fatty-acyl-CoA transferase to make phosphatidic acid. Phosphatidic acid, using phosphatase, loses one phosphate group and produces diglyceride (DAG). DAG combines with one extra acyl-CoA and produces TAG via the activity of triglyceride synthase. TAG is then transported to VLDL in the liver and stored in intrahepatic lipid droplets. In adipocytes TAG is sequestered in large lipid droplets (Chao *et al*., 1986). Lipid droplets consist of an organic core comprising neutral lipids (e.g. TAGs and sterol esters) that is bound by a monolayer of phospholipids (Kohlwein *et al*., 2013). This structure provides a unique separation of the aqueous and organic phases of the cell. Several types of proteins cover the lipid droplet such as structural proteins (e.g. perilipin), lipid synthesis enzymes, lipases and membrane trafficking proteins (Guo, 2009).

1.14 Triglyceride Degradation

TAGs are sequentially hydrolysed by the activity of adipose triglyceride lipase (ATGL), hormone-sensitive lipase (HSL) and monoglyceride (MAG) lipase (MAGL) to produce FAs and glycerol (Ahmadian *et al*., 2007; Duncan *et al* 2007*;* Jaworski *et al*., 2007) (Figure 1.5). The liberated FAs are used in different ways, either as the source of energy at the time of energy deprivation, for re-esterification in adipose tissue, for beta oxidation in other tissues or for storage as phospholipids or other lipid types. In the fasted state, the level of the catecholamines increases in adipose tissue due to absorption by circulation or by sympathetic innervations. Catecholamines increase the adenylate cyclase activity and therefore intracellular cAMP concentration and PKA activity. Consequently HSL is phosphorylated resulting in the stimulation of the hydrolytic activity of this enzyme as well as its translocation to the adipocyte-lipid droplets for TAG breakdown. Glucocorticoids, a class of steroid hormones, can also stimulate lipolysis via activation of PKA and subsequent stimulation of ATGL (Duncan *et* al., 2007). In the fed state, insulin inhibits lipolysis by dephosphorylation of HSL and activation of phosphodiesterase (PDE) that decreases the level of cAMP. Insulin, via the phosphoinositide-3-kinase/AKT (PI3K/AKT) pathway, phosphorylates and inhibits PDE3B which has an inhibitory effect on the cAMP activity. Another inhibitory effect of insulin on lipolysis is through phosphoprotein phosphatase-1 (PP1) and its negative regulation on HSL by

decreasing perilipin phosphorylation (Duncan *et* al., 2007). Other pathways for phosphorylation of HSL are via cGMP dependent kinase (Stralfors and Belfrage, 1985) and calcium-induced protein kinase C/mitogen-activated protein kinases/extracellular-signal-regulated kinase (PKC/MAPK/ERK) activity (Donsmark *et* al., 2003; Donsmark *et al.,* 2004) that activate HSL. AMPK inactivates HSL lipolytic properties and has a competitive effect with PKA in HSL phosphorylation and activity (Daval *et* al., 2006; Guilherme *et* al., 2008). Another regulator of HSL activity is perilipin A, a protein that associates with lipid droplets and enhances HSL lipolytic activity (Tansey *et* al., 2004; Daval *et* al., 2006). In basal states, perilipin A maintains a low rate of lipolysis in the lipid droplets. However, upon lipolytic stimulation, HSL translocates from the cytosol to the lipid droplet and in turn perilipin is phosphorylated by PKA which allows HSL to access the lipid droplet. Two circulating peptides called atrial natriuretic peptide (ANP) and brain natriuretic peptide (BNP) have also been implicated in HSL regulation. They are released at times of stress and bind to receptors that are coupled to the synthesis of cyclic guanosine monophosphate (cGMP), hence increasing its intracellular concentration. In turn this activates cGMP-dependent protein kinase causing the phosphorylation of perilipin and HSL and subsequently increasing lipolysis (Lafontan *et al*., 2005). HSL has an effect on broad substrates of lipid molecules including TAG, DAG, MAG, retinyl and cholesteryl esters, but it mostly affects DAG and cholesteryl ester (Ali *et al.,* 2005). ATGL contains a patatin-like domain that hydrolyses TAG but does not hydrolyse cholesteryl and retinyl esters (Ahmadian *et* al., 2007). *Atgl* is mainly expressed in adipose tissue and is overexpressed in adipocyte differentiation and glucocorticoid stimulation and is downregulated during feeding and insulin stimulation (Jaworski *et al*., 2007).

A number of hormonal signalling pathways influence TAG storage and liberation. For example, β-adrenergic hormones have a stimulatory effect on TAG degradation, via PKC/ERK (muscle contraction induced) and cAMP/PKA pathway (epinephrine stimulation) by stimulation of HSL (Donsmark *et* al., 2004; Watt *et al*., 2004; Guilherme *et* al., 2008). Adenylyl cyclase also has an important role in lipid metabolism. Adenylyl cyclase, via influence on ATP and conversion to cAMP, activates protein kinase using one ATP molecule. Activated PKA phosphorylates and activates ATGL (Watt *et al*., 2004). Hormones such as adrenaline, noradrenaline (Jensen *et* al., 1987) and glucagon (Miles and Jensen, 1993; Gravholt *et* al., 2001) influence adipocytes directly and stimulate adenylyl cyclase and lipolysis. Conversely, insulin inhibits lipolysis via

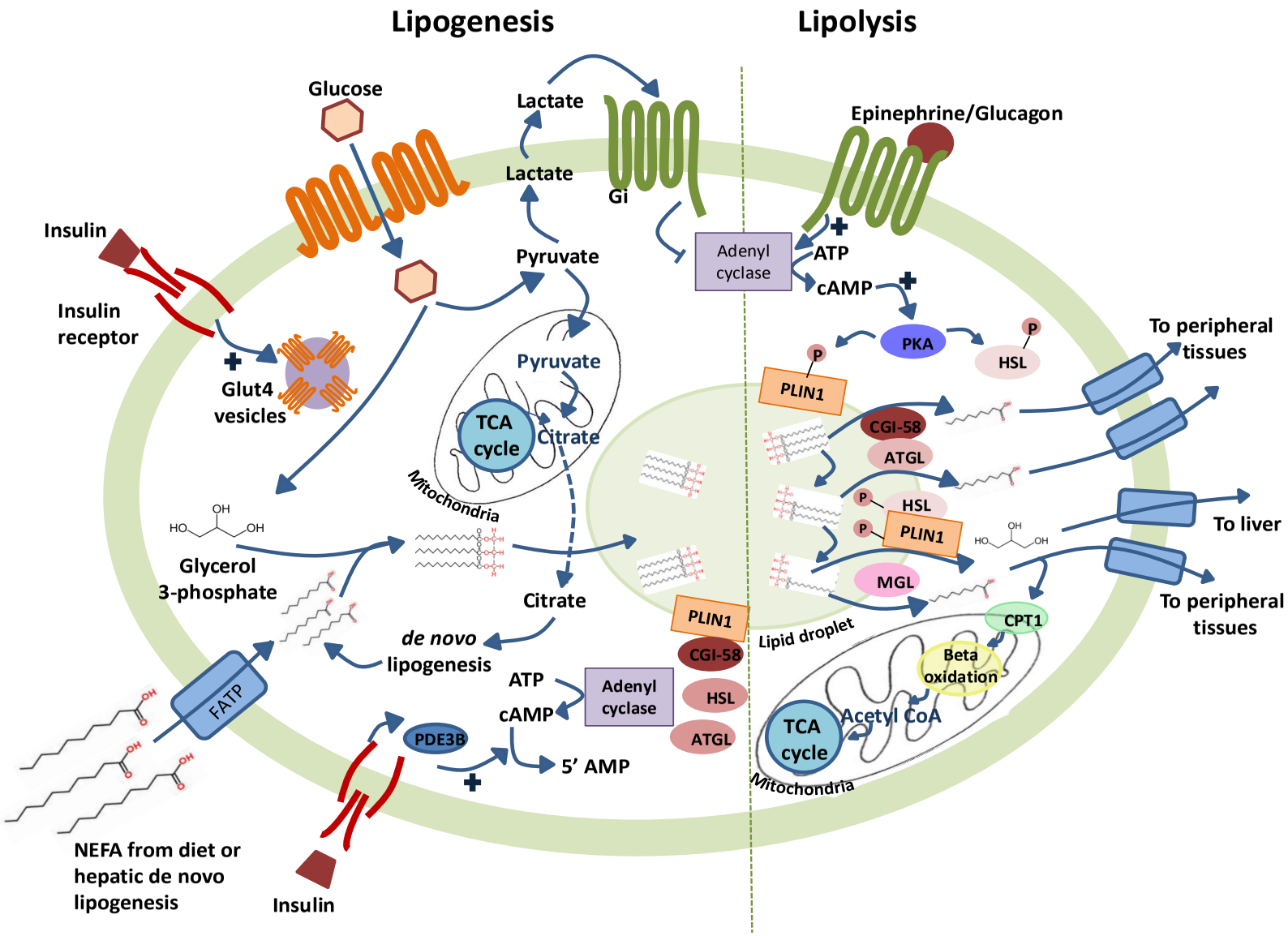
Lipogenesis
Lipolysis
Glucose
Lactate
Lactate
Gi
Epinephrine/Glucagon
Insulin
Insulin receptor
Glut4 vesicles
Pyruvate
Pyruvate
TCA cycle
Citrate
Mitochondria
Adenyl cyclase
ATP
cAMP
PKA
HSL
P
PLIN1
CGI-58
ATGL
To peripheral tissues
To liver
Glycerol 3-phosphate
Citrate
de novo lipogenesis
FATP
ATP
cAMP
Adenyl cyclase
PDE3B
5' AMP
PLIN1
CGI-58
HSL
ATGL
Lipid droplet
MGL
CPT1
Beta oxidation
Acetyl CoA
TCA cycle
Mitochondria
NEFA from diet or hepatic de novo lipogenesis
Insulin

Figure 1.5 - Overview of lipid metabolism within the adipocyte.

The main metabolic functions of adipose tissue are the storage of surplus fatty acids through TAG synthesis (lipogenesis) and then the mobilisation of fatty acids from triglyceride by hydrolysis (lipolysis). It is also sensitive to changing nutritional cues. For example, it is insulin-sensitive (insulin stimulates glucose uptake and lipogenesis and inhibits lipolysis) and subject to adrenergic regulation (stimulates lipolysis and adaptive thermogenesis (brown adipose tissue)). Abbreviations: ATGL, adipose triglyceride lipase; ATP, adenosine triphosphate; cAMP, cyclic adenosine monophosphate; CG1-58, comparative gene identification-58; CPT-1, carnitine palmitoyltransferase 1; Glut4, glucose transporter 4; HSL, hormone sensitive lipase; MGL, monoglyceride lipase; P, phosphorylated; PDE3B, phosphodiesterase 3B; PKA, protein kinase A; PLIN1, perilipin 1; TCA, tricarboxylic acid.

activation of PDE, and inhibition of adenylyl cyclase (Elks and Manganiello; 1985). Insulin also inhibits lipolysis indirectly by stimulating entrance of glucose to cells. Glycolysis then occurs which increases DHAP concentration, which is a substrate of FA synthesis. FAS is activated and TAG degradation via HSL is inhibited.

1.15 Ketone Bodies

Ketone bodies include acetone, acetoacetic acid and beta hydroxyl butyric acid; although only acetoacetic acid is used as an energy source by the body. Normally, the concentration of these products in the circulation is low (1 mg/dl); however in certain conditions, such as type 1 diabetes and starvation their concentration increases (leading to ketosis and metabolic acidosis). Ketone bodies are produced in the liver, testes and ovaries (Royo *et* al., 1993) and are transported to the brain and cardiac muscles for consumption as energy source via conversion to acetyl-CoA. Acetoacetic acid is made from acetyl-CoA using beta-ketothiolase, 3-hydroxy-3-methyl-glutaryl-CoA (HMG-CoA) synthase and HMG-CoA lyase (Figure 1.6). During fasting, adipocyte TAG is degraded to release its energy. However, over-supply of TAG in the liver induces synthesis of ketone bodies. This happens when the ratio of insulin/glucagon is altered in the fasting state. Therefore, when glucagon levels are high, ACC is inhibited and consequently FAO is stimulated. In FAO, fatty acyl-CoA is converted to acetyl-CoA to be used in the Krebs cycle for energy production. When there is a sufficient energy supply in hepatocytes extra acetyl-CoA is consumed in the ketogenesis pathway. In the chronic fasting state, gene expression of mitochondrial HMG-CoA synthase is stimulated that induces the ketogenesis pathway via acetoacyl-CoA and β-hydroxy-β-methylglutaryl-CoA (HMG-CoA).

1.16 Cholesterol Biosynthesis

Cholesterol is one of the main fat components of the body and is supplied both endogenously and exogenously. Inside the body cholesterol is made from acetyl-CoA in hepatocytes, enterocytes, testes and ovaries (Buhman *et al.,* 2000). Cholesterol biosynthesis occurs in the cytoplasm where 3 acetyl-CoA are joined to each other to produce HMG-CoA. HMG-CoA can be used to form cholesterol by HMG-CoA reductase (HMG-CoAR) or enter the ketogenesis pathway. HMG-CoAR is the key rate limiting sterol synthetic enzyme. High levels of cholesterol have a negative feedback effect on HMG-CoAR and its gene expression. For example, cholesterol stimulates HMG-CoAR polyubiquitination and degradation which is modulated by

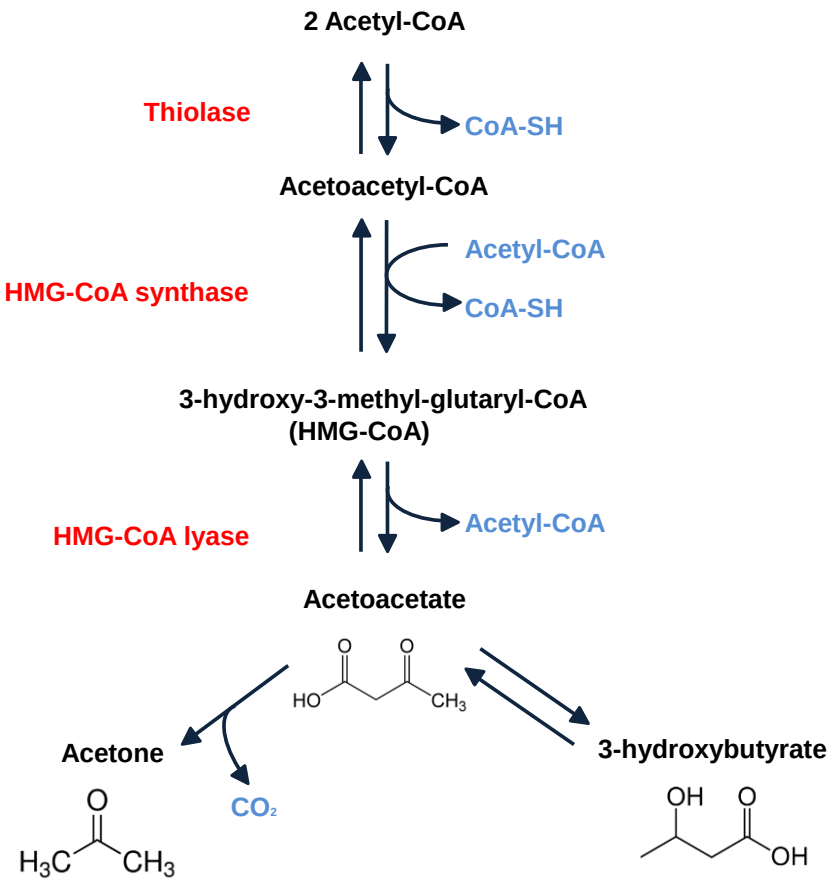

Figure 1.6 Reactions of ketogenesis.

Two Acetyl-CoA molecules are converted to Acetoacetyl-CoA which is then converted to HMG-CoA (beta-hydroxy-methylglutaryl-CoA). This molecule is then converted to acetoacetate which is converted to 3-hydroxybutyrate, this involves the release of NAD+ or acetone. Abbreviations: CoA, Coenzyme A, CoA-SH, Coenzyme A with Sulfhydryl Functional Group

its transmembrane sterol-sensing domain (SSD) and its role in proteasome degradation. HMG-CoAR is also regulated by phosphorylation and dephosphorylation. HMG-CoAR phosphorylation via activated AMPK (Curtis *et* al., 2005) or activated protein phosphatase inhibitor-1 (PPI-1) inhibits its function. Activated PPI-1 also inhibits HMG-CoAR phosphatase (also called PP2A), which dephosphorylates (and activates) HMG-CoAR. Glucagon and epinephrine decrease cholesterol synthesis through inhibiting PPI-1, while insulin dephosphorylates and activates HMG-CoAR (Espenshade and Hughes, 2007).

1.17 Transcriptional control of lipid metabolism

Transcriptional regulation of genes involved in metabolism is considered as the major long term regulatory mechanism controlling energy homeostasis. This regulation is executed by a variety of transcription factors among which are the PPARs, SREBPS and CCAAT/enhancer binding proteins.

PPARs are ligand activated transcription factors of nuclear hormone receptor subfamily comprising of the following three subtypes: PPARα, PPARγ, PPARβ/δ. PPARs can activate transcription through binding to PPAR response elements. PPARα target genes are involved in fatty acid catabolism and it is most abundantly expressed in the liver. PPARβ/δ is the most widely distributed of the subtypes and can be found in a wide variety of tissues including heart, kidney muscle and lung. Activation of PPARβ/δ enhances fatty acid metabolism.

PPARγ is mainly found in adipose tissue, macrophages and mammary tissue. Alternate promoter usage coupled with differential mRNA splicing results in two isoforms of PPARγ. $PPARγ_1$ is found in adipose tissue, liver, kidney and the heart whereas $PPARγ_2$ is found exclusively in WAT. Unliganded PPARγ associates with co-repressors, thereby supressing expression of target genes. In the presence of ligands, the corepressors are exchanged for coactivators, such as PPARγ coactivator 1 (PGC-1). PGC-1 was originally believed to function only in white and brown adipocytes but it is also expressed in hepatocytes where it plays a primary role in controlling the expression of genes involved in gluconeogenesis. Activation of PPARγ causes insulin sensitization and enhances glucose metabolism (Tyagi *et al*., 2011).

SREBPs are a family of transcription factors that regulate lipid homeostasis by controlling the expression of a range of enzymes required for endogenous cholesterol, FA, TAG and phospholipid synthesis, for example FASN and DGAT2. SREBP1C is involved in FA synthesis and insulin induced glucose metabolism (particularly lipogenesis) whereas SREBP2 is relatively specific to cholesterol synthesis. The SREBP1A isoform seems to be implicated in both pathways. SREBP processing is mainly controlled by cellular sterol content. The SREBP1c isoform, however, is mainly regulated at the transcriptional level by insulin. The unique regulation and activation properties of each SREBP isoform facilitate the coordination of the regulation of lipid metabolism (Eberlé *et al*., 2004).

CCAAT/enhancer binding proteins (C/EBPs) are leucine-zipper transcription factors whose sequences are characterised by the presence of a basic region followed by a leucine rich motif. A number of genes involved in adipose lipid metabolism are regulated by the C/EBP family of transcription factors, e.g. FABP4. Three members of the C/EBP family are expressed in adipocytes – α, β and δ. Temporal expression of the three isoforms during 3T3-L1 differentiation suggests that C/EBP genes are subject to exquisite regulatory controls. Studies have shown that C/EBPβ and C/EBPδ regulate the expression of C/EBPα (Lin and Lane, 1994). In addition, insulin regulates the transcription of the CEBP α, β and δ genes in fully differentiated 3T3-L1 adipocytes. Furthermore, glucocorticoids reciprocally regulate the expression of the C/EBP α and δ genes in WAT.

1.18 Adipose Tissue

Traditionally adipose tissue has been considered to be composed of two distinct forms, white (WAT) and brown (BAT) with fundamentally different functions. BAT is specialised for the generation of heat by non-shivering mechanisms fuelled primarily by the oxidation of fatty acids (Cannon and Nedergaard, 2004; Cannon and Nedergaard, 2009). WAT is specialised for fuel storage rather than oxidation, providing substrate to other tissues such as muscle during fasting and periods of high energy demand. Classically, lipid was considered to be deposited in a single unilocular droplet within white adipocytes, with multiple droplets in the case of brown fat cells. Brown adipocytes, in contrast to white, are derived from myogenic progenitor cells (Seale *et al*., 2008; Timmons *et al*., 2007). The concept of two distinct forms of adipose tissue has been challenged through the recognition that some fat depots have both white and brown adipocytes and a further 'brite' adipocyte has been identified. These brite cells express UCP1

but do not possess the complete molecular characteristics of brown adipocytes (Petrovic *et al*., 2010). In addition to different forms of adipocyte, several types of non-adipocyte cell are present in WAT depots. These include fibroblastic preadipocytes, vascular endothelial cells, macrophages and mast cells. Several types of immune cells are present in adipose tissue in addition to macrophages, for example lymphocytes and natural killer (NK) cells (Tilg and Moschen, 2006; Exley *et al*., 2014). WAT activity is strongly influenced sympathetic nervous system inputs (Hales *et al*., 1978); for example with marked activation of lipolysis during cold exposure or prolonged fasting (Garofalo *et al*., 1996; Migliorini *et al*., 1997). The extent of the sympathetic innervation in WAT is less than that of BAT as the sympathetic nervous system plays a central role in the initiation and regulation of thermogenesis in BAT, including mitochondrial biogenesis and the recruitment of UCP1 (Cannon and Nedergaard, 2004; Cinti, 2005).

1.19 Adipogenesis

Adipocytes derive from multipotent mesenchymal stem cells. Adipogenesis happens in 2 phases – determination and terminal differentiation. Determination results in the conversion of the stem cell to a pre-adipocyte, which cannot be distinguished morphologically from its precursor cell but has lost the potential to differentiate into other cell types. In the second phase, the preadipocyte takes on the characteristics of the mature adipocyte – it acquires the machinery that is necessary for lipid transport and synthesis, insulin sensitivity and the secretion of adipocyte specific proteins. Adipocyte differentiation involves a complex and highly orchestrated programme of gene expression and multiple signals, for example extracellular factors such as fibroblast growth factors 1 and 2, can influence whether stem cells form adipocytes. PPARγ and C/EBPs are considered to be the master regulators of adipogenesis.

PPARγ is both necessary and sufficient for adipogenesis (Rosen *et al*., 2000). Most pro-adipogenic factors seem to function at least in part by activating PPARγ expression or activity. Proadipogenic C/EBPs and Kruppel-like factors have been shown to induce at least one of the two PPARγ promoters. By contrast, anti-adipogenic GATA factors function by repressing PPARγ expression (Tong *et al*., 2000). Ligand activation of PPARγ is required to induce adipogenesis but not to maintain PPARγ-dependent gene expression in mature adipocytes. PPARγ is not only crucial for adipogenesis but also required for the maintenance of the differentiated state (Gerhold *et al*., 2002). As previously mentioned, several C/EBP family members are expressed

in adipocytes. C/EBPβ is crucial for adipogenesis in immortalised pre-adipocyte lines but its effect is less obvious in embryonic fibroblasts. C/EBPβ promotes adipogenesis in part by inducing C/EBPα and PPARγ expression. C/EBPα induces many adipocyte genes directly and is therefore an important factor in the development of adipose tissue. Despite the importance of C/EBPs In adipogenesis, the transcription factors cannot function efficiently in the absence of PPARγ which is required to release histone deacetylase-1 (HDAC1) from the *C/ebpα* promotor (Zuo *et al*., 2006).

1.20 Secretory role of WAT

In addition to energy storage, WAT adipocytes are major secretory cells, releasing a wide range of lipid and protein entities including a number of peptides hormones called adipokines (Fruhbeck *et al*., 2001). Adipokines influence a number of physiological processes including lipid homeostasis, inflammation and food intake (Ronti *et al*., 2006). The most prominent of these adipokines are leptin adiponectin and resistin.

1.20.1 Leptin

Leptin is a satiety hormone encoded by the *ob* gene and was discovered by means of the *ob/ob* mutation in mice. This mutation leads to hyperphagia, morbid obesity and insulin resistance, all of which can be reversed by leptin administration (Friedman and Halaas, 1998). Circulating levels of leptin are directly related to BMI or body fat (Considine *et al*., 1996, Maffei *et al*., 1995). It has also been found that leptin resistance, whereby the body no longer responds to this satiety signal, is present in obesity (Myers *et al*., 2008). After release by adipose tissue, leptin signals to the brain giving information about the status of the body energy stores. After leptin is released by adipose tissue into the bloodstream, it crosses the blood brain barrier and binds to hypothalamic leptin receptors influencing the activity of various hypothalamic neurones and the expression of various orexigenic and anorexigenic neuropeptides. This results in a decrease in food intake and an increase in energy expenditure to maintain the size of body fat stores. Orexigenic peptides influenced by leptin include NPY, melanin-concentrating hormone, AgRP and orexin (Meister, 2000). Anorexigenic peptides modulated by leptin include POMC and corticotrophin releasing hormone (CRH) (Meister *et al*., 2000). Several studies have also demonstrated that leptin is involved in the neuroendocrine response to starvation, including changes in hormone concentrations and possible changes in sympathetic nervous system activity and reproductive function (Klein *et al*., 2000; Chan *et al* .,

2003). Leptin has also been reported to have an influence on various biological mechanisms, including the immune and inflammatory response by stimulating the production of chemokines and macrophages (Kiguchi *et al*., 2009). Leptin levels can also be increased by pro-inflammatory stimuli such as lipopolysaccharaide (LPS) and interleukin 1 (IL-1) (Grunfeld *et al*., 1996).

1.20.2 Adiponectin

Adiponectin is a hormone synthesised almost solely by adipocytes and has important roles in glucose and lipid metabolism, as well as inflammation (Maeda *et al*, 2002; Waki *et al*., 2003). It is constitutively produced and constitutes approximately 0.01-0.05% of plasma protein (usually ranging from 2-20 µg/ml). Although secreted by adipose tissue, circulating levels of adiponectin are paradoxically decreased with increased central adiposity (Arita *et al*., 1999, Turer *et al*., 2011). Adiponectin has effects on metabolism by binding to adiponectin receptors 1 and 2 (ADIPOR1 sand ADIPOR2) that are predominantly expressed in skeletal muscle and liver (Yamauchi *et al*., 2003). As well as being expressed in muscle and liver, adiponectin receptors are expressed in pancreatic β-cells (Kharroubi *et al*., 2003; Huypens *et al*., 2005) with ADIPOR1 being the predominant form in the mouse. Adiponectin may act to increase glucose-mediated insulin secretion and transcription of insulin and related gene products (Wijesekara *et al*., 2010). Adiponectin has been shown to increase glucose-mediated insulin secretion in HFD fed mice (under insulin resistant conditions). Adiponectin has also been shown to have anti-apoptotic effects on β-cells in cell culture and islet preparations (Rakatzi *et al*., 2004; Wijesekara *et al*., 2010, Holland *et al*., 2011). This may be due to the activation of pro-survival kinases such as extracellular signal regulated kinases 1 and 2 (ERK 1/2) and AKT (Brown *et al*., 2010; Wijesekara *et al*., 2010). ADIPOR1 is the predominant adiponectin receptor found in skeletal muscle (Yamauchi *et al*., 2003). In muscle, adiponectin appears to act through AMPK (inhibiting acetyl-Co-A carboxylase) (Tomas *et al*., 2002) and PPARα (Yamauchi *et al*., 2003) to exert metabolic effects in muscle. Adiponectin binding results in an increase in glucose uptake via Glut4 translocation and non-oxidative glycolysis while at the same time reducing intramyocellular TAG content and promoting FA oxidation (Fruebis *et al*., 2001; Civitarese *et al.,* 2006). Adiponectin also has several effects on the liver. One of the most prominent of these is suppression of hepatic glucose output, lowering systemic glucose levels. It acts to supress the expression and activity of key regulators in gluconeogenesis (Yamauchi *et al*, 2002; Berge *et al*., 2001) such as phosphoenolpyruvate, carboxykinase and glucose-6-phosphatase. Adiponectin acts to sensitise hepatocytes to the effects of insulin. Adiponectin also acts on FA

metabolism in the liver which has secondary effects on circulating levels of TAG and NEFA. Even moderate overproduction of adiponectin in transgenic mice leads to substantial protection from hepatic steatosis in obesity (Kim *et al*., 2007; Asterholm and Scherer, 2010). AMPK activation, downstream from the adiponectin receptor has been recognised as a mechanism of adiponectin action in the liver. Adipocytes are also known to express adiponectin receptors and therefore adiponectin is able to act locally in an autocrine or paracrine fashion to influence adipose tissue function. One of adiponectin's most prominent affects in adipose tissue is seen when the adiponectin gene is overexpressed in the *ob/ob* mouse. This mouse model displays greater adiposity than the *ob/ob* mouse with the excess weight accounted for by greater subcutaneous fat mass. The adipose tissue of these mice is composed of a larger number of adipocytes with a significantly lower average cell size compared to lipid engorged *ob/ob* adipocytes. On top of this, mRNA levels of several key genes involved in TAG formation including *Pparγ* target genes upregulated in WAT of these mice, suggesting improved, safer lipid storage in adipose tissue (Kim *et al*., 2007).

In addition to adiponectin having effects on metabolism, it is also associated with inflammation. The absence of adiponectin leads to high levels of proinflammatory cytokine TNF-α in adipose tissue and serum which can be reduced upon adiponectin supplementation (Maeda *et al*., 2002). Adiponectin can also inhibit phagocytosis and LPS induced TNF-α expression in macrophages (Yokota *et al*., 2000). As well as reducing expression of proinflammatory cytokines, adiponectin also induces the expression of IL-10, an anti-inflammatory cytokine, in human macrophages (Kumada *et al*., 2004). Beyond suppressing local inflammation in adipose tissue, adiponectin has systemic anti-inflammatory effects which may impact global insulin sensitivity. Adiponectin polarises a wide-variety of tissue macrophages towards an anti-inflammatory M2 phenotype. Importantly, this includes effects on suppressing macrophage transformation into lipid-ladened foam cells in atherosclerotic plaque (Ouchi *et al*., 2001).

1.20.3 Other adipokines

There are also numerous other adipokines secreted from adipose tissue. Resistin is solely expressed in adipose tissue in mice (Steppan *et al*., 2001). However, in humans it is mostly expressed in macrophages and monocytes (Savage *et al*., 2001). Levels of resistin in serum correlate with increased obesity in both diet-induced and genetically obese mouse models. Resistin impairs the actions of insulin and glucose tolerance. Treatment with TZDs such as

rosiglitazone, which reduces expression of the resistin gene, restores glucose tolerance in these models (Steppan *et al*., 2001) whereas proinflammatory cytokines, for example TNF-α induce the expression of the gene (Kaser *et al*., 2003). Plasminogen activator inhibitor-1 (PAI-1) is an inhibitor of fibrinolysis which is produced in adipose tissue by adipocytes, preadipocytes, fibroblasts and immune cells. Its levels of expression are increased with an increase in weight gain (Mertens and Van Gaal, 2002). PAI-1 deficient mice have reduced weight gain and improved insulin sensitivity when on HFD (Ma *et al*., 2004).

1.21 Pathophysiology of obesity

Obesity is a complex multifactorial and heterogeneous disease. Weight gain is a normal physiological response to positive energy balance, yet if the imbalance persists, obesity results. Many factors contribute to the etiology of obesity, including genetic susceptibility, nutrition, physical activity and environment. Energy storage in the form of fat is an important adaptation for survival and therefore it is likely like a combination of genes have been selected during evolution to favour energy storage. In modern society however, increased food availability and decreased physical activity has resulted in these genes conferring susceptibility to the development of obesity and its maintenance. The involvement of genetic factors in the regulation of body weight has been indicated by studies of monozygotic twins showing a high concordance of body composition and response to overfeeding (Barsh *et al*., 2000). However, monogenic causes of obesity account for only a small fraction of obese individuals. Obesity, or perhaps more accurately, increased susceptibility to obesity is likely to be polygenic, with numerous modifier genes contributing the development of the disease. In addition to the fact that genetic factors can modulate nutrient storage, nutrients are also able to modulate gene expression (Foufelle and Ferré, 2002) and therefore obesity results from complex genetic and environmental interactions.

Nonetheless, a number of monogenic causes of obesity have been identified. Obesity has also been associated with >25 genetic syndromes, such as Prader-Willi and Bardet-Biedl. In human patients, homozygous carriers of a loss-of-function mutation in the leptin gene exhibit early onset morbid obesity and central hypothyroidism (Barsh *et al*., 2000). People affected by this mutation exhibit severe hyperphagia. Daily subcutaneous injection of recombinant human leptin for a year in patients homozygous for this mutation leads to sustained fat mass loss (Barsh *et al*., 2000). Mutations in the leptin receptor have also been discovered, which

abolishes leptin signalling and results in a phenotype similar to that of individuals with leptin deficiency (Rankinen *et al*., 2002).

Homozygous or compound heterozygous loss-of-function mutations in the POMC gene results in a phenotype including obesity and adrenal insufficiency reflecting the lack of POMC derived peptides α-MSH and adrenocorticotropic hormone (ACTH) (Krude and Gruters, 2000). Mutations of MC4R cause dominant and recessive inherited non-syndromic obesity, however the mutation is not always associated with obesity and a similar mutation can yield various degrees of obesity *(*Vaisse *et al.,* 2000*).* Human obesity caused by MC4R mutations has an early age of onset, with excessive hunger and food seeking behaviour (Rankinen *et al*., 2001).

Most of the genes involved in monogenic forms of obesity are involved in the regulation of food intake; however, in the most common (polygenic) forms of obesity, genes involved in numerous pathways, from nutrient absorption to energy expenditure play a role. Linkage studies, candidate gene association studies and genome-wide association studies (GWAS) have revealed a number of obesity related genes. The first *loci* identified through GWAS was the fat mass and obesity-associated (*FTO*) gene (Frayling *et al*., 2007), and now more than 50 genetic *loci* have been identified. Unsurprisingly, linkage and GWAS studies have provided evidence for the leptin gene locus in the development of obesity and its related phenotypes. For example, one gene variant adjacent to sequences involved in the leptin gene transcription, was shown to modulate the response to caloric restriction in severely obese women and homozygous obese girls carrying this variant allele had a 25% decrease in leptin levels despite a similar body fat mass (Le Stunff *et al*., 2000). Studies have also revealed candidate adiposity genes in the regulation of metabolism. In a study of early onset obesity, the effect of variants in the insulin gene amongst a large cohort of obese children was analysed. This study demonstrated that a specific allelic combination induces higher insulin secretion and a higher risk of developing juvenile obesity (Le Stunff *et al*., 2000).

1.22 Adipose Tissue Expansion

In response to over-nutrition, energy harvested in fatty acids either directly from the diet or via *de novo* lipogenesis is esterified into TAG and stored in large part within adipocyte lipid droplets. In a state of chronic positive energy balance this can lead to the dramatic adipocyte hypertrophy and expansion of adipose tissue bed (Sturley and Hussain, 2012). Adipocyte-specific proteins, such as perilipin, which coats lipid droplets in adipocytes acting as a protective coating from the body's natural lipases, are important for the metabolic flexibility of

adipocyte lipid storage and metabolism (Brasaemle *et al*., 2004; Digel *et al*., 2010). Fat specific protein 27 (FSP27/Cidec) is a lipid droplet-associated protein almost exclusively expressed in adipocytes where it facilitates unilocular lipid droplet formation (Puri *al*., 2007). Perilipin serves as an fsp27 activator, increasing FSP27-mediated lipid exchange, lipid transfer and droplet growth (Sun *et al.,* 2013*).* The dual role of perilipin in the regulation of adipose tissue lipolysis and lipid droplet expansion highlights the importance of lipid droplet proteins in the maintenance and regulation of adipocyte metabolism. Mice with adipocyte specific deletion of the *Fsp27* gene have impaired lipid storage capacity as indicated by small adipocyte size, resistance to weight gain upon HFD feeding, hepatic steatosis, dyslipidaemia and systemic insulin resistance (Tanaka *et al*., 2015). This supports the hypothesis that expansion of the lipid droplet and therefore WAT can be protective against the metabolic abnormalities associated with excess caloric intake. Further studies which have demonstrated the ability of adipocytes to expand the lipid droplet while maintaining insulin sensitivity further supports this protective, adaptive role (Kusminski *et al*., 2012). Expanding fat mass requires increased adipocyte size (hypertrophy) or increased adipocyte number (hyperplasia). Hypertrophy occurs prior to hyperplasia to meet the need for additional fat storage capacity in the progression of obesity. However, large hypertrophic adipocytes face limits of expansion based on multiple factors such as hypoxia, adipocyte cell death, enhanced chemokine secretion, and dysregulation in fatty acid fluxe that result in dysfunctional adipocytes (Halberg *et al*., 2009). Mature adipocytes are terminally differentiated cells. However, adipocyte precursors have been identified in adipose tissue that differentiate into fully mature white adipocytes under metabolic stimulation or PPARγ activation, both *in vitro* and *in vivo* (Rodeheffer *et al*, 2008; Tang *et al*., 2008, Gupta *et al*., 2012). Adipocyte hyperplasia may present a mechanism for "healthy" fat storage capacity, due to maintenance of insulin sensitivity. Adiponectin over-expressing mice display enhanced clearance of circulating fatty acids and increased expansion of subcutaneous adipose tissue with chronic HFD feeding. These adaptive changes to the HFD were associated with increased mitochondrial density in adipocytes, smaller adipocyte size and a general transcriptional upregulation of factors involved in lipid storage through efficient esterification of free fatty acids. Increased levels on adiponectin potently protect against HFD-induced hepatic lipid accumulation and preserve insulin sensitivity (Asterholm and Scherer, 2010).

1.23 Adipose tissue inflammation

Adipose tissue expansion is also associated with an increased accumulation of macrophages. Macrophages are important in the development of adipose tissue inflammation. (Weisberg *et al.*, 2003). In addition to an increased accumulation of macrophages, obese mice are also shown to switch the state of adipose tissue macrophages from M2 seen in lean mice to M1 macrophages which secrete pro-inflammatory cytokines (Lumeng *et al.* 2007). M1 macrophages accumulate around necrotic adipocytes forming 'crown-like structures' and releasing proinflammatory cytokines such as IL-6 and TNF-α (Lumeng *et al.* 2007). In addition to macrophages, other immune cells found in adipose are also affected by obesity. Eosinophils normally mediate activation of M2 macrophages. However, during obesity, numbers of eosinophils decline. Mice lacking eosinophils have increased M1 macrophage activation suggesting that this decline in eosinophils could contribute to obesity-induced inflammation (Wu *et al.* 2011). T regulatory cell (Treg) numbers also decline in obesity. These cells normally provide immunological tolerance and are abundantly expressed in lean adipose tissue. Reducing WAT Treg numbers leads to a worsening of inflammation (Feuerer *et al.* 2009). In addition to inflammatory cells, cytokine expression levels also alter in obesity. TNF-α and IL-6 are the most common cytokines released from adipose tissue. Levels of TNF-α and IL-6 are elevated in obese humans with the levels declining upon weight loss (Kern *et al.* 1995; Fried *et al*. 1998). An increase in secretion of TNF-α is also seen in animal models of obesity and diabetes (Hotamisligil *et al.* 1993). In addition to their inflammatory roles, IL-6 and TNF-α inhibit lipoprotein lipase, reducing lipogenesis, and TNF-α also stimulates lipolysis which could contribute to metabolic dysfunction (Kern *et al*. 2001).

1.24 Insulin resistance in obesity

Insulin resistance is a common metabolic consequence of obesity and this manifests itself as hyperinsulinemia in the presence of hyperglycaemia and dyslipidaemia. In obesity, the production of NEFAs, glycerol, hormones such as leptin and adiponectin and inflammatory cytokines such as TNFα and IL-6. The production of retinol-binding protein 4 (RBP4), the sole retinol transporter in blood which is secreted from adipocytes and liver is also increased in obesity. This induces insulin resistance through reduced phosphatidylinositol-3-OH kinase (PI(3)K) signalling in muscle and enhanced expression of the gluconeogenic enzyme phosphoenolpyruvate carboxykinase in the liver through a retinol-dependent mechanism (Yang *et al*., 2005). In addition to adipocyte-derived factors, increased release of TNF-α IL-6, monocyte chemoattractant protein-1 (MCP-1) and additional products of macrophages and other cells that populate adipose tissue might also have a role in the development of insulin

resistance (Wellen and Hotamisligil, 2005). TNF-α and IL-6 act through classical receptor-mediated processes to stimulate both the c-Jun amino-terminal kinase (JNK) and the IκB kinase-β/nuclear factor-κB pathways, resulting in upregulation of potential mediators of inflammation that can lead to insulin resistance. Pathways involving the induction of suppression of cytokine signalling proteins (Mooney *et al*., 2001) and inducible nitric oxide synthase (iNOS) (Perreault and Marette, 2001) may be involved in mediating cytokine-induced insulin resistance. Secretion of these proinflammatory proteins, particularly MCP-1 by adipocytes, endothelial cells and monocytes, increases macrophage recruitment and thereby contributes to a feedforward process.

The release of NEFAs may be the single most critical factor in modulating insulin sensitivity. Insulin resistance develops within hours of an acute increase in plasma NEFA levels in humans (Roden *et al*, 1996). Conversely, insulin mediated glucose uptake and glucose tolerance improves with an acute decrease in NEFA levels and treatment with an antilipolytic agent (Santomauro *et al*., 1999). Increased intracellular NEFAs might result in competition with glucose for substrate oxidation leading to the serial inhibition of pyruvate dehydrogenase, phosphofructokinase and hexokinase II activity (Hue and Taegtmeyer, 2009). It has also been proposed that increased NEFA delivery or decreased intracellular metabolism of fatty acids results in an increase in the intracellular content of fatty acid metabolites such as DAG and fatty acid acyl-CoA and ceramides, which in turn activate a serine/threonine kinase cascade leading to serine/threonine phosphorylation of insulin receptor substrates 1 and 2 and a reduced ability of these molecules to activate PI(3)K (Shulman, 2000). Subsequently, events downstream of insulin receptor signalling are diminished. Distribution of body fat itself is a critical determinant of insulin sensitivity. Intra-abdominal fat expresses more genes encoding secretory proteins and proteins responsible for energy production (Maeda *et al*, 1997). The delivery of NEFAs to the tissues might also be modulated by their source. Intra-abdominal fat is more lipolytic than subcutaneous fat and is also less sensitive to the antilipolytic effect of insulin (Montague and O'Rahilly, 2000).

Through Akt-mediated phosphorylation and activation of phosphodiesterase 3B, which controls intracellular cAMP pools, insulin exerts its antilipolytic effects by inactivating cAMP, preventing phosphorylation and this activation of ATGL and HSL (Choi *et al*., 2010). In systemic insulin resistance, in the absence of these downstream effects, upregulated adipose tissue lipolysis is permitted, resulting in ectopic deposition of lipid in non-adipose tissues (Choi *et al*., 2010). Dysregulated adipocyte lipolysis has been implicated as the primary source of NEFA flux

to the liver, which promotes non-alcoholic fatty liver disease and hepatic insulin resistance, leading to impairment of insulin actions to inhibit gluconeogenesis (Samuel *et al*., 2004). A variety of studies however have shown that obesity-related insulin resistance, hepatic steatosis and systemic inflammation can be prevented by manipulating energy metabolism in the adipocyte to drive lipid droplet expansion. This prevents excessive lipolysis and therefore ectopic lipid deposition and lipotoxicity in other cell types. Overexpression of PEPCK in adipose tissue leads to obesity without associated insulin resistance in the mouse by increased G3P substrate for re-esterification, therefore reducing NEFA release and increasing adipocyte TAG storage (Franckhauser *et al*., 2002; Tordjman *et al*., 2003). However, despite advantages of an expanding adipocyte, too much lipid in the cell results in reactive oxygen species (ROS) generation and leads to ER stress and increased lipid spillover, i.e. ectopic distribution (Koves *et al*., 2008; Gao *et al*., 2010).

1.25 Endoplasmic Reticulum (ER) stress

The ER plays an important role in protein and lipid synthesis and its dysfunction has been linked to disrupted cellular metabolism and local and systemic insulin resistance (Koves *et al*., 2008). Induction of ER stress, the accumulation of misfolded and unfolded proteins in the ER lumen, activates PKA and results in increased lipolysis through Plin1 phosphorylation (Deng *et al*., 2012), a potential mechanism for increased NEFA release and systemic lipotoxicity. ER stress also reduces adipocyte insulin sensitivity (Xu *et al*., 2010) and regulates adiponectin oligomerization, resulting in a decrease in high molecular weight forms of adiponectin (Huh *et al*., 2012). As the relative abundance of adiponectin high-molecular weight oligomers is better correlated with overall systemic insulin sensitivity that total adiponectin levels, this suggests a potential pathway by which adipocyte metabolic stress is communicated to other insulin sensitive tissues.

1.26 Hypoxia in fat expansion

As the adipocyte expands, adipose tissue interstitial oxygen tension decreases. HIFI1α is a transcription factor that serves as an oxygen sensor in many cell types. Under normoxic conditions, HIFI1α is rapidly degraded; however, hypoxic conditions stabilize HIFI1α and permit upregulation of genes containing HIF response elements (Nallamshetty *et al*., 2013). HIFIα protein is highly enriched in expanding adipocytes due to the need for increased adipose tissue vascularisation. In hypoxic conditions decreased oxygen availability shifts energy production to

increased dependence on glycolysis, which in turn increases local fatty acid concentrations which results in uncoupled respiration and therefore further increase oxygen consumption (Lee *et al*., 2014). Although HIFI1α induction enhances cell survival during hypoxia and facilitates increased tissue vascularization, its induction in hypertrophic adipose may not be entirely beneficial. For example, direct inhibition of HIFI1α improves adipose tissue health by supressing fibrosis and reducing local inflammation in WAT, and overexpression of HIFI1α in the adipocyte proved to be more pro-fibrotic and pro-inflammatory than pro-angiogenic (Halberg *et al*., 2009; Sun *et al*., 2013). The degree to which hypoxia in adipose tissue may be directly proportional to adipocyte size. Leptin secretion increases with adipocyte size and leptin is a direct HIFI1α transcriptional target (Sun *et al*., 2013). Therefore, local adipocyte hypoxia plays a signalling role for assessing systemic energy reserves and may be translated into altered leptin levels.

1.27 PPAR regulation in obesity

PPARs are involved in the regulation of energy homeostasis and inflammation and therefore represent important targets for obesity and metabolic syndrome. Currently synthetic PPAR agonists are widely used for treatment of insulin resistance and metabolic syndrome. In mice fed HFD, proper function of PPARα is essential to prevent the liver from storing large amounts of fat (Patsouris *et al*., 2006). By inducing mitochondrial, peroxisomal and microsomal FA oxidation, PPARα reduces hepatic fat accumulation in the liver during the development of fatty liver disease and therefore prevents steatosis (Ip *et al*., 2004). Although expression of PPARα expression in WAT is of relatively low abundance it has been shown that PPARα$^{-/-}$ mice gain more adipose mass compared to WT animals (Costet *et al*., 1998). An anti-obesity role for PPARα is also supported by several studies in which obese rodents were administered synthetic PPARα agonists (Guerre-Millo *et al*., 2000; Mancini *et al*., 2001; Vazquez *et al*., 2001). Although the anorexic effect of PPARα is due to decreased food intake, PPARα may also directly influence adipose tissue function. A study revealed that treatment of obese diabetic KKA$_{\gamma}$ mice administered with PPARα agonist (Wy-14643) decreased adipocyte hypertrophy as well as macrophage infiltration (Tsuchida *et al*., 2005). In PPARα$^{-/-}$ mice chronically fed with HFD, expression of inflammatory genes in adipose tissue is more pronounced than WT mice. Several abnormalities have been observed in mice lacing PPARβ/δ, for example decreased adipose tissue mass (Barish *et al*., 2006). PPARβ/δ has been directly linked to the development of obesity – decrease in adiposity is observed after PPARβ/δ activation. By stimulating fatty acid oxidation, PPARβ/δ activation leads to loss of adipose mass in different mouse models of

obesity (Wang *et al*., 2003). As previously mentioned, PPARγ is vital for adipogenesis and lipogenesis. Unsaturated fatty acids and several eicosanoids serve as endogenous agonists for PPARγ while antidiabetic drugs belonging to the TZD class act as synthetic agonists. Diet induced obesity is associated with increased inflammatory gene expression in adipose tissue via adipocyte hypertrophy and macrophage infiltration. It has been demonstrated that PPARγ is able to reverse macrophage infiltration and subsequently reduce inflammatory gene expression (Xu *et al*., 2003). Treatment of obese rats with the synthetic PPARγ agonist troglitazone dramatically reduced the size of adipocytes without changing the total weight of WAT. In parallel, the expression levels of the inflammatory marker TNFα were normalised compared to those of untreated rats (Okuno *et al*., 1998).

Disorders of lipid and lipoprotein metabolism and transport are responsible for the development of a large spectrum of pathologies, ranging from cardiovascular diseases to metabolic syndrome. Recently, increased knowledge of the molecular mechanisms that control our biological clock and circadian rhythms has been gained and from these studies is has clearly emerged how the molecular clock tightly regulates every aspect of our lives, including metabolism. PPARs, which clearly play essential roles in energy metabolism, are a prime example of this connection, as all PPAR isoforms have been found to be expressed rhythmically in given mouse tissues. PPARα and PPARγ have also been shown to be direct regulators of core clock genes, and PPARα is a direct target of the molecular clock. On top of this, PPARs have been shown to exert their functions in a circadian manner, further supporting that the clock and energy homeostasis are intertwined (Chen and Yang, 2014).

1.28 Circadian clocks

Circadian clocks, which are self-sustained biological oscillators with a period of approximately 24 hours. Having a robust internal timing system allows an organism to anticipate regular fluctuations in the environment (e.g. daylight, food availability) and adapt their physiology and behaviour appropriately. The word circadian is derived from the Latin *circa diem* which means “approximately a day”. Entrainment is the synchronization of endogenous oscillations to external cycles. The most predominant entrainment stimulus or zeitgeber (time giver) of the circadian clock is the external light environment (Reppert and Weaver, 2001). However, other external cues can also entrain the clock, such as food intake, temperature and physical activity. However, in the absence of environmental cues these 24 hour rhythms are maintained.

1.28.1 The Master Clock

The master clock in mammals, resides within the suprachiasmatic nucleus (SCN) of the anterior hypothalamus. The SCN is a bilateral structure and individual neurons within the SCN function as autonomous single cell oscillators which are tightly coupled with each other to produce a single SCN output (Welsh *et al*., 1995; Aton *et al.,* 2005). The importance of the SCN as a master clock is clear from lesioning studies in hamsters or rats in which the SCN was destroyed (Lehman *et al*., 1987). These lesioning experiments showed that the SCN was important for the rhythmicity of corticosterone secretion and locomotor activity as lesioning the SCN resulted in arrhythmia (Moore and Eichler, 1972, Stephan and Zucker, 1972). Impressively, transplantation of fetal SCN tissue into previously lesioned hamsters restored circadian locomotor activity (Lehman *et al*., 1987). Similarly, SCN grafts from wild-type mice could restore circadian rhythmicity in genetically arrhythmic mice (Sujino *et al*., 2003). When the SCN neurons were cultured *in vitro* they showed a circadian pattern in electrical activity (Green and Gilette, 1982; Groos and Hendriks, 1982; Shibata *et al.,* 1982), even after 3 weeks of culture. Furthermore, metabolic activity and glucose uptake in the SCN (Schwartz and Gainer, 1977), as well as clock gene (Sun *et al*., 1997; Tei *et al*., 1997) and protein expression (Hastings *et al*., 1999) exhibit a robust daily cycle which persist in absence of environmental cues.

The SCN synchronises physiology to environmental changes. The activity of the SCN is strongly influenced by three major input pathways, the retinohypothalamic tract (RHT), the geniculohypothalamic tract (GHT) and serotonergic (5HT) input from the dorsal raphe nucleus (DRN) and median raphe nucleus (MRN). The RHT mediates photic information and the major neurotransmitter of the RHT is glutamate. Two peptides present in the RHT, substance P and pituitary adenylate cyclase-activating peptide modulate the entrainment process.

The SCN synchronises physiology to environmental changes. Lighting information is conveyed to the SCN by several convergent pathways (Morin, 1994). The major light input pathway to the SCN is the retinohypothalamic tract (RHT), which arises from a widely distributed population of retinal ganglion cells (Moore *et al*., 1995). The major neurotransmitter of the RHT is glutamate. Two peptides present in the RHT, substance P and pituitary adenylate cyclase-activating peptide, modulate the entrainment process. Two indirect pathways provide retinal input to the SCN. The first is from the intergeniculate leaflet of the lateral geniculate nucleus, which receives input from the same retinal cells whose axons compose the RHT (Pickard, 1985). A

geniculohypothalamic tract, rich in γ-aminobutyric acid (GABA), neuropeptide Y, and encephalin converges on the retinorecipient region of the SCN (Morin, 1994). The second indirect pathway from the retina to the retinorecipient SCN is routed via the serotonergic raphe nuclei. Transmitters in both the intergeniculate leaflet and raphe pathways appear to play a role in mediating non-photic phase shifts, such as those caused by behavioural arousal (Byku and Gannon, 2000; Mistlberger *et al*., 2000). Finally, neurohumoral signals reach the SCN. The pineal hormone, melatonin, can subtly influence circadian rhythms in adult mammals, but it has a dramatic impact during development (Viswanathan and Davis, 1997; Weaver, 1999). MT1 melatonin receptor activation inhibits firing of SCN neurons, whereas both MT1 and MT2 receptors appear capable of mediating phase shifts (Liu *et al*., 1997). Signal transduction pathways activated by the glutamate receptor are mediated by the release of intracellular calcium via ryanodine receptors (Ding *et al*., 1998). The downstream actions of calcium likely include activation of calcium/calmodulin, MAP kinase, and other kinases. Subsequent phosphorylation of CREB results in its binding to cAMP response elements located in the promoters of target genes, i.e. clock genes, activating their transcription (Grewal *et al*., 1999).

To function as a pacemaker and synchronizer for other brain and peripheral clocks, the intrinsic time-keeping signal from the SCN has to be transmitted. SCN efferents terminate in many areas of the brain including regions of the hypothalamus, such as the subparaventricular zone and dorsomedial nucleus and thalamic regions such as the paraventricular nucleus, as well as many others (Saper *et al*., 2005; Leak and Moore, 2001). Ultrastructural studies have shown that around 30% of SCN axons contain both GABA and peptide neurotransmitters such as vasoactive intestinal peptide and arginine-vasopressin (Buijs *et al*., 1995; Castel and Morris, 2000), and electrophysiological studies have shown that glutamate, along with many other molecules is an SCN transmitter, converging circadian signals to hypothalamic target structures (Kalsbeek *et al*., 1996). Transplantation experiments of SCN tissue make evident that projections from SCN neurons are not required for the establishment of locomotor activity rhythms and therefore paracrine factors released from the SCN can act to coordinate the expression of rhythms in wheel running activity (Maywood *et al*., 2011). However, SCN grafts do not restore rhythms in the neuroendocrine axis, implying that SCN efferents control hormone rhythms such as melatonin and corticosterone (Meyer-Bernstein and Morin, 1999) and therefore the autonomic nervous system plays a major role. Studies indicate that apart from the classical neuroendocrine control of the adrenal cortex by the PVN-CRH-ACTH cascade the autonomic projections of the SCN via the PVN to the intermediolateral column of the

spinal cord determine daily changes in sensitivity of the adrenal gland to ACTH (Kalsbeek *et al*., 1996; Buijs *et al*., 1999). Light activates the murine adrenal gland and effects gene expression via the autonomic nervous system (Cailotto *et al*., 2009). The SCN therefore affects not only hormone secretion but modulates sensitivity of target organs of these hormones by neuronal mechanisms.

Despite the predominance of the master SCN clock in dictating circadian rhythms, it is now known that circadian clocks exist in other regions of the brain as well almost all cells and tissues of the periphery. Extra-SCN regions of the brain, such as the dorsomedial hypothalamus show circadian clock gene expression. However, when these regions are isolated from the SCN, rhythms in these extra-SCN cells persist for only a short period of time, indicating that the SCN is necessary for their synchronisation (Inouye and Kawamura, 1979; Guilding and Piggins, 2007). Cultured cells and tissue explants from a wide variety of peripheral organs, for example liver, lung, kidney, skeletal muscle and adipose tissue exhibit robust circadian oscillations in gene expression (Balsalobre *et* al., 1998; Yamazaki *et al*., 2000; Yamamoto *et al*., 2004; Yoo *et al*., 2004; Yamazaki *et al*., 2009). The circadian clocks in peripheral tissues are also synchronised to the external light environment via the SCN (Yamazaki *et al*., 2000).

1.28.2 Peripheral Clocks

In peripheral organs a large number of key physiological functions are subject to daily oscillations, such as carbohydrate and lipid metabolism by the liver, muscle and adipose tissue, as well as parameters of the cardiovascular system such as blood pressure and heart rate (Gachon *et* al., 2004; Lamia *et* al., 2008; Le Martelot *et* al., 2009). These peripheral functions can be coordinated by systemic cues originating at the SCN, such as neuronal signals and circulating hormones or metabolites, or by local peripheral oscillators synchronized by the SCN (Gachon *et* al., 2004; Stratmann and Schibler, 2006; Kornmann *et* al., 2007). Genome wide transcriptome profiling studies performed on a variety of tissues such as liver, heart and adrenal gland suggest that many cellular functions are subject to circadian regulation and between 2-10% of all transcribed genes in a given tissue are rhythmically expressed (Akhtar *et al*., 2002; Duffield *et al*., 2002; Oishi *et al.,* 2005; Hughes *et al*., 2009). Many genes that show circadian variation in the liver encode key enzymes involved in metabolic pathways, energy homeostasis and food processing (Gachon *et al*., 2006). Oscillation in peripheral gene expression allows for the limitation of metabolic processes to when they are needed. For example, simultaneously high expression of glycogen synthase and glycogen phosphorylase

would not be conducive to the conversion of glucose into glycogen and vice versa and therefore antiphasic expression of these genes is necessary (Ishikawa and Shimazu, 1980). Furthermore, mRNA synthesis has a high energy cost and cycling genes are expressed at high levels and constitute the most costly proteins to synthesise in the genome. For this reason, rhythmic gene expression optimises the metabolic cost of global gene expression and may therefore be a way in which energy is conserved (Wang *et al*., 2015).

It has been shown both *in vitro* and *in vitro* that if the SCN is ablated, oscillations in these organs still persist (Yoo *et al*, 2004; Gerber *et al*., 2015). Circadian timekeepers in liver and lung can generate around 20 cycles of *Per2*-luciferase expression when isolated in culture (Yoo *et al*., 2004). However, in SCN-lesioned animals, phase desynchrony within the tissues develops (Yoo *et al*., 2004). It has also been shown that the SCN is required to maintain the synchronisation of phase between hepatocytes of the same liver and hence peripheral oscillators do not appear to be highly coupled (unlike the SCN) (Guo *et al*., 2006).

The SCN uses many routes to establish phase coherence in the periphery. Feeding rhythms are strong Zeitgebers for many tissues (Damiola *et* al., 2000; Yamazaki *et* al., 2000). Restricted feeding studies, whereby food is only available to the animal for a set period of time outside of their normal activity period can uncouple the peripheral clocks from the SCN, whereby peripheral clocks entrain to mealtime whilst the SCN remains entrained to the external light environment (Damiola *et al*., 2000). Food entrainment is demonstrated by food anticipatory activity, such as increased body temperature and locomotor activity, in animals in the hours prior to the expected meal time (Stephan, 2002). In addition to a shift in behaviour, the phase of the clock in peripheral organs involved in metabolism, such as the liver, shifts to the entrained mealtime whereas the SCN remains entrained to the light environment (Stokkan *et al*., 2001). However, when returned to an ad libitum diet, entrainment to the restricted feeding schedule is lost (Mistlberger, 1994). The entrainment pathways from feeding-fasting cycles may include hormones secreted upon feeding and fasting, e.g. CCK, ghrelin and leptin (Konturek *et al*., 2004), food metabolites e.g. glucose and fatty acids and intracellular redox state (Schibler, 2009). Peripheral clocks are also synchronized by more direct signals, such as neural and humoral outputs. For example, glucocorticoid hormones possess clock-resetting properties and are an important phase-entrainment signal from the SCN. Plasma glucocorticoid hormones levels exhibit daily circadian variation in both laboratory rodents and humans and these cycles are driven by the SCN via the hypothalamic-pituitary-adrenal (HPA) axis (Basalobre *et al.,* 2000; Oster *et* al., 2006).

The autonomic nervous system also constitutes a direct synchronisation pathway utilised by the SCN and plays a role in the resetting of peripheral clocks after phase shift-inducing light exposure (Cailotto *et al*., 2009). It was shown by surgically disrupting liver innervation that light affects liver gene expression not only via the hormonal pathway but also via the autonomic pathway (Cailotto *et al*., 2009). It has also been shown that adrenal innervation is required for light-induced corticosterone secretion by the adrenal gland, thus representing a direct output from the SCN to the adrenal cortex.

1.28.3 Molecular clock

The circadian clock mechanism involves interlocking transcriptional-translational feedback loops built upon a core set of genes (Figure 1.7). This core set of genes is highly conserved among animals (Bell-Pedersen *et al*., 2005). The following genes make up the core circadian feedback loop in mammals: *Bmal1* (brain and muscle aryl hydrocarbon receptor nuclear translocator (ARNT)-like), *Clock* (circadian locomotor output cycles kaput), *Per1* (period homologue 1), *Per2*, *Per3, Cry1* (Cryptochrome 1), *Cry2* and *Npas2* (Neuronal PAS domain-containing protein 2). In the daytime, *Clock*, a basic helix-loop-helix (bHLH) transcription factor heterodimerises with *Bmal1* to initiate the transcription of the target genes containing E-box cis-regulatory enhancer sequences, including *Per* and *Cry* genes. PER and CRY proteins form oligomers that are transported from the cytoplasm to the nucleus. When located in the nucleus, CRY and PER repress their own transcription by inhibiting CLOCK/BMAL1 activity (Lee *et al*., 2001). As the PER:CRY repressor complex subsequently degrades through ubiquitin dependant pathways, the repression is lifted and a new cycle of transcription by the CLOCK-BMAL1 heterodimer is initiated with a 24 hour periodicity. Casein kinase 1δ/ε (CK1δ, CK1ε) play an important role in determining the intrinsic period of the clock by controlling the rate at which the PER:CRY complexes are either degraded or enter the nucleus. Their activity is opposed by the phosphates PP1 and PP5 respectively (Partch *et al*., 2006; Lee *et al*., 2011). The entire cycle takes close to 24 hours to be completed. In addition to the primary feedback loop, the CLOCK:BMAL1 heterodimer also activates the transcription of *Rev-erbα/β* and *RORα/β/γ* which are retinoic acid-related orphan nuclear receptors (NRs). REV-ERBα and RORα compete to bind to the BMAL1 promotor through interaction with retinoic acid-related orphan receptor elements (ROREs). It has been previously shown that both isoforms of ROR (β and γ) and REV-ERB (α and β) are able to regulate BMAL1 through RORE site binding (Guillaumond *et al*., 2005). RORs and REV-ERBs activate and repress the transcription of *Bmal1* respectively (Preitner *et al*., 2002; Sato *et al*., 2004) resulting in rhythmic changes in *Bmal1* transcription,

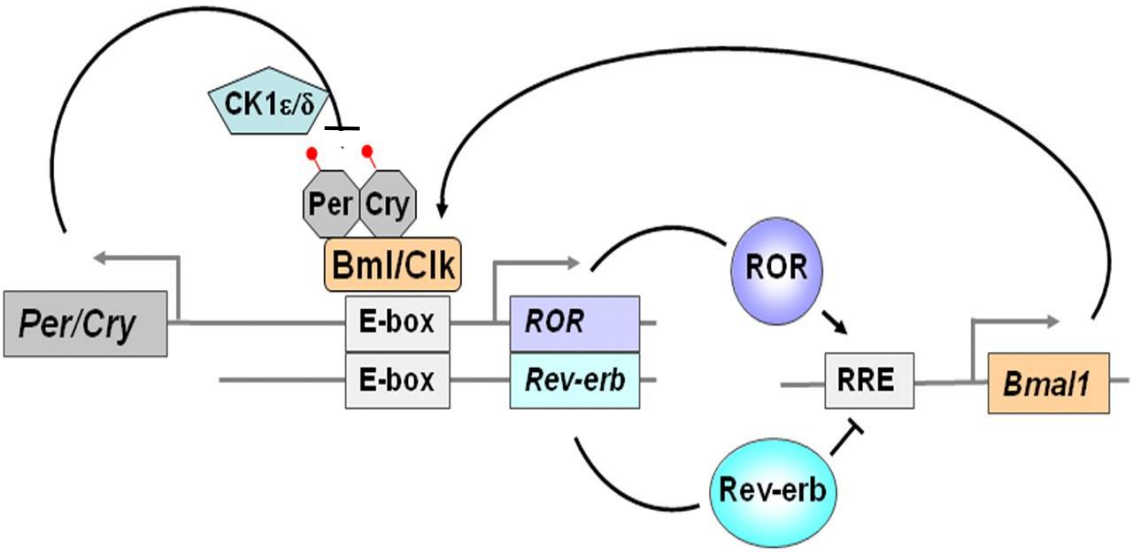

Figure 1.7 – Schematic representation of the transcriptional feedback loops of the circadian clock.

The positive feedback loop is regulated by the BMAL1:CLOCK complex and ROR which activates the expression of *Bmal1*. In this loop REV-ERB is responsible for repressing *Bmal1* transcription. The positive loop is also opposed by the repressor feedback loop which involves the proteins PER and CRY. Abbreviations: Bmal1, aryl hydrocarbon receptor nuclear translator-like protein 1; Clock, circadian locomotor output cycles kaput; CK1, casein kinase 1; E-box, enhancer box; Per, Period; ROR, retinoic acid receptor related orphan receptor; RRE, Rev-erbα/ROR-A response elements.

introducing a delay in *Cry1* mRNA expression that offsets it from genes regulated strictly by CLOCK:BMAL1 (Ukai-Tadenuma *et* al., 2011). This secondary loop is thought to strengthen the molecular clock and the presence of cooperative, interlocking feedback loops provides robustness against noise and environmental perturbations to help maintain accurate circadian timing (Brown *et al*., 2012). Until recently, it was believed that *Rev-erbα* and *Rev-erbβ* were auxiliary regulatory components of the clock mechanism, and not essential clock components. However, when both *Rev-erbα* and *Rev-erbβ* are deleted, arrhythmic expression of *Bmal1* and *Cry1* is observed in vitro, and *in vivo*, mice demonstrate disrupted wheel running behaviour; thus demonstrating that REV-ERB signalling is a vital component of the molecular clock (Cho *et al*., 2012; Bugge *et al*., 2012). Other feedback loops involve the proline and acidic amino acid-rich basic leucine zipper family members, albumin D-box binding protein (DBP), hepatic leukaemia factor (HLF) and thyrotroph embryonic factor (TEF); the bZip protein, Nuclear factor interleukin 3 regulated, and the bHLH proteins - deleted in oesophageal cancer 1 and 2 (DEC1 and DEC2/*Bhlhb2*, *Bhlhb3*), all of which are transcriptional targets of CLOCK-BMAL1 (Lowrey and Takahashi, 2004; Gachon 2007).

Other NRs and coactivators have been suggested to modulate the actions of BMAL1 and CLOCK, examples of which include the PPARs and PPARγ-coactivator 1α (PGC-1α). The *Bmal1* promotor contains PPAR-response elements and by binding to these PPARα is able to influence both the activity and expression of BMAL1 and CLOCK (Inoue *et al*., 2005). *Rev-erbα* also contains the PPAR-response element, and PPARα binding has been shown to increase expression of *Rev-erbα.* PGC-1α acts on the clock by a different mechanism, inducing transcription of *Bmal1* and *Rev-erbα* through co-activation of RORα (Liu *et al*., 2007).

1.29 Clock control

Simple autoregulatory feedback loops can lead to oscillations with periods as short as a few hours and therefore mechanisms need to be in place to observe periods of around 24 hours. The balance between synthesis and degradation of mRNA is key to the generation of circadian rhythms (Shu and Hong-Hui, 2004). For example, the analysis of mice with a *Per1*-luciferase transgene and the analysis of *Per1* mRNA 3' untranslated region (UTR) has suggested that *Per1* mRNA stability is tightly regulated (Kojima *et al*., 2003; Wilsbacher *et al*., 2002). The same appears to be true for *Per3* as the 3' UTR of its mRNA was shown to be important for its decay and for its circadian oscillations (Kwak *et al*., 2006). It has also been shown that non-rhythmic mRNAs can be translated into proteins that displace circadian rhythms (Reddy *et al*., 2006).

This can be attributed to either circadian regulation of protein synthesis or the modulation of post translational processing of the proteins. Because the core clock relies on TTFLs, one key feature is a timely orchestration in the dimerization, nuclear import/export, activity and degradation of clock proteins. Protein dynamics and degradation are a critical step in setting the period length.

Post-translational modulation, for example phosphorylation, acetylation and sumolation has a major impact on the stability, subcellular localisation and transcriptional activity of many core clock genes. One of the most important examples of the influence of post-translational modification on clock function is the Tau mutant hamster. The circadian phenotype (free-running period (Tau) = 20 hours) of the Tau mutant hamster is due to a point mutation in the gene encoding the casein kinase 1 ε (CK1ε) which results in hyperphosphorylation of PER1 and PER2 (Lowrey *et al.,* 2000) therefore showing that phosphorylation has a physiological significance in setting the pace of the clock. Phosphorylation of PER1-3 proteins by CK1δ or CK1ε has a number of functional effects – it destabilises PER proteins by promoting ubiquination and subsequent proteasomal degradation (Akashi *et al*., 2002; Yagita *et al*., 2002; Eide *et al*., 2005). This is mediated by ubiquitin ligase adapter protein β-TrCP (Shirogane *et al*., 2005). Phosphorylation of PER proteins also triggers subcellular relocation (Akashi *et al*., 2002; Vanselow *et al*., 2006). Therefore, PERs are regulated in a bimodal way (nuclear translocation and turnover) by CK1δ/CK1ε and other kinases and that may depend on the phosphorylated sites targeted on the PERs and on the extent of phosphorylation (Akashi *et al*., 2002; Partch *et al*., 2006). This was more recently supported by a study that demonstrated that phosphorylation acts as a switch, leading to two alternative fates of PER2 depending on the site phosphorylated – either increased stability or increased degradation. This 'phosphoswitch' was shown to be sensitive to changes in temperature and metabolic signals and therefore fine-tuned clock speed as necessary (Zhou *et al*., 2015). CRYs can also be phosphorylated by CK1ε, provided they are bound to PERs (Eide *et al*., 2002). Phosphorylation of the CRY proteins also results in their destabilisation and degradation (Yagita *et al*., 2002). F-box-type ubiquitin ligase FBXL3 ubiquinates CRYs, subjecting them to degradation. However, FBXL21 also ubiquinates CRYs but instead stabilises them, contributing to CRY protein accumulation in the daytime (Hirano *et al*., 2013). It has also been shown that the heterodimerisation of PER2 with CRY proteins stabilises and promotes their nuclear retention, therefore when PERs and CRYs are present at the same time they are stabilised and can exert repression. Glycogen synthase kinase-3 (GSK-3) has also been shown to phosphorylate CRY2 (Harada *et al*., 2005) PER2 (Iitaka *et al*., 2005) and REV-ERBα (Yin *et al.,* 2006). The phosphorylation of CRY2 and PER2 by GSK-3

promotes nuclear entry and/or retention in the nucleus and is accompanied by the degradation of CRY2 in the proteasome pathway (Harada *et al*., 2005). However, phosphorylation of REV-ERBα by GSK-3 leads to its stabilisation and inhibits degradation by the proteasome pathway (Yin *et al*., 2006). Phosphorylation events of given clock proteins modulate activity, subcellular localization, dimerization capabilities and stability of target protein.

1.30 Epigenetic control of circadian clock

The clock is able to regulate gene expression beyond the core clock genes. Transcription factors such as DBP, RORα and REV-ERBα are able to regulate cyclic expression of other genes. Mouse D site albumin promotor binding protein (DBP) binds to D-boxes whereas RORα and REV-ERBα bind to the Rev-erb/Ror- binding element (RRE). Whereas RRE binding elements follow a repressor-precedes-activator pattern, resulting in delayed transcriptional activity, the regulation of D-boxes follows a repressor-antiphasic-to activator mechanism which generates high amplitude transcriptional activity (Ueda *et al*., 2005).

Genes encoding circadian clock proteins are regulated by epigenetic mechanisms such as histone phosphorylation, acetylation and methylation which have been shown to follow circadian rhythm (Ripperger and Schibler, 2006; Masri and Sassone-Corsi, 2010). Light pulse during subjective night triggers phosphorylation of serine 10 of histone H3 which is a general mechanism necessary to unfold nucleosomes and allow the transcriptional machinery to activate transcription. This is closely paralleled by induction of c-fos and *Per1* suggesting that chromatin remodelling is an important step in light induced resetting of the clock (Crosio *et al*., 2000). Rhythmic histone acetylation appears to be crucial not only for light induced expression of *Per1* and *Per2* but also their regular circadian expression (Etchegaray *et al*., 2003). Histone acetylation status at a given promotor depends on the interplay between proteins bearing antagonistic enzymatic activity: histone acetyltransferase (HAT) proteins acetylate histones which results in an open chromatin state, while histone deacetylases (HDACs) deacetylate histones and thereby lock the chromatin so that it is inaccessible to the transcriptional machinery. CLOCK/BMAL1 can associate with factors harbouring HAT activity. Upon the transcription of the DBP rhythmic binding of CLOCK-BMAL1 to E-box cis-regulatory elements is seen, on top of acetylation of lysine 9 of histone H3 as well as trimethylation of lysine 4 of histone 3 leading to a reduction in histone density. CLOCK protein has HAT activity and can acetylate BMAL1, possibly controlling circadian function (Hirayama *et al*., 2007). Histone

deacetylase sirtuin 1 (SIRT1) not only interacts with CLOCK but also deacetylates lysine 537 of BMAL1 as well as two lysines of histone H3. As well as showing circadian expression, SIRT1 plays a role in the regulation of circadian gene expression of *Bmal1*, *Ror*, *Per2* and *Cry1*. It is able to regulate the expression of these genes via interactions with the CLOCK-BMAL1 heterodimer as well as through the deacetylation and degradation of PER2 (Asher *et al*., 2008). There is clearly a very close relationship between chromatin remodelling and transcription driven by CLOCK-BMAL1 not only with the autoregulatory feedback loop but also of the target genes downstream of the CLOCK-BMAL1 heterodimer.

Clock protein interactions with transcription factors are also able to regulate clock gene expression. The nuclear receptor corepressor 1 (NCoR1) recruits a histone deacetylase, termed HDAC3, which in turn mediates the transcriptional repression that REV-ERBα has on target genes including *Bmal1* (Alenghat *et al*., 2008). On top of this, PER2 forms a complex with PPARγ and regulates its function. PER2 represses PPARγ by interacting with the N-terminal domain (Grimaldi *et al*., 2010). Circadian co-regulators CRY1 and CRY2 interact with the glucocorticoid receptor in a ligand dependent fashion and globally alter the transcriptional response to glucocorticoids – crypotchromes broadly oppose GR activation and promote repression revealing a specific mechanism through which cryptochromes couple the activity of the clock and receptor target genes to complex genomic circuits (Lamia *et al*., 2011).

1.31 Linking the circadian clock to energy homeostasis

Growing evidence connects the circadian clock to energy metabolism. Circadian rhythms allow metabolic processes to be aligned with periodic environmental changes and behavioural cycles, for example fasting/feeding cycles. Disturbance of this alignment significantly increases the risk of metabolic disease. Meanwhile, the circadian clock receives signals from the environment and feedback from metabolic pathways.

In rodents, when food availability is restricted to the light phase, a time in which nocturnal animals are normally inactive, behavioural rhythms and peripheral clock gene expression can rapidly entrain to the new feeding schedule (Stokkan *et al*., 2001). During such restricted feeding (RF) paradigms, a variety of rhythms entrain to the timing of food presentation such as, peripheral clock gene expression, hormonal rhythms and body temperature.. An increase in locomotor activity also becomes apparent leading up to the time of predictable food presentation, commonly referred to as food anticipatory activity (FAA). Despite this, the

overall activity of the rodent remains to be synchronised with the SCN and the light-dark cycle (Mistlberger, 1994).

Metabolic challenges can also result in an impairment of circadian rhythms. The rise in prevalence of obesity goes hand in hand with an increase in sleep curtailment and obese people tend to exhibit disrupted sleep patterns (Resnick *et al*., 2003). On top of this the rhythmicity of glucose tolerance is severely blunted in obese patients, and compared to lean individuals, diurnal secretion patterns of ghrelin in obese patients are dramatically reduced (Van Cauter *et al*., 1997; Yildiz *et al.,* 2004). Intake of a high fat diet (HFD) in mice can result in disruption of the circadian clock. For example, Kohsaka *et al*. (2007) demonstrated that diet-induced obesity in mice led to altered expression of clock genes in multiple tissues, blunted feeding rhythms and a lengthened period of locomotor activity rhythms. Interestingly, the timing of HFD feeding is critical to its impact on metabolic consequences and the clock. Hatori *et* al. showed in 2012 that even when mice were put on a HFD but under dark-phase RF conditions, they were protected from obesity.

1.32 Circadian regulation of metabolism

Genome-wide transcriptome profiling studies identifying genes under circadian control consistently highlight pathways involved in intermediate metabolism (e.g. glycolysis, gluconeogenesis, lipid metabolism) and systemic energy balance (e.g. insulin signalling). Moreover, the fact that feeding–fasting cycles are a dominant zeitgeber for peripheral oscillators indicates that circadian clockwork is closely coupled to metabolic processes throughout the body. This is further supported by extensive metabolomic and lipidomic studies in laboratory rodents and humans, in which the levels of large numbers of metabolites are found to oscillate in tissues, plasma and saliva (Dallman *et al*., 2012; Kasukawa *et al*., 2012; Chua *et al*., 2013; Adamovich *et al*., 2014). Several recent studies have demonstrated a strong coupling between cellular energy and redox state and activities of circadian core clock components. For example, NAD levels, indicators of energy metabolism, can affect the activity of clock transcription factors directly or via NAD-dependent enzymes. NAD^+ is an important metabolic cofactor. The CLOCK-BMAL1 heterodimer is found to directly regulate the enzyme nicotinamide phosphoribosyltransferase (NAMPT) that provides the rate limiting step in the NAD^+ salvage pathway. This leads to rhythmic expression of the cofactor NAD^+ which is an important co-factor for SIRT1 which regulates a number of metabolic processes including insulin and glucose homeostasis (Nakahata *et al*., 2009; Haigis and Sinclair, 2010). SIRT1 can

perform deacetylation making it a key regulator of a variety of metabolic proteins. For example, SIRT1 is involved in gluconeogenesis by means of deacetylation and consequently activation of PGC-1α, responsible for the co-activation of hepatic nuclear factor 4α (HNF-4α) and glucocorticoid receptors and consequent induction of gluconeogenic genes (Yoon *et al*., 2001).

AMPK is an energy responsive enzyme that plays a role in cellular energy homeostasis as it has the ability to sense the energy status of the cell. It has been shown that the expression of AMPK has a circadian profile in a variety of tissues including the hypothalamus and the liver (Lamia *et al*., 2009; Um *et al*., 2011). There is evidence that AMPK itself can also regulate the circadian clock by phosphorylation of CRY and CK1ε. CRY1 becomes phosphorylated by AMPK drives ubiquination and subsequent degradation of CRY1 (Lamia *et al*., 2009). AMPK phosphorylation of CK1ε enhances its activity, with a resulting increase in PER2 degradation (Um *et al*., 2007). When AMPK is deleted in mice, circadian gene expression is modified in a tissue specific manner (Um *et al*., 2011). It has also been suggested that AMPK regulates circadian gene expression by activating SIRT1 (Canto *et al*., 2009).

The coupling of the clock to energy metabolism is also clearly observed at a systemic level. Indeed, many hormones involved in energy balance and metabolism such as insulin (La Fleur *et al*., 1999), glucagon (Ruiter *et al*, 2003), adiponectin (Ando *et al*., 2005), leptin and ghrelin (Bodosi *et* al., 2004) show circadian oscillations. In addition to endocrine control, the circadian clock is now known to regulate energy homeostasis in peripheral tissues by mediating the expression or activity of metabolic enzymes and transport systems. Further supporting the link between the circadian clock and metabolism, mutations in the essential clock genes have been found to disturb rhythmic expression of key metabolic genes and cause metabolic disorders. Drastic alterations in energy homeostasis are seen in homozygous *ClockΔ19* mutant. The phenotype of these mice is typical of metabolic syndrome, displaying low plasma insulin levels and in turn high plasma glucose levels as well as hyperlipidemia and obesity. The rhythmicity feeding in these mice is reduced with much a higher percentage of feeding occurring during the light phase which is associated with increased lipid absorption during the day, which is the opposite of what is seen in wild-type mice (Turek et al., 2005; Pan and Hussain, 2009; Pan et al., 2010).

1.33 Circadian control of carbohydrate metabolism

Time-of-day dependent oscillations in glucose metabolism are observed in both humans and rodent models. These rhythms are not purely mediated by fluctuations in behaviours such as exercise and feeding. For example, circulating glucose levels increase before waking, in both humans and rodents (Bolli *et al.,* 1984), and rhythms in blood glucose levels persist when rats are fasted (La Fleur *et al.,* 1999). Moreover, surgical ablation of the SCN disrupts glucose homeostasis (La Fleur *et al.,* 1999), suggesting that circadian timing is important not only to rhythms in circulating glucose, but also in basic homeostatic mechanisms which control glucose release and uptake.

As discussed above (section 1.9), glucose incorporation into glycogen represent a key depot for acute storage/liberation of energy in the body. Glycogen dynamics exhibit clear circadian control. For example, time of day dependent rhythms in glycogen levels persist in fasted rodents, suggesting that these rhythms are not simply secondary to feed-fasting cycles (Ishikawa and Shimazu, 1976). Activities of key glycogen metabolism enzymes oscillate over the course of the day, e.g. glycogen synthase displays maximum levels during the dark (i.e. active) phase in rodents whereas glycogen phosphorylase peaks towards the end of the light phase (Peret *et al.,* 1976, Ishikawa and Shimazu, 1980). Diminished oscillations in both hepatic glycogen levels and glycogen synthase expression and activity are observed in *Clock* mutant mice (*Clock*Δ19), with CLOCK identified as a transcriptional coactivator of glycogen synthase 2 (Gys2) (Doi et al., 2010). *Clock*Δ19 mice also develop hyperglycaemia and hyperinsulinemia (Turek et al., 2005).

Loss of BMAL1 attenuates diurnal variation in glucose and triglyceride levels, impairs gluconeogenesis and causes glucose intolerance (Rudic *et al*., 2004; Lamia *et al.,* 2008). Gluconeogenesis exhibits a diurnal variation, and increased rates are observed at the wake-to-sleep transition, which is paralleled by a diurnal rhythm in PEPCK (Kida *et al.,* 1980). Tissue specific deletion of *Bmal1* in the liver further supports the critical role of peripheral clocks in metabolic tissues. In hepatocyte specific BMAL1 knockout mice rhythmic expression of glucose metabolic genes e.g. *Pepck* and *Glut2* is abolished. Hypoglycaemia is also observed in these animals but only in the fasting phase of the day (Lamia *et al.,* 2008). Other clock components also play a role in glucose metabolism. CRYs inhibit gluconeogenic gene expression in a time of day dependent manner through regulation of β-adrenergic signalling and activation of CREB-protein. Therefore, hepatic depletion of CRY1/2 increases circulating glucose, while CRY1 overexpression reduces fasting blood glucose and improves whole body insulin sensitivity in

diabetic mice (Zhang *et al.,* 2010). CRYs also transrepress glucocorticoid-induced *Pepck* transcription, and loss of CRYs1/2 results in glucose intolerance (Lamia et al., 2011).

Clock mediated regulation of glucose homeostasis also involves the temporal regulation of endocrine factor release and sensitivity. Insulin dependent and independent whole body glucose disposal exhibits diurnal variations in humans and rodents (Whichelow *et al.,* 1974; Lee *et al*., 1992, La Fleur *et al*., 2001). *In vitro* studies showed that insulin secretion from isolated pancreatic rat islets display a circadian rhythm that originates within the islet. Plasma insulin concentrations in rats exhibit daily oscillations with distinct increments at every meal. These increments were highest during the dark phase and diminished during the second half of the light phase showing that circadian regulation of basal blood glucose and feeding-induced insulin responses, is *independent* of the temporal distribution of feeding activity (Kalsbeek and Strubbe, 1998). Studies also show that disruption of the circadian clock causes impaired insulin secretion and consequent hyperinsulinemia. A study in which young healthy patients were submitted to partial sleep restriction demonstrated marked alterations in glucose metabolism including decreased glucose tolerance and insulin sensitivity (Gottlieb *et al.,* 2005). A more recent study showed that circadian misalignment, when subjects ate and slept approximately 12 hours out of phase from their habitual times increased glucose levels despite increasing insulin (Scheer *et al.,* 2009). This work is also further supported in rodents. For example, specific loss of BMAL1 from pancreatic β-cells impairs insulin secretion (Marcheva *et al.,* 2010). Insulin sensitivity also exhibits a time of day dependence, which appears to be circadian clock dependent as both insulin and glucose tolerance are impaired in SCN ablated rats as well as *Clock*Δ19 and *Bmal1* null mice (La Fleur *et al.,* 2001; Rudic *et al.,* 2004). Similarly, insulin signalling is impaired in various tissues isolated from germline *Bmal1* null and *Per2* mutant mice (Anea *et al*., 2009; Durgan *et al*., 2010). Glucagon has also been shown to display diurnal patterns of release (Tasaka *et al*., 1980). 24 hour plasma glucagon concentrations are regulated by feeding and the circadian clock (Ruiter *et al.,* 2003). Melatonin also influences pancreatic glucagon expression as well as peripheral glucagon action (Bahr *et al.,* 2011). All of this evidence indicates that cell autonomous circadian clocks contribute towards rhythms in glucose homeostasis through the regulation of either the release or sensitivity to endocrine factors.

1.34 Circadian control of lipid metabolism

Lipid metabolic pathways are among the most enriched in circadian gene array studies. In the liver, Panda *et al.* 2002 demonstrated that of the 1,262 oscillating transcriptions, 1,160 were protein coding, and many of these were well-characterised genes implicated in metabolic regulation, for example the cholesterol metabolism regulator Insig2. Microarray analyses suggest that approximately 10-20% of the murine transcriptome in adipose tissue shows circadian rhythm in its expression, and a particular high ratio of these are involved in metabolism (Ptitsyn *et al*., 2006; Zvonic, *et al.,* 2006; Zhang *et al*., 2014), suggesting a pronounced impact of the clock on adipose physiology.

Multiple core clock genes have been shown to be vital for adipocyte differentiation *in vitro* suggesting a strong link between clocks and adipose physiology. During the differentiation of adipocytes, the expression of both *Bmal1* and *Rev-erbα* increases 3-4 fold, both have been shown to promote the differentiation of adipocytes, and deletion of either *Bmal1* or *Rev-erbα* inhibits the differentiation of pre-adipocytes in culture (Chawla *et al*., 1993; Shimba *et* a*l.,* 2005; Wang and Lazar, 2008). *Rev-erbα* expression cycles in adipose tissue and is induced during the adipogenic process by *PPARγ* activation by rosiglitazone in rat adipose tissue (Chawla *et al*., 2003; Fontaine *et al*., 2003). Ectopic overexpression of *Rev-erbα* 3T3-L1 preadipocytes promotes their differentiation into mature adipocytes and enhances lipid storage (Fontaine *et al*., 2003; Wang and Lazar, 2008). The *in vivo* evidence however contradicts this as adipose tissue appears normal in both *Rev-erbα* null and *Bmal* null mice (Chomez *et al*., 2000; Kondratov *et al*., 2006). *Per2* also affects adipocyte differentiation through a direct interaction with PPARγ (Grimaldi *et al*., 2010).

Studies have shown in both humans and rodents that levels of TAGs in plasma oscillate following a circadian pattern (Schlierf and Dorow, 1973; Fukagawa *et al., 1994).* In humans, two separate spikes in plasma TAG levels are observed - at 8 and 20 hours after arousal. When the sleep schedule was desynchronised, the first peak remained but the second peak was lost, therefore suggesting that although the second peak is likely related to sleep cycles, the first peak is dependent on an endogenous circadian clock (Morgan *et al*., 1998). Using metabolomics, it was shown that of the 15% of all small molecular weight metabolites that display circadian variation, more than 75% of them were lipids, most of which were fatty acids (Dallmann *et al.,* 2012). As changes in feeding or sleeping schedule did not affect these oscillations, it emerged that the endogenous circadian clock was the principal regulator of these fluctuations (Dallmann *et al.,* 2012).

It has long been known that cholesterol synthesis in rodents shows a circadian pattern in the liver and the intestine, which peaks during the night and is lower during the day (Back *et al.,* 1969; Edwards *et al.,* 1972; Mortimer *et al., 1998).* This regulation was mainly achieved through the circadian expression of HMG-CoA reductase *(*Back *et al.,* 1969; Oishi *et al.,* 2003). In rodents, bile acid showed circadian variation in the serum, liver, gallbladder and intestine and was in antiphase to cholesterol biosynthesis in the serum and intestine, but not in the liver and gallbladder (Ho, 1976). In rodents, diurnal variations of bile acid concentrations may play important roles in coordinating daily nutrient absorption and energy homeostasis by influencing the circadian expression of bile acid metabolising genes in the liver and ileum and of key proteins involved in bile acid biosynthesis and transport (Mirani-Oostdijk *et al.,* 1985; Zhang *et al.,* 2011). On top of this, levels of several key proteins implicated in the regulation of TAG metabolism such as lipolytic enzymes and PPARα oscillated with circadian periodicity both in rodents and humans and in mice, FAS, ACC, SREBP1c and FABP4 have been shown to fluctuate in a circadian manner in both adipose tissue and liver (Kudo *et al.,* 2007; Kohsaka *et al.,* 2007).

Various studies have also highlighted a direct role of clock genes in the control of lipid metabolic pathways. As discussed above, drastic alterations in energy homeostasis are seen in homozygous *ClockΔ19* mutant (Turek *et al.,* 2005; Pan and Hussain, 2009; Pan *et al.,* 2010). Interestingly, when *Clock* mutant mice were outbred onto an ICR genetic background a lean phenotype resulted due to impaired lipid absorption (Oishi *et al*., 2006). *Clock*-deficient mice also displayed a reduced hepatic TAG accumulation under high fat diet conditions, due to the suppressed expression of key genes involved in lipid biosynthesis such as Fabp1 (Kudo *et al.,* 2007).

Loss of *Bmal1* in the mouse results in a severe phenotype that completely loses all rhythmicity as well as abolishing the oscillations of glucose and triglyceride levels normally seen throughout the day (Rudic *et al*., 2004). Overexpression of *Bmal1* resulted in an induction of lipid synthesis and lipogenesis (Shimba *et* al., 2005). It has, however, been difficult to separate out whether the metabolic consequences caused by the loss of *Bmal1* are because of a loss of rhythmicity in the SCN or in peripheral clocks. When *Bmal1* is specifically lost from the liver or the pancreas blood glucose homeostasis is lost but it would seem that locomotor activity remains unaffected (Lamia *et al*., 2008). On top of this, in the liver specific *Bmal1* knockout the expression of a variety of key metabolic genes, most notably *Glut2* is lost which means that glucose cannot be taken up by the liver resulting in hypoglycaemia (Lamia *et al.,* 2008). In

2012, Paschos *et al.* showed that mice with an adipocyte specific deletion of *Bmal1* were more susceptible to diet induced obesity.

Per2 was implicated in metabolism by Bae *et al*., in 2001 when homozygous *Per2* null mice had lower body weights than WT controls. Grimaldi *et al*., in 2010 then went on to show the importance of *Per2* in lipid metabolism as mice lacking *Per2* showed drastic alterations in lipid metabolism and a reduction in total TAG and NEFAs. *Per2* is responsible for the specificity of PPARγ transcriptional activity and PER2 blocks PPARγ mediated transcriptional activation by impeding recruitment to target promoters. Lipidomic profiling of white adipose tissue of the mutant mice has shown that *Per2* is required for normal lipid metabolism (Grimaldi *et al*., 2010).

1.35 Role of Rev-erbα in lipid metabolism

Initially, it was thought that the main role of the nuclear receptor REV-ERBα was in both adipogenesis and lipid metabolism, acting downstream of PPARα, so when it was discovered that it was also involved in the control of *Bmal1* expression a clear link between energy homeostasis and the molecular mechanism of the circadian clock was uncovered (Preitner *et al*., 2002).

NCoR1 recruits a histone deacetylase, termed HDAC3, which in turn mediates the transcriptional repression that REV-ERBα has on target genes including *Bmal1* (Alenghat *et al*., 2008). Pharmacological activation of *Rev-erbα* increases recruitment of NCoR and *Rev-erbα* transcriptional activity. Heme has been identified as the endogenous ligand for the REV-ERBα receptor, and when bound heme increases REV-ERBα stability and improves the interaction with NCoR1. Heme levels in the cell are dictated both by metabolic status of the cell, and by the circadian clock. Aminolevululinate synthase 1 (ALAS1) which is a rate limiting enzyme in heme biosynthesis shows circadian oscillations and is a target gene for the NPAS2-BMAL1 heterodimer - NPAS2 being a paralog of CLOCK (Kaasik and Lee, 2004). Heme is also involved in mitochondrial respiration and cellular redox balance and therefore REV-ERBα functions as a sensor for the metabolic state of the cell and likely entrains the clock to metabolic cues (Yin *et al*., 2007; Kaasik and Lee, 2004). Interestingly, heme is required for the efficient differentiation process of the adipocyte (Chen and London, 1981) and it is also required for the proper functioning of enzymes such as cytochrome p450 and peroxidases (Ponka *et al*., 1999).

Rev-erbα plays an important role in regulating whole body metabolism via the control of cholesterol and bile acid metabolism in the liver (Duez *et al*., 2008; Le Martelot *et al*., 2009). Cholesterol 7α-hydroxylase (Cyp7A1) gene which encodes the first and rate controlling enzyme of the major bile acid biosynthetic pathway exhibits a strong diurnal pattern of expression (Chiang *et al*., 1990). *Rev-erbα* cross talks with bile acid receptor FXR in order to regulate the small heterodimer partner Shp and modulates Cyp7A1 expression through altered circadian expression of the two CYP7A1 regulators Shp and E4BP4 (Duez *et al*., 2008). *Rev-erbα* also downregulates the expression of liver apolipoprotein C-III and *Rev-erbα* deficient mice exhibit dyslipidaemia characterised by increased TAG levels (Duez *et* al., 2008; Raspe *et al*., 2002). *Rev-erbα* has also been suggested to repress the expression of *elovl3*, a gene encoding a very long chain fatty acid elongase (Anzulovich *et al*., 2006). Both *Rev-erbα* and *β* coordinate circadian hepatic fatty acid synthesis and storage (Bugge *et al*., 2012; Cho *et al*, 2012). The anticipatory induction of lipogenic programmes prior to animal waking is facilitated by the HDAC3-dependent repression of *Rev-erbα* and *β* target genes (Feng *et al*., 2011). HDAC3 repression of lipogenesis also influences hepatic glucose production (Sun *et al*., 2012) and *Rev-erbβ* has been shown to coordinate multiple phases of circadian transcription in the liver.

Rev-erbα also contributes to WAT metabolism through rhythmic expression of *Lpl*. Chow fed *Rev-erbα* null mice displayed increased adiposity and mild hyperglycemia without insulin resistance. It was also shown that *Rev-erbα* null mice utilize more fatty acids during the daytime. High fat diet feeding exaggerated metabolic disturbances, including the expression of lipogenic factors. *Lpl* was constitutively upregulated in muscle and adipose tissue, which facilitates muscle and fatty acid utilisation and contributes to fat overload (Delezie *et al*., 2012). Circadian control has also been implicated in BAT thermogenesis (Redlin *et al*., 1992; Zvonic *et al*., 2006; Yang *et al*., 2011). This function was found to be significantly regulated by *Rev-erbα* in mice (Gerhart-Hines *et al*., 2013). *Rev-erbα* binds directly to the promoter of *Ucp1* and supresses its expression. Upon cold exposure, *Rev-erbα* levels and promotor occupancy are significantly reduced, aiding maximal induction of *Ucp1* and BAT thermogenesis (Gerhart-Hines *et al*., 2013; Li *et al*., 2013).

Loss of *Rev-erbα* also significantly impacts on glucose stimulated insulin release from β-cells of the pancreas (Viera *et al*., 2013). The nuclear receptor also exhibits a regulatory role in liver glucose mediated glucagon secretion from α cells (Viera *et al*., 2013). *Rev-erbα* also plays a role in skeletal muscle energy homeostasis as it alters the dynamics of mitochondrial biogenesis and autophagy (Woldt *et al*., 2013). Genetic ablation of *Rev-erbα* reduced activation of the

LKB1-AMPK-SIRT1-PGC-1α axis and therefore decreased the generation of new mitochondria and increased the turnover of existing mitochondria (Woldt *et al*., 2013). Pharmacological activation of *Rev-erbα* in skeletal muscle increased the number and enhanced the functionality of the mitochondria as well as improving exercise capacity. PGC1-α has also been shown to impact on the clock through upregulation of *Rev-erbα (*Liu *et al.,* 2007*). Rev-erbα* has also been shown to be involved in the interaction between the host and microbiome through transcriptional control of toll-like receptors in collaboration with RORα (Mukherji *et al*., 2013).

Circadian and metabolic physiological are therefore intricately linked and *Rev-erbα* exemplifies this. However, *Rev-erbα* has been shown to modulate the clock and metabolism by different genomic mechanisms. Clock control requires *Rev-erbα* to bind directly to the genome and its cognate sites where it competes with activating ROR transcription factors. However, *Rev-erbα* regulates metabolic genes by recruiting HDAC3 corepressor to sites to which it is tethered by cell type specific transcription factors. This means that self-sustained control of the molecular clock across all tissues is due to direct competition between *Rev-erbα* and ROR transcription factors whereas lineage-determining factors are used by *Rev-erbα* to convey a tissue specific epigenomic rhythm that regulates metabolism in a certain tissue (Zhang *et al*., 2015).

1.36 Overall Aims

Although circadian dysfunction and disease pathogenesis are clearly linked, much information is yet to be gained with regards to the role of the circadian clock in adipose tissue and its involvement in lipid metabolism. A significant percentage of genes in adipose depots display robust and coordinated circadian expression profiles which is evidence for the presence of a peripheral clock in adipose tissue. In order to broaden our understanding of the bidirectional relationship between the circadian clock and lipid metabolism, we hypothesise:

1. The molecular clock will be affected by diet
2. *Rev-erbα* will play a critical role in energy homeostasis
3. The adipose tissue clock will play a vital role in energy balance

To address this, we will:

- Determine how Diet Induced Obesity (DIO) affects both behavioural and molecular rhythmicity in mice

- Investigate the metabolic effects of the loss of *Rev-erb*α$^{-/-}$ by a range of challenges such as DIO and fasting
- Determine the role of the circadian clock specifically in adipocytes by the use of adipose specific clock gene knockouts (*Bmal1* and *Rev-erb*α)

Chapter 2 - Materials and Methods

2.1 Animal maintenance

All experimental procedures were licenced under the 1986 Home Office Animal Procedures Act (UK) and received ethical approval of the local animal welfare committee. C57BL/6J mice were purchased from Charles River (UK). *Rev-erbα*$^{-/-}$ mice (Preitner *et* al., 2002) were initially provided by Ueli Schibler (University of Geneva) and subsequently bred at GlaxoSmithKline (Stevenage). mPER2::luc mice were originally obtained from Joe Takahashi (Yoo *et al.,* 2004) and subsequently bred locally. Adipoq-Cre (Eguchi *et al*., 2011) and *Bmal1*$^{flox/flox}$ (Storch *et al.*, 2007) transgenic mice were purchased from The Jackson Laboratory (USA). *Bmal1*$^{flox/flox}$ mice were mated with *PER2*$^{luc/luc}$ mice. *Rev-erbα*$^{flox/flox}$ mice were purchased from Institut Clinique de la Souris (France). *Adipoq*$^{CRE/+}$ mice were mated with *Bmal1*$^{flox/flox}$*/Per2*$^{luc/luc}$ or *Rev-erbα*$^{flox/flox}$ mice and cohorts were established by mating the F1 male *Adipo*$^{CRE/+}$*/Bmal1*$^{flox/+}$*/Per2*$^{luc/+}$ with female *Bmal1*$^{flox/flox}$*/ Per2*$^{luc/luc}$ and the F1 male *Adipo*$^{CRE/+}$*/Rev-erbα*$^{flox/+}$ with female *Rev-erbα*$^{flox/flox}$. Mice were given ab-libitum access to standard rodent chow (NC) (Special Diets Services) and water unless otherwise stated. Mice were housed in standard housing conditions of a 12h:12h light:dark (LD) with lights on at 07:30 hours with an ambient temperature of 20±2°C (unless otherwise stated), humidity 55±5%.

2.2 Dietary Manipulation

2.2.1 HFD feeding

For diet-induced obesity (DIO) studies, mice were provided with *ad libitum* access to high fat diet (HFD; 61.6 % kcal from fat, 20.3% kcal from carbohydrates, 18.1% kcal from protein; TestDiet, London, UK) or normal chow (NC). Body weight was measured on a weekly basis and upon culling the animals, fat pad weights were measured. For DIO studies of WT mice, 8-10 week old male C57BL/6J mice were maintained on HFD (n=30) or NC (n=30) for 2, 8 or 16 weeks. For *Rev-erbα*$^{-/-}$ mice, 8-10 week year old KO and WT littermates were maintained on either HFD (n=8 per genotype) or NC (n=8 per genotype) for 14 weeks. Day/night food intake was measured for 5 days after 8 weeks on HFD. In separate experiments, 8 week old female *Adipo*^{CRE}*Bmal1*$^{flox/flox}$*, Adipo*^{CRE}*Rev-erbα*$^{flox/flox}$ and their respective control littermates were maintained on HFD or NC for 12 weeks (n=5 per diet per genotype).

2.2.2 Fasting

Leading up to fasting experiments standard rodent chow and water were supplied ad libitum. To assess fasting response, mice were fasted for 24 or 48 hours, with removal of food at approximately 11 am. Body weight was measured pre and post-food withdrawal. Fasting/fed comparisons were performed in three cohorts of *Rev-erbα*$^{-/-}$ mice (n=6 per group for serum TAG levels, n=8 per group for metabolic parameters, n=8 per group for 24 and 48 hour fast qPCR analysis). Fasting was performed on two separate cohorts of *Adipo*^{CRE}*Bmal1*$^{flox/flox}$ and *Adipo*^{CRE}*Rev-erbα*$^{flox/flox}$ mice and littermate controls (n=6 per genotype per feeding regime for telemetry analysis, n=4 per genotype per feeding regime for metabolic parameters) for 48 hours. Upon replacement of food, food intake was monitored for 24 hours post-refeeding.

2.3 Remote Telemetry

Mice were anaesthetised with isoflurane (2-5% in O_2) and underwent surgical implantation of a temperature transmitter (TA-F10, Data Sciences International) to allow continuous monitoring of core-body temperature. Briefly, mice were implanted intraperitoneally with the temperature transmitter. Surgical preparation consisted of shaving the abdominal fur and making an incision (length, approximately 1cm) through the skin and abdominal muscle layer by using aseptic technique. The peritoneal muscle layer and skin were closed with sutures. Following the operation mice were given analgesic (Vetergesic, 0.03mg/kg) and allowed to recover in their cages for 1 week post-surgery prior to telemetry recording. Mice were individually housed on receiver pads which transmitted core body temperature and activity measurements to the data acquisition software every 5 minutes. For DIO studies, n=10 mice per group were implanted with a telemetry remote prior to switch to HFD, and subsequently monitored for the first 2 weeks of HFD/NC feeding and the final two weeks of the study (14-16 weeks of HFD). *Rev-erbα*$^{-/-}$animals and control littermates (n=8 per genotype) were also implanted with telemetry remotes, as well as *Adipo*^{CRE}*Bmal1*$^{flox/flox}$ and *Adipo*^{CRE}*Rev-erbα*$^{flox/flox}$ and control littermates (n=6 per genotype).

2.4 Comprehensive Lab Animal Monitoring System (CLAMS)

To assess metabolic rate, mice were placed in CLAMS indirect calorimetric cages (Columbus Instruments, Columbus, OH, USA). Mice were acclimated to cages for two days and standard rodent chow and water were supplied *ad libitum*. Oxygen consumption (VO_2) and carbon dioxide consumption (VCO_2) were measured every 10 min until the termination of the experiment (7 days typically). Respiratory Exchange Ratio (RER) was then calculated from this

data using the following formula: VCO_2/ VO_2. Heat (energy expenditure) was also calculated using the following formula CV * VO_2, where CV (calorific value) = 3.815 + 1.232 * RER (Ferrannini, 1988). Carbohydrate oxidation rate (COX) and fatty acid oxidation rate (FOX) were also derived using the following equations: COX: 4.5 * VCO_2 – 3.21 * VO_2**;** FOX: 1.67 * VO_2 – 1.67 * VCO_2. Metabolic parameters were assessed in *Rev-erbα*$^{-/-}$, *Adipo*^{CRE}*Bmal1*$^{flox/flox}$, *Adipo*^{CRE}*Rev-erbα*$^{flox/flox}$ mice and control littermates (n=8 per genotype).

2.5 TSE Feeding Cages

Food intake was monitored using the Labmaster Metabolism Research Platform (TSE systems), with meal size and feeding events recorded over 7 days. Mice were placed individually into plastic cages to which feeding and drinking sensors were attached. Animals were habituated for at least one week before experimentation. Food and water were available *ad libitum* and intake was measured every 10 minutes. For WT DIO studies, n=8 per diet regime and for *Adipo*^{CRE}*Bmal1*$^{flox/flox}$ and control littermate food intake analysis, n=8 per genotype.

2.6 Glucose Tolerance Test (GTT) and Insulin Tolerance Test (ITT)

Before administration of insulin or glucose, mice were fasted for 6 hours. Blood glucose was monitored pre-administration by tail bleeds using an Accu-chek Aviva glucose meter (Roche). 1 g/kg of glucose (Sigma Aldrich) or 0.75 U/kg of insulin (Sigma Aldrich) was administered to the mice I.P at ZT6. Blood glucose measures were collected 20, 40, 60 and 120 minutes post glucose/insulin administration. These tests were performed on *Rev-erbα*$^{-/-}$mice and control littermates on NC and HFD (n=8 per genotype per diet regime). Average weights of all animals on NC and all animals on HFD were taken, regardless of genotype. A set dose of insulin/glucose was then administered to the mice based on these average weights. An ITT test was also performed on *Adipo*^{CRE}*Rev-erbα*$^{flox/flox}$ mice and control littermates (n=6 per genotype).

2.7 *In vivo* lipogenic/lipolytic challenge

Before lipogenic challenge experiments took place mice were fasted for 6 hours. *Rev-erbα*$^{-/-}$mice and WT littermates (n=8 per genotype/treatment) were then injected I.P. with either 0.75 U/kg insulin or saline as a control. Blood samples, by means of tail bleeds, were taken before and 4 hours post stimulation. Blood was allowed to clot at room temperature (approximately 5 minute) prior to being placed on ice. Serum was recovered by low speed

centrifugation (9,600 x g for 10 minutes). Mice were sacrificed 4 hours post stimulation by cervical dislocation and various tissues collected, placed immediately on dry ice and subsequently stored at -80°*C* for further qPCR and protein analysis. For the lipolytic challenge *Rev-erbα*$^{-/-}$mice and WT littermates (n=5 per genotype/treatment) were injected intraperitoneally (I.P.) with either 0.1 or 1 mg/kg of CL316,243 (Sigma Aldrich) or saline as a control. At the termination of the experiment (4 hours post injection), mice were sacrificed by cervical dislocation, and tissues collected, placed immediately on dry ice and subsequently stored at -80°*C* until qPCR and/or western blot analyses.

2.8 Cold Exposure

Adipo^{CRE}*Bmal1*$^{flox/flox}$ mice were individually housed in a modified upright 1200 L industrial fridge (Polar Refrigeration, UK). The fridge was adapted to include an Akor ventilation unit (Akor Systems, France) to allow an internal external air exchange. Internal temperature was maintained between 4°C -16°C, as stated for each experiment. Body temperature was recorded by remote telemetry as described in section 2.3. Mice that were implanted with a telemetry remote I.P. (n=6 per genotype) and maintained at normal room temperature for 4 weeks post-surgery were then were individually housed on top of telemetry pads inside the refrigeration cabinet set at a temperature of 4°C for 5 hours. After 5 hours the temperature was reset to 16°C and the temperature inside the refrigeration cabinet subsequently ramped up to the desired temperature. After a 7 day acclimatisation to the 16°C temperature mice were then fasted for 24 hours and food was then reintroduced to the cages. Body temperature was recorded throughout the experiment.

2.9 Serum collection and lipid analysis

Serum was either collected by tail bleeds throughout experiments or from trunk blood at sacrifice. Serum, which had been stored at -80°C was allowed to thaw at 4°C. To determine lipid concentrations in serum, a Free Fatty Acid fluorometric kit (Cayman) and Serum Triglyceride Determination kit (a quantitative enzymatic assay) to measure triglyceride and free glycerol (Sigma) were used according to manufacturer's instructions with sample absorbance measured using a GloMax®-Multi+ fluorometer (Promega).

2.10 *Ex vivo* bioluminescence

For *ex vivo* analysis of circadian rhythms for WT DIO studies, mice (n=4 mice per group, >16 slices per tissue/mouse) were culled by cervical dislocation and tissues (WAT, lung, liver) were extracted and placed in phenol red free HBSS (Sigma Aldrich, UK). Tissue was then further dissected into 5 slices per animal and placed into sterile 35 mm dishes containing 1 ml DMEM recording media containing Sodium Bicarbonate (0.035%), HEPES buffer (10Mm), Streptomycin (25 µg/ml), Penicillin (25 units), 5% FBS, Beetle Luciferin K salts (0.1 mM, Promega, UK) (All Sigma Aldrich UK, unless otherwise stated).The slices were placed on a Millicell low profile, 0.4 µM membrane insert (Millipore, UK) to provide an air-liquid interface and prevent slice movement. The dishes and slices were sealed with a 40mm sterile glass cover slip (VWR) and high vacuum grease (Dow Corning) and placed in a Lumicycle (Actimetrics) and bioluminescence recordings taken over a 5-7 day period. The temperature of the incubator was set to 37°C.

2.11 RNA extraction, conversion, and quantitative Real Time PCR

For all studies, animals were killed by cervical dislocation; tissues were removed rapidly and immediately dissected, using a sterile blade. Where appropriate, organ weight was measured, for example scWAT and gWAT before being frozen on dry ice and stored at -80°C for protein/RNA extraction. For most of the larger tissues, approximately 100 mg blocks were dissected, but in the case of scWAT and gWAT all tissue was taken due to low RNA yield. For circadian tissue collections, mice were placed in constant darkness (DD) for 24 hours prior to the collection. Mice were sacrificed by cervical dislocation every 4 hours (n=5-10 mice/time-point/diet condition) and a range of tissues were collected. Tissue was rapidly frozen on dry ice and stored at -80°*C* for further analysis.

RNA was extracted from frozen adrenal glands, adipose tissue (WAT, scWAT and BAT), hypothalamus, liver, lung, lymph nodes, muscle, and spleen using a phenol-chloroform method. Tissue was homogenised using lysing matrix D tubes (MP Biomedicals) in 1 ml (TRIzol; Ambion, Life Technologies, UK) using a FastPrep-24 system (MP Biomedicals) at 4°C. For most tissues, phase separation was carried out immediately following homogenisation but for WAT, prior to phase separation, samples were centrifuged at 4℃ 16,200 x g for 5 minutes, to separate excess lipids into a top layer which was then removed. For phase separation, samples were incubated at room temperature for 5 minutes before addition of 200 µl chloroform (Sigma, UK) and then thoroughly mixed by vigorous inversion. After incubation for 3 min at room temperature, samples were centrifuged at 4℃ 16,200 x g for 5 minutes. The resting

solution separated into different phases with total RNA in the upper aqueous phase. 500 µl of the aqueous phase was removed and mixed with 500 µl isopropanol, mixed by gentle inversion, and incubated on ice for 10 min to precipitate the RNA. This mixture was then centrifuged at 4°C 16,200 x g for 10 minutes and the isopropanol solution was removed. The resulting RNA pellet was washed in 75% ethanol and centrifuged at 4°C 16,200 x g for 5 min. The ethanol was removed and the RNA pellet was left to air-dry before being resuspended in 15-200 µl nuclease free H_2O. RNA concentration (ng/µl) and purity was determined using a NanoDrop 1000 spectrophotometer (Thermo Scientific). RNA samples were either stored at -80°C *or* used as a template for cDNA synthesis using a high capacity cDNA reverse transcription kit (Applied Biosystems, UK).

2 µg total RNA was used per 20µl reaction, with the assumption that all RNA was converted to cDNA, to yield a final concentration of 100 ng/µl cDNA. Prior to conversion to cDNA, RNA was treated for 30 min at 37°C with 1µl RNase free DNase (Promega). The reaction was stopped with 1µl DNase stop buffer (Promega), incubated at 65°C for 10 min. A High Capacity RNA to cDNA Kit (Applied Biosystems) was then used for the conversion reaction, with the addition of 10µl 2x buffer and 1µl of 20x enzyme mix and deionised H_20 so that the total volume came to 20µl. The reverse transcription reaction was incubated at 37°C for 60 min before the reaction stopped by denaturing the enzyme with incubation at 95°C for 5 min. Resulting cDNA was stored at -20°C

RT qPCR was performed and analysed using an Applied Biosystems 7900HT Fast Real-Time PCR System with 2 x GoTaq® qPCR Master Mix and 0.5 µM primers (see sequences in table 2.1). Individual qPCR reactions were carried out in 10µl volumes in a 384 well Fast-prep plate (Applied Biosystems), using the following protocol: 2 min at 50 °C, followed by 15 min at 95°C, then 40 cycles of 15 sec at 94 °C, 30 sec at 60 °C and 30 sec at 72 °C. Relative expression levels (relative quantification/RQ) were determined using the comparative C_T method to normalize target gene mRNA to 18S.

Table 2.1 – Primer Sequences

Target mRNA	Primer Sequence
18s	F: 5'-TCCGACCATAAACGATGCCGACT-3' R: 5'-TCCTGGTGGTGCCCTTCCGTCAAT-3'
Atgl	F: 5'- TGTGGCCTCATTCCTCCTAC -3' R: 5'- TCGTGGATGTTGGTGGAGCT -3'
Bmal1	F: 5'-GTCGAATGATTGCCGAGGAA-3' R: 5'-GGGAGGCGTACTTGTGATGTTC-3'

Cry1	F: 5'- TCGCCGGCTCTTCCAA -3' R: 5'- TCAAGACACTGAAGCAAAAATCG -3'
Clock	F: 5'- TTGCTCCACGGGAATCCTT -3' R: 5'- GGAGGGAAAGTGCTCTGTTGTAG -3'
Dbp	F: 5'-CCGTGGAGGTGCTAATGACCT-3' R: 5'-CCTCTGAGAAGCGGGCC -3'
Dgat2	F: 5'- AGTGGCAATGCTATCATCATCGT -3' R: 5'- TCTTCTGGACCCATCGGCCCCAGGA -3'
Fabp4	F: 5'-GAAAACGAGATGGTGACAAGC -3' R: 5'-TTGTGGAAGTCACGCCTTT -3'
Fasn	F: 5'- CCCAGAGGCTTGTGCTGACT -3' R: 5'- CGAATGTGCTTGGCTTGGT -3'
F4/80	F: 5'- AAGACTTGATACTCCAAAGTGAGC -3' R: 5'- GAAGGAAGCATAACCAAGATCCC -3'
Gk	F: 5'- CCCTGAGTGGCTTACAGTTC -3' R: 5'- ACGGATGTGAGTGTTGAAGC -3'
Glut4	F: 5' -GTCCTCCTGCTTGGCTTCTT -3' F: 5'-AGCTGAGATCTGGTCAAACG -3'
Hk2	F: 5' -GAAGATGATCAGCGGGATGT -3' R: 5' –TCTGGATTCCGTCCTTATCG -3'
Hsl	F: 5'- GCTGGGCTGTCAAGCACTGT -3' R: 5'- GTAACTGGGTAGGCTGCCAT -3'
Lpl	F: 5'- AGGGCTCTGCCTGAGTTGTA -3' R: 5'- CCATCCTCAGTCCCAGAAAA -3'
Pepck	F: 5' - GGCCACAGCTGCTGCAG - 3' R: 5' – GGTCGCATGGCAAAGGG - 3'
Per2	F: 5'-GCCTTCAGACTCATGATGACAGA-3' R: 5'- TTTGTGTGCCTCAGCTTTGG-3'
Ppary α	F: 5' – GAGGGTTGAGCTCAGTCAGG -3' F: 5' – GGTCACCTACGAGTGGCATT - 3'
Ppar γ	F: 5' – AGGCCGAGAAGGAGAAGCTGTTG - 3' F: 5' – TGGCCACCTCTTTGCTCTGCTCM - 3'
Rev-erb α	F: 5'- GTCTCTCCGTTGGCATGTCT -3' R: 5'- CCAAGTTCATGGCGCTCT -3'
Rev-erb β	F: 5'- TCATGAGGATGAACAGGAACC -3' R: 5'- GAATTCGGCCAAATCGAAC -3'
TNFα	F: 5' - TCTCTTCAAGGGACAAGGCTG - 3' F: 5' – ATAGCAAATCGGCTGACGGT – 3'

2.12 SDS-Page and Western Blot analyses

For protein extraction, gWAT and liver tissue samples were placed in 400 or 1000 µl respectively of T-PER Tissue Protein Extraction Reagent (Pierce) supplemented with protease inhibitor (Roche) in Lysing Matrix D Tubes. Tissue was homogenised using the FastPrep®-24 for 40 seconds, placed on wet ice to cool for 30 seconds and then homogenised for a subsequent

40 seconds. Homogenised fat samples were then spun down for 5 minutes at 4° at 16,200 x g in order to separate out the solubilized material from the lipid layer. This was repeated 3-4 times and the supernatant was collected. In order to assess protein concentration, a standard curve was made using known concentrations of protein standards of bovine serum albumin (BSA) (Sigma, UK). 10 µl of the protein standards; 0, 100, 200, 400, 800 and 1000 µg/ml BSA diluted in lysis buffer and samples diluted 1:15-50 in lysis buffer were added to 96 well plate with 200 µl of 20% Protein Assay Reagent (BioRad). Samples were read at 560 nm on a plate reader (Bio-Rad).

12 µl of 20-50µg quantified protein lysates were denatured at 95°C for 5 min in the presence of 4 µl 5 x Laemmli sample buffer (Bio-Rad) with 10% 2-Mercaptoethanol. The samples were separated by sodium dodecyl sulphate–polyacrylamide gel electrophoresis using 4–15% Mini-PROTEAN® TGX™ Precast Gels in Mini-PROTEAN 3 apparatus (Bio-Rad) according to manufacturer's instructions at 150 V until the proteins were sufficiently resolved, in a Tris-SDS running buffer (192 nM glycine, 25 mM Tris, 0.01% SDS). A pre-stained molecular weight protein marker (Precision Dual Colour Marker, BioRad) was resolved in parallel with samples to allow estimation of the molecular sizes of the separated proteins.

The separated protein was then transferred to a nitrocellulose membrane using an iBlot gel transfer system (Invitrogen). Membranes were blocked with 5% skimmed milk in TBS-T buffer (150 mM NaCl, 20 mM Tris-HCl, pH 7.4, 0.1% Tween-20) for 1 hour. Membranes were then probed overnight at 4°C with primary antibodies diluted in blocking buffer (as described in table 2.2)

Table 2.2 – Antibody Weights and Concentrations

Antibody	Weight	Concentration	Supplier
Anti-ATGL	55	1:200	Santa Cruz Biotech
Anti-DGAT2	44	1:1000	Santa Cruz Biotech
Anti-LPL	53	1:5000	Santa Cruz Biotech
Anti-GAPDH	37	1:1000	Santa Cruz Biotech
Anti-HSL	81,83	1:1000	Cell Signalling Technology
Anti-pHSL (Ser563)	81,83	1:1000	Cell Signalling Technology
Anti-PPARα	58	1:1000	Santa Cruz Biotech
Anti-PPARγ	58	1:1000	Santa Cruz Biotech
Anti-FASN	273	1:20000	Abcam
Anti-FABP4	15	1:20000	Santa Cruz Biotech

Blots were then incubated in appropriate secondary antibody (2hr, room temp), either horseradish peroxidase-linked sheep anti-mouse IgG or horseradish peroxidase-linked goat anti-rabbit IgG (GE Healthcare). Protein bands were detected with an enhanced chemiluminescence substrate kit (Thermo Scientific) and exposed to Kodak film (KodakBioMax Light) for 0.5–5 min at room temperature. The developed films were quantified using Image J and protein levels expression in relation to GAPDH.

2.13 WAT explant cultures

Mice were sacrificed by cervical dislocation at CT 6 and gWAT, removed by dissection, was placed in ice-cold Hanks Balanced Salt Solution (HBSS). Connective tissue and blood vessels were removed from the gWAT and 10 mg of the gWAT explant was minced and placed into a 24-well plate and cultured in 1 ml of Dulbecco's modified Eagles Medium (DMEM) (Sigma-Aldrich, UK) supplemented with 10% foetal bovine serum (Fisher Scientific, UK) and a mixture of penicillin-streptomycin (Sigma-Aldrich, UK) for 24 hours in a humidified atmosphere containing 5% CO_2. One animal provided 6 explants. A media change took place after one hour. In order to validate the model, another media change took place but this time supplemented with either 0, 10 nM, 100 nM, 1 µM or 10 µM insulin (Sigma-Aldrich, UK). The explants were cultured for a further 24 hours before the tissue was removed and frozen at -80°C for qPCR analysis. From this validation, it was determined that 1 µM of insulin was the optimum stimulation concentration and this was used for subsequent explant experiments.

2.14 Statistical Analysis

Data are presented as mean ± standard error (SEM). Students' t-test was used when two groups were tested, one-way ANOVA with Dunnett's multiple comparisons or two-way ANOVA followed by Sidak post-hoc analyses were used when more than two groups and/or factors were analysed using Graphpad Prism. Statistical significance was assessed at the first level of the ANOVA using @ symbol and by post-hoc test using * symbol.

Results

Chapter 3 - High-fat diet disrupts molecular circadian rhythms in mice

3.1 Introduction

There is a well-established link between the circadian clock and energy metabolism. Lifestyles associated with circadian dysregulation, such as rotating shift work and chronic sleep deprivation, are associated with increased risk of obesity and its comorbidities (Karlsson *et al*., 2001; Di Lorenzo *et al*., 2003; Pan *et al*., 2011). Similarly, transgenic mouse models in which critical elements of the circadian clock have been deleted often results in a metabolic phenotype. For example, *ClockΔ19* mutant mice exhibit pronounced obesity and hyperglycaemia (Turek *et al*., 2005). Human genetic studies report associations between polymorphisms of *Clock* and obesity (Scott *et al*. 2008) as well as many other clock genes.

While the influences of the molecular clock on metabolic processes have been well documented, it is less clear how metabolic disturbance may feedback onto the circadian clock. Studies have been performed in mice to address how obesity affects circadian rhythmicity but have provided conflicting results (Ando *et al*., 2005; Yanagihara *et al*., 2006; Kohsaka *et al*. 2007). In 2005, Ando *et al*. used mice models of mild and severe spontaneous obese diabetes (KK and KK-A^Y respectively). Rhythmic expression of clock genes was mildly attenuated in WAT of KK mice and strongly attenuated in KK-A^Y mice in comparison to C57BL/6 WT controls. However, in a diet induced obesity (DIO) model in which female C57BL/6 mice were fed HFD for 8 weeks from 4 weeks of age, peak levels of clock genes did not differ in any of the tissues examined (Yanagihara *et al*., 2006). Conversely, in male C57BL/6 mice fed HFD for 6 weeks from 4 weeks of age, circadian period was lengthened in DIO mice, and HFD attenuated diurnal pattern of feeding behaviour (Kohsaka *et al*. 2007). This work and a subsequent study (Prasai *et al.,* 2013) also demonstrated a DIO-associated damping of clock gene expression in WAT of obese mice, when compared with normal weight controls.

Adipose tissue physiology demonstrates a strong correlation with circadian mechanisms (Bray and Young, 2007; Zvonic *et al*. 2007). For example, circulating levels of secreted adipokines such as adiponectin and leptin (Yildiz *et al*., 2004) display as oscillating profile with a 24 hour period, as do adipose and macrophage derived inflammatory cytokines IL-6 and TNF-α (Vgontzas *et al*. 1999; Vgontzas *et al*. 2002). Murine WAT, as with many other tissues, contains endogenous circadian timing properties (Johnston *et al.* 2009; Gimble and Floyd, 2009) and it is estimated that 10-20% of the murine WAT transcriptome shows circadian variations (Ptitsyn *et al*., 2006; Zvonic *et al.* 2006; Zhang *et al*., 2014).

Here we determine the impact of DIO on the circadian clock of C57BL/6 mice by conducting broad analysis of behavioural and molecular rhythms in HFD fed mice and to examine how HFD affects clock-metabolic regulators. A large number of tissues were examined and the expression of clock genes determined to allow for a comprehensive analysis of how DIO affects the circadian clock. Previous studies have used varying HFD-challenge lengths, which may be responsible for the difference in results obtained. For this reason, we also monitored clock gene expression at various time points during the development of obesity in order to determine if HFD-feeding itself causes disruption of the molecular clock.

3.2 Methods

Detailed methodological approaches can be found in the methods (Chapter 2). Below are specific experimental details.

For DIO studies, 8-10 week old mice (C57BL6/J, Charles River, UK) were provided *ad libitum* access to high fat diet (HFD; 60% energy from fat; DIO Rodent Purified Diet, IPS Ltd) or normal chow (NC) for 2 (n=4-5/diet), 8 (n=4-5/diet) or 16 (n=25-40/diet) weeks. In the 16 week HFD group, body temperature and locomotor activity were recorded using radiotelemetry (Data Sciences International), and metabolic gas exchange measured by indirect calorimetry using the CLAMS system (Columbus Instruments). Food intake was monitored using the Labmaster Metabolism Research Platform (TSE systems), with meal size and feeding events recorded over 6 days (n=30 per diet). Prior to tissue collection, mice were placed in constant darkness (DD) for 24h, following which tissues (liver, muscle, adrenal glands, inguinal lymph nodes, spleen, pancreas, BAT, gWAT, and scWAT) were collected every 4h (n=5-10/time-point/diet condition).

For *ex vivo* analysis of circadian rhythms, 8 week old male mPER2:luc mice were fed HFD or NC for 16 weeks. Bioluminescence was recorded from gWAT samples maintained in DMEM recording media at 37°C using a Lumicycle (actimetrics). Amplitude of mPER2-dependent luminescence was determined for each animal (n=4 mice/diet), using the mean of 16 samples/mouse.

3.3 Results

3.3.1. Circadian behaviour of obese mice

To determine if DIO has an effect on behavioural and physiological rhythms, adult male C57BL/6 mice were maintained on either NC or HFD (60% energy from fat) for 16 weeks (n = 30 mice per diet). Mice fed HFD gained significantly more weight than NC control mice and as to be expected significant WAT accumulation was observed in animals on a HFD feeding regime in comparison to NC control mice (Figure 3.1A). Activity and core body temperature rhythms were monitored during the 16 week study by remote telemetry. Recording of both parameters at the transition to HFD and following chronic HFD feeding revealed robust diurnal rhythms were maintained in NC and HFD fed mice (Figure 3.1B). However, HFD-fed mice showed a reduction in dark phase activity, and reduced amplitude in day/night temperature profiles, indicating a damping of diurnal rhythms in these mice. Studies of HFD feeding in mice commonly report increased daytime feeding, and we therefore assessed the diurnal feeding structure in these animals (Figure 3.1B). Food intake (g/hr) was monitored continuously across the 24hr cycle for >10 days using TSE systems' cages, with mice switched from NC to HFD after 5 days of recording (n=8). Mice on NC consumed more food in the dark phase than in the light phase. The proportion of calories consumed during the light phase was significantly higher in HFD fed mice but this was largely due to the decrease in night time feeding rather than an increase in feeding during the day (Figure 3.1C, $p<0.05$, one-way ANOVA with repeated measures). This was reflected in a decrease in meal events (>0.05g of food consumed in 10 minutes) observed during the dark phase in mice fed HFD in comparison to mice fed NC. Mean meal size (in g) remained consistent for both NC and HFD fed animals across the light and dark phase. Decreased nocturnal feeding was apparent within days of the mice being placed on HFD which suggests that altered feeding patterns reflect a homeostatic response to a HFD-related alteration of circadian regulation of feeding rhythms. Taken together, these data suggest that obesity did not dramatically disrupt diurnal rhythmicity in HFD-fed mice. Nevertheless, the flattening of food-related zeitgeber due to increased energy intake shifted towards the day.

3.3.2. Molecular clock disruption in response to obesity

We next assessed the impact of obesity on clock gene rhythms in a panel of central and peripheral tissues. From 8 weeks of age, male C57BL/6J mice were maintained on either HFD or NC for 16 weeks (n=30 mice per diet). Prior to tissue collection, mice were placed under constant darkness (DD) for 24 hours to remove the direct influence of light. Tissues were

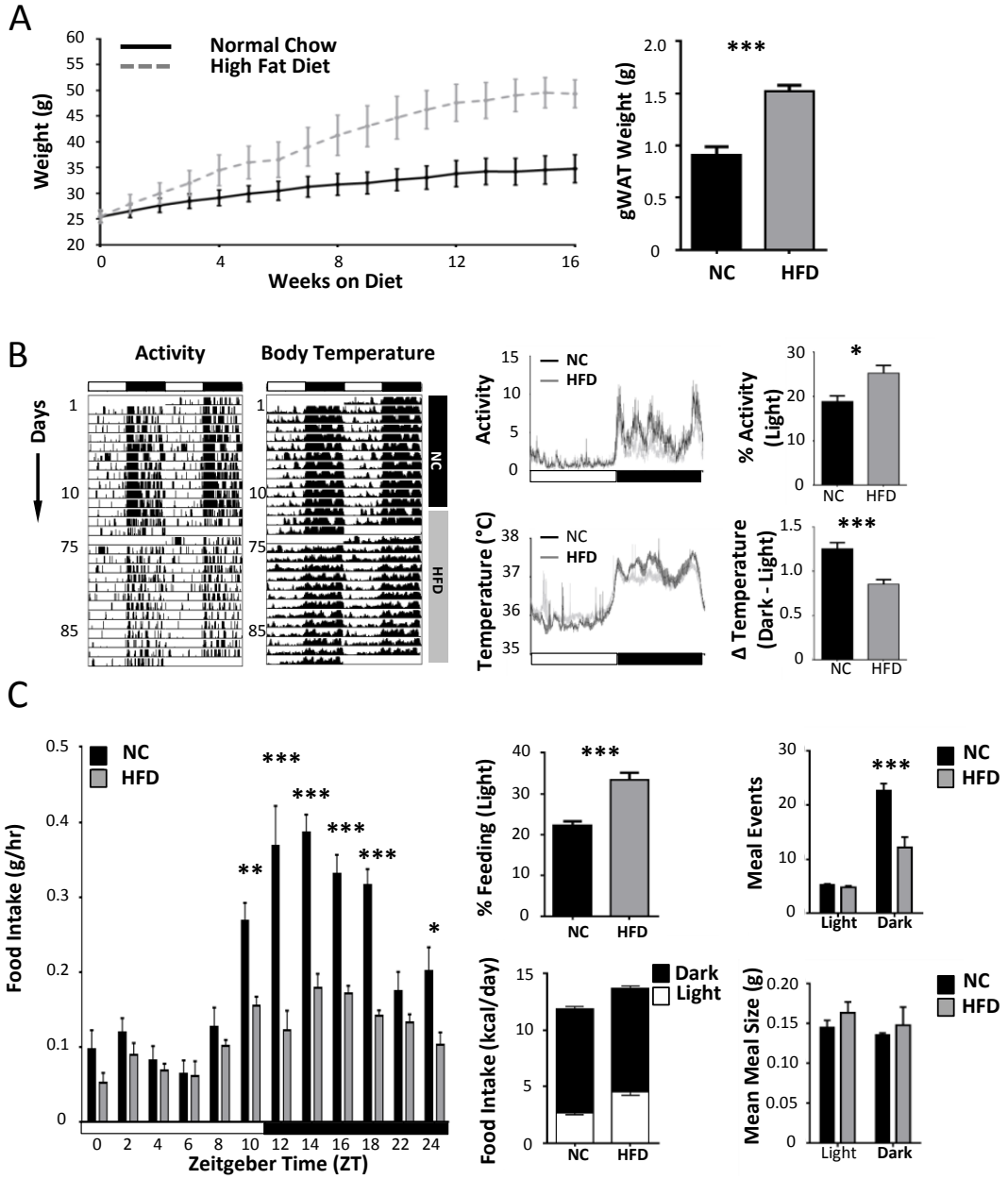

Figure 3.1 – Physiological changes in diet induced obesity.
Male C57BL/6J mice were put on HFD and monitored for 16 weeks (Growth curve = 30-40/ diet). Mice on HFD gained weight and developed obesity with increased accumulation of perigonadal white adipose tissue (A). The impact of HFD on diurnal activity and body temperature rhythms was measured by real time telemetry recording. Data reflect mean ± SEM, * = diet difference, student's unpaired t-test, *** = $p < 0.0005$. (B). Diurnal rhythms are maintained when mice are fed HFD, however, a reduction in activity during the active phase and lower amplitude body temperature rhythms is observed (n=7/diet). Data reflect mean ± SEM, * = diet difference, student's paired t-test, * = $p < 0.05$, *** = $p < 0.0005$. Diurnal feeding structure was then assessed (C). The proportion of calories eaten during the light phase increased upon HFD feeding (n=4-6/diet/timepoint) which was due to a reduction in meal events during the active phase. Meal size (g) is unaffected by HFD feeding during both the light and dark phase. Data reflect mean ± SEM, * = diet difference, student's unpaired t-test or 2-way ANOVA, Sidak post hoc test, * = $p < 0.05$, ** = $p < 0.005$, *** = $p < 0.0005$. *Full description of statistical analysis can be found in Appendix 1.*

collected every 4 hours over the circadian cycle and snap frozen, mRNA was extracted, and for qPCR analyses run for a set of core clock genes. Overall, HFD feeding did not appear to have a dramatic impact on clock gene rhythms in most tissues, with robust clock gene rhythms being observed in both NC and HFD fed mice (Figure 3.2A). For example, no alteration in circadian gene expression was observed in hypothalamic tissue. Interestingly, the adrenal gland and liver showed a phase advance of clock gene rhythms in HFD-fed mice, whereas other tissues showed virtually alteration (e.g. muscle and BAT). This suggests that HFD feeding leads to altered synchrony amongst different tissue clocks.

The most significant attenuation of clock gene expression was observed in gWAT. This attenuation in expression was most notable in *Rev-erbα*, which displayed both lower expression levels and decreased amplitude of the rhythm. In comparison, however, *Rev-erbβ* expression was unaffected by obesity in the animals. Interestingly, clock gene rhythms within scWAT remain largely unaffected by HFD feeding, despite pronounced adipose tissue hypertrophy being observed in both scWAT and gWAT tissue beds. This suggests that HFD-induced disruption of the circadian clockwork is highly tissue-specific and not due to increased lipid storage/tissue expansion *per se*. We next went on to determine if HFD-induced disruption in gWAT clock gene rhythms would be maintained *ex vivo*. gWAT was collected from *mPer2::Luc mice* (Yoo et al., 2004) after 16 weeks NC or HFD (n=3 animals/diet, 12 slices per mouse, collected ZT4) and maintained in culture during which time PER2::Luc driven bioluminescence was recorded using a lumicycle (Actimetrics) (Figure 3.2B). Robust oscillations were observed in tissue derived from mice maintained on NC or HFD; however, oscillations in HFD-fed mouse derived gWAT tissue explants exhibited a significantly lower amplitude in PER2::Luc rhythms ($p<0.05$, student's unpaired t-test. Taken together this data highlights that profound dampening of clock gene rhythms are observed specifically in gWAT.

3.3.3. Effect of obesity of lipid handling genes

Clock gene expression in gWAT was clearly affected by long term HFD-feeding; therefore, we next determined if DIO resulted in dysregulation in the diurnal expression of genes involved in lipid metabolism. A small panel of genes was selected to reflect different aspects of lipid metabolism, all of which have been shown to be under some clock control. The panel of genes

A

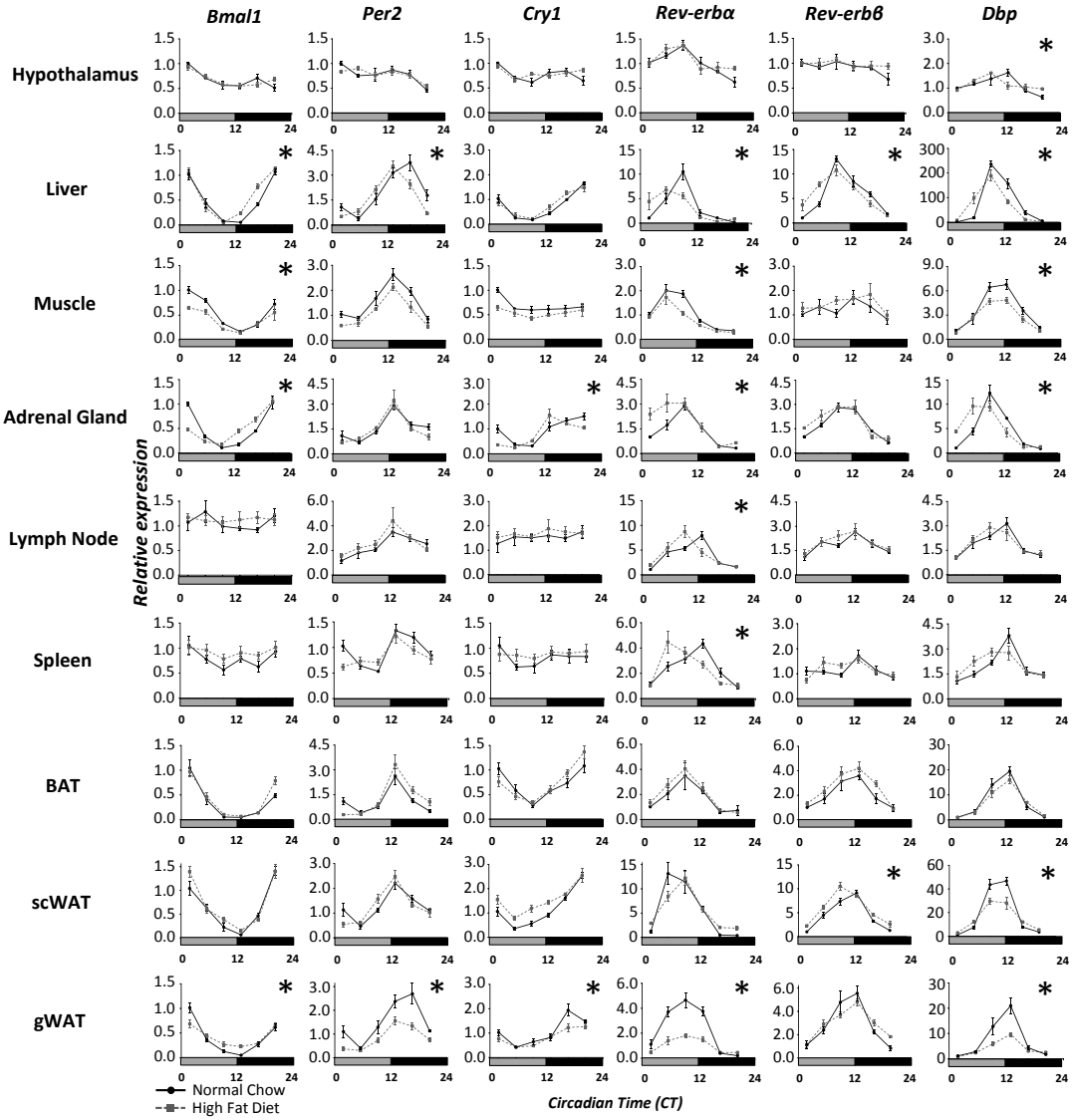
Bmal1
Per2
Cry1
Rev-erbα
Rev-erbβ
Dbp
Hypothalamus
Liver
Muscle
Adrenal Gland
Lymph Node
Spleen
BAT
scWAT
gWAT
Relative expression
Normal Chow
High Fat Diet
Circadian Time (CT)

B

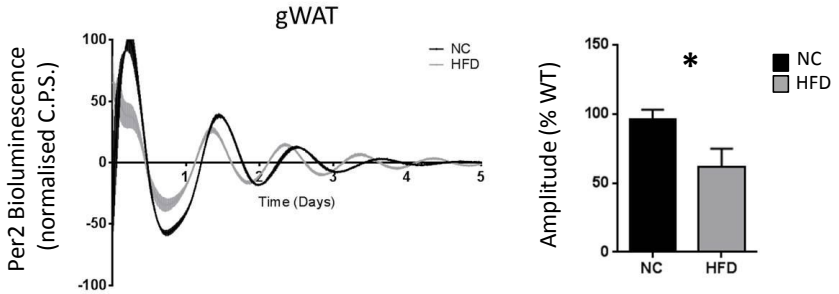
gWAT
Per2 Bioluminescence (normalised C.P.S.)
Time (Days)
NC
HFD
Amplitude (% WT)
NC
HFD

Figure 3.2 – Tissue-specific effects on the molecular clock associated with HFD feeding. Broad analysis clock gene expression over the circadian day was performed in tissues most relevant to circadian regulation, metabolism and inflammation of C57BL/6J mice after 16 weeks of HFD (A, n=4-5/diet/timepoint). Significant differences are observed at a number of individual time-points, in gWAT there is attenuation of clock gene expression with a reduction in amplitude in *Bmal1*, *Dbp*, *Rev-erb α* and *Per2* (* = significant difference between diets at one or more time-points , 2-way ANOVA, * = $p < 0.01$, Sidak post hoc test). *Ex vivo* analysis (B) of the circadian clock in gWAT taken from 16 week HFD challenged mPER2::luc male mice (n=3 – 3 slices per animal/diet) showed decreased amplitude of mPER2::luc oscillation in DIO mice . Data reflect mean ± S.E.M, * = diet difference, student's unpaired t-test, * = $p < 0.05$. *Full description of statistical analysis can be found in Appendix 1.*

consisted of those involved in lipogenesis (*Dgat2, Fasn*), fatty acid transport (*Fabp4*), fatty acid liberation and uptake (*Lpl*) and lipolysis (*Hsl, Atgl*).

From 8 weeks of age, male C57BL6/J mice were maintained on either HFD or NC for 16 weeks (n=30 mice per diet; Tissue samples were the same as those used above for clock gene analysis). Robust rhythms were observed in some lipid handling gene, most notably with *Dgat2* and *Fasn* showing strong circadian variation in gWAT of NC-fed mice (Figure 3.3A). A pronounced, yet highly tissue-specific alteration in metabolic gene expression was observed in response to HFD feeding. HFD-fed mice exhibited an attenuation in the rhythms of *Dgat2* and *Fasn* ($p<0.05$, 2-way-ANOVA) and a dramatic reduction in the expression of most genes examined within gWAT. However, HFD-dependent changes in gene expression were profoundly different among the two fat depots examined (i.e. scWAT and gWAT). The lipolytic genes *Hsl* and *Lpl* were upregulated in scWAT of HFD-fed mice, which contrasts with the profound reduction in expression observed in gWAT. Upregulation of *Dgat2* in scWAT of HFD-fed mice also contrasts with the downregulation measured in gWAT. This most likely reflects differences between gWAT and scWAT. For example, scWAT has a greater long term storage capacity compared to gWAT (Frayn, 2002) and therefore during a positive energy balance, formation of TAGs would be beneficial in this depot. *Fasn* was downregulated in both scWAT and gWAT of HFD-fed mice, reflecting the robust inhibition of *de novo* lipogenesis in states of increased adiposity. A robust rhythm in *Atgl* expression was observed in the liver, which was not affected by HFD feeding. Interestingly, *Hsl* did not show rhythmicity in the liver from NC-fed mice, yet upon HFD-feeding a rhythm was induced (1 way-ANOVA, $p<0.05$). *Fabp4* expression was also upregulated in the liver of HFD-fed mice. gWAT was most dramatically affected by HFD-feeding in terms of both metabolic and clock gene expression, raising the possibility that disruption of the clock in this tissue is linked to metabolic disruption.

We next assessed protein expression of the two of the most rhythmic genes in gWAT – *Dgat2* and *Fasn.* gWAT from the same DIO (16 week HFD) and normal weight mice used for transcript analysis were collected at CT0 and CT12, snap frozen, and protein was extracted for SDS-PAGE and Western Blot analyses (Figure 3.3B). A small time of day difference was observed in FAS expression in NC-fed mice although this did not reach significance. In line with transcript analysis, HFD caused a profound downregulation of FAS protein expression, and loss of any circadian variation. In contrast, no time of day difference was observed in DGAT2, and

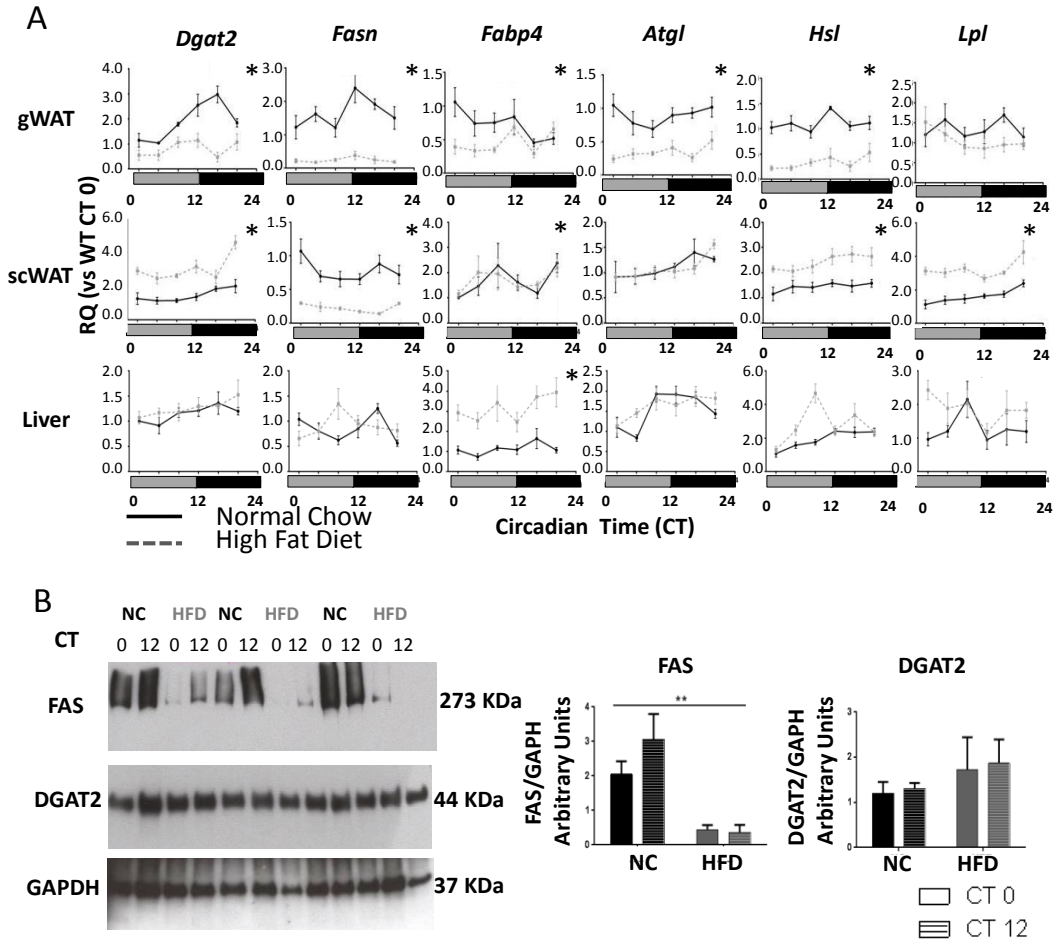

Figure 3.3 – Circadian variation of lipid handling genes differentially affected by HFD feeding in different tissues.

The circadian expression of genes involved in lipid metabolism was examined in gWAT, scWAT and liver from C57BL/6J mice fed HFD (n=25-30/diet) (A). In gWAT HFD challenge resulted in the attenuation of the expression most lipid handling genes, and in the case of *Dgat2* and *Fasn* a dampening of circadian variation. In contrast, *Dgat2, Hsl* and *Lpl* are upregulated in HFD in scWAT (A). *Fabp4* is upregulated in the obese state and HFD challenge potentially induces a rhythm in *Hsl* mRNA. (* = significant difference between diets at one or more time-points, 2-way ANOVA, Sidak post-hoc test, * = $p < 0.01$). Circadian variation in FAS and DGAT2 was not observed upon Western Blot analysis (n=4-5/diet) (B). Data reflect mean ± S.E.M, * = diet difference, 2-way ANOVA, Sidak post-hoc test , * = $p < 0.05$, ** = $p < 0.005$. *Full description of statistical analysis can be found in Appendix 1.*

downregulation of its expression following HFD was not observed at a protein level. Caution must therefore be observed in assuming mRNA levels correlated to protein levels.

3.3.4. Tissue specific reprogramming of the clock-metabolic regulators

We have demonstrated that both clock gene expression and lipid handling gene expression is differentially affected in peripheral tissues by chronic HFD-feeding. *PPARα, PPARγ* and *PGC-1α* are metabolic regulators reciprocally linked with the circadian clock, and therefore we sought to determine the temporal dynamics of their expression in DIO mice (Figure 3.4A). Circadian variation in *Pparα*, *Pparγ* and *Pgc1α* was observed across the panel of tissues, with *Pparα* and *Pparγ* exhibiting robust rhythms in gWAT (2-way ANOVA, $p<0.05$). The expressions of *Pparα*, *Pparγ* and *Pgc1α* were significantly affected by HFD feeding in adipose tissue and liver. Attenuation of the rhythm and downregulation in expression of all three of these metabolic regulators was observed in gWAT. The circadian variation in expression of *Pparα* and *Pgc1α* was also attenuated in scWAT of HFD-fed mice, although overall expression was not reduced. In contrast to gWAT, HFD feeding caused an upregulation of *Pparα* and *Pparγ* in the liver, when compared to control mouse tissue. Analysis of protein expression by Western Blot analyses confirmed the tissue-specific alteration in PPARγ expression, with an increase in expression observed in the liver of mice fed HFD (Figure 3.4B). This is most notably seen in the PPARγ2 isoform. Expression of both PPARγ2 and PPARγ1 were significantly downregulated in mice fed HFD. These data highlight a similar tissue-specific diet-induced reprogramming of circadian clock gene and PPARγ/PPAR*α* expression in mice fed HFD, suggesting that these changes may be directly linked.

3.3.5. Effect of obesity on glucose handling genes

PPARs are major regulators of glucose handling. We therefore examined the expression profiles of *Glut2/4, Gk* (liver)*/Hk* (gWAT, muscle), *Pepck* in NC and HFD fed mouse tissues (Figure 3.5). Robust rhythms were observed in *Glut4*, *Gk* and *Pepck* in the liver of mice fed NC. Rhythmic expressions of *Glut4* and *Gk* were dampened in the liver of HFD-fed mice (2-way ANOVA, $p<0.05$). In contrast, no loss of rhythmicity was observed in *Pepck*. The expression of these genes did not vary across the circadian cycle in muscle, but HFD-feeding did cause a significant downregulation in all three. Rhythmic expression profiles of *Glut4, Hk* and *Pepck*

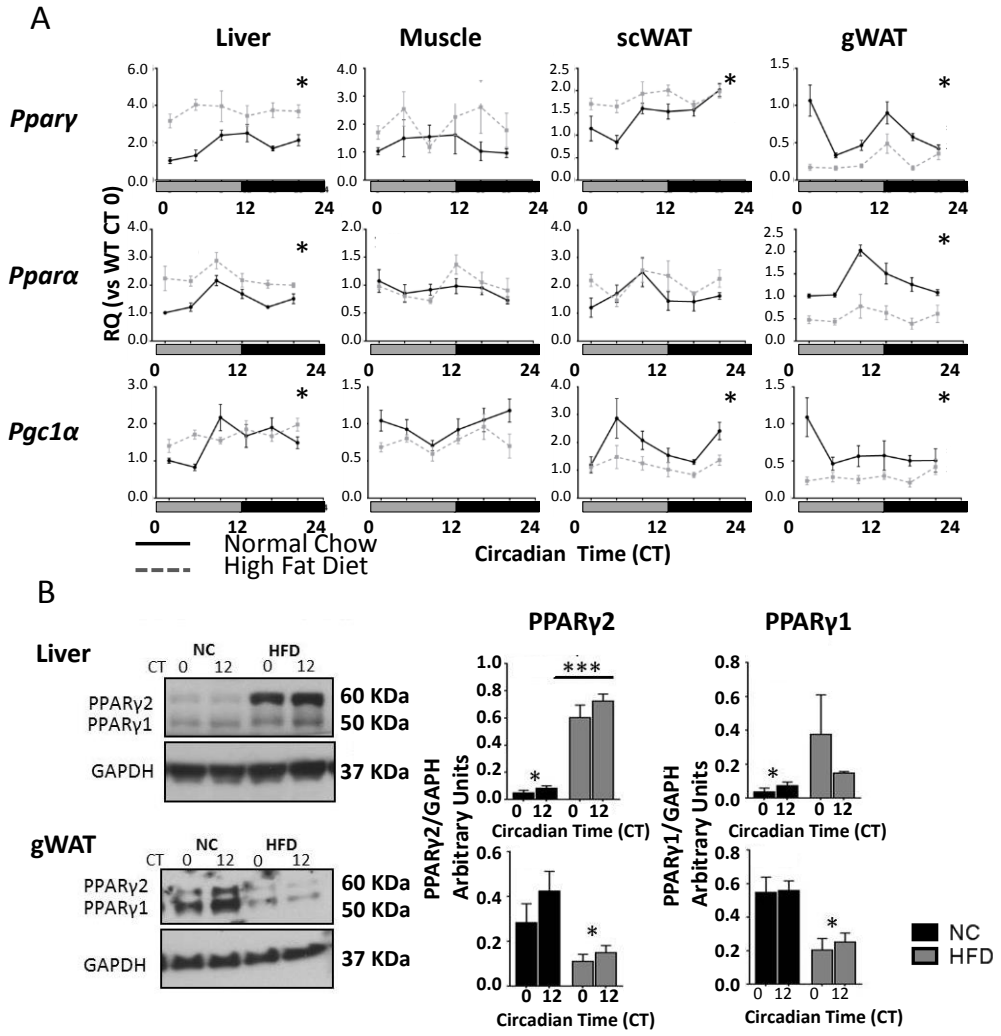

Figure 3.4 – Disruption of downstream pathways is affected in a tissue-specific manner by High Fat Diet feeding.

Expression of key transcriptional regulators of metabolism PPARα, PPARγ and PGC1α in liver, muscle, scWAT and gWAT of C57BL/6J male mice fed HFD for 16 weeks (n=25-30/diet). *PPAR*γ expression was significantly increased in the liver of those animals fed HFD as dis *PPAR*α (A). The expression of these regulators was unaffected by HFD feeding in muscle. The temporal expression of *PPAR*γ and *PGC1*α is affected by HFD feeding in subcutaneous WAT and in gWAT expression of PPARγ, *PPARα* and *PGC1*α was reduced and dampened. Data reflect mean ± S.E.M, * = difference between diets at one or more time-points, 2-way ANOVA, Sidak post-hoc test, * = $p < 0.01$). These tissue specific changes in expression of PPARγ were confirmed by protein expression analysis by immunoblot (gWAT n=9-10/diet, liver n=4-5/diet) (B). Data reflect mean ± SEM, * = diet difference, 2-way ANOVA, Sidak post-hoc test, * = $p < 0.05$, ** = $p < 0.005$, *** = $p < 0.0005$. *Full description of statistical analysis can be found in Appendix 1.*

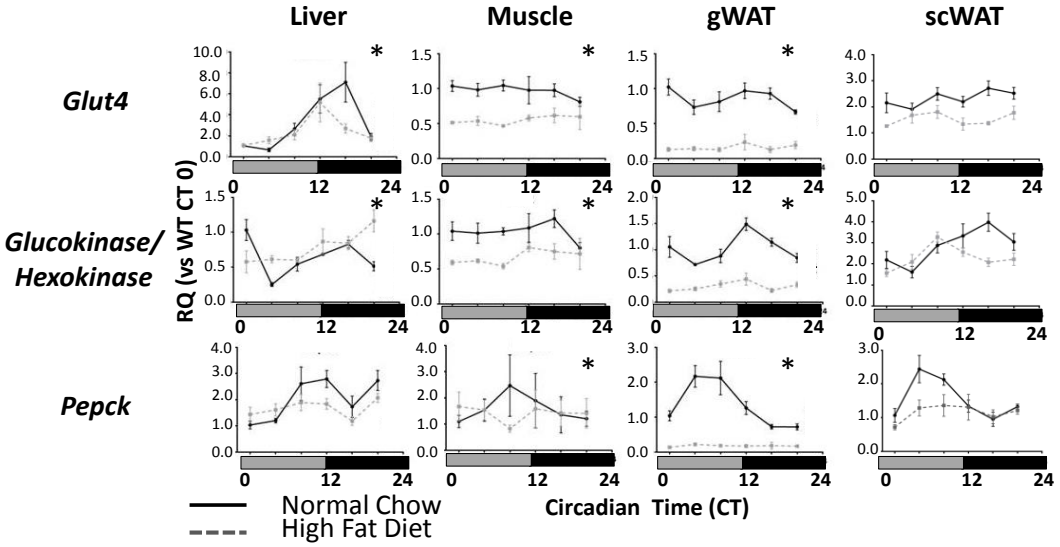

Figure 3.5 – Diurnal variation of glucose handling genes differentially affected by HFD feeding in different tissues.

The rhythmicity and expression of glucose handling genes was also assessed in liver, muscle, gWAT and scWAT (n=25-30/diet). Strong circadian variation was seen in *Glut4, GK* and *Pepck* in the liver under both diet conditions. These genes showed little diurnal variation in muscle with slight attenuation of expression. In gWAT, diurnal variation is seen under NC conditions but in HFD expression of *Glut4, HK2* and *Pepck* is greatly attenuated with a loss of rhythm. This is not reflected in scWAT tissue. Data reflect mean ± S.E.M, * = $p < 0.01$, * = difference between diets at one or more time-points , 2-way ANOVA, Sidak post-hoc test). *Full description of statistical analysis can be found in Appendix 1.*

were observed in gWAT of NC-fed mice, and dramatic damping and downregulation in expression of all three was observed in response to HFD-feeding. A similar effect was observed in scWAT, although to a lesser extent than observed in gWAT (which failed to reach statistical significance). Thus, as observed in circadian and lipid handling pathways, the impact of chronic HFD-feeding on this subset of rhythmic glucose metabolism genes was highly tissue-specific manner, with the most dramatically effects on gene rhythmicity observed in gWAT.

3.3.6. Damping of gene rhythmicity in gWAT associated with the development of obesity and tissue inflammation

Obesity is often associated with an increased inflammatory state, especially in WAT. Moreover, inflammation has been previously linked to clock disruption (Castanon–Cervantes *et al.,* 2010). Indeed, as shown in Figure 3.6A, the levels of inflammatory markers (*TNFα* and *F4/80*) were significantly increased in mice fed HFD for 16 weeks. The increase in *TNFα* and *F4/80* (indicative of macrophage/monocyte content) was particularly pronounced in gWAT of HFD-fed mice (Figure 3.6A). No effect of diet was observed in inflammatory marker gene expression in the lymph nodes or the spleen. We then investigated the timing of DIO-induced inflammation. Male C57BL/6J mice were maintained on HFD for 2 weeks (n=5), 8 weeks (n=5), 16 weeks (n=5), following which gWAT was collected at CT0 and CT12 and mRNA extracted for qPCR analysis (Figure 3.6B). Although a decrease in amplitude was observed in *Bmal1* expression at 8 and 16 week of HFD-feeding, the gene retained a significant circadian variation at all time-points. As shown in above (Figure 3.2), *Rev-erbα* expression was profoundly reduced after 16-weeks HFD-feeding; however, this was not observed after 2 or 8 weeks of HFD-feeding. This demonstrated that HFD-feeding *per se* does not drive attenuated clock gene expression, but that it is the chronic nature of this feeding and likely the resultant obesity that leads to clock disruption. Similarly to *Rev-erbα*, attenuation reduced *Pparα* and *Pparγ* expression only occurred after 16-weeks HFD feeding.

3.4. Summary

HFD-feeding for 16 weeks did not profoundly disrupt behavioural rhythms in C57BL/6 mice, at least not in an LD environment. This contrasts data obtained by Kohsaka *et al*. (2007) which

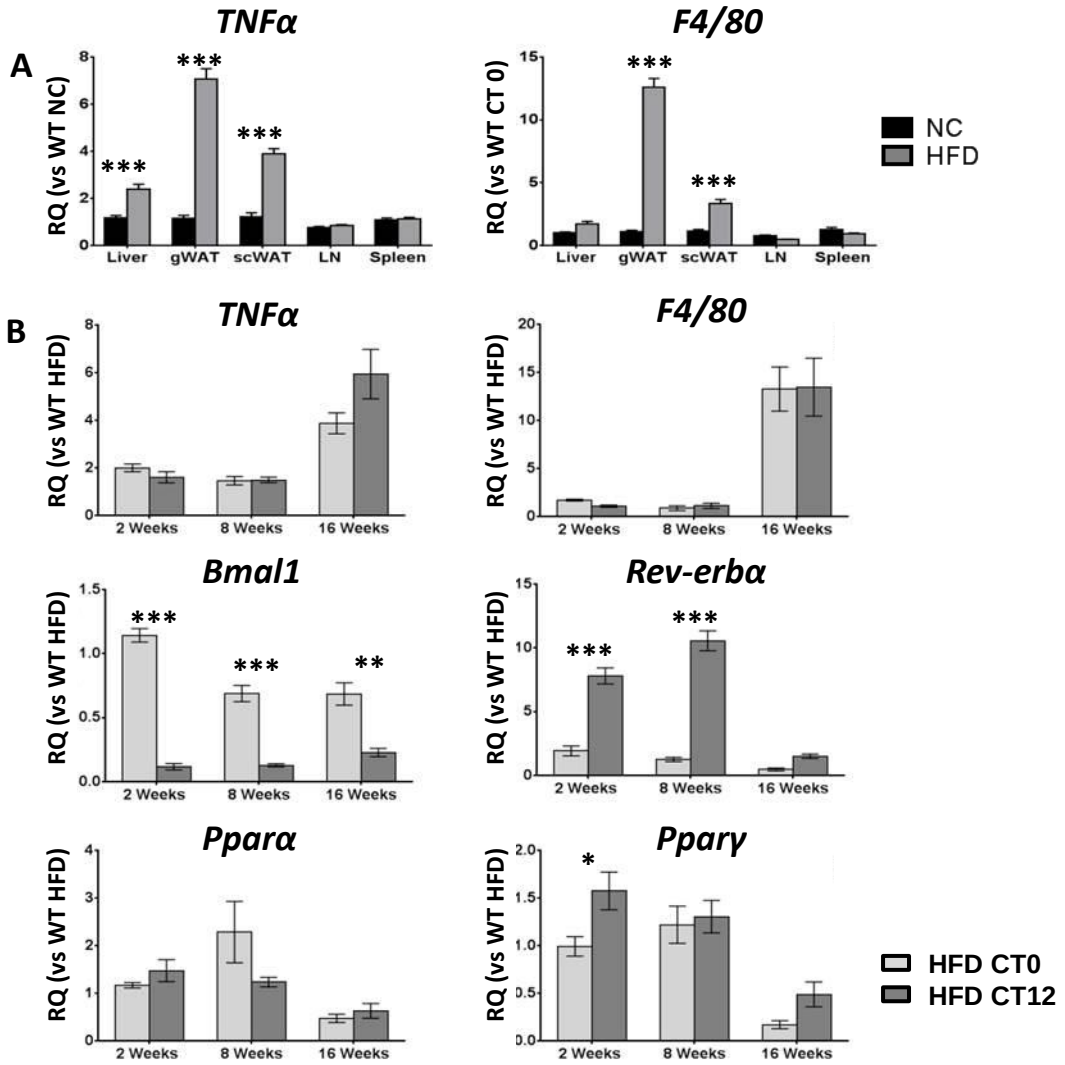

Figure 3.6 – Attenuation of the clock in gWAT was acutely affected by HFD feeding and associated with increased inflammation.

F4/80 and TNFα expression levels were measured in a range of tissues of C57BL/6J mice fed HFD for 16 weeks (n=25-30/diet). Inflammation was highest in gWAT of HFD challenged animals which links to the breakdown of the clock in this tissue (A). Data reflect mean ± S.E.M, * = diet difference, student's unpaired t-test, *** = $p < 0.0005$. Mice maintained on HFD for 2 and 8 weeks showed no attenuation of *Bmal1* and *Rev-erbα* expression when compared to the 16 week HFD animals (n=4-5/diet/time). This lack of attenuation also correlated with low levels of inflammatory markers TNFα and F4/80 at that time. Attenuation of *PPARγ* and *PPARα* expression in gWAT was also only seen after 16 weeks HFD (B). Data reflect mean ± SEM, normalised to NC mice in each case (data not shown), * = time of day difference, student's unpaired t-test, * = $p < 0.05$, ** = $p < 0.005$, *** = $p < 0.0005$. *Full description of statistical analysis can be found in Appendix I.*

demonstrated that HFD resulted in dampened diurnal rhythm of locomotor activity selectively in LD conditions as equivalent levels of activity and preserved amplitude was observed in activity rhythms in DD conditions. However, our studies do indicate reduced amplitude of day/night body temperature and flattening of calorie intake across the day, which are important zeitgebers.

These studies revealed a pronounced disruption of the circadian clockwork in gWAT. This parallels data obtained from Kohsaka *et al*. (2007) and Prasai *et al*. (2013), whose work demonstrated that the amplitude of clock gene expression rhythms was severely attenuated in fat with a smaller effect in liver. Clock gene rhythms in gWAT are more susceptible to obesity related dysfunction compared to scWAT, likely representing depot-specific differences in the metabolic and inflammatory response to obesity-related hypertrophy. *Rev-erbα* is downregulated throughout the circadian series and shows the strongest attenuation of rhythm in the DIO model. Together this data may suggest that the right regulation of the *Rev-erbα* 'auxiliary' loop may be of critical importance for metabolic homeostasis in gWAT.

Damping of *Bmal1* and *Rev-erbα* expression in gWAT was not observed following 2 or 8 weeks of HFD-feeding, and was most pronounced in mice that had been maintained on HFD for 16 weeks. The time scale of HFD-feeding required to bring about clock disruption (16 weeks) also reflected the length of time at which inflammatory markers, *TNFα* and *F4/80,* were dramatically upregulated. This may be indicative that obesity related inflammation may be responsible for clock breakdown, as although no diurnal variation is observed in these inflammatory markers at any point during the development of obesity, upregulation is observed at 16 weeks when loss of diurnal variation of the clock is observed.

Interestingly, a similar attenuation in *Pparα* and *Pparγ* expression was observed in gWAT in response to DIO. Given that PPARα/γ receptors are both regulated by the clock, yet also feed-back directly onto the clock through transcriptional regulation (Peek *et al*., 2012; Chen and Yang, 2014) it seems likely that the disruption of these pathways are linked. Our studies support the PPARs as a potential interface between the metabolic challenge and the disruption of the clock. *Pparγ* has been shown to be essential for the survival of mature adipocytes (Imai *et al*., 2004). Eckel Mahan *et al.* (2013) demonstrated that HFD feeding generated a profound reorganisation of specific metabolic pathways, leading to widespread remodelling of the liver clock. In this study, HFD also resulted in *de novo* oscillating transcripts due to the pronounced

cyclic activation of pathways through PPARγ. A further study, in which diurnal feeding reversed from the active to the rest phase, resulted in increased FFA and glycogen levels. Increased FFA levels resulted in enhanced *Pparα* activation which resulted in aberrant activation of *Rev-erbα* and *Per2* (Mukherji *et al.,* 2015). It is therefore possible that chronic positive energy balance leads to PPAR dysregulation which in turn drives Clock/Rev-erb dysregulation. This may also result in dyschrony of peripheral body clocks, for example between the liver and adipose clock.

Although altered PPAR signalling and/or local tissue inflammation are likely to play a role, additional studies are required to fully elucidate events and molecular pathways which lead to attenuated clock function in gWAT during obesity. Importantly, it also remains to be determined whether loss of robust circadian rhythms in WAT contributes to obesity-related metabolic dysfunction, such as insulin resistance. The studies outlined in this chapter revealed *Rev-erba* to be particularly attenuated in gWAT of obese mice. In the chapter 4, we examine specifically how genetic targeting of *Rev-erbα* impacts on metabolic function.

Results

Chapter 4 - Loss of *Rev-erbα* results in an obese phenotype and severe dysregulation of lipid handling in the mouse

4.1. Introduction

Rev-erbα is an important regulator of the circadian clock. In addition, this nuclear hormone receptor has been implicated in numerous metabolic pathways, including lipid metabolism and bile acid homeostasis in the liver (Raspe *et al*., 2002; Le Martelot *et al.* 2009), adipocyte differentiation (Fontaine *et al*., 2003; Wang and Lazar, 2008) and insulin secretion (Viera *et al*., 2012). Beyond the circadian clock, REV-ERBα binds to over 14,000 genomic locations in the liver at ZT10 when its expression peaks, but binds to very few at ZT22 when its expression is the lowest (Feng *et al*., 2011). A large number of the genes loci to which *Rev-erbα* binds are involved in lipid metabolism, including for example >100 genes involved in lipid biosynthesis such as *Fasn* (Feng *et al*., 2011). REV-ERBα recruits a repressive complex, which includes NCoR1 and HDAC3, which drives diurnal variation in histone acetylation and gene expression required for normal hepatic lipid homeostasis (Feng *et al*., 2011).

Rev-erbα also functions as a sensor for the metabolic state of the cell. Heme binds reversibly to *Rev-erbα* and regulates its interaction with a nuclear receptor corepressor complex. Heme also suppresses hepatic gluconeogenic gene expression and glucose output through *Rev-erbα*-mediated gene expression. Therefore, by acting as a heme sensor, *Rev-erbα* coordinates the cellular clock, glucose homeostasis and energy metabolism, entraining the clock to metabolic cues (Yin *et al*., 2007). Recent work also provides further evidence that *Rev-erbα* is central to the entrainment of peripheral tissue clocks to restricted feeding. Restricted feeding in mice results in hypoinsulinemia during the active phase, causing increased FFA and glucagon levels which in turn leads to the activation of PPARα and CREB, respectively, and consequently aberrant activation of expression of *Rev-erbα* is observed. Moreover, hypoinsulinemia leads to an increase in glycogen synthase kinase 3β (GSK3β) activity and through phosphorylation this stabilizes and increases the level of the REV-ERBα protein (Mukherji *et al*., 2015). Chapter 3 also highlighted *Rev-erbα* as being particularly affected by chronic HFD feeding further supporting the fact that its expression regulated by the metabolic state of the animal.

Recent studies have also shown that *Rev-erbα* plays an important role in regulating cholesterol and bile acid metabolism in the liver (Duez *et al.* 2008). *Rev-erbα*-deficient mice display a lower synthesis rate and an impaired excretion of bile acids into the bile and faeces. CYP7A1, a rate-limiting enzyme of the neutral pathway, exhibits decreased expression in the livers of *Rev-erbα*-deficient mice, but when *Rev-erbα* is overexpressed in the liver expression of CYP7A1 is induced. By means of either overexpression or deletion of *Rev-erbα,* Le Martelot *et al.* showed

that *Rev-erbα* drives circadian rhythms in sterol regulatory element binding protein (SREBP) activity and therefore the daily expression of SREBP target genes involved in cholesterol and lipid metabolism (2009). This occurs via the cyclic transcription of *Insig2*, a gene that encodes a trans-membrane protein that sequesters SREBP proteins to the endoplasmic reticulum membranes and thereby interferes with activation of SREBPs in Golgi membranes. Le Martelot *et al.* (2009) also demonstrated that circadian control of REV-ERBα on CYP7A1 involves LXR.

Mice lacking *Rev-erbα* display an altered balance between carbohydrate and lipid fuel usage (Delezie *et al*., 2012). Specifically, indirect calorimetry studies suggest that chow-fed *Rev-erbα* knockout mice utilise more fatty acids during the daytime (Delezie *et al*., 2012). When these mice are fasted for 24 hours, further fatty acid mobilisation at the expense of glycogen utilization and gluconeogenesis is observed, yet without triggering hypoglycaemia and hypothermia. A role for *Rev-erbα* has also been implicated in maintenance in rhythms in BAT thermogenesis (Gerhart-Hines *et al*., 2013). Uncoupling protein 1 (UCP1) is BAT-specific transport protein of the inner mitochondrial membrane is a canonical thermogenic regulator. *Rev-erbα* represses UCP1 expression. UCP1 is physiologically induced by cold temperature and this induction is preceded by rapid downregulation of *Rev-erbα* in BAT. As *Rev-erbα* represses UCP1 expression, mice lacking *Rev-erbα* show attenuated temperature oscillations. The circadian expression of *Rev-erbα* is in antiphase with body temperature and mice exposed to cold at ZT22 display a higher survival rate when *Rev-erbα* is barely expressed than at ZT 10 when *Rev-erbα* is abundant.

Given the tight coupling of *Rev-erbα* and energy metabolism, and our observation of pronounced decreased in *Rev-erbα* during DIO, we sought to further understand how altered *Rev-erbα* expression may contribute to obesity and its co-morbidities.

4.2 Methods

Detailed methodological approaches can be found in the methods (Chapter 2). Below are specific experimental details. For some studies, male/female only cohorts were used due to the difficulty generating sufficient numbers of males. WT controls were C57BL/6 *Rev-erbα*$^{+/+}$.

Activity rhythms were assessed in male *Rev-erbα*$^{-/-}$ mice and WT littermates (n=5/genotype) using Wheel Running. For *ex vivo* analysis of circadian rhythms, male *Rev-erb*$^{-/-}$mice were bred against *mPER2::Luc* reporter mice (Yoo *et al.,* 2002). Bioluminescence was recorded from

gWAT, liver and lung samples collected from *Rev-erb*$^{-/-}$ mice and wild-type littermates, maintained in DMEM recording media at 37°C using a Lumicycle (actimetrics). Amplitude of mPER2-dependent luminescence was determined for each animal (n=3/genotype) using the mean of 5 samples/tissue/mouse. For circadian transcript analysis, male mice were placed in constant darkness (DD) for 24h, following which gWAT was collected every 4h (n=8/time-point/genotype).

Basal metabolic gas exchange was measured in male *Rev-erbα*$^{-/-}$ mice and WT littermates by indirect calorimetry using the CLAMS system (Columbus Instruments) (n=4/genotype). Basal transcript analysis was also performed on tissues collected from sacrificed male *Rev-erbα*$^{-/-}$mice and WT littermates (n=9-14/genotype).

For negative energy balance studies, mice were either fasted for 24 or 48 hours. Physiological response to fasting (weight loss, food intake post fast, biochemical serum analysis) was monitored in male *Rev-erbα*$^{-/-}$mice and WT littermates (n=6/genotype). Metabolic gas exchange was measured in male *Rev-erbα*$^{-/-}$ mice and WT littermates fasted for 48 hours using the CLAMS system (n=4/genotype). Male *Rev-erbα*$^{-/-}$ mice and WT littermates were also sacrificed in either their fed, 24h or 48h fasted state in order to perform transcript analysis (n=5-6/genotype/challenge).

For the lipolytic challenge male *Rev-erbα*$^{-/-}$mice and WT littermates (n=4/genotype/treatment) were injected I.P. with either 0.1 or 1 mg/kg of CL316,243 (Sigma Aldrich) or saline as a control. At the termination of the experiment (4 hours post injection), mice were sacrificed and tissues collected for protein/transcript analysis. Before lipogenic challenge mice were fasted for 6 hours. Male *Rev-erbα*$^{-/-}$ mice and WT littermates (n=5/genotype/treatment) were then injected I.P. with either 0.75 U/kg insulin or saline as a control. Blood samples, by means of tail bleeds, were taken before and 4 hours post stimulation for biochemical analysis. Mice were sacrificed 4 hours post stimulation and tissues collected for transcript/protein analysis.

For DIO studies, 8 week old female mice were provided *ad libitum* access to high fat diet (HFD; 60% energy from fat; DIO Rodent Purified Diet, IPS Ltd) or normal chow (NC) for 14 weeks (n=8/genotype/diet). Body weights and food intake were monitored in these animals and ITT/GTT tests were performed. Upon sacrifice, a range of tissues were taken for protein and transcript analysis as well as gWAT for *ex vivo* studies. For *ex vivo* studies, gWAT was minced and maintained in DMEM supplemented with FBS and penicillin/streptomycin before being stimulated with insulin and subsequently collected for transcript analysis.

4.3 Results

4.3.1. Rhythmicity in locomotor activity and local tissue clocks in *Rev-erbα*$^{-/-}$ mice

As previously demonstrated (Preitner *et al*., 2002), mice which lack *Rev-erbα* retain a functional clockwork, albeit with an accelerated circadian period of activity rhythms under free running conditions. This was confirmed in our line of *Rev-erbα*$^{-/-}$ mice (Figure 4.1A), which exhibited robust entrainment of wheel-running activity rhythms to a 12:12hr LD cycle, and displayed a shortened period once released into constant darkness (DD) (male mice, n=5 per genotype). To gain a further understanding of the circadian clock function in individual peripheral tissues, *Rev-erbα*$^{-/-}$ mice were bred against *mPER2::Luc* reporter mice (Yoo *et al.,* 2004). Tissues were collected from *Rev-erb*α$^{+/+}$ (WT) and *Rev-erb*α$^{-/-}$ littermates (male mice, n=3 mice/genotype, 5 samples/tissue/mouse, collected at ZT4) and maintained in culture during which time mPER2::Luc driven bioluminescence was recorded (Figure 4.1B). Amplitude was assessed by measuring height of second peak to height of the second trough. Robust circadian oscillations were observed in all tissues for both genotypes; however, the amplitude of PER2::Luc rhythms was significantly reduced in gWAT derived from *Rev-erb*α$^{-/-}$ mice (2.6 fold reduction, $p<0.001$, student's t-test) when compared to WT mouse-derived tissue. A small but significant attenuation in the amplitude of bioluminescence was also observed in the liver of *Rev-erb*α$^{-/-}$ mice (1.4 fold reduction, $p<0.01$, student's t-test) with no effect of the loss of *Rev-erb*α$^{-/-}$ observed in the lung.

To examine whether the attenuation of the clock gene rhythms in gWAT of *Rev-erbα*$^{-/-}$ mice was also evident *in vivo*, mRNA expression was quantified in gWAT collected at 6 time-points across the circadian cycle from WT and *Rev-erbα*$^{-/-}$ mice (male mice, n=4/time-point/genotype; Figure 4.1C). A strong de-repression of *Bmal1* expression was observed in *Rev-erb*α$^{-/-}$ tissue ($p<0.01$, 2-way ANOVA, Sidak post-hoc), consistent with the normal role of REV-ERBα in transcriptional repression of *Bmal1*. In line with *ex vivo* recording, *Per2* expression in gWAT was damped in the KO mice ($p<0.01$, 2-way ANOVA, Sidak post-hoc). The extent of PER2 dampening was more pronounced in *ex vivo* bioluminescence recording, suggesting perhaps, that the impact of *Rev-erbα* deletion may be minimised by systemic synchronisation or entrainment cues. In contrast, the circadian rhythm of *Dbp* expression was not dampened in gWAT of *Rev-erbα*$^{-/-}$ mice, and in fact an increase in expression was observed ($p<0.01$, 2-way ANOVA, Sidak post-hoc).

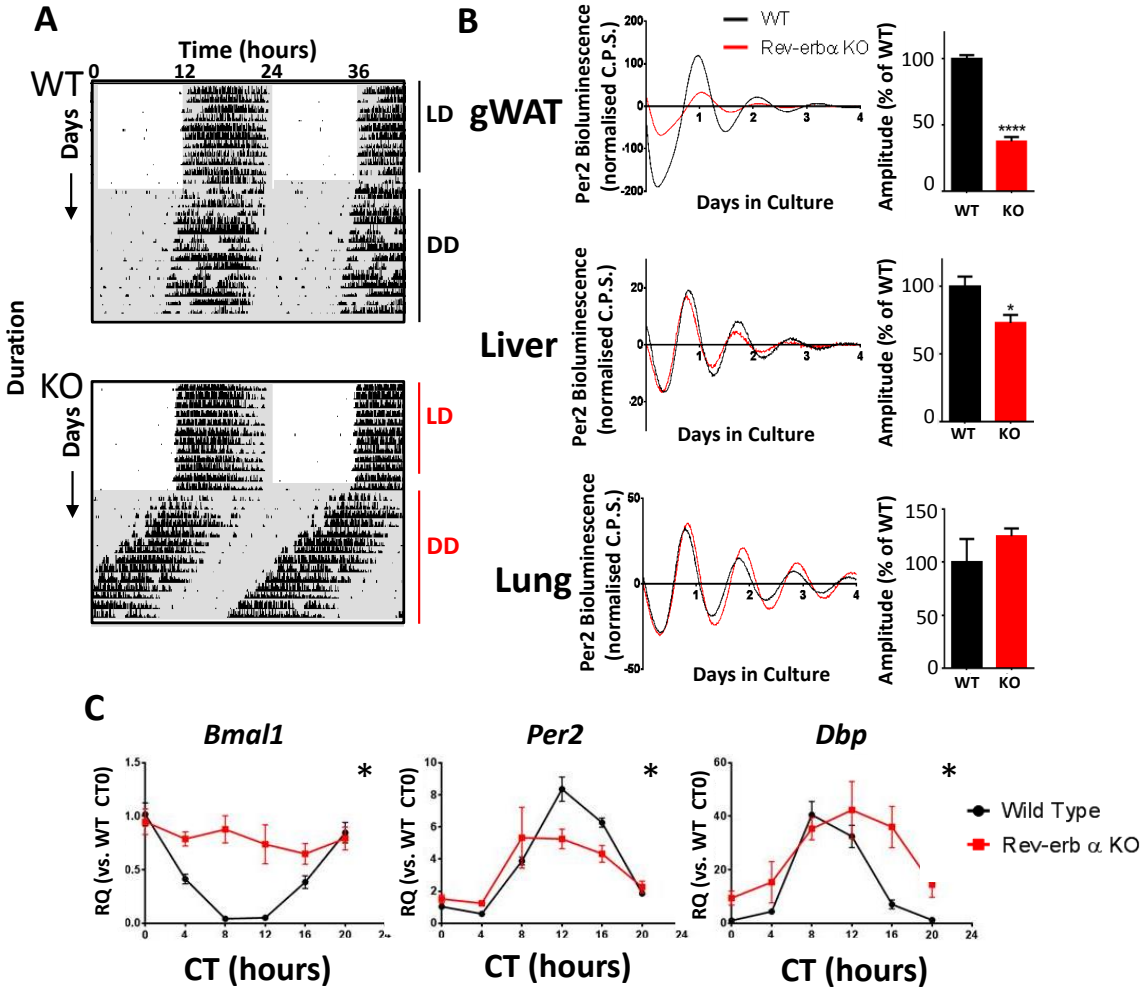

Figure 4.1– Circadian rhythmicity in *Rev-erbα*$^{-/-}$ mice.

Activity rhythms were assessed in male *Rev-erbα*$^{-/-}$ mice and WT littermates (n = 5 per genotype) in both LD and DD. WT animals showed strong activity rhythms in LD which were maintained in DD. Despite loss of *Rev-erbα*, KO animals remained rhythmic in LD but had a shorter period in DD (A). *Ex vivo* analysis of the circadian clock (B) in gWAT, liver and lung in male KO animals and their WT littermates bred on an mPER2::luc background (n=3 per genotype) showed severely decreased amplitude of mPER2::luc oscillation in gWAT and a slight dampening in liver. Amplitude is expressed as a % of WT bioluminescence based on an average of three oscillations from each mouse. Data reflect mean ± S.E.M., * = genotype difference, student's unpaired t-test, *= $p < 0.01$, **** = $p<0.00001$. The diurnal expression of clock genes (C) was examined in gWAT from male *Rev-erbα* KO mice and WT littermates (n= 8 per genotype). This loss of *Rev-erbα* resulted in an attenuation of *Bmal1* and *Per2* with decreased amplitude of the oscillations and a possible phase shift of *Dbp* expression. Data reflect mean ± S.E.M., * = significant difference between genotypes at one or more time points, 2-way ANOVA, Sidak post-hoc test, * = $p < 0.01$). *Full description of statistical analysis can be found in Appendix 2.*

Nonetheless, despite the fact that *Rev-erbα*$^{-/-}$ mice maintain robust circadian rhythms in locomotor activity, local tissue clocks appear compromised with gWAT being particularly affected by deletion of this clock component.

4.3.2. Metabolic phenotype of *Rev-erbα*$^{-/-}$ mice

Given the strong effect of diet-induced obesity on *Rev-erb*α expression in many tissues including WAT (Figure 3.2), and altered clock gene rhythms in the adipose tissue of *Rev-erbα*$^{-/-}$ mice, we next characterised the metabolic phenotype of these mice. *Rev-erb*α$^{-/-}$ mice and WT littermates exhibited little difference in body weight up to 16 weeks of age (n=15-20/genotype; Figure 4.2A). However, despite the similarity in body weight, these mice showed a significant increase in fat pad weight, with gWAT mass ~2 fold higher than that observed in WT littermates (gWAT – WT: 0.018 ± 0.002 g/g BW, *Rev-erbα*$^{-/-}$ 0.034 ± 0.005 g/g BW; scWAT – WT: 0.009 ± 0.002 g/g BW, *Rev-erbα*$^{-/-}$ 0.013 ± 0.003 g/g BW). The increased adiposity observed in the *Rev-erb*α$^{-/-}$ mice was not due to an increase in food intake relative to WT mice, as no significant difference was observed in total daily food intake, or in the proportion of food consumed during the day and during the night (Figure 4.2B).

We next examined energy expenditure and metabolic rate in *Rev-erbα*$^{-/-}$ mice and control littermates using indirect calorimetry (n=4/genotype). A pronounced diurnal variation in oxygen consumption (VO_2) and carbon dioxide production (VCO_2) was observed in WT mice, with elevated VO_2 and VCO_2 associated with the active (dark) phase of the day (Figure 4.3). Interestingly, *Rev-erbα*$^{-/-}$ mice were found to have a damped diurnal rhythm in oxygen consumption, with no significant difference observed in mean VO_2 across the light and dark phases of the cycle. Lack of statistical significance between mean daytime and night-time VO_2 in the KO mice was likely due to an increase in daytime bouts of elevated VO_2 evident in these mice. A damping in rhythmicity was also observed in respiratory exchange rate (RER) profile from *Rev-erbα*$^{-/-}$ mice, with significant diurnal variation observed in WT mice ($p<0.001$, 2-way ANOVA) but not in KO animals (Figure 4.3). A significant difference between genotypes was not observed however. Diurnal rhythms in VCO_2 were observed in both genotypes, although VCO_2 in the light phase was significantly increased in the KO mice when compared with WT littermates ($p<0.01$, 2-way ANOVA; Figure 4.3). Measures of energy expenditure (kcal/hr) were not different between genotypes, and exhibited robust diurnal variation in both genotypes (Figure 4.3). Although all metabolic parameters showed diurnal variation in *Rev-*

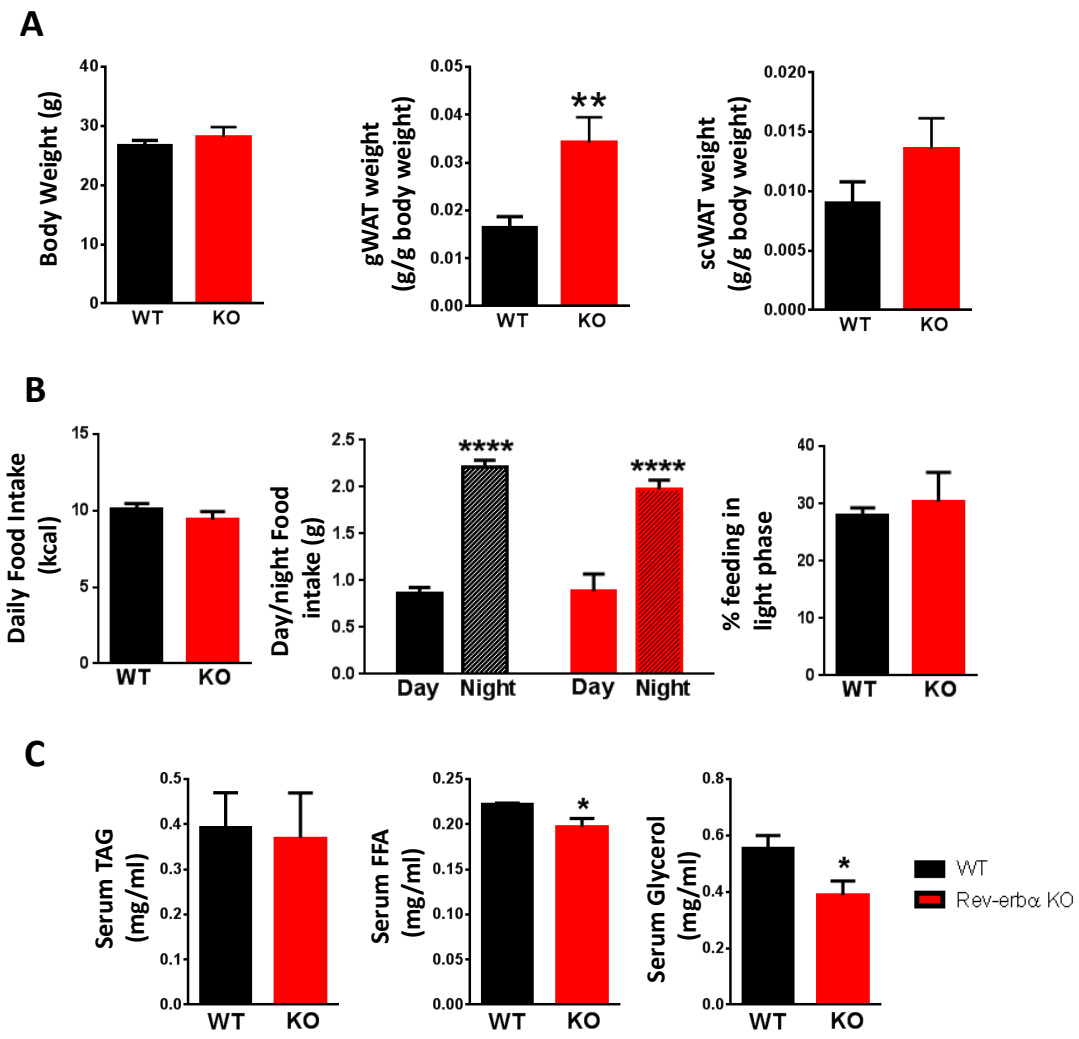

Figure 4.2 - Physiological and behaviour changes in *Rev-erbα*$^{-/-}$ mice.
Despite no difference in body weight (female mice, n=15-20 per genotype), *Rev-erbα*$^{-/-}$ mice have increased gWAT and scWAT. (A) No difference in food intake was observed in these mice (average of 3 days, n=4-8/genotype), with the majority of feeding taking place during the dark phase (B). Serum analysis of blood collected at ZT 6 showed decreased FFA and Glycerol levels in *Rev-erbα*$^{-/-}$ mice (C). Data reflect mean ± S.E.M., * = genotype difference (student's unpaired t-test) or time difference (2-way ANOVA, sidak post hoc test, *= $p < 0.01$, **= $p < 0.001$, **** = $p<0.00001$ *Full description of statistical analysis can be found in Appendix 2.*

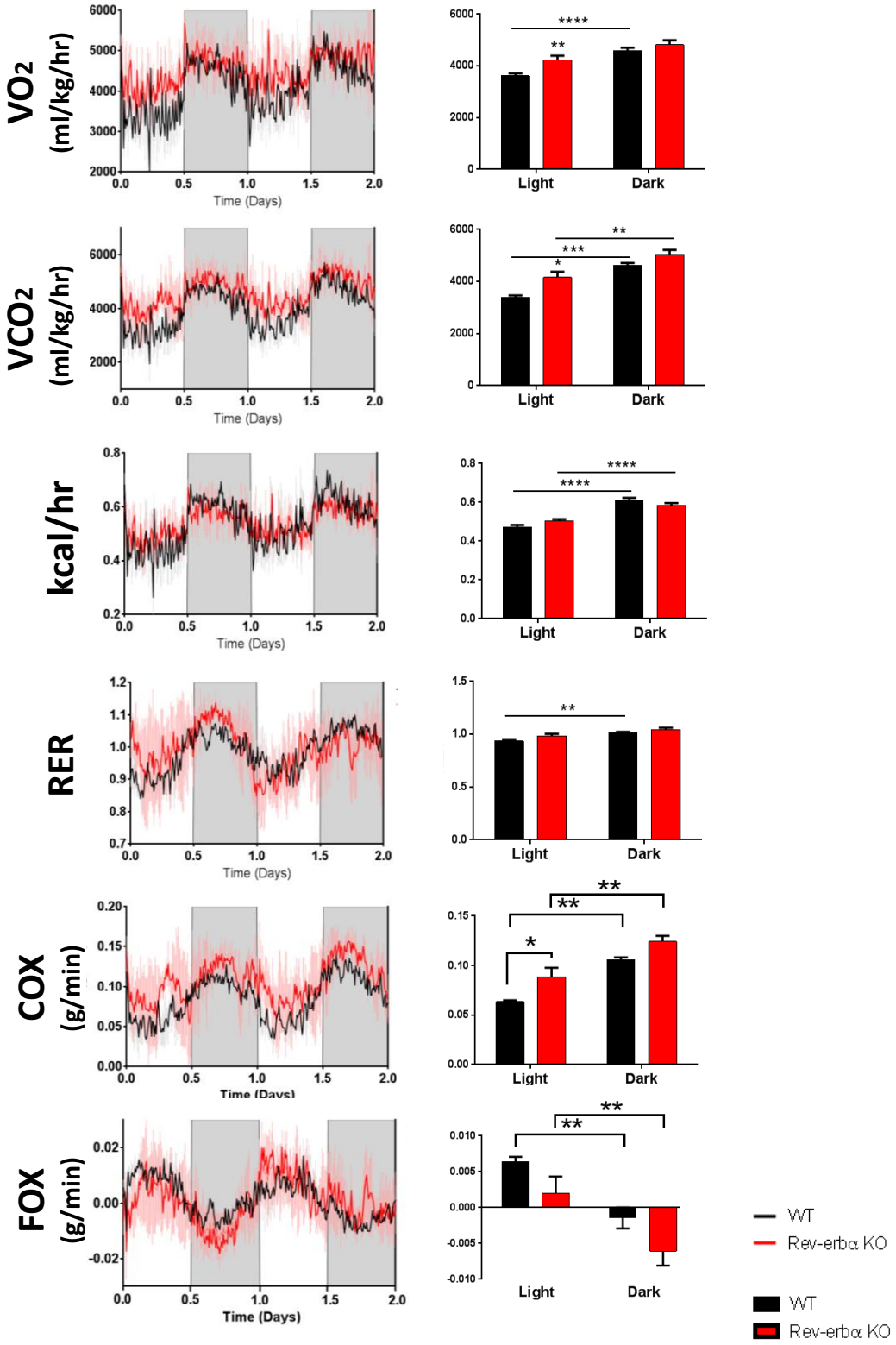
VO2 (ml/kg/hr)
VCO2 (ml/kg/hr)
kcal/hr
RER
COX (g/min)
FOX (g/min)
Time (Days)
Light
Dark
WT
Rev-erbα KO

Figure 4.3 – Alterations in metabolic parameters in *Rev-erbα*$^{-/-}$ mice.
Male *Rev-erbα*$^{-/-}$ mice and WT littermates (n=4 per genotype) were housed in CLAMS cages to assess metabolic parameters. As expected kcal/hr and VCO_2 were higher in the dark phase for both genotypes. VO_2 and RER however only showed diurnal variation in WT animals but resting VO_2 and VCO_2 in *Rev-erbα*$^{-/-}$ animals was higher. COX and FOX calculations showed diurnal variations in both genotypes. Data reflect mean ± S.E.M. , * = genotype difference, student's unpaired t-test, *= $p < 0.01$, **= $p < 0.001$, ***=$p<0.0001$ **** = $p<0.00001$. *Full description of statistical analysis can be found in Appendix 2.*

erbα$^{-/-}$, the fact that there is no significant difference in day/night VO_2 consumption and RER indicates a decreased amplitude of these rhythms.

Rates of carbohydrate oxidation (COX) and fatty acid oxidation (FOX) were derived from metabolic gas exchange rates. Diurnal variation was observed in both COX and FOX in *Rev-erbα*$^{-/-}$ mice and WT littermates. The *Rev-erbα*$^{-/-}$ mice exhibited an elevated rate of COX during the inactive phase relative to WT mice ($p>0.01$, 2-way ANOVA; Figure 4.3). This suggests an increased dependence on carbohydrate use in the KOs during the light phase. Some studies in our laboratory show that *Rev-erbα*$^{-/-}$ mice have increased feeding in the daytime (Cunningham, Unpublished Work), therefore, although not consistent in all mice, there may be an increased bias towards COX.

Thus, *Rev-erbα*$^{-/-}$ mice exhibited lower amplitude rhythms in metabolic gas exchange and altered COX and FOX profiles. This suggests a shift in fuel use in these mice. Nevertheless, these results certainly demonstrate that the increased adiposity in the *Rev-erbα*$^{-/-}$ mice was not due to increased food intake or decreased energy expenditure relative to WT mice. Thus, loss of *Rev-erbα* leads to increased energy efficiency and/or incorporation of absorbed energy into adipose tissue.

To examine the potential bias towards lipolysis and/or lipid incorporation in *Rev-erbα*$^{-/-}$ mice we measured the expression levels of lipid-handling genes in gWAT, scWAT, muscle and liver (n=9-14 per genotype, collected at ZT 6) by qPCR (Figure 4.4). A pronounced impact of *Rev-erb*α deletion on the expression of lipid-related genes was observed in gWAT. There was not, however, a bias towards lipid storage as both lipogenic (*Dgat2, Fasn*) and lipolytic (*Hsl*) sides of the pathway were upregulated in gWAT. Loss of *Rev-erbα* had no significant effects on these lipid handling genes in other peripheral tissues. *Lpl* was significantly up-regulated in gWAT and liver of *Rev-erbα*$^{-/-}$ mice, and although not reaching statistical significance was also increased in scWAT and muscle (Fig. 4.4). Since *Lpl* is responsible for the liberation of fatty acids from circulating triglycerides for uptake into tissues, the increased expression may contribute to the increased adiposity in *Rev-erbα* mice. Aside from *Lpl*, none of the other transcripts examined were significantly different between genotypes in scWAT, liver and muscle.

Biochemical analysis of circulating triglyceride (TAG), free fatty acids (FFA), and glycerol within the serum of WT and *Rev-erb*α$^{-/-}$ mice (n=5 per genotype, collected at ZT 6) revealed a significant reduction in both circulating FFA and glycerol levels in *Rev-erb*α$^{-/-}$ mice (Figure 4.2).

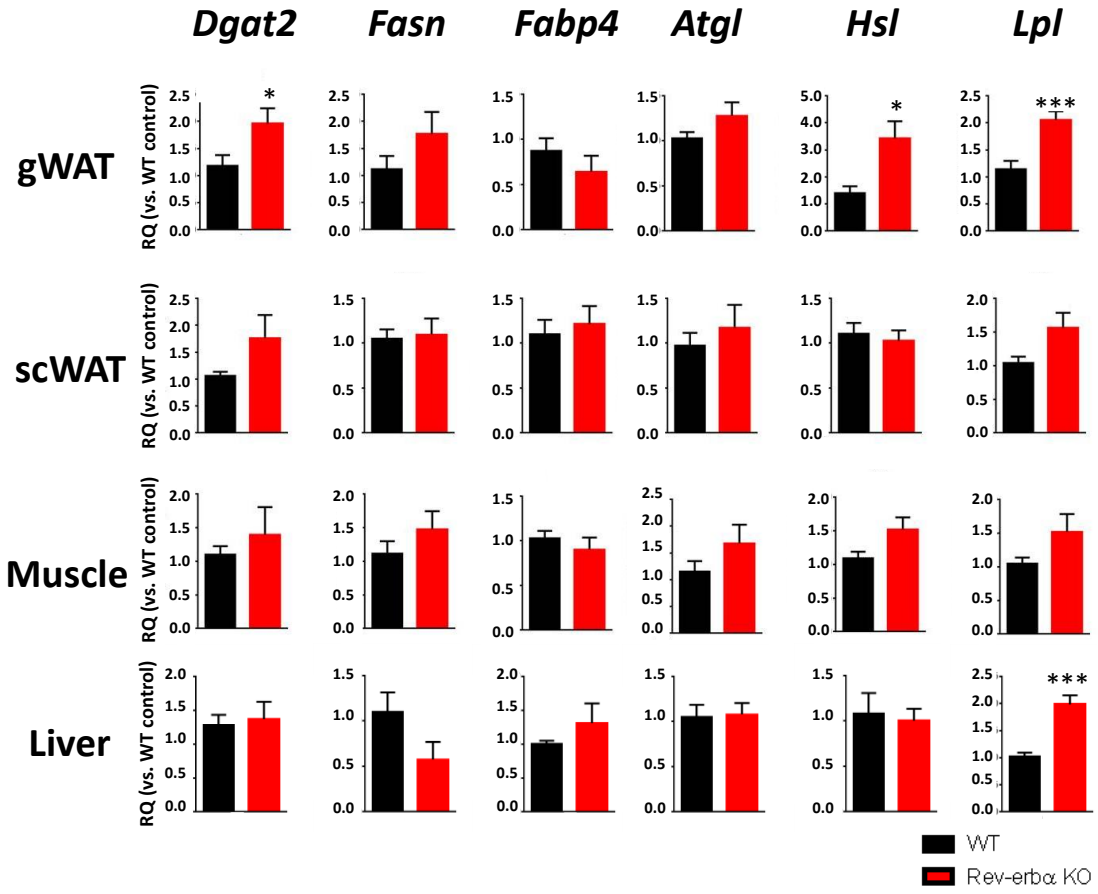

Figure 4.4 –Tissue specific effects of loss of *Rev-erbα* on lipid handling genes.
Transcript analysis of male *Rev-erbα*$^{-/-}$ and WT littermates was performed on gWAT, scWAT, Muscle and Liver (n=9-14 per genotype) at ZT6. On the whole, gWAT was most affected by the loss of *Rev-erbα* with most dysregulation of lipid handling genes seen most in this tissue, for example upregulation of *Dgat2*, *Hsl* and *Lpl.* There was a trend for upregulation of *Lpl* in all tissues. Data reflect mean ± S.E.M. , * = genotype difference, student's unpaired t-test, *= p < 0.01, *** = p<0.0001. *Full description of statistical analysis can be found in Appendix 2.*

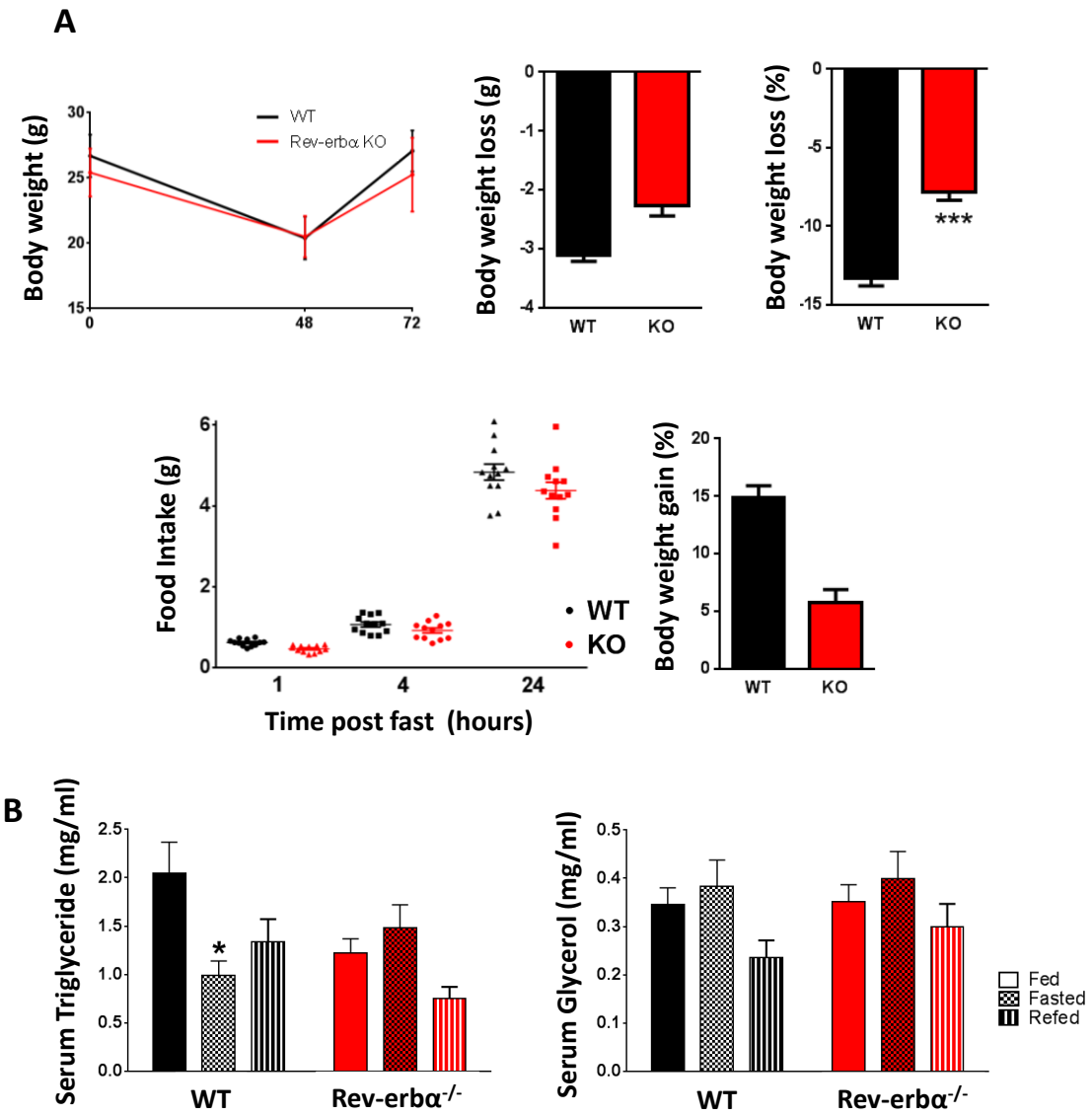

Figure 4.5 –Differential physiological responses to fasting in *Rev-erbα*$^{-/-}$ mice.
Male *Rev-erbα-/-* and WT littermates were fasted for 48 hours and weight loss, food intake and weight gain was measured (n = 6 per genotype) (A). *Rev-erbα*$^{-/-}$ mice lost less weight during the fast than their WT littermates and subsequently gained less weight after post-fast feeding. No difference, however, was seen in their food intake post-fast. Data reflect mean ± S.E.M., * = genotype difference, student's unpaired t-test, *** = p<0.0001. Serum analysis was performed on serum from these fasted animals, and as expected, in WT animals TAG levels decreased and there was a trend for an increase in glycerol (B). However, this reduction in circulating TAG was not observed in *Rev-erbα*$^{-/-}$ mice. Data reflect mean ± S.E.M., * = feeding regime difference, 2-way, ANOVA, Sidak post-hoc test, *= p < 0.01. *Full description of statistical analysis can be found in Appendix 2.*

This is compatible with an increased uptake and storage of FFA and glycerol within peripheral tissues.

4.3.3 Fasting response in *Rev-erbα*$^{-/-}$ mice

To further investigate how loss of *Rev-erb*α alters lipid storage and breakdown, we compared the responses of WT and *Rev-erb*α$^{-/-}$ mice to states of negative energy balance (i.e. fasting). Mice (n=6 per genotype) were fasted for 48 hours and we tested body weight, feeding and gene expression as well as metabolic parameters. *Rev-erbα*$^{-/-}$ mice lost less weight during the fast, in terms of absolute weight loss (WT: 3.09 ± 0.085 g, *Rev-erbα*$^{-/-}$: 2.21 ± 0.11 g; $p<0.001$, student's t-test) and as a % of initial body weight (7.97% compared to 13.10% loss in WTs, $p<0.001$, student's t-test) (Figure 4.5A). No difference was observed in food intake after 1, 4 and 24 hours of refeeding. *Rev-erbα*$^{-/-}$ mice gained less weight upon re-feeding, in terms of % weight gain from refeed (5.83% compared to 14.99% gain in WTs); however this reflected the degree of weight loss observed in the animals as both genotypes return to their original body weight after 24 hours re-feeding.

Serum analyses showed that while circulating TAG levels were significantly reduced in WT animals in response to 24 hr of fasting, a similar reduction in was not observed in *Rev-erbα*$^{-/-}$ mice (Figure 4.5B). This suggests that the KO mice exhibit more efficient/continued release of TAG from the liver during fasting. Circulating glycerol levels in both genotypes were not altered by fasting.

Energy expenditure and metabolic rate were examined in fasted *Rev-erbα*$^{-/-}$ or WT mice using indirect calorimetry (Figure 4.6). Mice (n=4 per genotype) were acclimatised to the cages for 4 days before being fasted for 48 hours. A fast induced decrease in all parameters of metabolic gas exchange (VO_2, VCO_2, kcal/hr and RER) was observed in both genotypes. Interestingly fast induced reductions in VO_2 and EE (kcal/hr) observed in *Rev-erbα*$^{-/-}$ mice were significantly less pronounced than those observed in WT mice. Specifically, a 27.7± 3.17% reduction in VO_2 was observed in WT mice whereas KO mice exhibited a 17.6 ± 4.84% reduction during fast ($p<0.05$, student's t-test). As expected, RER approached a value of ~0.7 in both genotypes during the fasting period, which reflects a reliance on fatty acid oxidation for energy. In line with this, derivation of FOX rate demonstrated that fatty acid oxidation was profoundly increased in both genotypes during the fasting period. Interestingly, FOX rates were significant higher in fasted *Rev-erbα*$^{-/-}$ mice compared with WT littermates, especially during the final 6 hour of the

fast. This likely reflects the increased adiposity of these animals, and may underlie their ability to maintain higher rate of EE and VO2 across the fasting period (Figure 4.6).

Fasting-induced changes in the expression of metabolic genes were examined in the liver and gWAT of *Rev-erbα*$^{-/-}$ and WT mice (n=5-6/genotype, collected at ZT6) in response to 24 or 48 hr fast (Figure 4.7). As expected, fasting caused a dramatic down-regulation of lipogenic pathways in both genotypes. This was most clearly evidenced by reduced expression of *Dgat2* (reflecting a downregulation in lipid incorporation into stored TAG) and *Fasn* (reflecting reduced *de novo* lipogenesis) in gWAT. A significant fast-induced reduction of *Fasn* was also observed in the liver of WT and *Rev-erbα*$^{-/-}$ mice, while a reduction in *Dgat2* was observed in the liver of *Rev-erbα*$^{-/-}$ mice but not in WT mice. Similar to *Dgat2*, fasting led to a reduction in *Lpl* expression in the gWAT and liver of *Rev-erbα*$^{-/-}$ mice, yet not within the WT mouse tissues. These differential responses may reflect a normalisation of elevated *Lpl* and *Dgat2* expression in the KO mice to WT level. In parallel to downregulation of lipogenesis, fasting leads to an increase in lipolysis, as fatty acids are liberated from lipid stores to provide energy for the body. In line with this, *Atgl* transcription was significantly increased in WT animals in response to fast in both gWAT and liver. Interestingly, a similar increase in *Atgl* expression was not seen in either tissue of *Rev-erbα*$^{-/-}$ mice, suggesting a defect in fast-induced regulation of Atgl specifically or lipolytic responses in general within these animals. The expression of *Hsl* was not increased in either line of mice in response to the fasting.

4.3.4 Adrenergic stimulation of *Rev-erbα*$^{-/-}$ mice

β_3-adrenergic receptor signalling in adipose tissue is the major route for sympathetic control of lipolysis and thermogenesis (Collins and Surwit, 2001). Due to the attenuated *Atgl* response in fasted *Rev-erbα*$^{-/-}$ mice, lipolytic drive in the animals was stimulated directly through administration of the β_3-adrenergic receptor agonist, CL316,243. WT and *Rev-erbα*$^{-/-}$ mice were treated with vehicle or CL316,243 (n=4/group, ZT6, 0.1 mg/kg, I.P.), and culled 4 hours post drug administration, at which time tissue samples were rapidly dissected and snap frozen. Adrenergic stimulation did not lead to a reduction in lipogenic gene expression in gWAT or scWAT in either genotype, however, *Fasn* expression was attenuated in both genotypes in BAT (Figure 4.8). CL316,243 administration cause a pronounced upregulation of *Hsl.* In contrast to the response in fasted mice, *Atgl* was not upregulated in gWAT by pharmacological adrenergic stimulation, although it was significantly upregulated in scWAT of both genotypes. It is not clear why the different adipose tissue depots respond differently; however, these results

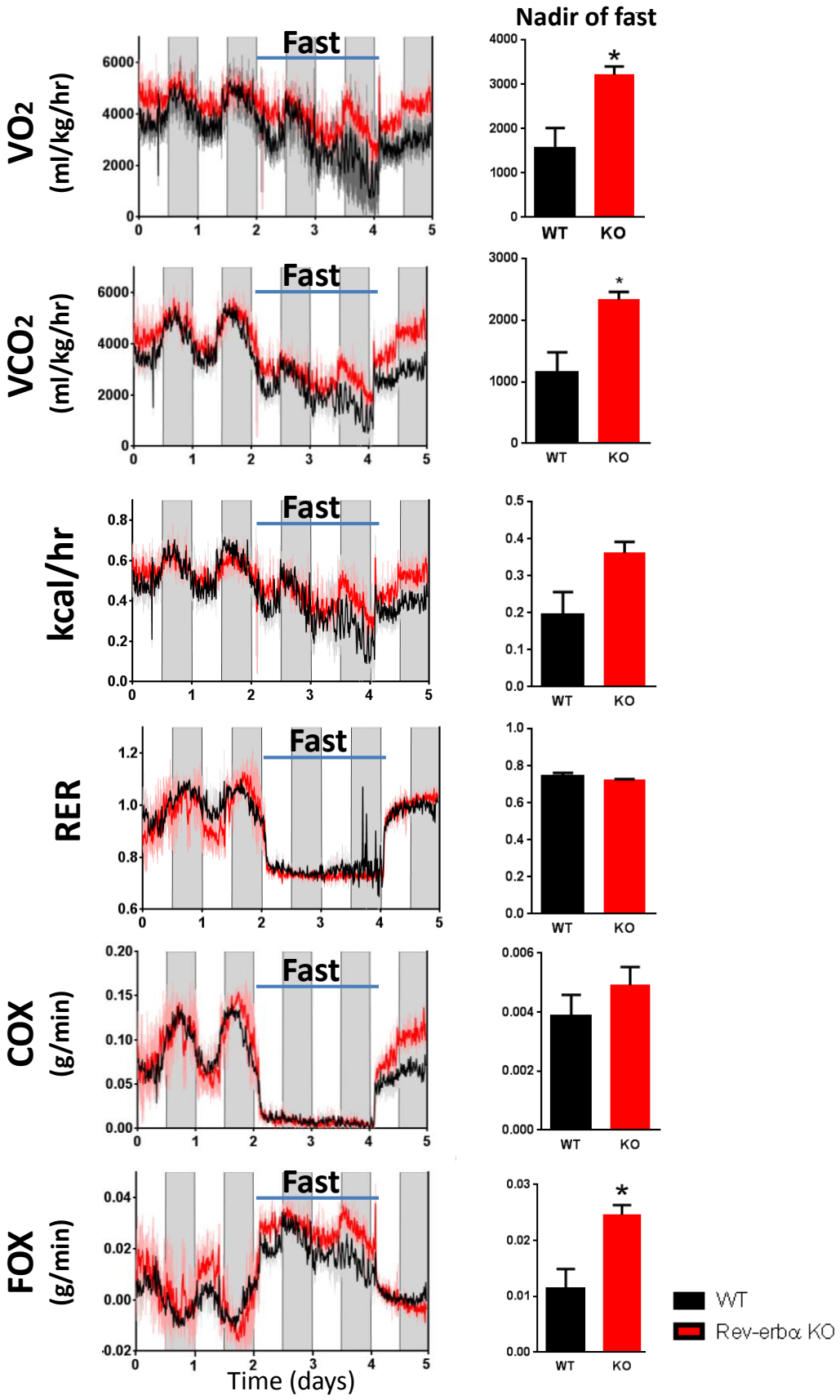
Nadir of fast
VO2 (ml/kg/hr)
VCO2 (ml/kg/hr)
kcal/hr
RER
COX (g/min)
FOX (g/min)
Fast
WT
KO
Time (days)
WT
Rev-erbα KO

Figure 4.6 – Differential metabolic response to fasting in *Rev-erbα*$^{-/-}$ mice.

Male *Rev-erbα*$^{-/-}$ mice and WT littermates n=8 per genotype) housed in metabolic CLAMS cages were fasted for 48 hours (n = 8 per genotype). Histograms show the average of the metabolic parameters at the nadir of the fast (between 42-47 hours). As expected, there was a reduction in all metabolic parameters (VO_2, VCO_2, kcal/hr, RER) but this reduction was blunted in *Rev-erbα-/-* mice. A significant increase in FOX was observed in *Rev-erbα-/-* mice during the fast. Data reflect mean ± S.E.M. , * = genotype difference, student's unpaired t-test, * = $p < 0.01$. *Full description of statistical analysis can be found in Appendix 2.*

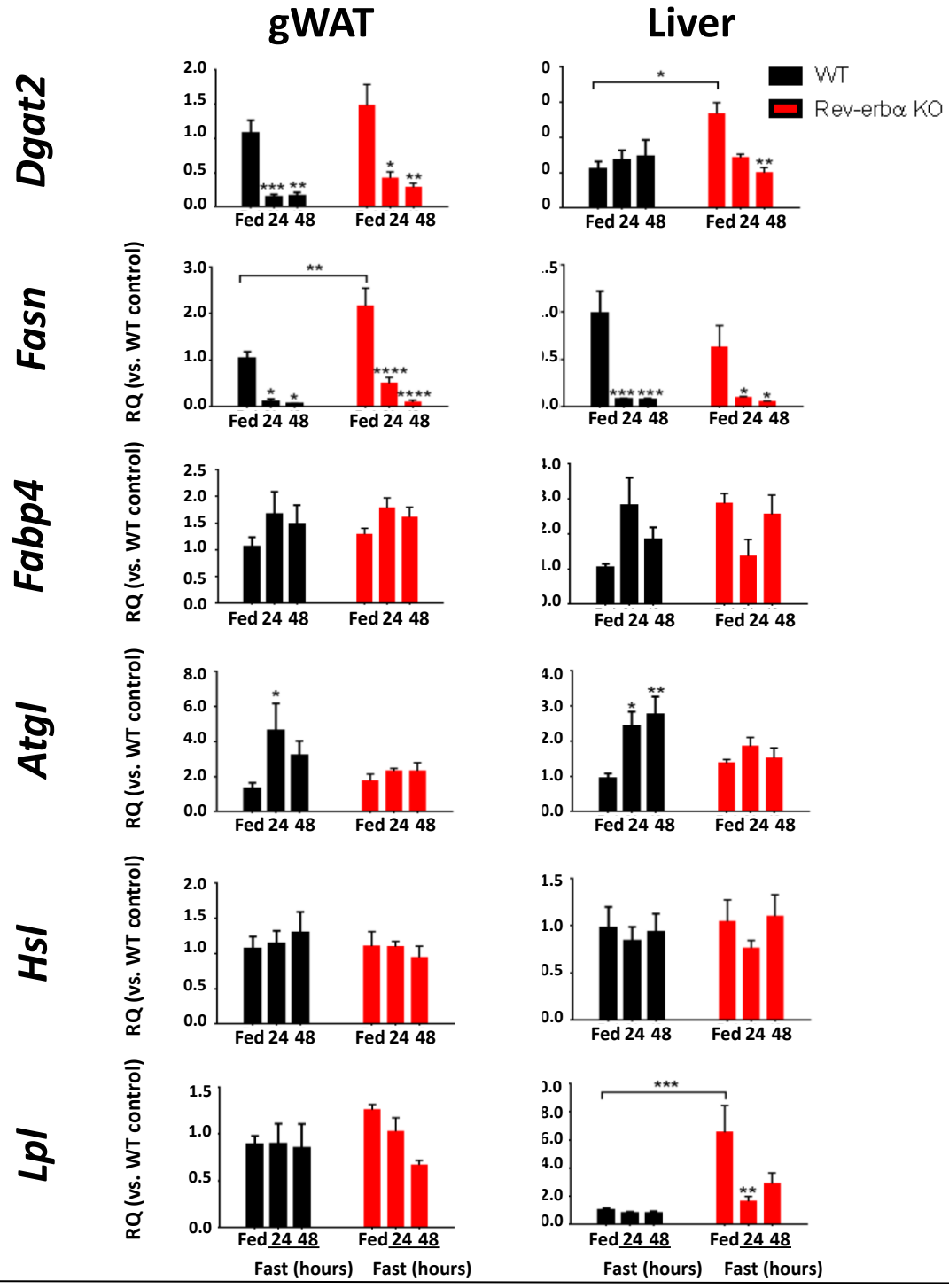

Figure 4.7 - Differential effects on lipid handling genes to a fast of *Rev-erbα*$^{-/-}$ mice. Transcript analysis was performed on lipid handling genes from tissue collected from 48 hour fasted male *Rev-erbα*$^{-/-}$ mice and WT littermates (n=5-6 per genotype). As expected, lipogenic gene expression (*Dgat2, Fasn*) was attenuated during the fast. In WT animals, an increase in *Atgl* was observed in fasted animals which was expected, but this increase was not seen in *Rev-erbα*$^{-/-}$ animals . Data reflect mean ± S.E.M., 2-way, ANOVA, Sidak post-hoc test , *= $p < 0.01$ **= $p < 0.001$, ***= $p < 0.0001$, ***= $p < 0.0001$, **** = $p<0.00001$ vs WT of same challenged group or vs control of same genotype. *Full description of statistical analysis can be found in Appendix 2.*

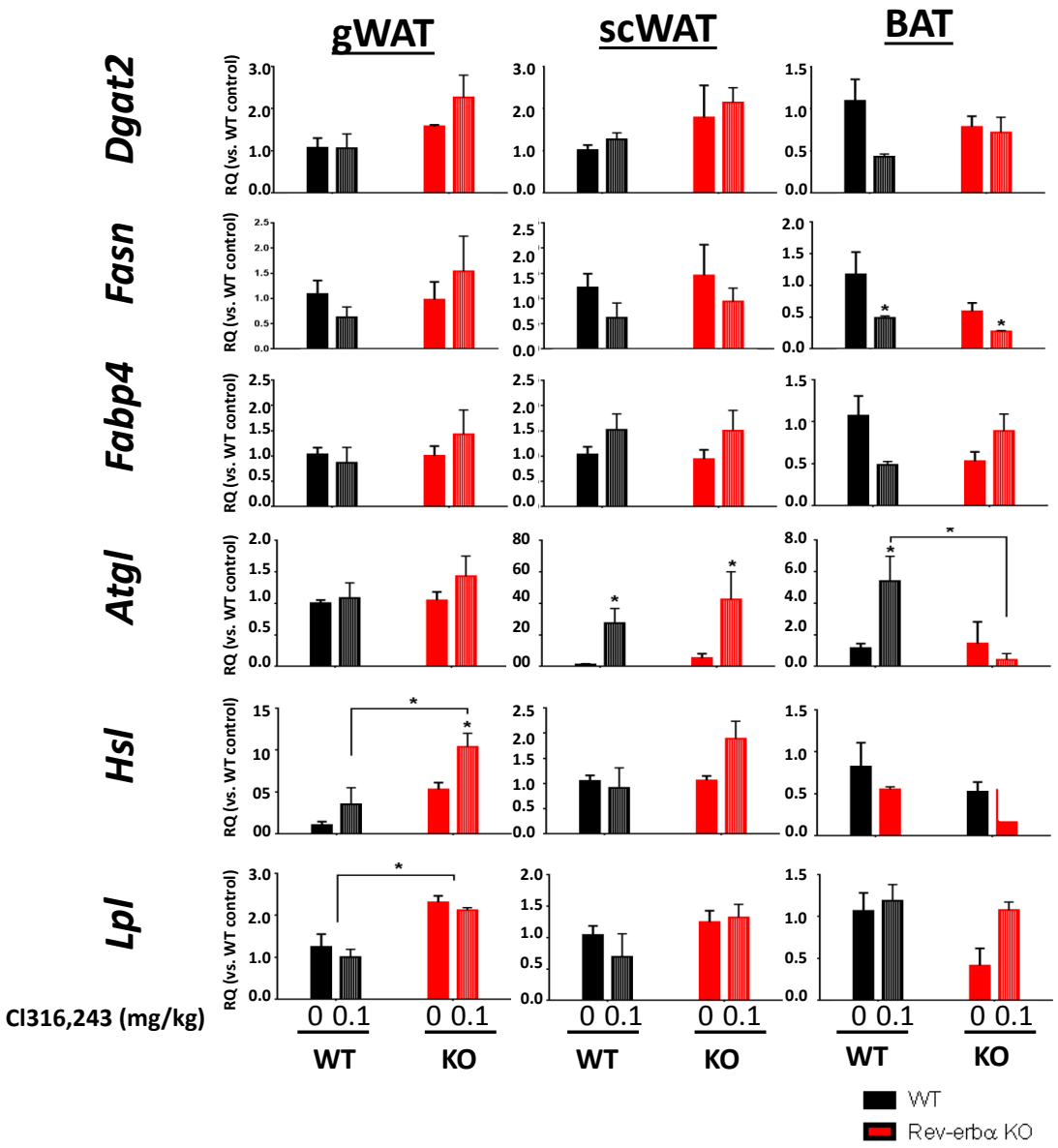

Figure 4.8 – *In vivo* adrenergic stimulation of *Rev-erbα*$^{-/-}$ mice.

Male *Rev-erbα-/-* mice and WT littermates (n=4/genotype/treatment) were administered 0.1 mg/kg CL316,243 I.P. And culled 4 hours post administration. Transcript analysis was performed on lipid handling genes in a variety of tissues. Data reflect mean ± S.E.M., 2-way, ANOVA, Sidak post-hoc test, *= $p < 0.01$ vs WT of treatment group or vs control treated group of same genotype. *Full description of statistical analysis can be found in Appendix 2.*

suggest that *Atgl* remains responsive to lipolytic stimulation in the KO mice (at least in scWAT). CL316,243 administration also resulted in an increase in *Atgl* expression in BAT of littermate controls which was not observed in *Rev-erbα*$^{-/-}$ mice. Taken together, these results suggest that the influence of REV-ERBα on *Atgl* regulation may be tissue and/or stimulus-specific.

Post-translational modifications play an important role in regulating the activity of HSL (Lorente-Cebrián *et al*., 2011). We therefore assessed the phosphorylation of HSL at serine 563, a well characterised activation site for HSL (Lorente-Cebrián *et al*., 2011) in response to CL316,243 administration (Figure 4.9). Western blot analyses of gWAT protein demonstrated similar basal expression levels of HSL in the two genotypes, with no significant upregulation of expression with both 0.1 and 1 µM CL316,243 in both genotypes. A dramatic increase in phosphorylated HSL (pHSL) was observed in gWAT from the CL316,243 treated littermate control mice, in comparison to vehicle-treated mice. Adrenergic stimulation also increased HSL phosphorylation in the *Rev-erbα*$^{-/-}$ mice, but this induction reached statistical significance only at the higher concentration of CL316,243 (1 mg/kg). This suggests that *Rev-erbα*$^{-/-}$ mice may have a blunted lipolytic response to fasting and adrenergic stimulation.

Together these results highlight a possible bias towards lipogenesis in the *Rev-erbα*$^{-/-}$ mice, with evidence of enhanced lipogenic drive (e.g. Increased basal expression of *Fasn* and *Lpl*) and decrease responsiveness of lipolytic pathways (e.g. blunted responses of *Atgl* to fasting and CL316,243 and HSL phosphorylation to CL316243).

4.3.5 HFD-feeding in *Rev-erbα*$^{-/-}$ mice

Given the altered response of the *Rev-erbα*$^{-/-}$ mice to negative energy balance (fasting) and the increased adiposity of the mice when maintained on normal chow, we next examined their response to HFD feeding. Briefly, female mice (8 weeks of age, n=8/genotype/diet) were fed HFD for 14 weeks with food intake and body weight monitored throughout. *Rev-erbα*$^{-/-}$ mice exhibited a profound increase in HFD-induced weight gain relative to WT littermates (Figure 4.10A). Exacerbated diet-induced obesity (DIO) was reflected by greater adiposity, with significantly increased gWAT and scWAT mass in the knockout mice. Interestingly, and in contrast to feeding behaviour when maintained on NC, weight gain on HFD was associated with hyperphagia in the *Rev-erbα*$^{-/-}$ mice. KO mice consumed significantly more calories on HFD compared to WT littermates maintained on HFD or knockout mice fed NC (Figure 4.10B). Similar results are observed in male mice (Cunningham, Unpublished Data). Provision of HFD led to an increase in daytime calorie intake in C57BL/6 mice (28.0± 1.4 % daytime

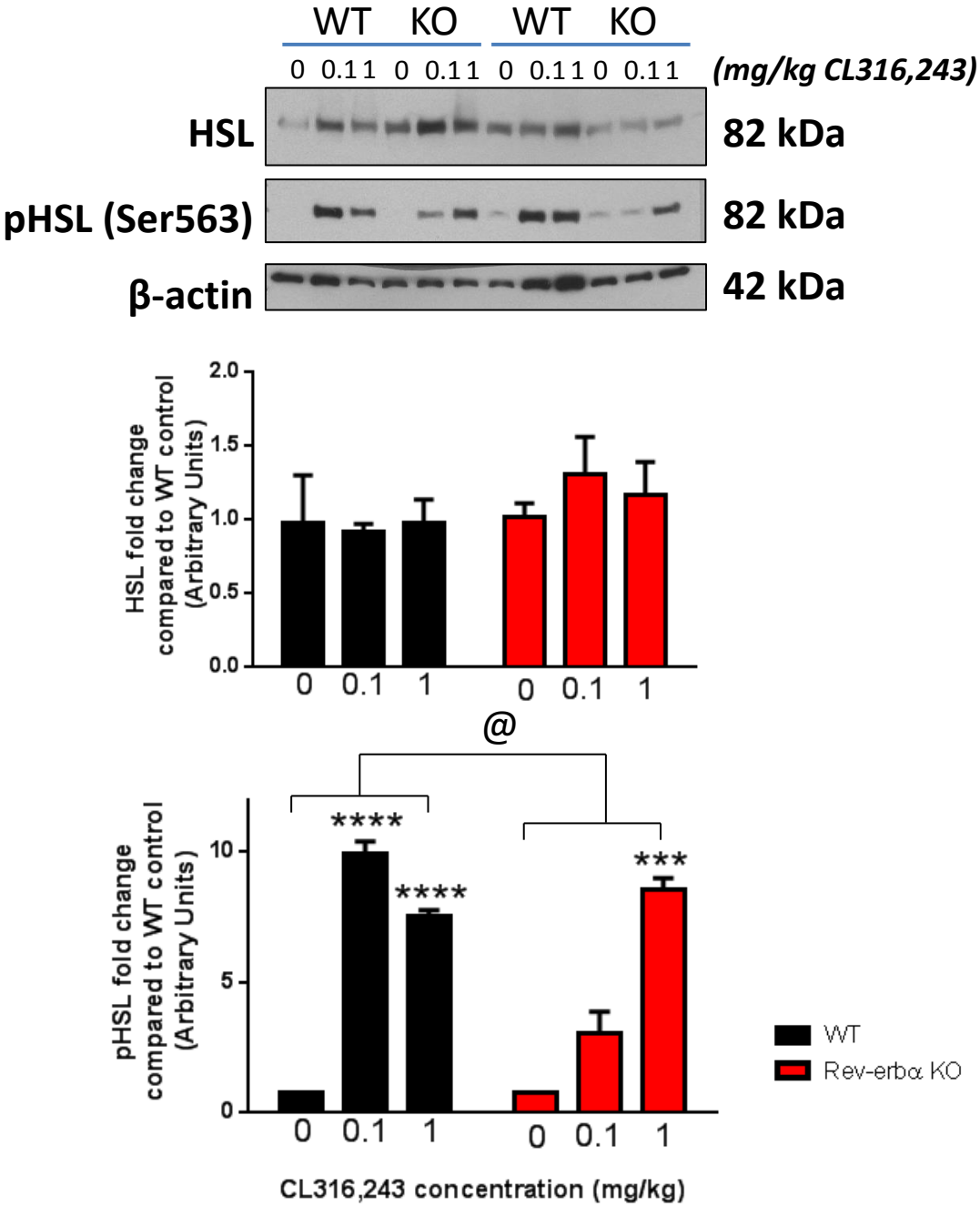

Figure 4.9 –*Rev-erbα*$^{-/-}$ mice show decreased sensitivity to adrenergic induction of HSL phosphorylation.

gWAT of male *Rev-erbα*$^{-/-}$ mice and WT littermates was harvested 4 hours post adrenergic stimulation (n=4 per genotype per treatment). Values are expressed as relative abundance (mean) after normalization to both β-actin and total HSL. Increased phosphorylation of HSL was seen after adrenergic stimulation, although the response was attenuated in *Rev-erbα*$^{-/-}$ mice at the lower dose of CL316-243. Data reflect mean ± S.E.M. , 2-way, ANOVA, Sidak post-hoc test *= $p < 0.01$ ***= $p < 0.0001$, **** = $p<0.00001$ vs control treated group of same genotype. @ = difference in response between genotypes $p <0.01$. *Full description of statistical analysis can be found in Appendix 2.*

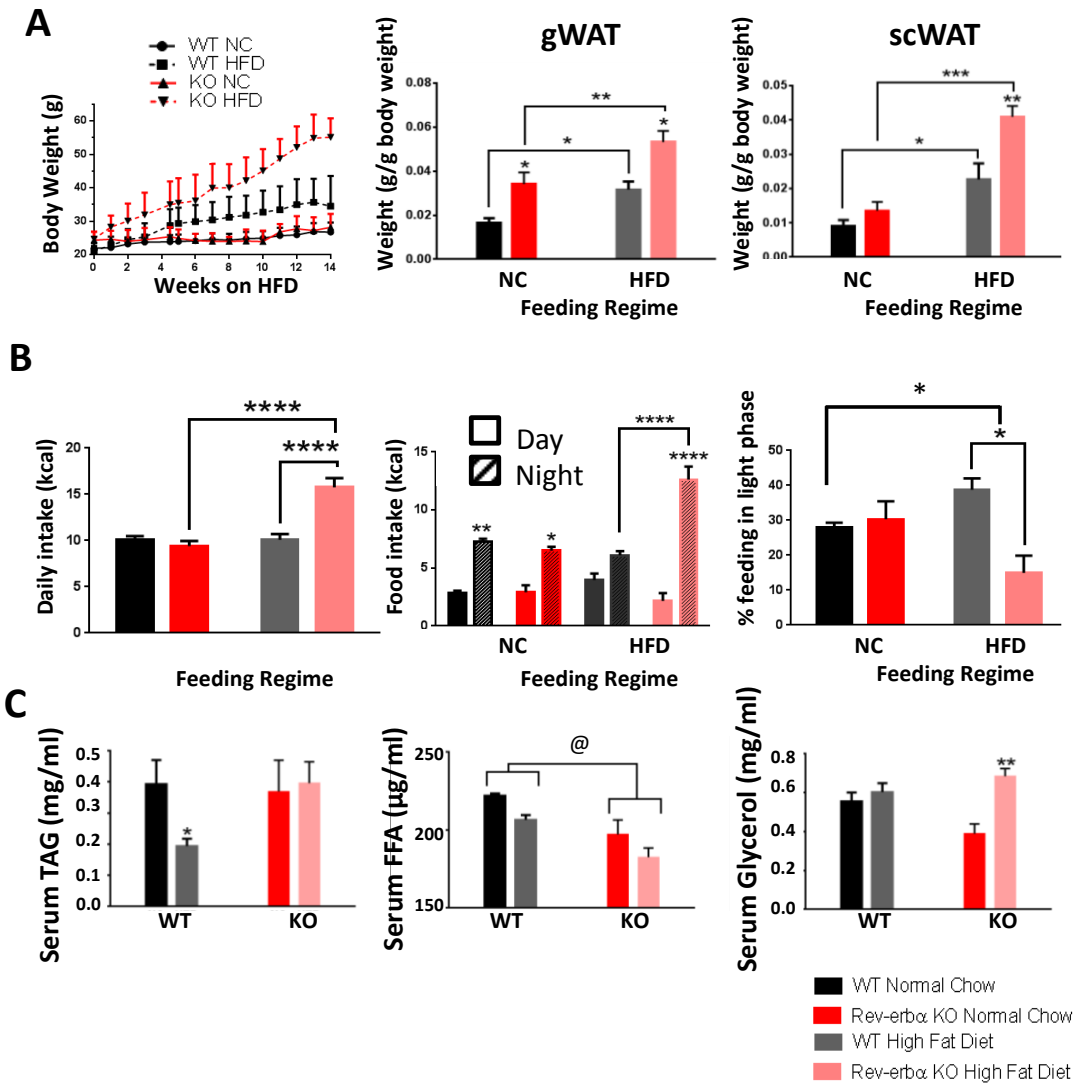

Figure 4.10 – Differential effect of diet induced obesity on *Reverbα*$^{-/-}$ mice.
Female *Rev-erbα*$^{-/-}$ mice and WT littermates (n=8/genotype) were maintained on either NC or HFD for 14 weeks from 8 weeks of age. *Rev-erbα*$^{-/-}$ mice are more susceptible to diet induced obesity with vast increases in gWAT and scWAT weight observed (A). This was linked to hyperphagia in these mice but with decreased light phase feeding observed (B). Serum analysis was performed and decreased circulating TAG was observed in WT mice but not in KO mice. FFA were lower in the KO animals on both feeding regimes and there was a significant increase in glycerol in the KO animals on HFD (C). Data reflect mean ± S.E.M., 2-way, ANOVA, Sidak post-hoc test *= $p < 0.01$ **= $p < 0.001$, ***= $p < 0.0001$, ***= $p < 0.0001$, **** = $p<0.00001$ vs WT of same diet group or vs NC of same genotype. Differential response to HFD between genotypes represented by @ = $p < 0.01$. *Full description of statistical analysis can be found in Appendix 2.*

feeding on NC but 38. 8±3.4 % on HFD). In contrast, *Rev-erbα*$^{-/-}$ mice on HFD retained a strong diurnal pattern in HFD feeding, with the majority of kcal consumed in the active phase (31.6 ± 5.9% daytime feeding on NC, 15.6 **±** 1.45% daytime feeding on HFD (Figure 4.10B). Separate studies in our laboratory have demonstrated that normalisation of HFD intake (to that of WT mice) by restriction of food access reduces HFD-induced weight gain and adiposity in these *Rev-erbα*$^{-/-}$ mice but does not return HFD-weight gain back to WT levels. This indicates that HFD-induced hyperphagia is not solely responsible for excessive diet-induced weight gain in the *Rev-erbα*$^{-/-}$ mice.

Unexpectedly, circulating TAG levels were decreased in WT mice after 14 weeks of HFD feeding (Figure 4.10C). However, this has been reported previously in C57BL6 mice (Biddinger *et al.,* 2005). This was not observed in *Rev-erbα*$^{-/-}$ mice and circulating TAG levels were similar in HFD and NC mice. Circulating levels of FFA were lower in *Rev-erbα*$^{-/-}$ mice when compared to WT littermates regardless of diet type, although a significant effect of diet was not observed in either genotype. However, glycerol levels were significantly higher in *Rev-erbα*$^{-/-}$ mice on HFD, which contrasted with WT littermates as no diet difference was observed in these levels.

To further investigate the increased propensity of weight gain in *Rev-erbα*$^{-/-}$ mice on HFD, gene expression analyses was carried out on gWAT, liver and muscle collected from mice maintained on HFD for 14 weeks (n =7-11/group/diet). Despite the fact that *Pparα* and *Pparγ* are regulated by the clock and showed profound changes in expression in C57BL/6J DIO mice (Figure 3.4A), deletion of *Rev-erbα* did not cause a alter *Ppar* gene expression in gWAT, liver, or muscle (Figure 4.11). As observed previously (Figure 3.4), *Pparα* and *Pparγ* transcripts were upregulated in the liver of WT animals on HFD. However, upregulation of *Pparα* in the liver of *Rev-erbα*$^{-/-}$ mice on HFD was not observed. Significant down-regulation of the *Ppar* expression in response to 14 week HFD feeding was not observed in the gWAT of WT or *Rev-erbα*$^{-/-}$ mice. This contrasts with observation made in Chapter 3, and may be due to the sex difference and/or relatively low body weight in these WT mice (35.4 ± 8.7 g). Overall, this data would suggest the effect that loss of *Rev-erbα* has susceptibility to DIO is not due to altered transcription of *Ppars.* Similarly, few significant genotype differences were observed in HFD-induced lipid handling gene expression in gWAT, liver, and muscle (Figure 4.12). Chronic HFD feeding caused a downregulation of *Fasn* in gWAT and muscle in both genotypes (Figure 4.12). HFD feeding did cause a decrease in *Atgl* expression in gWAT of *Rev-erbα*$^{-/-}$ mice which was not observed in WT mice. Once again, this suggests a possible bias towards lipid storage in the *Rev-erbα*$^{-/-}$ mouse even amid profound adipocyte hypertrophy.

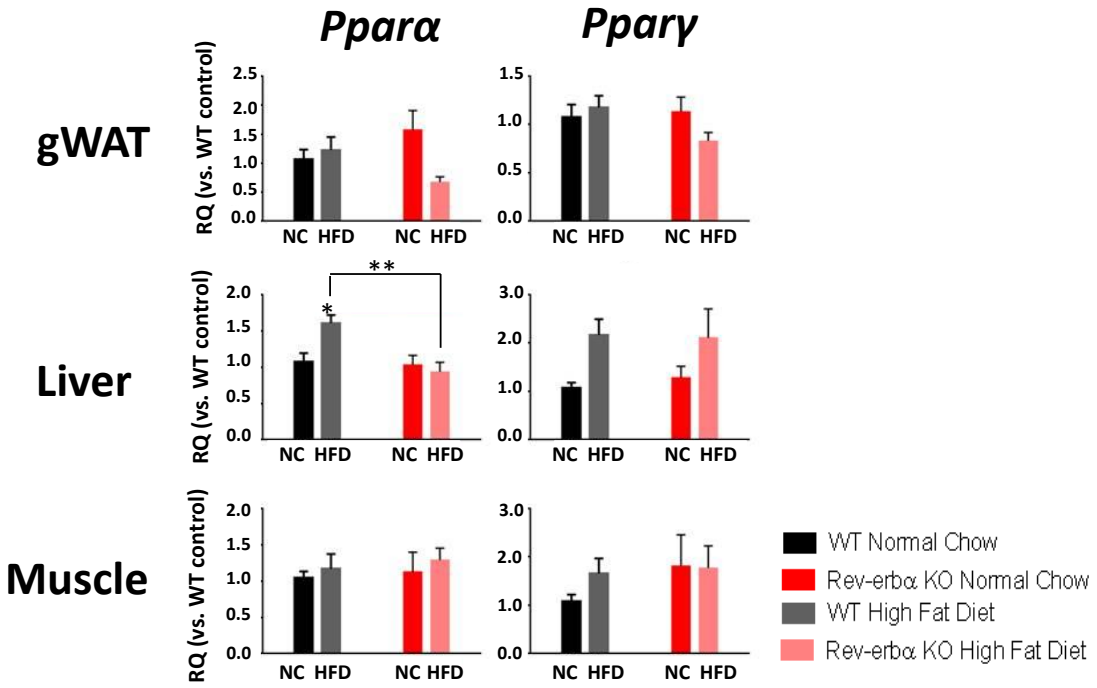

Figure 4.11 – Effects of diet induced obesity on *Ppar* genes in *Rev-erbα*$^{-/-}$ mice.

Female *Rev-erbα*$^{-/-}$ mice and WT littermates (n=7-11/genotype/diet) were maintained on either NC or HFD for 14 weeks from 8 weeks of age. Transcript analysis was performed on *Ppar* genes in a variety of tissues. On the whole HFD did not affect *Ppar* expression in these tissues, but an increase in *Ppar*α expression was observed in the liver in WT mice on HFD which was not seen in *Rev-erbα*$^{-/-}$ mice . Data reflect mean ± S.E.M. , 2-way, ANOVA, Sidak post-hoc test, *= $p < 0.01$ **= $p < 0.001$ vs WT of same diet group or vs NC of same genotype. *Full description of statistical analysis can be found in Appendix 2.*

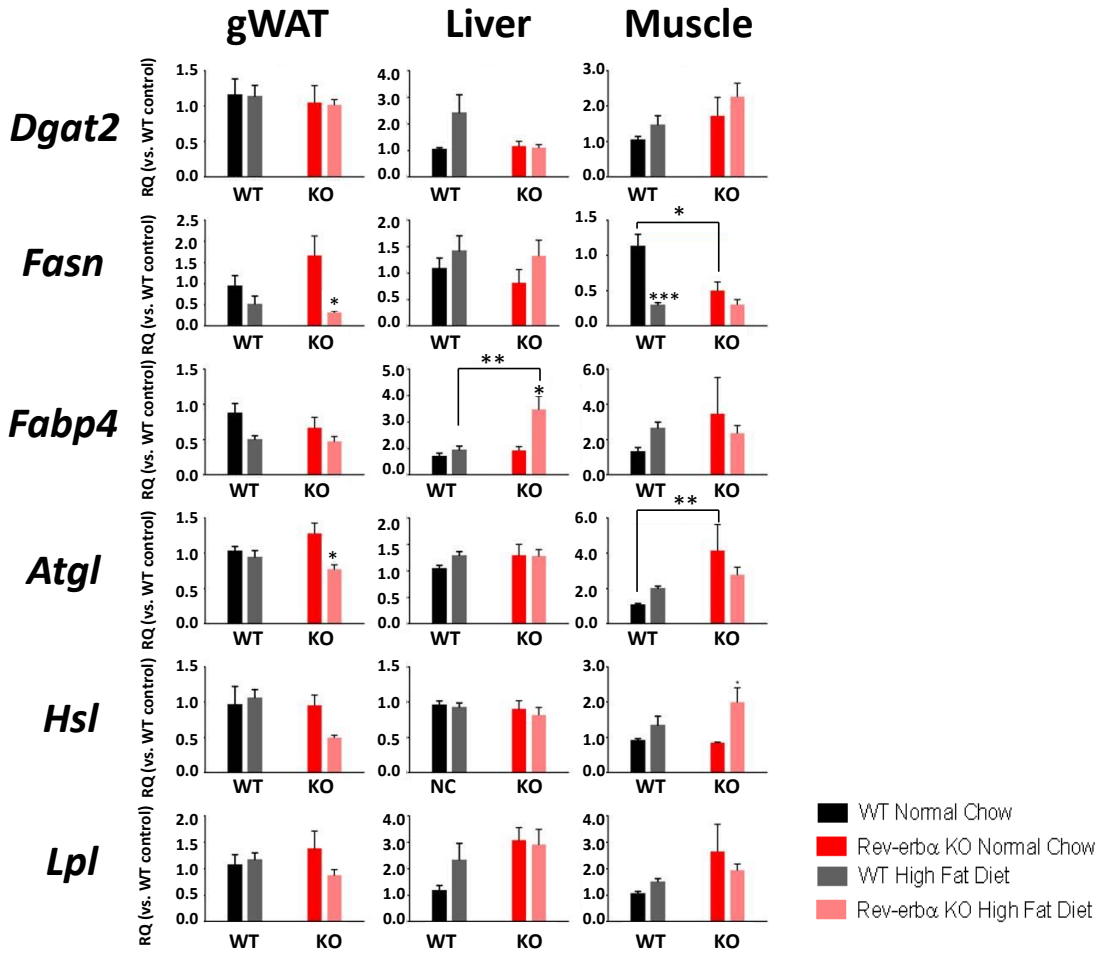

Figure 4.12 – Tissue specific effects of diet induced obesity on lipid handling genes in *Rev-erbα*$^{-/-}$ mice.

Female *Rev-erbα*$^{-/-}$ mice and WT littermates (n=7-11/genotype/diet) were maintained on either NC or HFD for 14 weeks from 8 weeks of age. Transcript analysis was performed on lipid handling genes in a variety of tissues. HFD caused a reduction in *Fasn* in gWAT both genotypes which was to be expected and interestingly *Fasn* was attenuated in both feeding regimes in muscle of KO mice. Data reflect mean ± S.E.M., 2-way, ANOVA, Sidak post-hoc test *= $p < 0.01$ **= $p < 0.001$, ***= $p < 0.0001$, ***= $p < 0.0001$, **** = $p<0.00001$ vs WT of same diet group or vs NC of same genotype. *Full description of statistical analysis can be found in Appendix 2.*

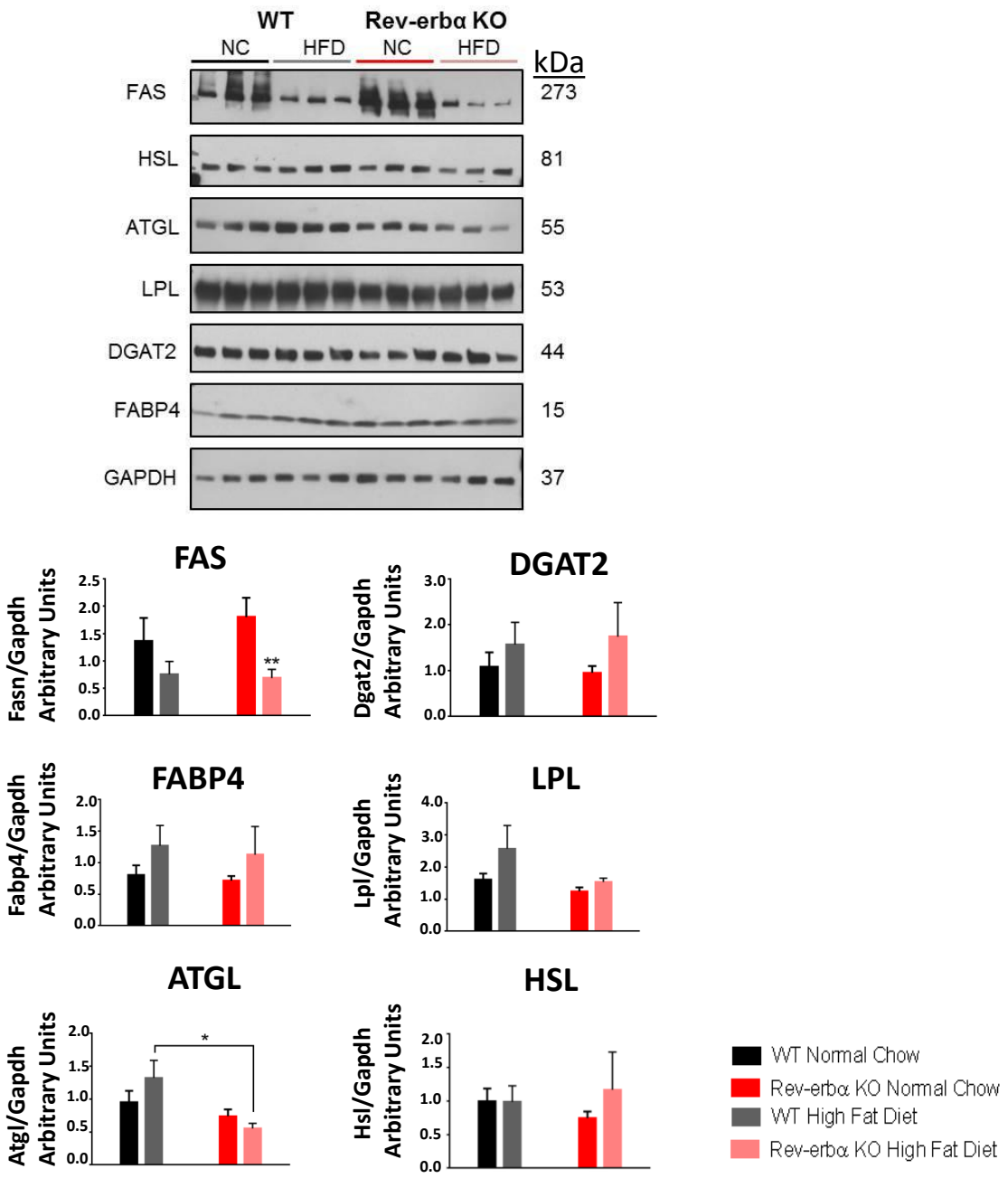

Figure 4.13 - Effects of diet induced obesity on lipid handling proteins in *Rev-erbα*$^{-/-}$ mice. Female *Rev-erbα*$^{-/-}$ mice and WT littermates (n=6/genotype/diet) were maintained on either NC or HFD for 14 weeks from 8 weeks of age. Values are expressed as relative abundance (mean) after normalization to GAPDH. FAS was attenuated in both genotypes on HFD and ATGL expression in the KO mice was significantly attenuated on HFD. Data reflect mean ± S.E.M., 2-way, ANOVA, Sidak post-hoc test *= $p < 0.01$ **= $p < 0.001$ vs WT of same diet group or vs NC of same genotype. *Full description of statistical analysis can be found in Appendix 2.*

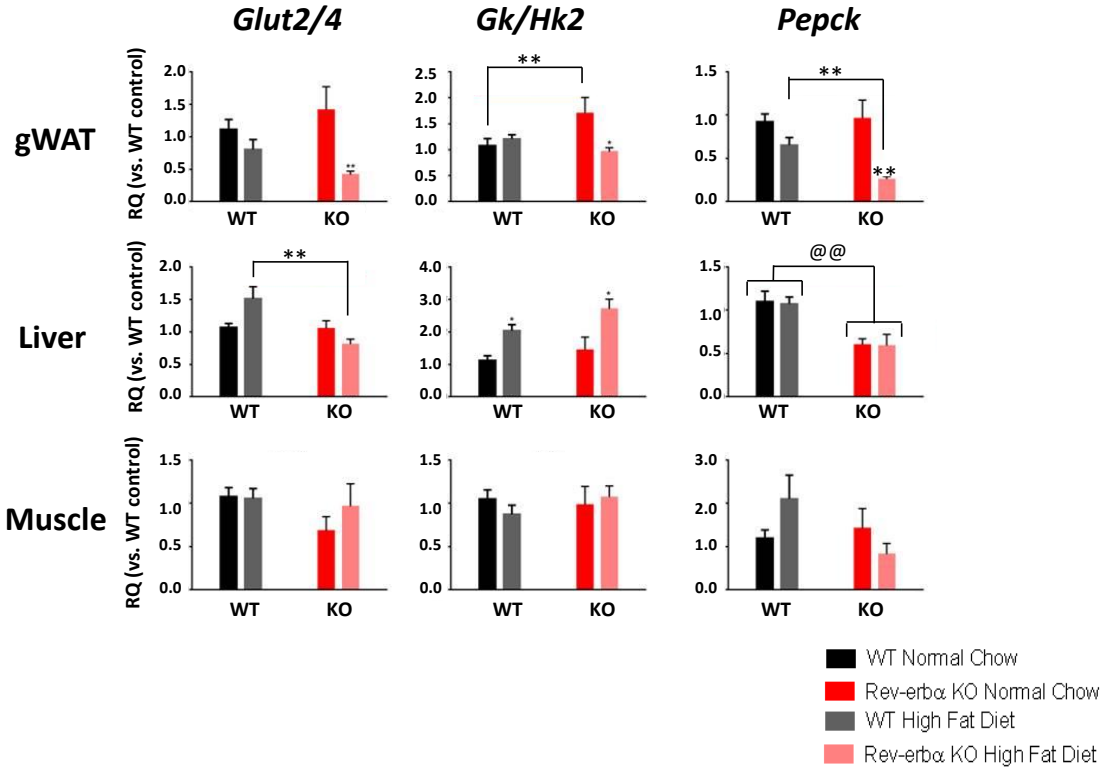

Figure 4.14 – Effects of diet induced obesity on glucose handling genes in *Rev-erbα*$^{-/-}$ mice. Female *Rev-erbα*$^{-/-}$ mice and WT littermates (n=7-11/genotype/diet) were maintained on either NC or HFD for 14 weeks from 8 weeks of age. *Pepck* expression in gWAT was highly attenuated in KO mice on HFD and in the liver *Pepck* expression was reduced in the KO under both feeding regimes. Data reflect mean ± S.E.M., 2-way, ANOVA, Sidak post-hoc test *= $p < 0.01$ **= $p < 0.001$. Differential response to HFD between genotypes represented by @@ = $p < 0.001$ vs WT of same diet group or vs NC of same genotype. *Full description of statistical analysis can be found in Appendix 2.*

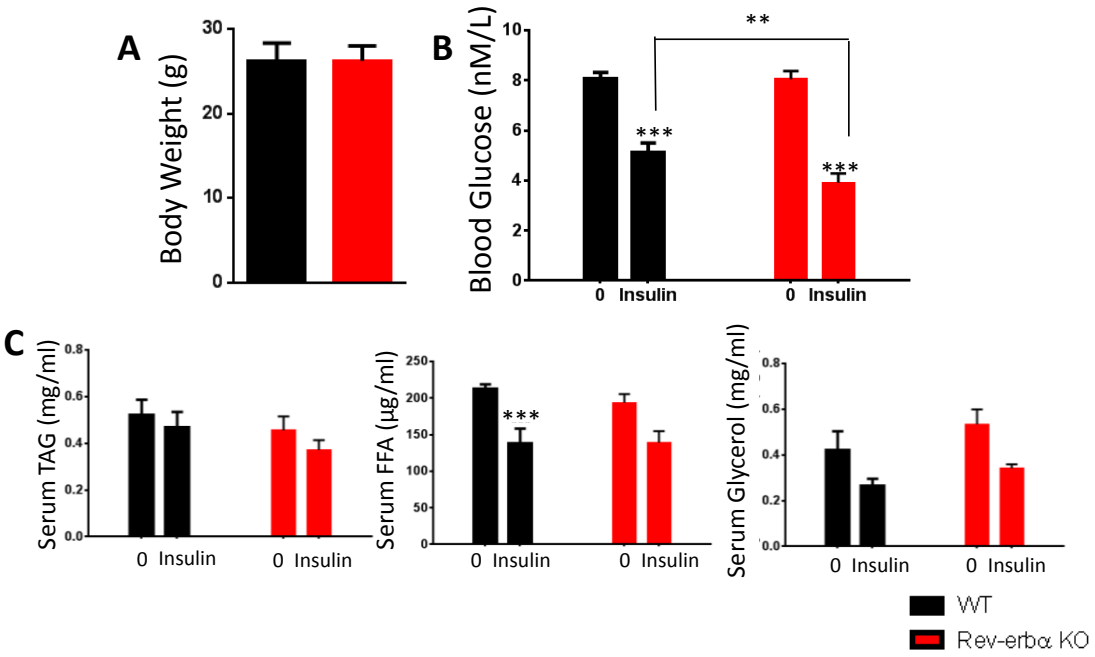

Figure 4.15 – Effect of insulin administration on blood glucose and circulating triglycerides in *Rev-erbα*$^{-/-}$ mice.

Male *Rev-erbα*$^{-/-}$ mice (n=14-15/genotype) were administered 0.75 U/kg of insulin I.P. Animals were weight matched (A) and 1 hour post administration blood glucose concentration was measured (B). *Rev-erbα*$^{-/-}$ mice show higher insulin sensitivity than WT littermates. Serum analysis of circulating TAGs was performed and as expected in WT animals FFAs were reduced, with a trend for this also seen in the *Rev-erbα*$^{-/-}$ mice (n=6/genotype) (C). Data reflect mean ± S.E.M., 2-way, ANOVA, Sidak post-hoc test, *= $p < 0.01$ **= $p < 0.001$, ***= $p < 0.0001$ vs WT of same treatment group or vs control of same genotype. *Full description of statistical analysis can be found in Appendix 2*.

We next performed protein analysis on gWAT from *Rev-erbα*$^{-/-}$ mice and WT littermates (n=6/genotype, collected at ZT 6) maintained on NC or HFD for 14 weeks using SDS-PAGE and Western Blot analysis (Figure 4.13). Notably, many genotypic differences observed at level of mRNA expression were not observed at the level of protein expression; for example, Western Blotting for LPL did not reveal an increase in protein expression between WT and KO mouse adipose. Under NC-fed conditions, an elevated expression of FAS levels was observed in the *Rev-erbα*$^{-/-}$ mice compared with WT littermates, although this did not reach significance upon quantification. FAS was strongly affected by diet in both genotypes with decreased expression observed in response to HFD. Transcript analysis had highlighted a reduction in *Atgl* expression in *Rev-erbα*$^{-/-}$ mice in response to HFD (Figure 4.11) and this is reflected at a protein level (although not reaching statistical significance).

We performed transcript analysis of glucose handling genes in gWAT, liver and muscle from *Rev-erbα*$^{-/-}$ and WT littermates (Figure 4.14). Overall, relatively few genotypic differences were observed in the expression of glucose regulatory genes profiled. Expression of the glucose transporters, *Glut2* and *Glut4*, as well as *Pepck* were down regulated in response to HFD in both genotypes, although these decreases were accentuated in the knockout mice. *HKII* was upregulated in gWAT of *Rev-erbα*$^{-/-}$ mice under NC conditions, and *Gk* expression in the liver was upregulated in both genotypes on HFD.

Proteomic analysis was also performed on WT and *Rev-erbα*$^{-/-}$ mice (n=6, collected at ZT 6) gWAT depots using LC-MS by the Centre for Advanced Discovery and Experimental Therapeutics (CADET) (data not shown). In line with our Western Blot analyses, LPL levels were not different between genotypes. This may indicate that although *Rev-erbα* may play a role in the regulation of *Lpl* transcript, this does not translate to the functional protein. Proteomics analyses did confirm the upregulation of FAS in the qWAT of knockout animals.

4.3.6 *In vivo* insulin stimulation of *Rev-erbα*$^{-/-}$ mice

Insulin regulates energy homeostasis in the body in a variety of ways, including enhancing uptake and incorporation of glucose, decreasing gluconeogenesis, and increasing lipogenesis (Le Roith and Zick, 2001). We were therefore interested whether insulin stimulation of lipogenesis may be accentuated in the *Rev-erbα*$^{-/-}$ mice. Weight matched *Rev-erbα*$^{-/-}$ and WT littermates (n=14-15/genotype) were administered 0.75 U/kg insulin (I.P., administered at ZT6; Figure 4.15A). Blood glucose was measured 1 hour post-administration to assess insulin action. Insulin administration resulted in a significant reduction in blood glucose in both genotypes.

Interestingly, the insulin-induced glucose decrease was accentuated in the knockout animals, despite their increased adiposity (Figure 4.15B). Mice were culled 1 hour post-insulin administration, and trunk blood was collected for serum analysis of circulating lipids (Figure 4.15C). Insulin caused a decrease in circulating TAG, FFA, and glycerol in both genotypes, although the effect of insulin only reached statistical significance in the FFA analyses.

We next performed transcript analysis on a variety of tissues from insulin treated animals to assess the impact of insulin treatment on expression of lipid handling genes. Overall, the transcriptional response to insulin observed in the *Rev-erbα*$^{-/-}$ mice was similar to that observed in WT animals, but with some notable differences (Figure 4.16). Specifically, insulin enhanced lipogenic gene expression in gWAT (*Dgat2, Fasn*, and *Lpl* expression) and scWAT (*Dgat2*) in WT animals. However, this was not observed in *Rev-erbα*$^{-/-}$ mice. Insulin administration did not significantly effect lipolytic gene expression, although decreased expression of *Hsl* was observed in some tissue (although not with a statistically significant effect). In WT mice, insulin caused upregulation of *Atgl* in scWAT, BAT and muscle, but no effect of insulin treatment was observed in these tissues of *Rev-erbα*$^{-/-}$ mice, once again highlighting *Rev-erbα* as potential modulator of *Atgl* expression.

Due to the initial finding of heightened glucose response to insulin treatment in the *Rev-erbα*$^{-/-}$ mice, we went on to perform glucose and insulin tolerance tests (GTT and ITT, respectively) on littermate WT and *Rev-erbα*$^{-/-}$ mice maintained on NC or HFD feeding regimes (n=8/group, 1 mg/kg glucose, 0.75 U/kg insulin respectively, I.P.).

The average weight of all mice on NC, regardless of genotype (WT: 24.7 ± 1.0 g, *Rev-erbα*$^{-/-}$: 22.9 ± 1.1 g, overall 23.8 ± 0.8 g) and HFD (WT: 36.0 ± 1.1 g, *Rev-erbα*$^{-/-}$: 42.6 ± 2.4G, overall 39.3 ± 1.6 g) was calculated. Glucose or insulin was administered according to the whole diet group mean body weight (i.e. all WT/ *Rev-erbα*$^{-/-}$ mice on NC, and all WT/ *Rev-erbα*$^{-/-}$ mice on HFD), to ensure that mice of each genotype were administered with an equivalent amount of insulin or glucose. This was to prevent the super obese *Rev-erbα*$^{-/-}$ mice on HFD from receiving dramatically more glucose or insulin than WT littermates on the same diet. *Rev-erbα*$^{-/-}$ mice on both diet regimes have slightly elevated glucose clearance in response to bolus glucose administration (GTT), with increased blood glucose observed at 60 minutes post-injection relative to WT mice (Figure 4.17A). This effect was only significant in NC fed mice ($p>0.01$). In contrast however, *Rev-erbα*$^{-/-}$ mice exhibited a more pronounced insulin-induced reduction in circulating glucose compared with WT littermates regardless of diet regime, and despite their obese phenotype(Figure 4.17 B).

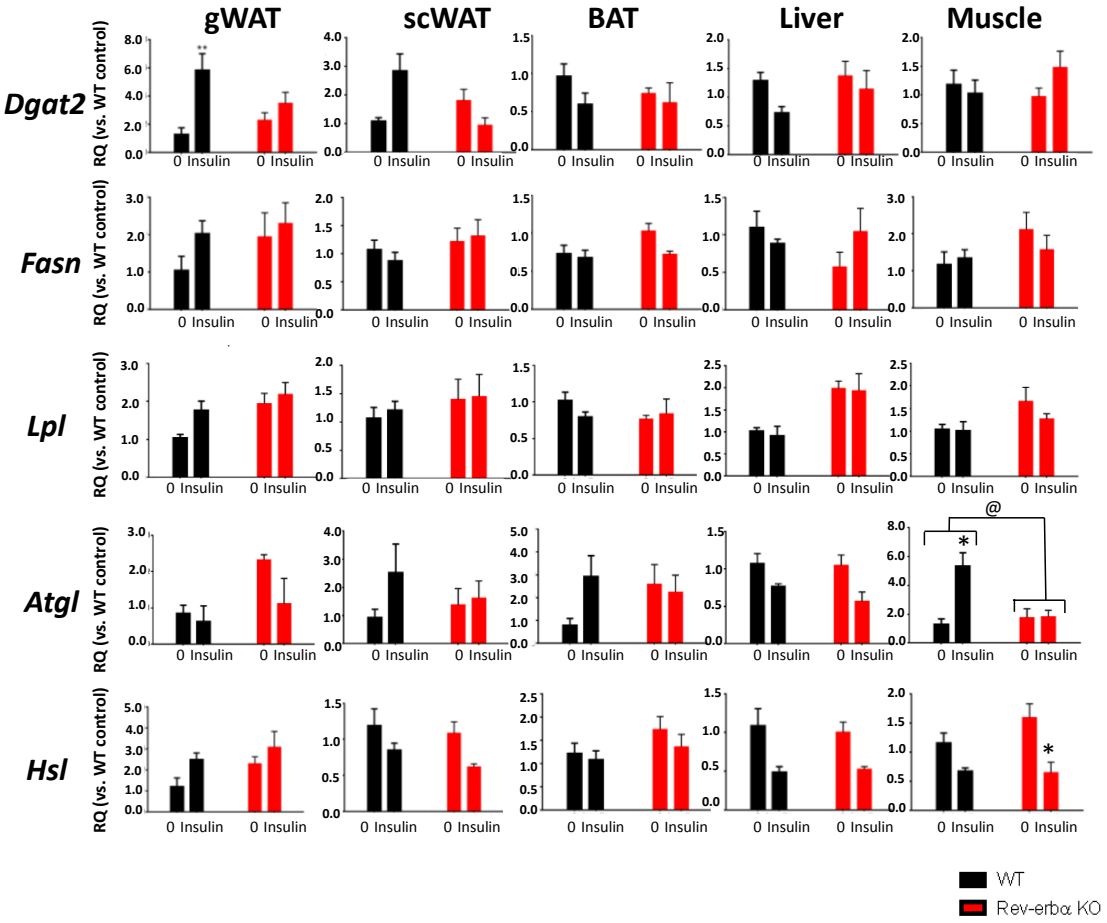

Figure 4.16 – Transcript analysis of *in vivo* insulin stimulation of *Rev-erbα*$^{-/-}$ mice.
Male *Rev-erbα*$^{-/-}$ mice (n=5/genotype) were administered 0.75 U/kg of insulin I.P. and culled 1 hour post administration. Tissues were harvested and transcript analysis was performed. In gWAT, KO animals seemed to show decreased insulin sensitivity with no up regulation of *Dgat2* and *Fasn* observed, unlike WT littermates. Data reflect mean ± S.E.M., 2-way, ANOVA, Sidak post-hoc test *= $p < 0.01$ **= $p < 0.001$. Differential response to insulin between genotypes represented by @ = $p < 0.01$. *Full description of statistical analysis can be found in Appendix 2.*

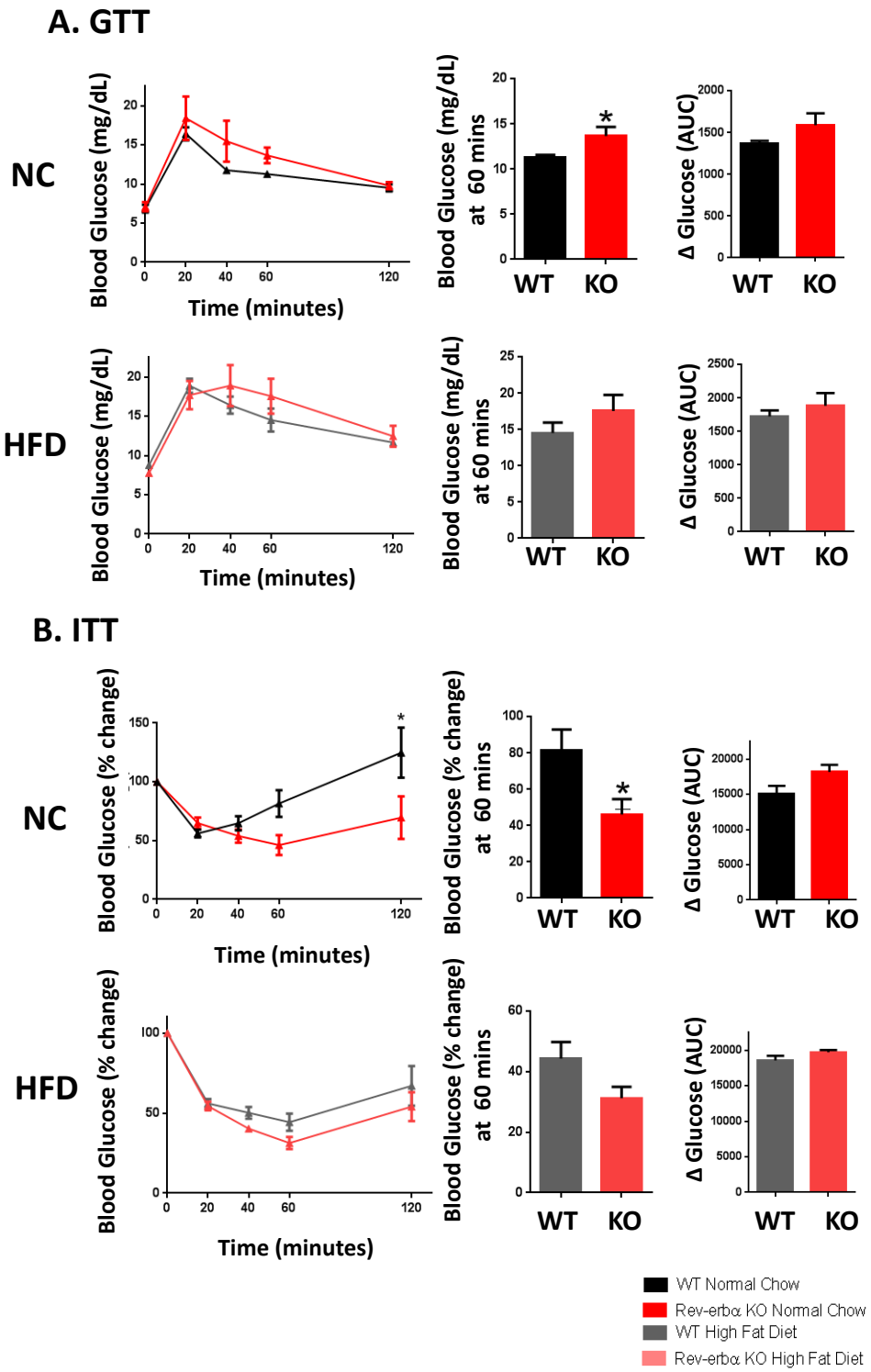

Figure 4.17 – Glucose and insulin tolerance tests in *Rev-erbα*$^{-/-}$ mice.
Female *Rev-erbα*$^{-/-}$ mice and WT littermates (n=6/genotype) were maintained on either NC or HFD for 12 weeks from 8 weeks of age. Mice were administered either 1 mg/kg glucose or 0.75 U/kg insulin for GTT and ITT. On NC, *Rev-erbα*$^{-/-}$ mice showed decreased glucose tolerance (A) but appeared to show increased insulin sensitivity (B) Data reflect mean ± S.E.M. , * = genotype difference, student's unpaired t-test, *= $p < 0.01$. *Full description of statistical analysis can be found in Appendix 2.*

4.3.7 *Ex vivo* insulin stimulation of *Rev-erbα*$^{-/-}$ mice

To remove the influence of systemic responses and directly control insulin exposure to the tissue, an *ex vivo* gWAT explant model was utilised. Initial dose response studies were used to determine the effect of insulin administration on lipogenic and lipolytic pathways in the *ex vivo* gWAT explants. Mice were culled by cervical dislocation and gWAT collected. gWAT was stripped of major blood vessels and further dissected into small (~20mg) tissue pieces (n=8 mice, 3 explants/mouse). Explants were cultured in (DMEM) supplemented with 10% fetal bovine serum and a mixture of penicillin-streptomycin for 24 hours, at which time insulin (dose range from 0-10 µM) was added to the media. Explants were cultured for a further 24 hours before tissue and media was collected for analyses. Insulin stimulation of gWAT explants resulted in decreased expression of lipolytic genes (*Atgl* and *Hsl*), as well as enhanced expression of lipogenic genes (*Dgat2* and *Fasn*) (Figure 4.18). A robust response was seen in all lipolytic/lipogenic genes in response to 1 µM insulin (Figure 4.18) and this dose was carried forward to further studies. We next collected explants from *Rev-erbα*$^{-/-}$ and WT mice (n = 12/genotype/diet, 2 explants/mouse, representative of 2 independent experiments).

Interestingly, and in contrast to *in vivo* responses, gWAT from *Rev-erbα*$^{-/-}$ mice showed an enhanced insulin-driven lipogenic gene expression compared to WT littermates. Insulin administration caused a significant upregulation of *Dgat2* and *Fasn* in explants derived from NC fed C57BL/6 mice, which was significantly more profound in gWAT explants from KO animals. Insulin also caused a pronounced reduction in *Lpl*, *Atgl* and *Hsl* mRNA expression. In gWAT explants derived from *Rev-erbα*$^{-/-}$ mice, insulin treatment reduced *Lpl* expression, but had no impact on *Atgl* or *HSL* expression. Once again this highlights the potential influence of *Rev-erbα* on regulation of *Atgl* and *Hsl*. In general, all insulin-dependent responses were maintained explants derived from control *Rev-erbα*$^{+/+}$ HFD-fed mice. This was not the case for explant cultures derived from HFD-fed KO mice, which showed strongly attenuated transcriptional response to insulin. This supports data obtained from fresh gWAT transcript analysis in which *Atgl* and *Hsl* were downregulated in DIO *Rev-erbα*$^{-/-}$ mice (Figure 4.12) and may be due to the profound adiposity of the animals rather than a true genotypic difference.

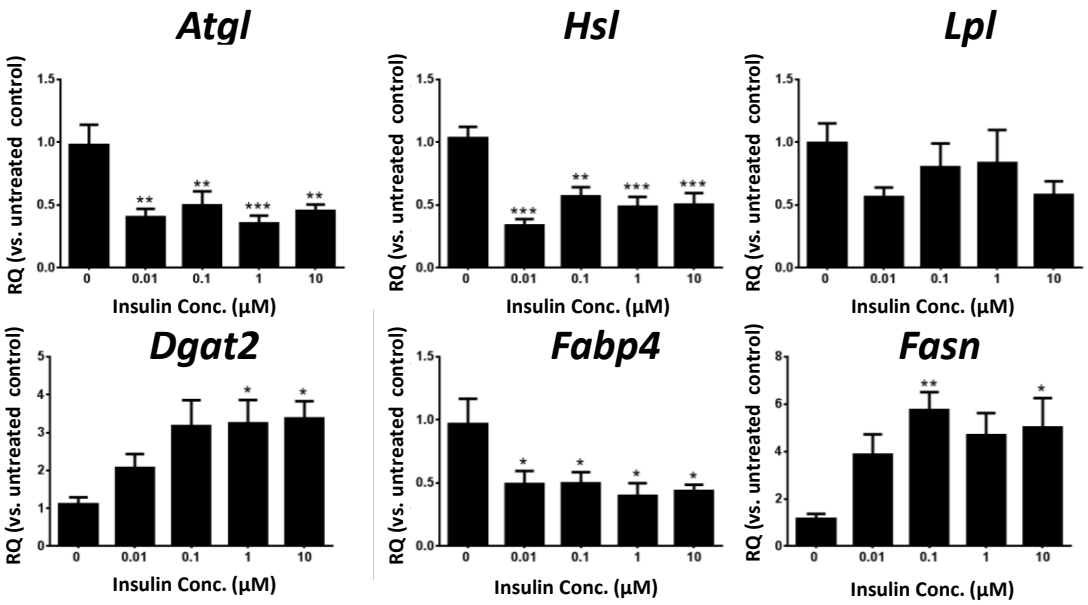

Figure 4.18 – Insulin dose response of WT gWAT explants.

gWAT from male C57BL6 mice was harvested (n=8) and cultured *ex vivo* for 24 hours. It was then treated with varying concentrations of insulin in the media. Insulin caused the downregulation of lipolytic genes (*Atgl, Hsl*) and the upregulation of lipogenic genes (*Dgat2, Fasn*) which was expected. Data reflect mean ± S.E.M., 1-way, ANOVA, *= $p < 0.01$, **= $p < 0.001$ ***= $p < 0.0001$ vs control treated group. *Full description of statistical analysis can be found in Appendix 2.*

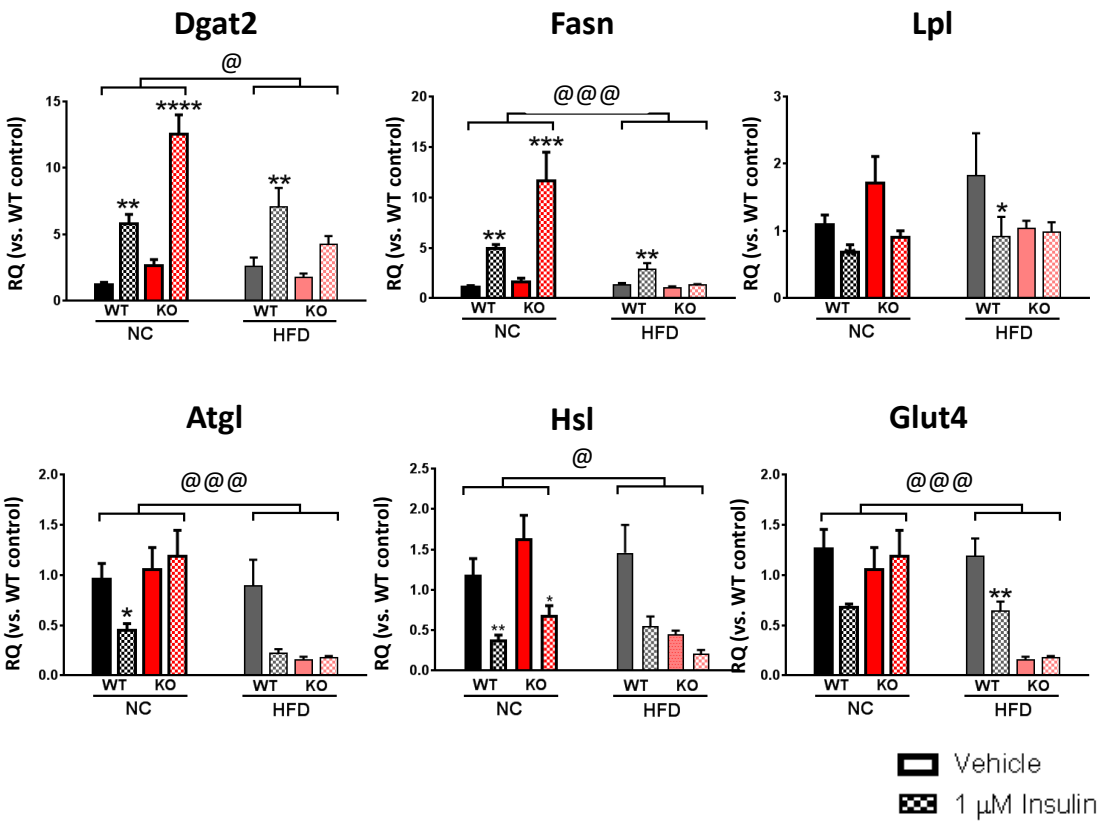

Figure 4.19 – *Ex vivo* insulin stimulation of gWAT from *Rev-erbα*$^{-/-}$ mice.
gWAT from female *Rev-erbα*$^{-/-}$ mice (NC or HFD for 14 weeks from 8 weeks of age, n = 12/genotype/diet) was harvested and cultured *ex vivo* before being treated with 1 uM insulin. Tissue was collected 24 hours later and transcript analysis of key lipid handling genes performed. As expected, HFD resulted in attenuation of lipogenic drive of insulin but interestingly gWAT from *Rev-erbα*$^{-/-}$ animals seemed to show heighted lipogenic drive with enhanced expression of *Dgat2* and *Fasn*. In WT gWAT insulin resulted in the down regulation of *Atgl* but this wasn't observed In gWAT from *Rev-erbα*$^{-/-}$ mice. Data reflect mean ± S.E.M. , 3-way, ANOVA, *= $p < 0.01$, **= $p < 0.001$ ***= $p < 0.0001$, ****= $p < 0.00001$ vs untreated control of same genotype. Diet difference in gene expression represented by @@= $p < 0.001$ @@@= $p < 0.0001$, @@@@= $p < 0.00001$. *Full description of statistical analysis can be found in Appendix 2.*

4.4 Summary

In this chapter we assessed the impact of global *Rev-erbα* deletion on physiological and metabolic parameters under normal conditions as well as during negative (fast) and positive (HFD) energy balance. Loss of *Rev-erbα* in mice, despite maintenance of robust physiological rhythms, results in a compromised gWAT clock, with attenuation of clock gene rhythms observed specifically in gWAT. This is interesting as *Rev-erbα* null mice are an obese phenotype and gWAT specific clock disruption was observed in diet-induced obese WT mice in chapter 3. This may be a suggestion that a disrupted clock in gWAT of *Rev-erbα*$^{-/-}$ is due to their increased adiposity. Increased inflammation has been proposed as a potential reason for clock disruption in obesity, but *Rev-erbα*$^{-/-}$ mice exhibit an attenuation of typical pro-inflammatory stimuli with enhanced anti-inflammatory signalling. Reduced inflammation in *Rev-erbα*$^{-/-}$ is supported by reduced circulating FFA and glycerol which is indicative of reduced lipolysis, a known inflammatory signal (Zhang *et al*., 2014).

A defect in lipolysis may play a role in the obese phenotype exhibited by *Rev-erbα*$^{-/-}$mice. Widespread dysregulation of lipid handling genes in gWAT of *Rev-erbα*$^{-/-}$ mice was observed but there was not, however, a bias towards lipid storage as both lipogenic (*Dgat2, Fasn*) and lipolytic (*Hsl*) sides of the pathway were upregulated in gWAT. *Lpl* was consistently upregulated in all tissues examined, suggesting that *Rev-erbα* may be a direct regulator of this gene throughout the body. As *Lpl* is responsible for the liberation of fatty acids from circulating triglycerides for uptake into tissues, the increased expression may contribute to the increased adiposity in *Rev-erbα*$^{-/-}$ mice.

Rev-erbα$^{-/-}$ mice do not show the normal metabolic and genetic response to fast, again potentially indicating a defect in lipolysis in these mice. The attenuated fast induced reduction in metabolic rate in the knockout mice may reflect increased energy stores available to these mice to due to increased adiposity. Derivation of FOX rate demonstrated that fatty acid oxidation was profoundly increased in both genotypes during the fasting period. Interestingly, FOX rates were significantly higher in fasted *Rev-erbα*$^{-/-}$ mice compared with WT littermates, especially during the final 6 hour of the fast. It is therefore likely that increased adiposity in *Rev-erbα*$^{-/-}$ animals underlies their ability to maintain higher rate of EE and VO_2 across the fasting period. However, the attenuated response was maintained even during 48 hr of fasting, a relatively extreme fast for mice. This suggests that these mice may not perceive the state of negative energy balance, or that they cannot engage in hypermetabolic processes (such as

torpor) to decrease energy expenditure during negative energy balance. However, when looking at the genetic profile of lipid-handling transcripts in these animals, strikingly, both a 24 and 48 hour fast did not result in the upregulation of *Atgl* in both adipose tissue and liver, as it does in control animals. The dysregulation of *Atgl* expression during fasting may be attributed to the increased levels of *Bmal1* present due to lack of *Rev-erbα* inhibition. *Atgl* expression is also regulated by CLOCK/BMAL1 expression via E-box activation and *Bmal1* expression is constitutively higher in *Rev-erbα*$^{-/-}$ mice (Shostak *et al*., 2013). A normal homeostatic response to fasting (reduced lipogenesis) is maintained in the *Rev-erbα*$^{-/-}$ mice, with decreased *Dgat2* expression observed. This highlights a possible specific defect in the homeostatic mechanism to upregulate lipolysis in a state of negative energy balance. To further investigate this, direct stimulation of lipolysis *in vivo* using CL316,243, a β_3-adrenoceptor was performed. This resulted in an upregulation of *Hsl* in gWAT of both *Rev-erbα*$^{-/-}$ mice and WT controls which contrasts results obtained from the negative energy balance study suggesting that the β-adrenoceptor is a potent regulator of *Hsl* expression. Post-translational modifications are important for the function of lipase enzymes, and they need to be phosphorylated in order for them to be lipolytically active. However, β-adrenergic stimulation caused significantly less phosphorylation of HSL in *Rev-erbα*$^{-/-}$ mice compared to WT controls. This further supports a defect in lipolysis in these animals.

When faced with HFD challenge, *Rev-erbα*$^{-/-}$ mice become super obese. All of this suggests that there is an increased propensity for fat storage and decreased liberation of fatty acids within *Rev-erbα*$^{-/-}$mice. The susceptibility of *Rev-erbα*$^{-/-}$ to DIO is not due to altered transcription of *Ppars.* However, *Pparγ* may be protected from the obesity related decrease in expression in *Rev-erbα*$^{-/-}$ mice, because a similar response to that observed in chapter 3 (i.e. downregulation of *Pparγ)* would have been expected due to their vast adiposity. The reduction in *Atgl* expression in response to chronic HFD feeding may reflect the more profound adiposity of the knockout animals compared to WT littermates. However, many studies have demonstrated that long-term or pronounced obesity is associated with an upregulation in lipolytc drive (Reynisdottir *et al.,* 1995; Ryden *et al.,* 2002; Ryden *et al.,* 2004). Despite their increased adiposity on NC and super obesity on HFD, *Rev-erbα*$^{-/-}$ mice remain insulin sensitive, which may point to the fact that increased storage of TAG within adipose tissue is 'safe' and it is ectopic fat storage in obesity that results in metabolic syndrome and insulin resistance. However, in an *ex vivo* environment, insulin does not cause the expected reduction in *Atgl* expression in gWAT from *Rev-erbα*$^{-/-}$mice, highlighting *Atgl* as a potential key point metabolic regulation responsible for the obese phenotype of this mouse.

Results

Chapter 5 - Adipocyte-specific *Bmal1* null mice showing attenuated feeding rhythms and sever lipid handling gene dysregulation whereas adipocyte specific loss of *Rev-erbα* has negligible physiological consequences

5.1 Introduction

We and others (Zvonic *et al*., 2006; Kohsaka *et al.* 2007) have shown that murine adipose tissue has robust rhythms in clock gene expression. Microarray analyses suggest that approximately 10-20% of the murine transcriptome in adipose tissue shows circadian rhythm in expression, within which metabolic pathways are particularly enriched (Zvonic, *et* al., 2006; Ptitsyn et al., 2005; Zhang et al., 2014). This suggests a pronounced impact of the clock on adipose physiology. Interestingly, WAT tissue rhythms in clock and metabolism related genes were found to be particularly sensitive to obesity-related damping (Chapter 3), implicating clock disruption in metabolic disease. In addition to orchestrating rhythms in gene expression, multiple lines of evidence connect circadian rhythms with adipose tissue physiology. For instance, *in vitro* data has demonstrated that a number of clock genes (including *Rev-erbα, Per2, Bmal1*) play a role in adipocyte differentiation. For example, *Rev-erbα* mRNA levels increase dramatically during the differentiation of 3T3-L1 cells into adipocytes (Chawla and Lazar, 1993). In more recent years, Wang and Lazar (2008) demonstrated that during adipogenesis, *Rev-erbα* gene expression initially declines and subsequently increases. In contrast, protein levels initially increases and subsequently declines, as REV-ERBα protein represses *Pparγ* expression, a transcriptional regulator of adipogenesis (Wang and Lazar, 2008). *Rev-erbα* has been further implicated in adipogenesis as heme, a physiological ligand for *Rev-erbα* can promote differentiation of fibroblasts to adipocytes and increased intracellular heme levels are observed during 3T3-L1 adipogenesis (Chen and London, 1981; Raghuram *et al*., 2007; Kumar *et al*., 2010). Despite this, *Bmal1*$^{-/-}$ and *Rev-erbα*$^{-/-}$ mice do not exhibit abnormalities in the development of adipose tissue, and in fact mice with either *Bmal1* or *Rev-erbα* deletion in all tissues have greater adipose tissue mass compared to WT controls (Bunger *et al*., 2000; Bunger *et al*., 2005; Lamia *et al*., 2008 Delezie *et al*., 2012; Chapter 4). Conversely, a lack of *Per2* results in enhanced adipocyte differentiation of cultured fibroblasts (Grimaldi *et al.,* 2010), and *Per2*$^{-/-}$ mice have significantly less epididymal fat than WT littermates (Grimaldi *et al*., 2010).

A role for Rev-erbα has also identified in BAT thermogenesis (Gerhart-Hines *et al*., 2013). In the mouse, expression of *Rev-erbα* in BAT peaks at ZT10, which is in antiphase to the circadian rhythm of body temperature. Cold temperatures induce the expression of UCP1, and it has been shown that this is preceded by rapid downregulation of *Rev-erbα* in BAT. UCP1 levels are high in *Rev-erbα* null mice as *Rev-erbα* represses *Ucp1* in a brown-adipose-cell autonomous manner. Therefore, when mice are subjected to 6 hours of cold, there is a higher survival rate

at ZT 16-22, when *Rev-erbα* is minimally expressed in comparison to ZT 4-10 when *Rev-erbα* is abundant. To further support this, deletion of *Rev-erbα* markedly improves cold tolerance at ZT10, suggesting that overcoming *Rev-erbα* dependant repression is an important feature of the thermogenic response to cold. Data from our lab also shows that body temperature is maintained in fasted *Rev-erbα* null mice in contrast to WT littermates whose temperature drops during this challenge. This parallels metabolic data obtained from these mice during a fast, which demonstrates that fast induced reductions of VO_2 and EE (kcal/hr) are significantly less pronounced in *Rev-erbα* null mice. It is therefore thought that *Rev-erbα* is necessary for maintaining body temperature rhythms in a way that is adaptable to environmental and metabolic cues.

In chapter 4, dramatic metabolic differences were observed in global *Rev-erbα*$^{-/-}$ mice compared to WT littermates. Robust physiological rhythms were maintained but the local gWAT clock was compromised in these mice. Dysregulation of lipid handling genes was also observed in these animals, with an upregulation of lipogenic genes being observed, which also corresponded to an increased adiposity in these mice as well as increased susceptibility to D.I.O. Despite increased adiposity, these mice remained insulin sensitive. Taken together, these data indicate a key role for *Rev-erbα* in adipose tissue. It has also been shown that mice with *Bmal1* deletion in all tissues have a higher body weight and greater adipose tissue mass compared to WT controls (Bunger *et al*., 2005; Lamia *et al*., 2008). Here we address the role of the circadian clock in adipose tissue by deleting *Bmal1* or *Reverb*α specifically in adipocytes. Tissue selective deletion of *Bmal1* renders the tissue arrhythmic (as it is an essential component of the circadian clockwork), but also results in a profound attenuation of *Rev-erbα* expression (Bunger *et al*., 2000). Although *Rev-erbα* reinforces the robustness of circadian oscillation, circadian rhythm generation persists in its absence (Preitner *et al*., 2002). Therefore clock functionality would be maintained in adipose tissue lacking *Rev-erbα*. By characterising these mice models it is possible to dissect the specific role that either the clock or clock components play in adipose physiology.

5.2 Methods

Detailed methodological approaches can be found in the methods (Chapter 2). Below are specific experimental details. Male or female only cohorts were used in some studies due to the difficulties in breeding the *Adipo*^{CRE} clock knockout mice.

Genotyping was performed by PCR using ear clip biopsies and QIAamp DNA Mini Kit (Qiagen) according to manufacturers' instructions.

Adipo^{CRE} expression:

2 µL of extracted DNA was added to a DNA amplification reaction containing (in final concentration): 1 X Go TAQ reaction buffer (Promega), $MgCl_2$ 2 mM (Sigma Aldrich), dNTP 0.2 mM (Sigma Aldrich) and Go Taq Hotstart polymerase (0.15 U). Four primers were added to the mixture – forward primer 5'-GCGGTCTGGCAGTAAAAACTATC-3' (1 µM) and reverse primer 5'GTG AAA CAG CAT TGC TGT CAC TT- 3' (1 µM) amplified the CRE transgene, which was 100bp. The forward primer 5'-CTAGGCCACAGAATTGAAAGATCT-3' (1 µM) and reverse primer 5'GTAGGTGGAAATTCTAGCATCATCC-3' (1 µM) amplified an internal positive control, which was 324bp. The PCR protocol consisted of 3 min at 94 °C, then 35 cycles of 30 sec at 94 °C, 1 min at 51.7 °C and 1 min at 72 °C and a subsequent 2 min at 72 °C. Products were separated by electrophoresis on 3% agarose gels stained with Safeview (NBS Biologicals).

Bmal1^{flox} expression: 1 µL of extracted DNA was added to a DNA amplification reaction containing (in final concentration): 1 X Go TAQ reaction buffer (Promega), $MgCl_2$ 2 mM (Sigma Aldrich), dNTP 0.2 mM (Sigma Aldrich) and Go Taq Hotstart polymerase (0.625 U). Two primers were added to the mixture – forward primer 5'-ACTGGAAGTAACTTTATCAAACTG-3' (0.2 µM) and reverse primer 5'-CTGACCAACTTGCTAACAATTA-3' (0.2 µM) amplified either a band of either 327 bp which represents the WT band or 431 bp which represents the floxed band. The PCR protocol consisted of 2 min at 94 °C, then 2 cycles of 30 sec at 94 °C, 1 min at 61.6 °C and 1 min at 72 °C and a subsequent 5 min at 72 °C. Products were separated by electrophoresis on 2% agarose gels stained with Safeview (NBS Biologicals).

Rev-erbα^{flox} expression: 3 µL of extracted DNA was added to a DNA amplification reaction containing (in final concentration): 1 X Go TAQ reaction buffer (Promega), $MgCl_2$ 2 mM (Sigma Aldrich), dNTP 0.5 mM (Sigma Aldrich) and Go Taq Hotstart polymerase (1 U). Two primers were added to the mixture – forward primer 5'-TCTCCGTTGGCATGTCTAGAGATGG-3' and reverse primer 5'-GAAGAGTGTGTGTTTGCCCAAGAGG-3' which amplified the floxed band of 291 bp. The PCR protocol consisted of 3 min at 94 °C, then 2 cycles of 1 min at 94 °C, 1 min at 62 °C and 1 min at 72 °C and a subsequent 5 min at 72 °C. This was followed by a 5 min

incubation period at 72 °C before 30 cycles of 30 sec at 94 °C, 30 sec at 62 °C and 30 sec at 72 °C before finally 3 min at 72 °C. Products were separated by electrophoresis on 3% agarose gels stained with Safeview (NBS Biologicals).

Confirmation of adipose specific targeting was performed by sacrificing male *Adipo*^{CRE}*Bmal1*$^{flox/flox}$ mice and control littermates (n=4-6/genotype) and *Adipo*^{CRE}*Rev-erbα*$^{flox/flox}$ mice and control littermates (n=4-6/genotype) and collecting a range of tissues for transcript analysis. Body weights and adipose tissues weights were measured in male and female *Adipo*^{CRE}*Bmal1*$^{flox/flox}$ and *Adipo*^{CRE}*Rev-erbα*$^{flox/flox}$ mice and control littermates (n=8/genotype/sex). Basal metabolic gas exchange was measured in male *Adipo*^{CRE}*Bmal1*$^{flox/flox}$ and *Adipo*^{CRE}*Rev-erbα*$^{flox/flox}$ mice and control littermates (n=4/genotype) by indirect calorimetry using the CLAMS system (Columbus Instruments). Basal transcript analysis was also performed on tissues collected from sacrificed male *Adipo*^{CRE}*Bmal1*$^{flox/flox}$ and *Adipo*^{CRE}*Rev-erbα*$^{flox/flox}$ mice and control littermates (n=8/genotype). Food intake of both male and female *Adipo*^{CRE}*Bmal1*$^{flox/flox}$ mice and control littermates was monitored using the Labmaster Metabolism Research Platform (TSE systems), with meal size and feeding events recorded over 6 days (n=4/genotype/sex).

For DIO studies, 8 week old male and female *Adipo*^{CRE}*Bmal1*$^{flox/flox}$ and control littermates (n=6/genotype/diet/sex) and female *Adipo*^{CRE}*Rev-erbα*$^{flox/flox}$ mice and control littermates (n=5/genotype/diet) were provided *ad libitum* access to high fat diet (HFD; 60% energy from fat; DIO Rodent Purified Diet, IPS Ltd) or normal chow (NC) for 14 weeks. For negative energy balance studies, male *Adipo*^{CRE}*Bmal1*$^{flox/flox}$ and *Adipo*^{CRE}*Rev-erbα*$^{flox/flox}$ mice and control littermates (n=4/genotype) were fasted for 48 hours. Physiological parameters, including body temperature using radiotelemetry (Data Sciences International) were monitored as well as metabolic gas exchange using the CLAMS system. Male *Adipo*^{CRE}*Bmal1*$^{flox/flox}$ and control littermates *were* also subjected to a cold challenge using an upright 1200 L industrial fridge (Polar Refrigeration, UK) (n=6/genotype). Body temperature was measured using radiotelemetry.

A further cohort of male *Adipo*^{CRE}*Bmal1*$^{flox/flox}$ mice and control littermates were used for *ex vivo* insulin stimulation. Upon sacrifice, gWAT was collected, minced and maintained in DMEM supplemented with FBS and penicillin/streptomycin before being stimulated with insulin and subsequently collected for transcript analysis (n=7-9/genotype, 2 independent studies). An *in vivo* ITT was performed on male *Adipo*^{CRE}*Rev-erbα*$^{flox/flox}$ mice (n=6/genotype/treatment).

5.3 Results

5.3.1 Confirmation of Adipose Specific Targeting

To study the role of the adipocyte circadian clock in energy homeostasis, mice were generated that lacked either *Bmal1* or *Rev-erbα* specifically in adipocytes, using an adiponectin (*Adipoq*) promotor driven Cre-recombinase driver mouse line (Eguchi *et al*., 2011), ensuring the genes were only knocked out of adipocytes. *Bmal1*^{flox} mice were created by inserting lox P sites either side of exons and 8 of the *Bmal1* gene (Storch *et al.,* 2007) (Figure 5.1A). Rev-erbα^{flox} mice were generated by inserting lox P sites either side of exons 3 and 4 of the *Rev-erbα* gene (Figure 5.1A) (Institut Clinique de la Souris). *Bmal1*^{flox}or *Rev-erbα*^{flox} mice were then bred locally with *Adipo*^{CRE} mice. Floxed mouse lines were C57BL/6J mice. Upon receipt, *Adipo*^{CRE} mice were approximately 70% C57BL/6, and so mice were backcrossed to the founder floxed mouse line for three generations before F1 mice were used for breeding.

Genotyping was performed using the genotyping strategy explained in section 5.2. Example agarose gels showing the presence/absence of the Adipo-cre transgene and the presence of the floxed *Bmal1* or *Rev-erbα*. To confirm adipose specific targeting, a variety of targeted and non-targeted tissues (gWAT, scWAT, BAT, liver, lung) were collected from male mice (n=10/genotype) and gene expression assessed by qPCR (Figure 5.1 B). In the *Adipo*^{CRE}*Bmal1*$^{flox/flox}$ mice, *Bmal1* expression was significantly reduced in all adipose tissue depots (gWAT, scWAT and BAT) with no difference in expression observed in liver and lung, showing that selective loss of *Bmal1* in adipose tissue has occurred. In line with reduced *Bmal1* expression, *Rev-erbα* expression was also significantly reduced in all adipose tissue depots (gWAT, scWAT and BAT) and unchanged in liver and lung. A similar approach was used to confirm the loss of *Rev-erbα* specifically in adipose tissue. *Rev-erbα* expression was significantly reduced in all adipose tissue depots (gWAT, scWAT, BAT) of *Adipo*^{CRE}*Rev-erbα*$^{flox/flox}$ compared to control *Rev-erbα*$^{flox/flox}$ *mice*, and expression remained unaltered in non-adipose tissues, liver and lung. To further confirm adipose specific targeting *Bmal1* expression was measured in these animals. Indeed, a significant increase in *Bmal1* expression in gWAT, scWAT and BAT was observed with no difference in expression observed in liver or lung compared to control mice. Once established and validated both lines were bred up for metabolic phenotyping to determine the impact of the loss of *Bmal1* and *Rev-erbα* on adipose physiology.

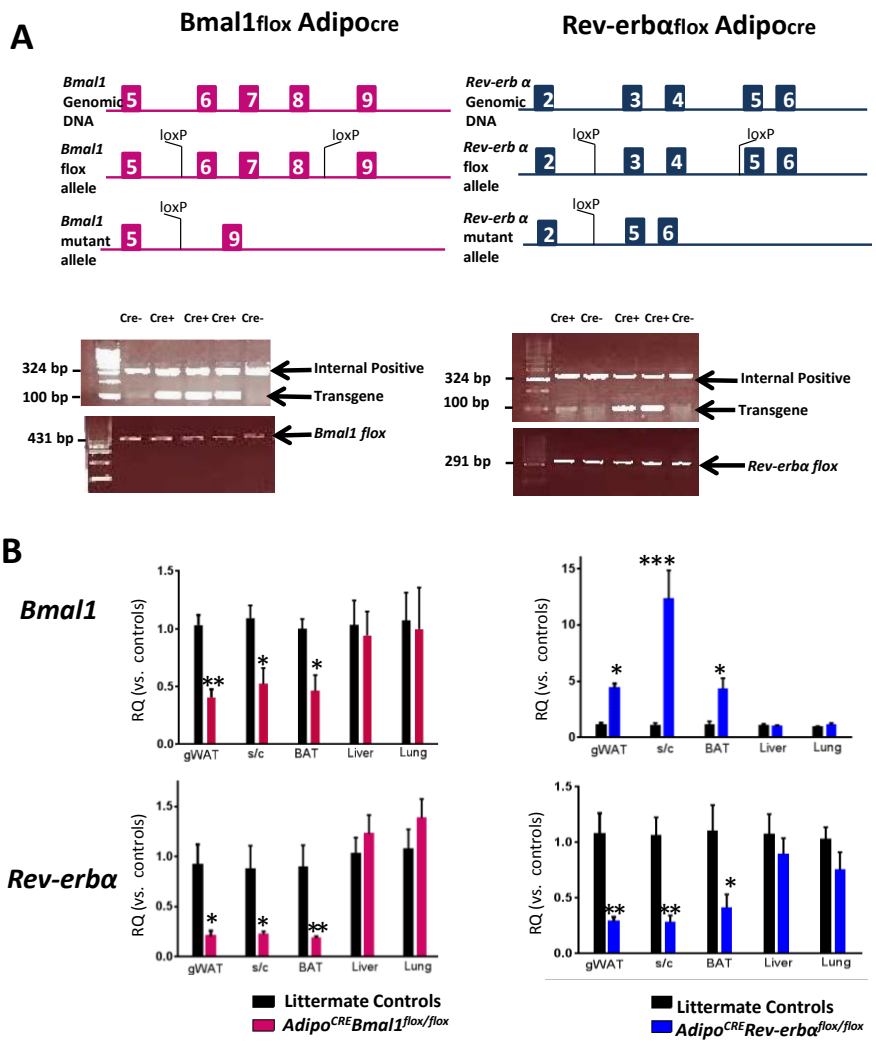

Figure 5.1 – Confirmation of adipose specific targeting.

Mice were generated that lacked either *Bmal1* or *Rev-erbα* specifically in adipocytes, using an adiponectin (*Adipoq*) promotor driven Cre-recombinase driver mouse line. *Bmal1*^{flox} mice were created by inserting lox P sites either side of exons and 8 of the *Bmal1* gene and Rev-erbα^{flox} mice were generated by inserting lox P sites either side of exons 3 and 4 of the *Rev-erbα* gene (A). Example agarose gels show the presence/absence of the Adipo-cre transgene and the presence of the floxed *Bmal1* or *Rev-erbα* (A). To confirm adipose specific targeting, a variety of targeted and non-targeted tissues (gWAT, scWAT, BAT, liver, lung) were collected from male mice (n=4-6/genotype) and gene expression assessed by qPCR (B). In the *Adipo*^{CRE}*Bmal1*$^{flox/flox}$mice, *Bmal1* expression was significantly reduced in all adipose tissue depots (gWAT, scWAT and BAT) with no difference in expression observed in liver and lung. *Rev-erbα* expression was also significantly reduced in all adipose tissue depots and unchanged in liver and lung.. *Rev-erbα* expression was significantly reduced in all adipose tissue depots of *Adipo*^{CRE}*Rev-erbα*$^{flox/flox}$ compared to control *Rev-erbα*$^{flox/flox}$ *mice*, and expression remained unaltered in non-adipose tissues, liver and lung. In these mice, a significant increase in *Bmal1* expression in gWAT, scWAT and BAT was observed with no difference in expression observed in liver or lung compared to control mice (B). Data reflect mean ± SEM, 2-way ANOVA, Sidak post hoc test, * = $p < 0.05$, ** = $p < 0.005$, *** = $p < 0.0005$. *Full description of statistical analysis can be found in Appendix 3.*

5.3.2 Metabolic phenotype of *Adipo^{CRE+}Bmal1$^{flox/flox}$* mice

No difference in body weight was observed between control and adipose-targeted mice. At 20 weeks of age, male and female *Adipo^{CRE}Bmal1$^{flox/flox}$* and *Bmal1$^{flox/flox}$* littermate mice showed no significant difference in body weight, or gWAT fat pad mass (n=5 per genotype per sex; Figure 5.2). A significant increase in scWAT weight in male *Adipo^{CRE}Bmal1$^{flox/flox}$* mice was observed compared to their control littermates (Figure 5.2) which may suggest a subtle impact on adiposity.

Continual monitoring of food intake over 4 days (using TSE feeding cages) revealed no difference in total daily food intake in male or female *Adipo^{CRE}Bmal1$^{flox/flox}$* mice compared to control littermates (n=4 per genotype). However, attenuated light/day feeding rhythms were observed in *Adipo^{CRE}Bmal1$^{flox/flox}$* mice (Figure 5.3).

We next examined energy expenditure in the *Adipo^{CRE}Bmal1$^{flox/flox}$* mice using indirect calorimetry (male mice, n= 4/genotype). Pronounced diurnal variations in VO_2, VCO_2 and RER were observed in control mice, with a significant elevation in VO_2, VCO_2 and RER in the active (dark) phase of the day (Figure 5.4). A similar profile was observed in the *Adipo^{CRE}Bmal1$^{flox/flox}$* mice. Similarly, RER, COX, and FOX profiles did not differ between the two genotypes. This pattern of RER does not correlate with attenuated feeding rhythms observed in these mice. Interestingly, although both control and *Adipo^{CRE}Bmal1$^{flox/flox}$* mice showed rhythmicity in the kcal/hr consumption, this only reached significance in the *Adipo^{CRE}Bmal1$^{flox/flox}$* mice. Core body temperature was recorded for 7 days using remote radio-telemetry in control and *Adipo^{CRE}Bmal1$^{flox/flox}$* animals (n=6/genotype). Diurnal variation was observed in the body temperature of both *Adipo^{CRE}Bmal1$^{flox/flox}$* (Day: 36.0°C± 0.03, Night: 37.2°C± 0.04) and control mice (Day: 36.1°C± 0.04, Night: 37.4°C± 0.1).

Taken together, these studies indicate that a functional clock in adipose tissue is not necessary to maintain diurnal rhythms in metabolic rate or body temperature.

5.3.3 Fasting response in *Adipo^{CRE}Bmal1$^{flox/flox}$*

As discussed above, global *Rev-erbα$^{-/-}$* mice exhibit an attenuated metabolic and thermogenic response to acute fasting when compared to WT littermates (Figures 4.6 and 4.7). We were therefore interested to examine the response of *Adipo^{CRE}Bmal1$^{flox/flox}$* to negative energy balance. *Adipo^{CRE}Bmal1$^{flox/flox}$* and littermate controls were fasted for 48 hours (male mice, n=6/

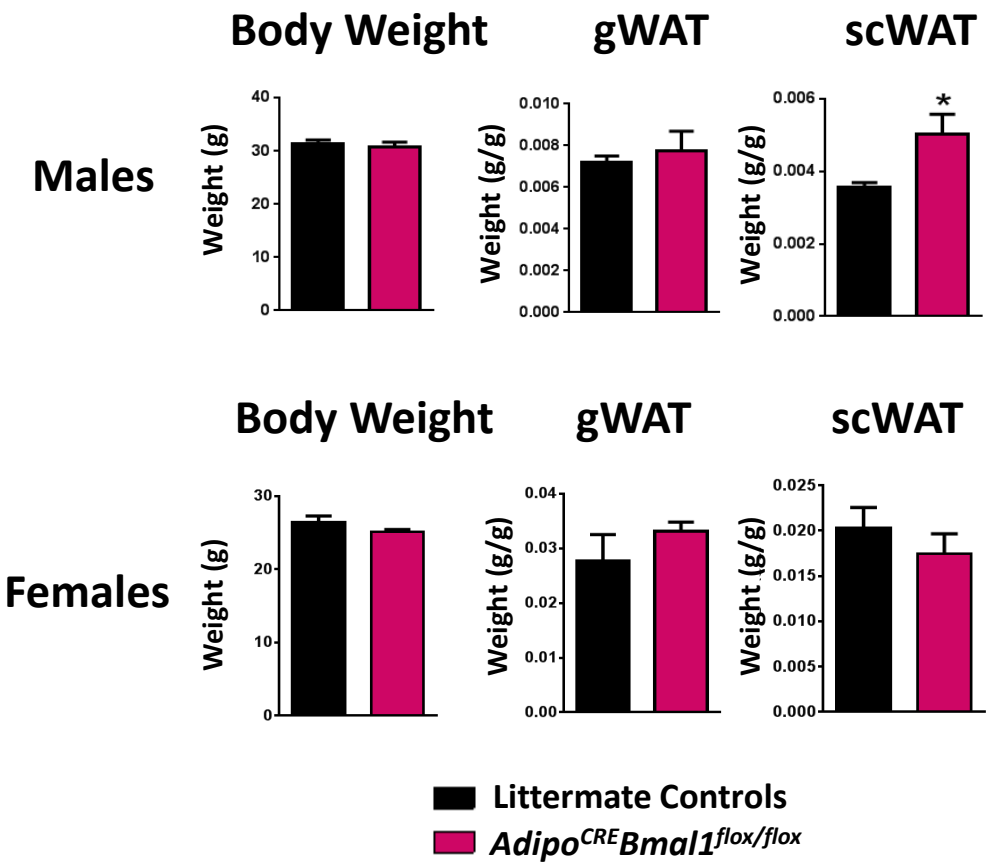

Figure 5.2 – Body weight profiles of *Adipo^{CRE}Bmal1$^{flox/flox}$* mice.
Body weights of male and female *Adipo^{CRE}Bmal1$^{flox/flox}$* mice (n=5 per genotype) were measured at 20 weeks of age (Fig. 5.2 A). Mice were culled and gWAT and scWAT fat pads dissected and weighed and expressed as g/g of bodyweight. No significant difference was seen between the body weights and gWAT weights of each genotype in both sexes. However, scWAT fat pad weight was significantly higher in male KO mice. Data reflect mean ± SEM, student's unpaired t-test, * = $p < 0.05$. *Full description of statistical analysis can be found in Appendix 3.*

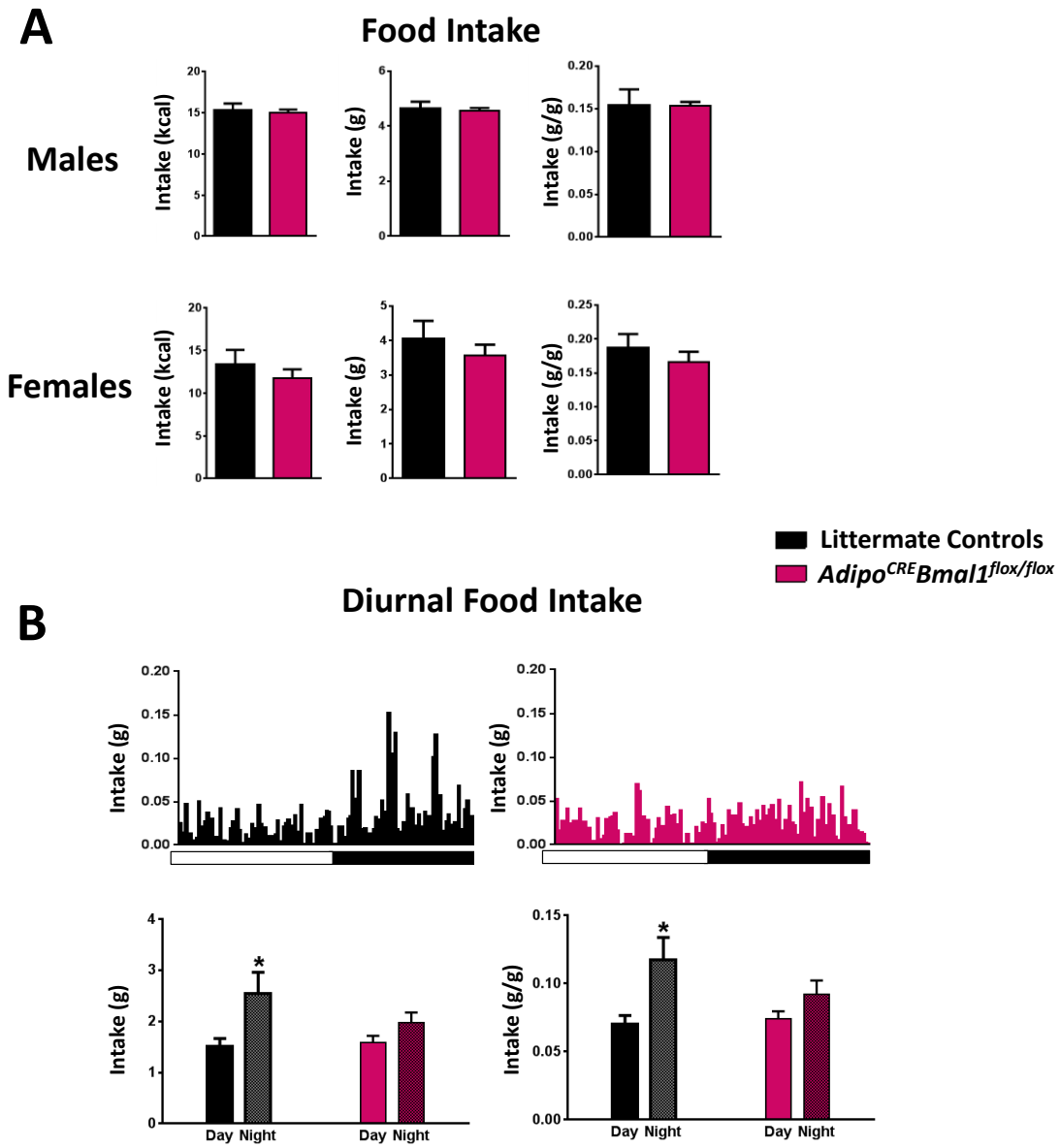

Figure 5.3 – Food intake in *Adipo^{CRE}Bmal1$^{flox/flox}$* mice.

No difference was observed in daily food intake between the genotypes of both sexes (n=4/genotype/sex) (A). Data reflect mean ± SEM, student's unpaired t-test, * = $p < 0.05$. Temporal food intake was monitored (B) in the female mice. In control mice, as expected, there was a significant increase in food intake during the active phase; however a temporal feeding rhythm seemed to be attenuated in *Adipo^{CRE}Bmal1$^{flox/flox}$* mice with no significant day/night difference observed. Data reflect mean ± SEM, 2-way ANOVA, Sidak post-hoc test * = $p < 0.05$. *Full description of statistical analysis can be found in Appendix 3.*

genotype). No difference was observed in the weight loss of these animals over the 48 hour fast (control: 19.1% ± 0.8 BW loss; *Adipo*^{CRE}*Bmal1*$^{flox/flox}$: 18.8% ± 0.6 BW loss). Both genotypes returned to their original body weight within 48 hours of refeed (Figure 5.5A). In line with the post-fast weight gain, no difference in food intake over 24hr post-fast was observed between the two genotypes (Figure 5.5B). Interestingly, over the short term (4 hr post fast) the *Adipo*^{CRE}*Bmal1*$^{flox/flox}$ mice consumed significantly more food than littermate control mice. This observation may be linked to the increased day-time feeding exhibited by these mice when fed ad libitum.

The body temperature profile of the mice across the fasting period was similar between genotypes. Both genotypes exhibited a pronounced reduction in core body temperature (control: 35. 6°C± 0.1, Δ1.6°C± 0.2 (n= 6, $p<0.05$); *Adipo*^{CRE}*Bmal1*$^{flox/flox}$ 35.5°C± 0.2, Δ1.5°C± 0.2) (n= 6, $p<0.05$). No difference was observed in the fasting temperature (between hours 42-47) between the control and *Adipo*^{CRE}*Bmal1*$^{flox/flox}$ animals (control: 32.6°C± 0.5; *Adipo*^{CRE}*Bmal1*$^{flox/flox}$: 32.5°C± 0.5). Indirect calorimetry of male mice (n=4/genotype) was performed during the fast (Figure 5.6). VO_2, VCO_2, kcal/hr and RER decreased during the fast in control animals, with no difference observed in *Adipo*^{CRE}*Bmal1*$^{flox/flox}$ mice compared to controls. RER reduced at the same rate between both genotypes during the fast, indicating the switch from carbohydrate use (RER ~ 1) to fat use (RER ~ 0.7) and the rate at which RER then rose to ~ 1 (carbohydrate use) upon re-feeding is also similar in both genotypes. COX rates were significantly reduced during the fast in both genotypes and FOX rates were significantly increased. This suggests similar transitions in fuel use in both genotypes, indicating that loss of *Bmal1* and subsequent loss of a functional clock in adipose tissue has no effect on the fasting response in mice. Taken together, this suggests that the loss of *Bmal1* and indirectly *Rev-erbα* expression in white and brown adipose tissue does not account for the dramatic attenuation of fast-induced hypothermia and hypo-metabolism observed in the global *Rev-erbα*$^{-/-}$ mice.

5.3.4 Cold challenge in *Adipo*^{CRE}*Bmal1*$^{flox/flox}$ mice

When *Rev-erbα* expression is disrupted a less significant decrease in core body temperature is observed when mice are exposed to acute cold (Gerhart-Hines *et al*., 2013). As our targeting strategy also disrupts *Bmal1* expression in BAT, we examined the response of *Adipo*^{CRE}*Bmal1*$^{flox/flox}$ mice to acute and chronic cold exposure. *Adipo*^{CRE}*Bmal1*$^{flox/flox}$ mice and Littermate control mice (n=6 per genotype) were implanted with remote telemetry devices for continual recording of core body temperature. Mice were maintained at room temperature

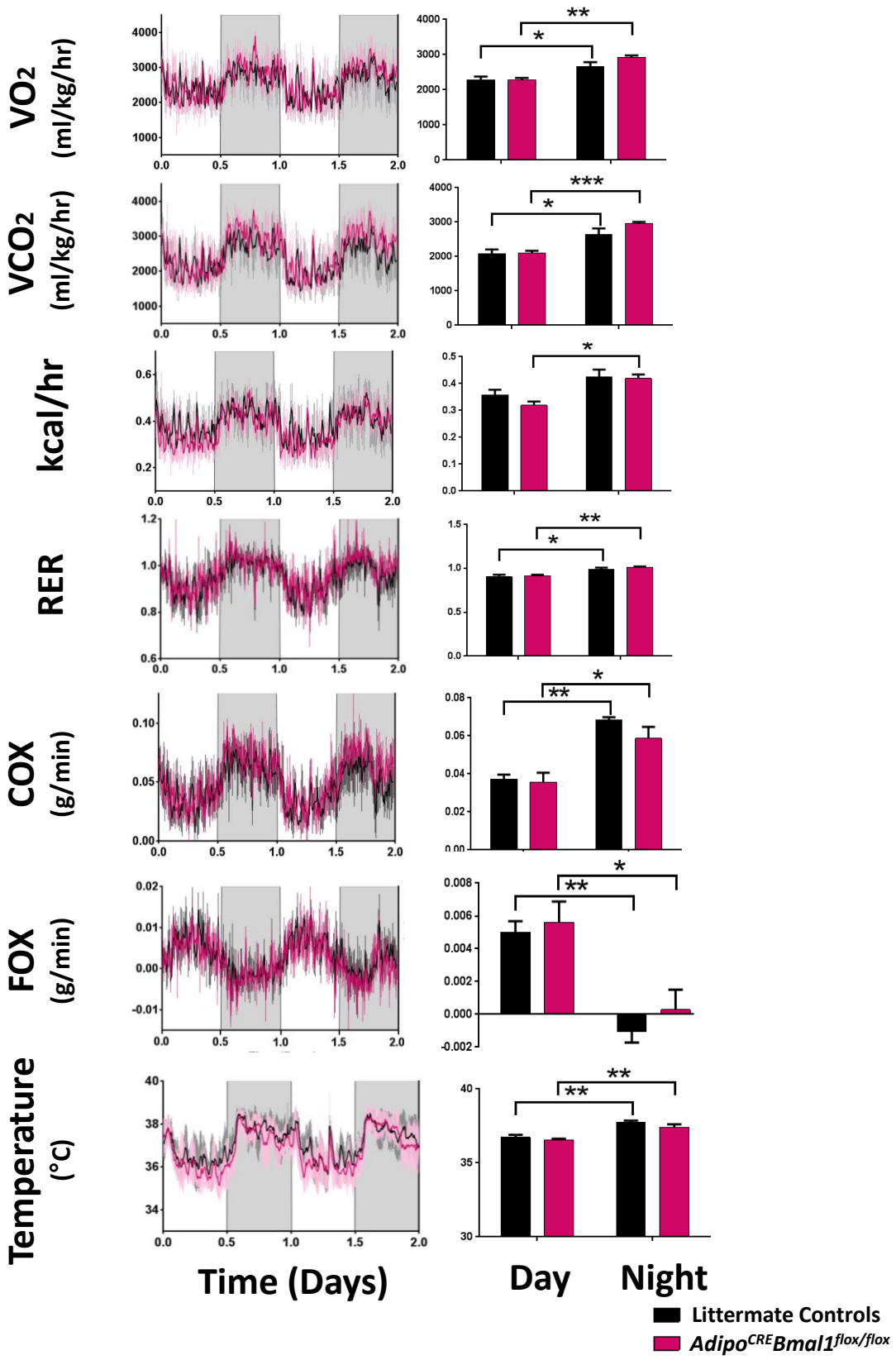
VO2 (ml/kg/hr)
VCO2 (ml/kg/hr)
kcal/hr
RER
COX (g/min)
FOX (g/min)
Temperature (°C)
Time (Days)
Day
Night
Littermate Controls
AdipoCREBmal1flox/flox

Figure 5.4– Metabolic parameters of *Adipo^{CRE}Bmal1$^{flox/flox}$* mice.

Male *Bmal1floxAdipocre* mice (n=4 per genotype) were placed in metabolic cages and a range of parameters were recorded. Temporal changes in all parameters were observed in all genotypes, with a higher metabolic rate and RER seen during the active phase. This temporal difference seemed to be more pronounced in the *Bmal1floxAdipocre* mice. Data reflect mean ± SEM, 2-way ANOVA, Sidak post-hoc test, * = $p < 0.05$, ** = $p < 0.005$, *** = $p < 0.0005$, **** = $p < 0.00005$ vs. same genotype during the day. *Full description of statistical analysis can be found in Appendix 3.*

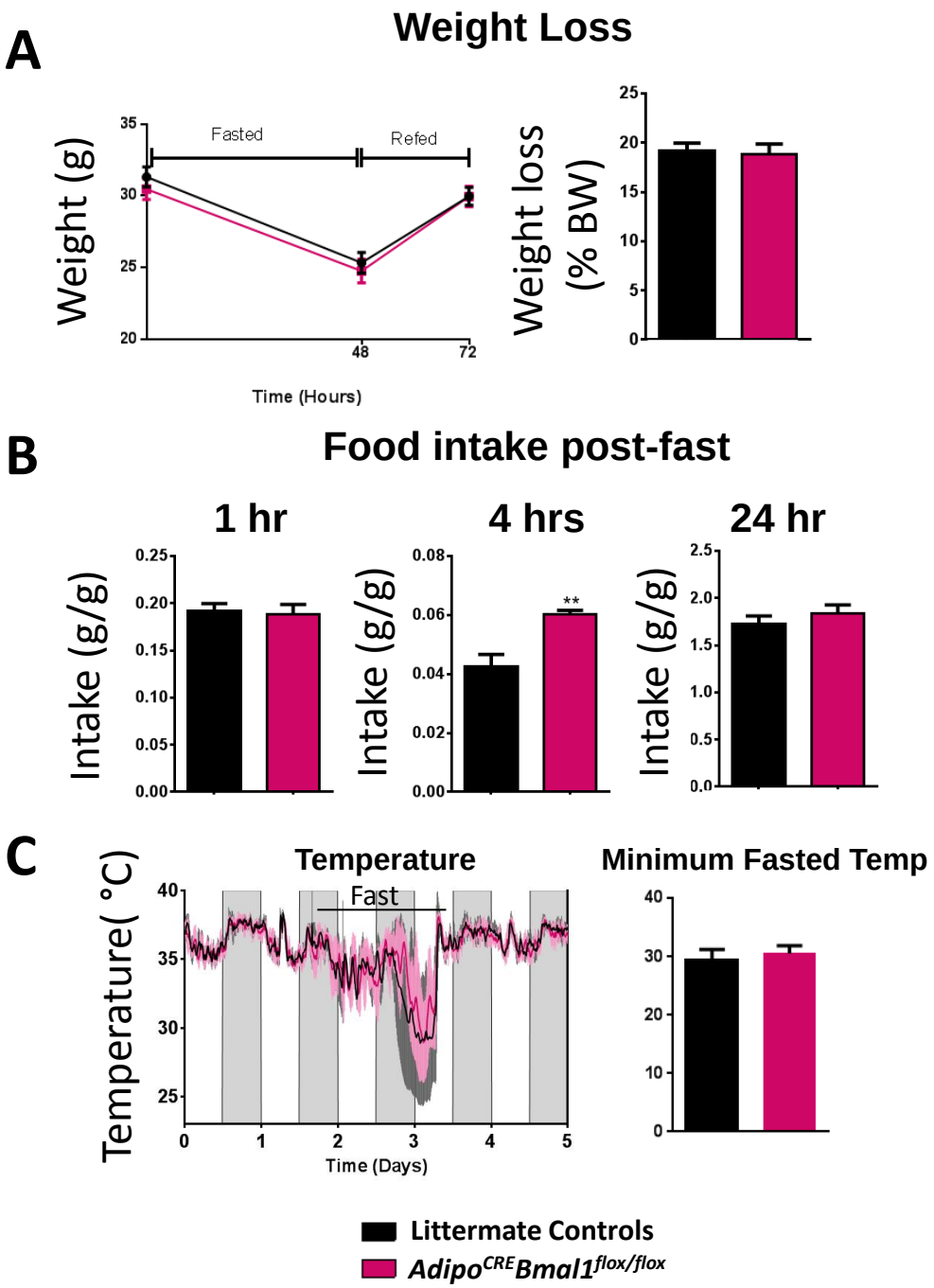

Figure 5.5 – Fasting response of *Adipo^{CRE}Bmal1$^{flox/flox}$* mice.

Male *Adipo^{CRE}Bmal1$^{flox/flox}$* mice (n=6 per genotype) were fasted for 48 hours. No difference in weight loss was seen between the genotypes (A). Food intake post fast was measured (B). Although there was a significant increase of food intake in the *Adipo^{CRE}Bmal1$^{flox/flox}$* mice after 4 hours of re-feeding, on the whole food intake post fast was the same for each genotype. As expected, the 48 hour fast caused a reduction in body temperature, with no significant difference seen between this drop in temperature between the genotypes (C). Data reflect mean ± SEM, unpaired student's t-test, * = $p < 0.05$, ** = $p < 0.005$.

(21°C+/- 2) for 28 days before being exposed to both an acute temperature challenge of 4°C for 6 hr, and a subsequent chronic exposure to 16°C for 7 days (Figure 5.7A). In response to the acute cold challenge, core body temperature of both *Adipo*^{CRE}*Bmal1*$^{flox/flox}$ and control littermates at room temperature dropped from 2.7°C ± 0.3 and 2.7°C ± 0.4 respectively, with no differential response to temperature being observed between the genotypes. After 6 hours, ambient temperature was raised to 16°C and mice were maintained at the temperature for a further 7 days (Figure 5.7B). No differences were observed in the body temperature profiles of the two genotypes during these 7 days. Mice were then subject to a 24 hour fast to further increase the metabolic challenge to the mice. Core body temperature dropped in control mice during the fast, and this was also observed in *Adipo*^{CRE}*Bmal1*$^{flox/flox}$ mice (control 35.9°C ± 0.1; *Adipo*^{CRE}*Bmal1*$^{flox/flox}$ 35.9°C ± 0.1, based on difference in temperature pre-fast compared to average temperature at nadir of fast). Also, no difference was recorded between the genotypes with regards to average fasted temperature and minimum fasted temperature (Figure 5.7 B). Thus, despite the lack of a functional clock in WAT and BAT, the *Bmal1* targeted mice showed no differences in body weight, adiposity, metabolic rate and or thermogenic response to cold challenge or fasting. The only difference observed was the temporal change in feeding behaviour.

5.3.5 Dysregulation of lipid handling genes in gWAT *Adipo*^{CRE}*Bmal1*$^{flox/flox}$ mice

As detailed in pervious chapters and previously published work, many genes involved in lipid metabolism oscillate within white adipose tissue. We demonstrated that global deletion of *Rev-erbα* alters the expression of genes involved in lipid handling (e.g. *Lpl, Atgl*), both in terms of constitutive expression, and in transcriptional response to changing energy status. Therefore, the impact of the tissue-specific deletion of *Bmal1* on the expression of these genes was examined. Basal gene expression was examined in male mouse tissues collected at ZT6 (n=5/genotype). Somewhat surprisingly, a severe attenuation was observed in the expression of the lipolytic genes, *Atgl* and *Hsl* in gWAT from *Adipo*^{CRE}*Bmal1*$^{flox/flox}$ mice (Figure 5.8, $p<0.05$, student's unpaired t-test), when compared with littermate controls. Similar to the global *Rev-erbα*-/- mice, *Fasn* expression was upregulated in the *Bmal1*-targeted mice, suggesting the FAS may be a direct target of *Rev-erbα* transcriptional repression. However, in contrast to in the global *Rev-erbα*$^{-/-}$ mice (Fig. 4.4), *Lpl* and *Dgat2* expressions were downregulated in *Adipo*^{CRE}*Bmal1*$^{flox/flox}$ mice. No difference in the expression of these genes was observed in the liver.

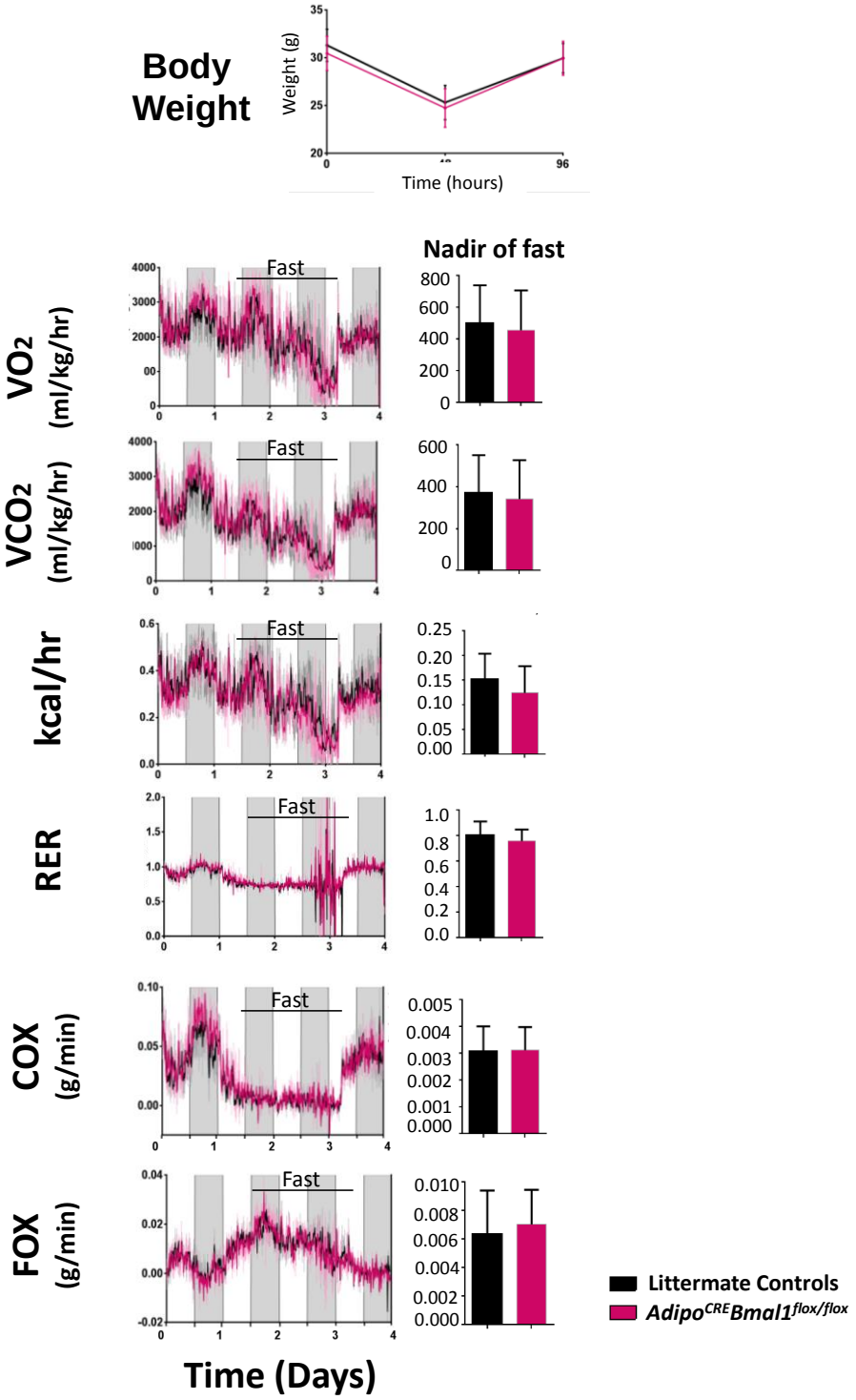

Figure 5.6 – Metabolic response to fasting in *Adipo^{CRE}Bmal1$^{flox/flox}$* mice.
Male *Adipo^{CRE}Bmal1$^{flox/flox}$* mice (n=4 per genotype) were fasted for 48 hours in metabolic cages. No difference was observed in weight loss and subsequent gain between the genotypes. As expected, during the fast a decrease in all metabolic parameters was observed (histograms show average values between hours 42-47 of fast), but with no significant difference between genotypes. Data reflect mean ± SEM, unpaired student's t-test, * = $p < 0.05$.

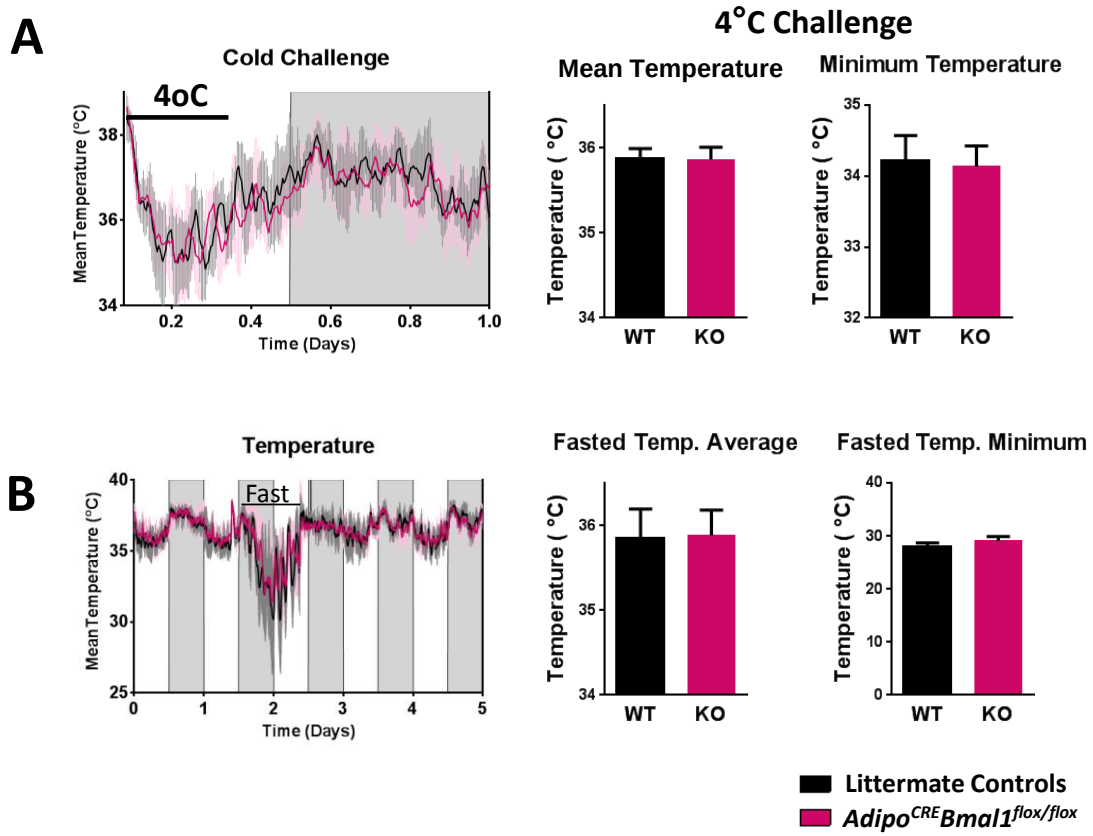

Figure 5.7 – Cold challenge of *Adipo^{CRE}Bmal1$^{flox/flox}$* mice.

Male *Adipo^{CRE}Bmal1$^{flox/flox}$* mice (n=6 per genotype) from room temperature were held at 4oC for 6 hours, after which the temperature was ramped progressively to 16°C (A). Body temperature of all mice dropped, with no significant difference seen in the average temperature and minimum temperature between the different genotypes during the 4°C challenge. Mice were held at 16°C for 1 week before being subjected to a 24 hour fast (B). Body temperature of all animals decreased, with no difference seen in average fasted temperature and minimum fasted temperature between genotypes. Data reflect mean ± SEM, unpaired student's t-test, * = $p < 0.05$.

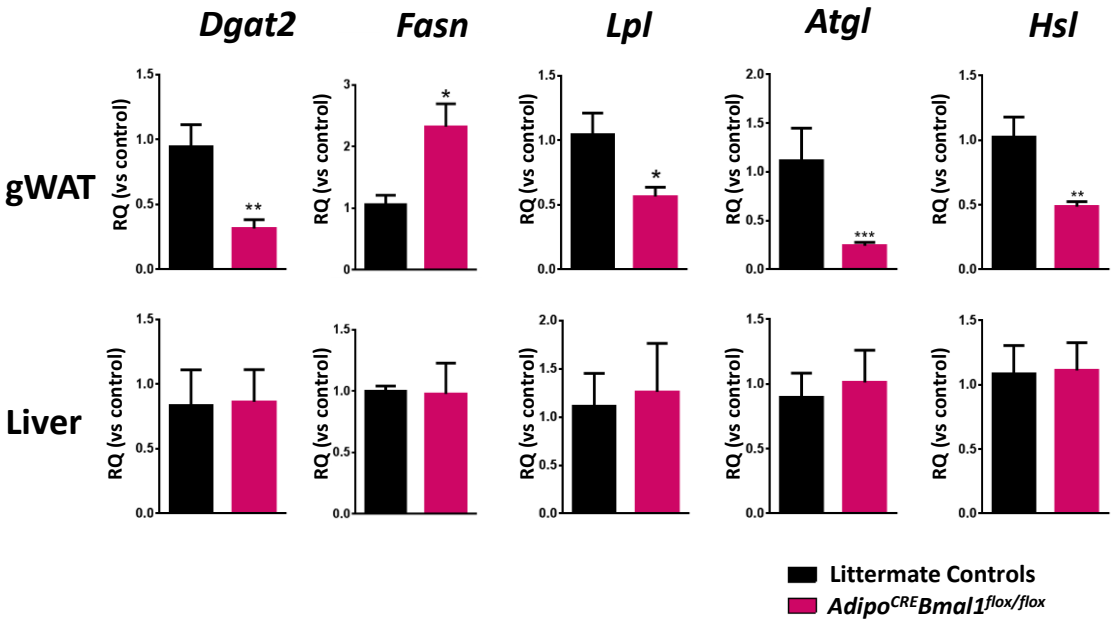

Figure 5.8 –Transcript analysis of lipid handling genes in *Adipo^{CRE}Bmal1$^{flox/flox}$* mice.
gWAT and liver from male *Adipo^{CRE}Bmal1$^{flox/flox}$* mice (n=5 per genotype) was obtained and qPCR analysis carried out at ZT6. As expected, no difference in gene expression was observed in the liver due to the specificity of the genetic targeting. However, severe dysregulation of both lipolytic and lipogenic genes was seen in gWAT from *Adipo^{CRE}Bmal1$^{flox/flox}$* mice. Data reflect mean ± SEM, unpaired students t-test, * = $p < 0.05$, ** = $p < 0.005$, *** = $p < 0.005$. *Full description of statistical analysis can be found in Appendix 3.*

As basal gene expression appeared to be profoundly different, next examined the response of isolated gWAT explant cultures to lipogenic (insulin) stimulation. gWAT from *Adipo*^{CRE}*Bmal1*$^{flox/flox}$ and control littermates was collected and cultured as small tissue explants, as described above (male mice, n=7-9/genotype). gWAT explant cultures were maintained in culture for 24 hours before being treated with insulin (1 µM). In gWAT explants derived from control animals, insulin stimulation caused an up-regulation of lipogenic genes *Dgat2* and *Fasn*, and this was also observed in gWAT explants from *Adipo*^{CRE}*Bmal1*$^{flox/flox}$ mice (Figure 5.9). The response to insulin was somewhat more pronounced in these animals similar to what was observed in gWAT from global *Rev-erbα* mice. The expected responses were seen with regards to lipolytic genes in both genotypes – downregulation of *Atgl* and *Hsl.* Although insulin caused no change to the expression of *Lpl* and *Glut4*, both of these genes seemed to be expressed at higher levels in gWAT from *Adipo*^{CRE}*Bmal1*$^{flox/flox}$ mice ($p<0.05$). It must be noted, however, that the dramatic differences in lipid handling gene expression observed in freshly dissected tissue (2 experiments, n=5-8 animals per genotype) were not maintained *in vitro* (Fig 5.8).

5.3.6 Response of *Adipo*^{CRE}*Bmal1*$^{flox/flox}$ mice to positive energy balance

From 8 weeks of age, male and female mice were maintained on HFD for 16 weeks (n=4-9 mice/sex/genotype/diet). Males and females of both genotypes exhibited significant weight gain on HFD (Figure 5.10), but no significant difference was observed between *Adipo*^{CRE}*Bmal1*$^{flox/flox}$ mice and control littermates when matched for diet. A significant increase in gWAT and scWAT accumulation was observed in both genotypes on HFD, but again no genotypic difference was observed.

Although there was no difference in body weight, adiposity or diet-induced weight gain between *Adipo*^{CRE}*Bmal1*$^{flox/flox}$ mice and control littermates, gene expression was very different.

5.3.7 Metabolic phenotype of *Adipo*^{CRE}*Rev-erbα*$^{flox/flox}$ mice

As demonstrated in chapter 4, global *Rev-erbα* knockout mice exhibit an obese phenotype even when maintained on normal chow, and are profoundly sensitive to DIO. To determine whether selective loss of *Rev-erbα* in adipose tissue was sufficient to recapitulate this

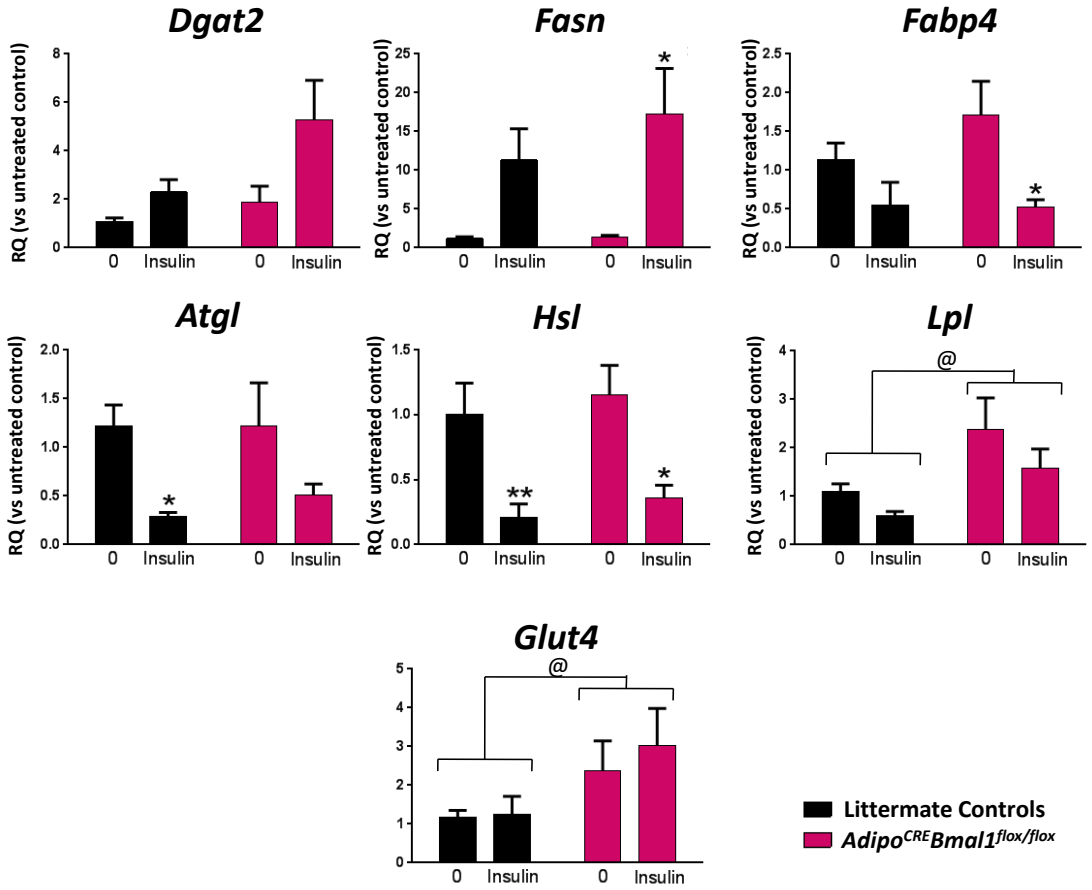

Figure 5.9 – *Ex vivo* insulin stimulation of *Adipo^{CRE}Bmal1$^{flox/flox}$* mice.
gWAT from male *Adipo^{CRE}Bmal1$^{flox/flox}$* mice (n=7-9 per genotype) was cultured for 24 hours before being treated with either a vehicle or 1 µM insulin. Tissue was collected 24 hours post insulin stimulation and qPCR analysis performed. Insulin stimulation resulted in an upregulation of lipogenic genes *Dgat2* and *Fasn*, with this response being heightened in the KO mice. Conversely, lipolytic drive was attenuated in both genotypes upon insulin stimulation. There was a trend for upregulation of Glut4 in gWAT from *Adipo^{CRE}Bmal1$^{flox/flox}$* mice Data reflect mean ± SEM, Two-way ANOVA, Sidak post-hoc test, * = $p < 0.05$, ** = $p < 0.005$ vs untreated explant of same genotype. Genotypic differences represented by @. *Full description of statistical analysis can be found in Appendix 3.*

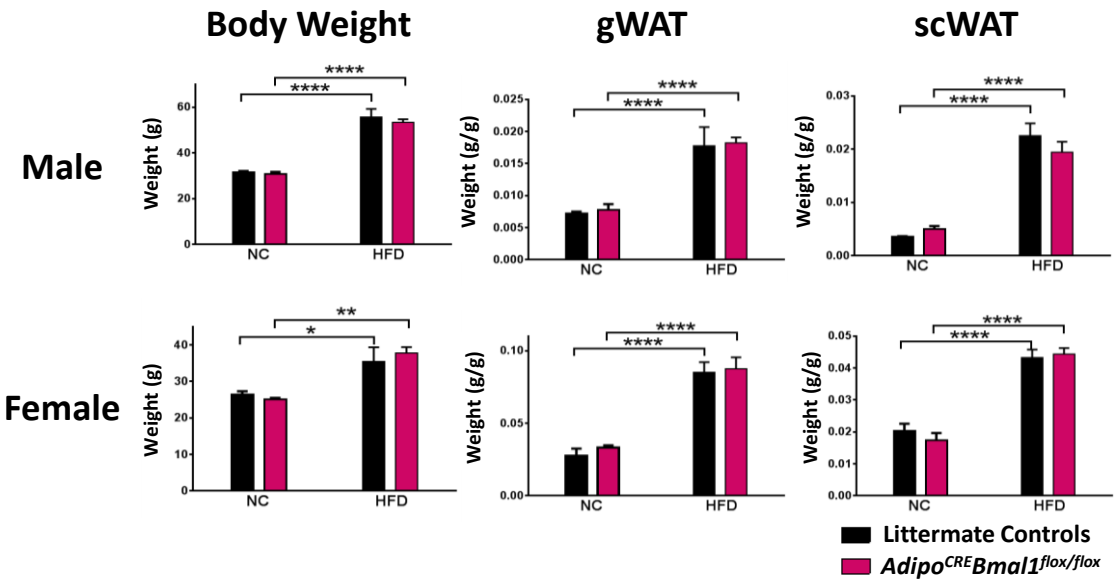

Figure 5.10 – High Fat Diet challenge of *Adipo^{CRE}Bmal1$^{flox/flox}$* mice.
Body weights of male (n=4-6 per genotype per diet) and female (n=8-9 per genotype per diet) *Adipo^{CRE}Bmal1$^{flox/flox}$* mice on either NC or HFD were measured after 14 weeks of HFD challenge starting at 8 weeks of age. Mice were culled and gWAT and scWAT fat pads dissected and weighed and expressed as g/g of bodyweight. HFD resulted in an increase in body weight, gWAT weight and scWAT weight in both males and females of both genotypes with no genotypic difference observed. Data reflect mean ± SEM, 2-way ANOVA, Sidak post-hoc test, * = $p < 0.05$, ** = $p < 0.005$, *** = $p < 0.0005$, **** = $p < 0.00005$ vs NC of same genotype. *Full description of statistical analysis can be found in Appendix 3.*

phenotype, we established the *Adipo*^{CRE}*Rev-erbα*$^{flox/flox}$ line. Targeted mice and littermate controls were maintained on either NC or HFD from 8 weeks of age for 14 weeks. Body weights were measured, and then mice were culled and fat pads were dissected and weighed (n= 5 mice/genotype/diet). On NC, no difference in bodyweight or fat pad weights were observed between genotypes. However, female *Adipo*^{CRE}*Rev-erbα*$^{flox/flox}$ mice consumed significantly more grams of food compared to control littermates, indicating possible hyperphagia in these animals (Figure 5.11). All mice gained a significant amount of weight in response to HFD feeding (Figure 5.12), but in contrast to the global *Rev-erbα*$^{-/-}$ mouse line, no genotypic differences were observed in HFD-induced weight gain. Both control and *Adipo*^{CRE}*Rev-erbα*$^{flox/flox}$ mice showed increased adiposity on HFD, with significant increase in scWAT and gWAT fat pad mass, yet no genotypic differences were evident.

We next examined energy expenditure and metabolic rate in *Adipo*^{CRE}*Rev-erbα*$^{flox/flox}$ using indirect calorimetry (male mice, n= 4 mice/genotype). Pronounced diurnal variations in VO_2, VCO_2, kcal/hr, and RER were observed in control mice, with a greatly elevated of gas exchange and RER evident in the active (dark) phase of the day (Figure 5.13). This diurnal variation was also observed in *Adipo*^{CRE}*Rev-erbα*$^{flox/flox}$ mice, although day/night differences in RER did not reach statistical significance in the knockout mice, which was similar to the global *Rev-erbα* knockout mice. This may indicate an increased reliance on carbohydrate metabolism within this genotype. However, diurnal variations in both COX and FOX were clearly observed in both genotypes, suggesting similar substrate oxidation in these mice. Core body temperature of *Adipo*^{CRE}*Rev-erbα*$^{flox/flox}$ mice was recorded using radiotelemetry. Diurnal variation was observed in the body temperature of both *Adipo*^{CRE}*Rev-erbα*$^{flox/flox}$ and control mice (Daytime - *Adipo*^{CRE}*/Rev-erbα*$^{flox/flox}$*:* 36.2°C ± 0.3; littermate controls: 36.2°C± 0.1; Night time - *Rev-erbα*$^{flox/flox}$: 37.4°C± 0.2; littermate controls: 37.4 ± 0.1).

5.3.8 Fasting response in *Adipo*^{CRE}*Rev-erbα*$^{flox/flox}$

In Chapter 4, we demonstrated that global *Rev-erbα*$^{-/-}$ mice showed differential fasting responses compared to WT C57BL/6 littermates. Therefore, male *Adipo*^{CRE}*Rev-erbα*$^{flox/flox}$ mice and littermate controls (n=6 mice/genotype) were fasted for 48 hours. No differences were observed in fast-induced weight loss of these animals during the 48 hour fast (*Adipo*^{CRE}*Rev-erbα*$^{flox/flox}$ mice: 17.3% ± 1.9 loss in BW; littermate controls: 16.8%± 0.8 loss in BW). Both genotypes also recovered body weight at a similar rate (Figure 5.14A). Food intake upon re-

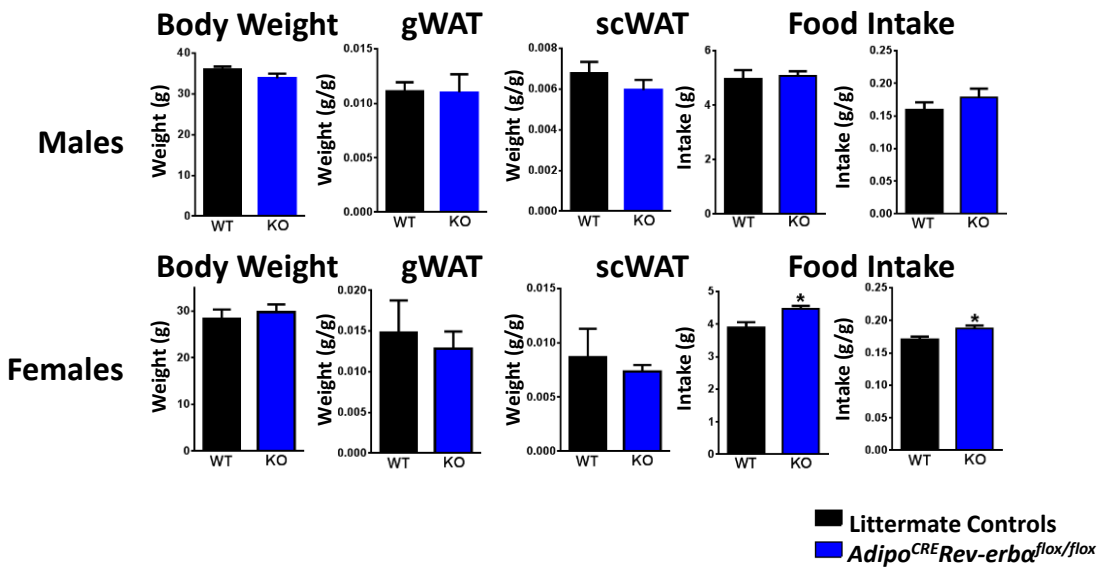

Figure 5.11 –Body weight profiles and food intake of *Adipo^{CRE}Rev-erbα$^{flox/flox}$* mice.
Body weights of male and female *Adipo^{CRE}Rev-erbα$^{flox/flox}$* mice (n=5 per genotype) were measured at 20 weeks of age (A). Mice were culled and gWAT and scWAT fat pads dissected and weighed and expressed as g/g of bodyweight. No significant difference was observed between the body weights and gWAT/scWAT weights of each genotype in both sexes. No difference was observed in daily food intake in male mice but increased food intake was seen in female *Adipo^{CRE}Rev-erbα$^{flox/flox}$* mice. Data reflect mean ± SEM, student's unpaired t-test, * = $p < 0.05$. *Full description of statistical analysis can be found in Appendix 3.*

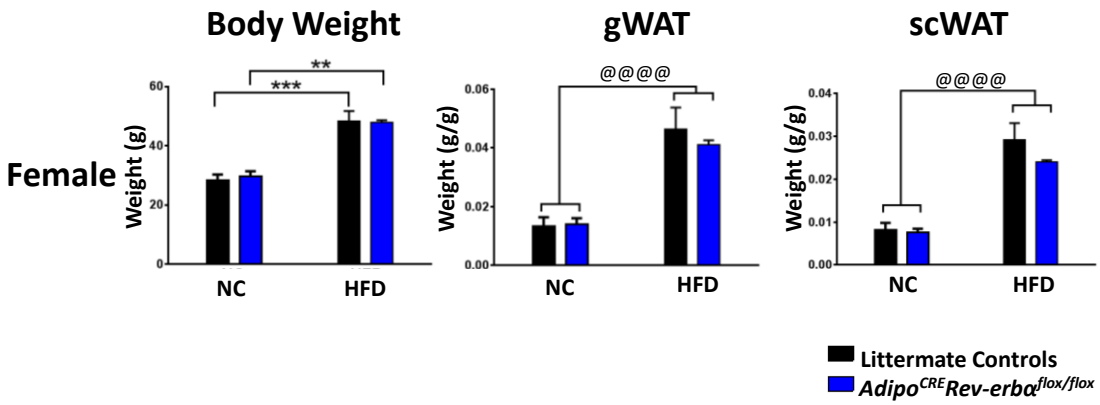

Figure 5.12 –High Fat Diet of *Adipo^{CRE}Rev-erbα$^{flox/flox}$* mice.

Body weights of female *Adipo^{CRE}Rev-erbα$^{flox/flox}$* mice on either NC or HFD (n=5 per genotype per diet) were measured at 20 weeks of age. Mice were culled and gWAT and scWAT fat pads dissected and weighed and expressed as g/g of bodyweight. HFD resulted in an increase in body weight gWAT and scWAT weight with no genotypic difference observed. Data reflect mean ± SEM, 2-way ANOVA, Sidak post-hoc test, ** = $p < 0.005$, *** = $p < 0.0005$ vs NC fed mice of same genotype. @ represents effect of HFD on both genotypes compared to NC mice (@@@@ = $p < 0.00005$). *Full description of statistical analysis can be found in Appendix 3.*

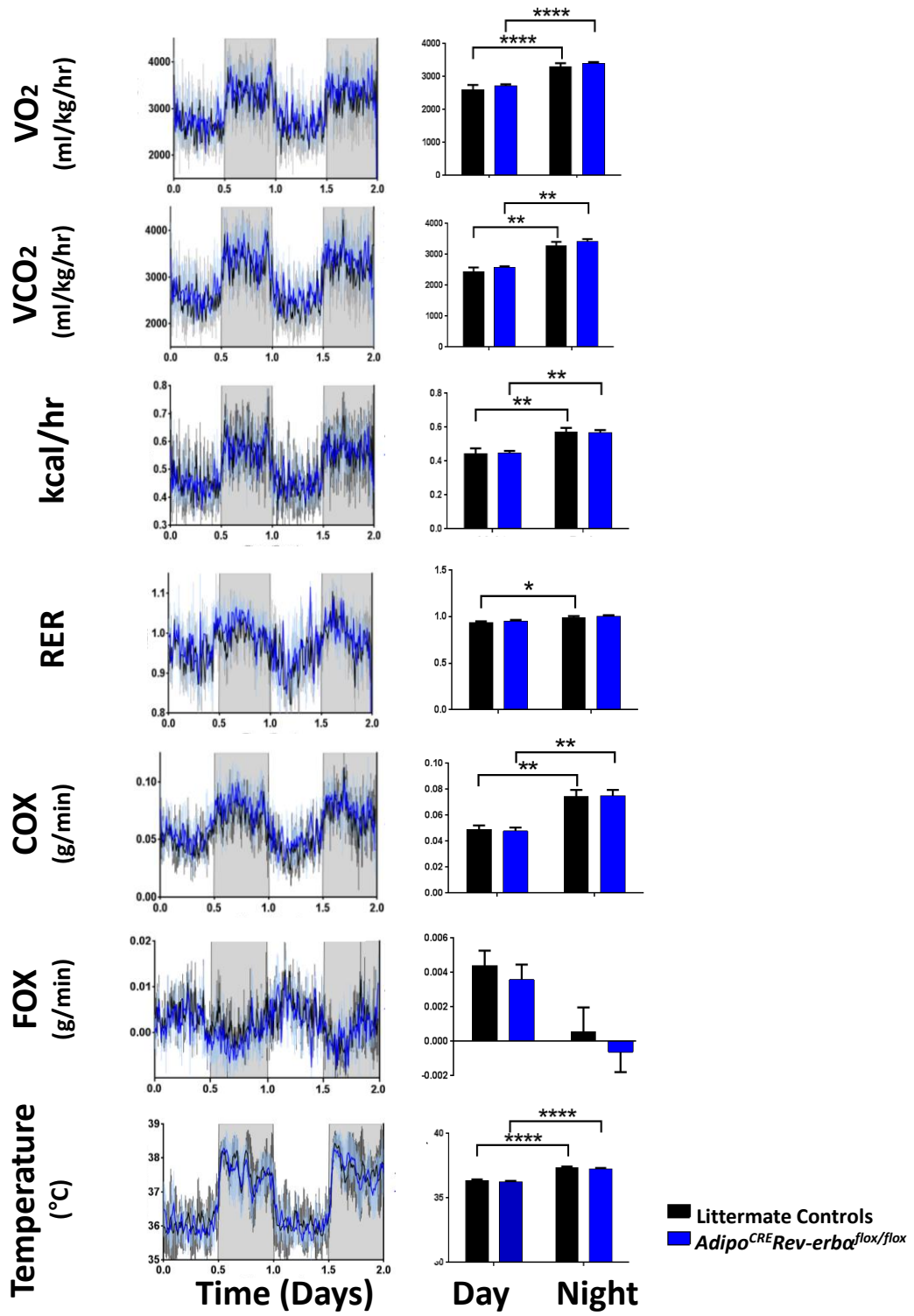

5.13 –Metabolic parameters of *Adipo^{CRE}Rev-erbα$^{flox/flox}$* mice.

Male *Adipo^{CRE}Rev-erbα$^{flox/flox}$* mice (n=4 per genotype) were placed in metabolic cages and a range of parameters were recorded. Temporal changes in all parameters were observed in all genotypes, with a higher metabolic rate and RER seen during the active phase. Data reflect mean ± SEM, 2-way ANOVA, Sidak post-hoc test * = $p < 0.05$, ** = $p < 0.005$, *** = $p < 0.0005$, **** = $p < 0.00005$ vs same genotype during the day. *Full description of statistical analysis can be found in Appendix 3.*

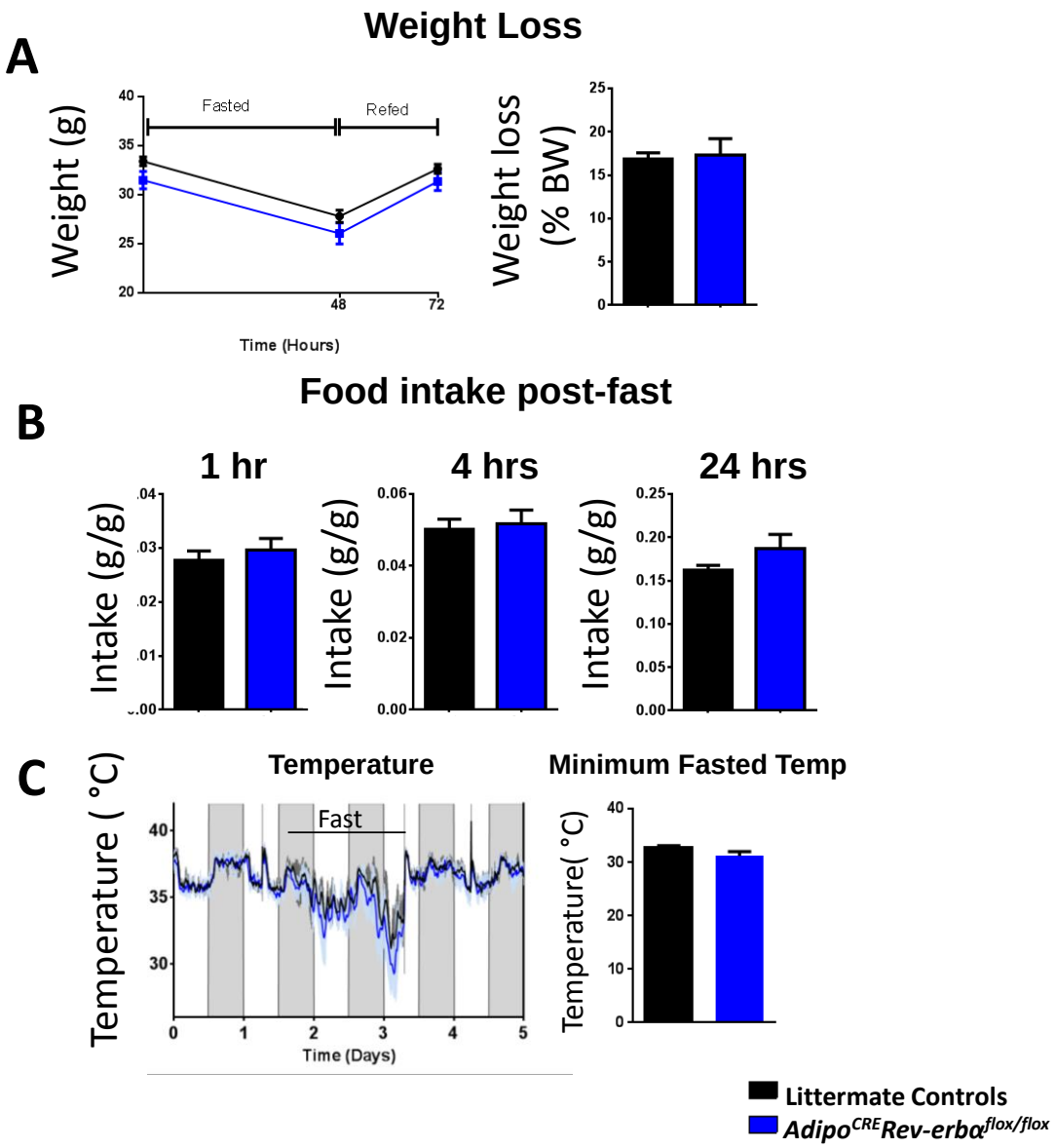

Figure 5.14 – Fasting response of *Adipo^{CRE}Rev-erbα$^{flox/flox}$* mice.
Male *Adipo^{CRE}Rev-erbα$^{flox/flox}$* (n=6 per genotype) were fasted for 48 hours. No difference in weight loss was seen between the genotypes (A). Food intake post fast was measured (B). Food intake post fast was the same for each genotype. As expected, the 48 hour fast caused a reduction in body temperature, with no significant difference observed in this drop in temperature between the genotypes (C). Data reflect mean ± SEM, unpaired student's t-test, * = $p < 0.05$.

feeding was also monitored. At 1, 4 and 24 hours of refeeding, *Adipo*^{CRE}*Rev-erbα*$^{flox/flox}$ mice consumed the same amount of food as control animals. Core body temperature of the control animals decreased during the fast, with a reduction of 4.0°C± 0.6 observed, based on mean temperature at time 0 and mean temperature during hours 42-47 of the fast, with a similar response observed in the *Adipo*^{CRE}*Rev-erbα*$^{flox/flox}$ mice (5.3°C± 0.7). Minimum temperature *Adipo*^{CRE}*Rev-erbα*$^{flox/flox}$ mice and littermate controls reached during the fast was also similar (29.0°C± 0.8 and 30.1°C± 0.6 respectively). Metabolic rate of male mice (n=4 per genotype) were also monitored during the fast using indirect calorimetry (Fig. 5.15). Fasting-induced reductions in VO_2, VCO_2, kcal/hr and RER were evident in control animals, and similar changes observed in *Adipo*^{CRE}*Rev-erbα*$^{flox/flox}$ mice. Similarly, fasting profiles in COX and FOX were observed in both genotypes, suggesting that fuel usage was similar between the mice.

Taken together, this suggests that expression of *Rev-erbα* in adipose tissue is not critical for the maintenance of rhythmicity in VO_2, VCO_2, kcal/hr, which is similar to what was observed in *Adipo*^{CRE}*Bmal1*$^{flox/flox}$ mice. To further support data obtained from *Adipo*^{CRE}*Bmal1*$^{flox/flox}$ mice, *Adipo*^{CRE}*Rev-erbα*$^{flox/flox}$ mice also maintained temperature rhythms, indicating that disruption of the clock in BAT does not result in loss of rhythmicity in body temperature.

5.3.9 Expression of lipid handling genes in gWAT *Adipo*^{CRE}*Rev-erbα*$^{flox/flox}$ mice

Targeting of *Rev-erbα* globally or *Bmal1* locally disrupted the expression of lipid metabolism genes (shown above), suggesting that the clock as a whole, or *Rev-erbα* specifically, is critical in the regulation of these pathways. To differentiate between loss of clock function (*Bmal1* targeting, which results in loss of both *Bmal1* and *Rev-erbα)* and loss of *Rev-erbα* specifically, we studied the expression of lipid handling genes in mice with adipose specific loss of *Rev-erbα.* Male mice (n=8 mice/genotype) were culled at ZT6 and gWAT and liver were dissected and used for qPCR analysis. Surprisingly, no significant differences were observed in expression of lipid handling genes examined (*Fasn, Dgat2, Lpl, Atgl, Hsl, Fabp4)* in gWAT from *Adipo*^{CRE}*Rev-erbα*$^{flox/flox}$ mice (Figure 5.16). *Fasn* did show up-regulated expression in gWAT from *Adipo*$^{CRE/+}$*/Rev-erbα*$^{flox/flox}$ mice when compared to control littermates, although this did not reach statistical significance. The lipogenic genes *Atgl* and *Hsl* showed no genotypic difference in expression, but most surprising was the fact that *Lpl* was expressed at the same levels in gWAT from *Adipo*^{CRE}*Rev-erbα*$^{flox/flox}$ and control mice. No difference in the expression of these genes was observed in the liver.

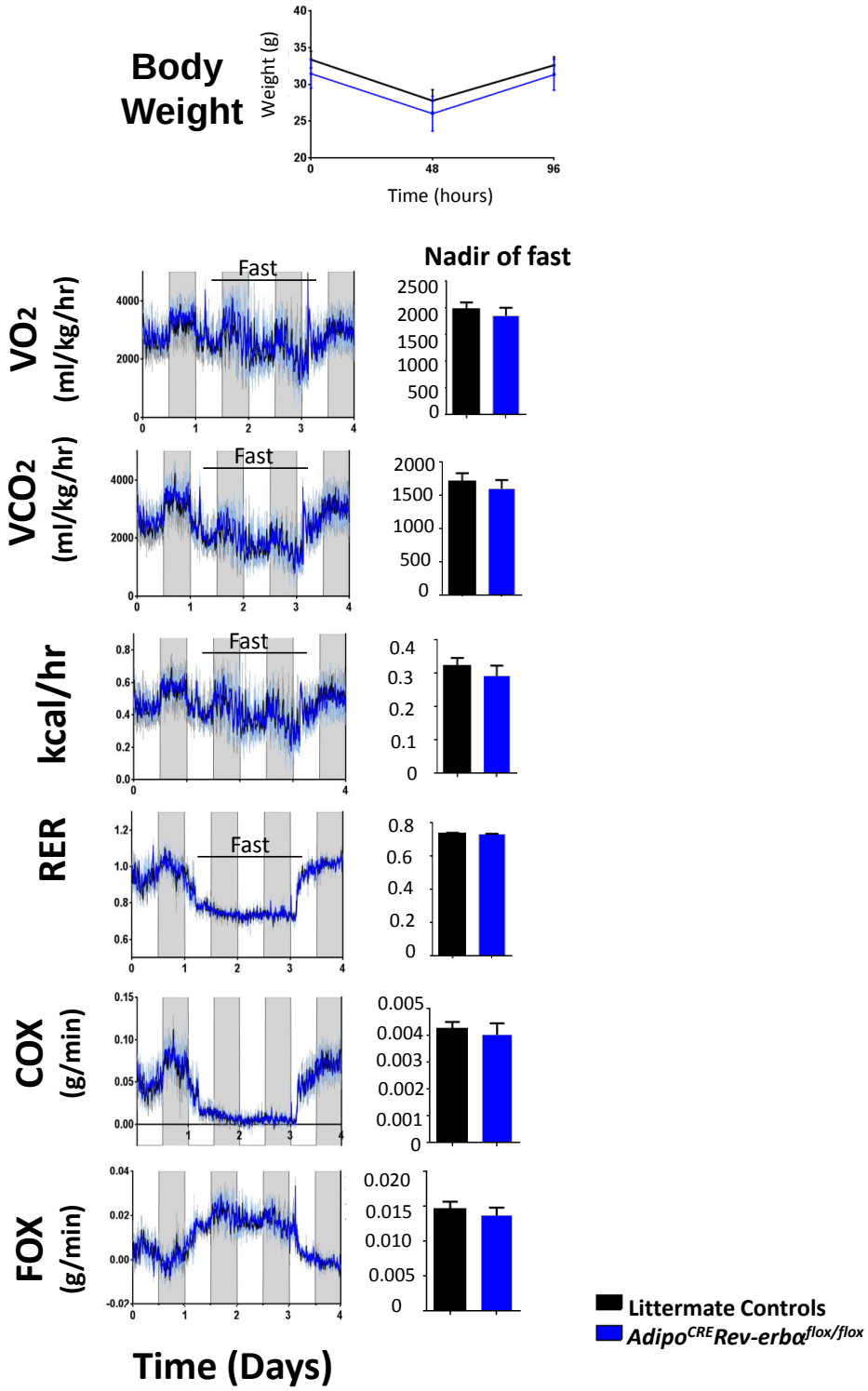

Figure 5.15 – Fasting response *Adipo^{CRE}Rev-erbα$^{flox/flox}$* mice.

Male *Adipo^{CRE}Rev-erbα$^{flox/flox}$* mice (n=6 per genotype) were fasted for 48 hours in metabolic cages. No difference was observed in the weight loss and subsequent gain between the genotypes. As expected, during the fast a decrease in all metabolic parameters was observed (histograms show average values between hours 42-47 of fast), but with no significant difference between genotypes. Data reflect mean ± SEM, unpaired student's t-test, * = $p < 0.05$.

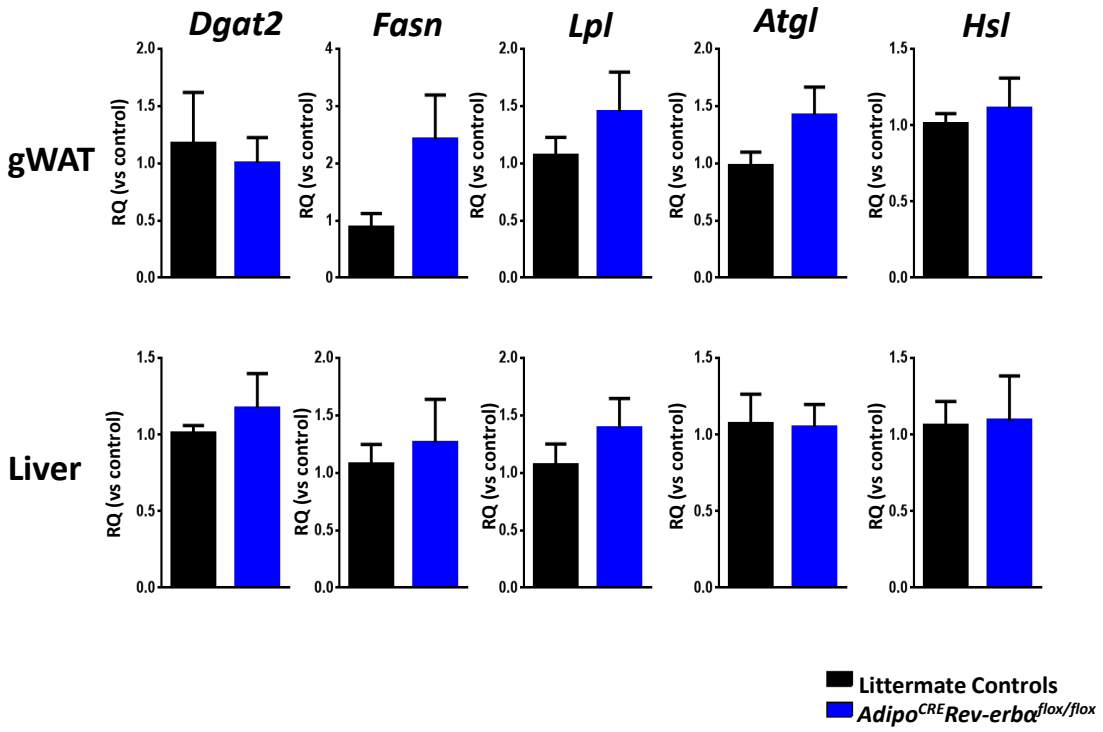

Figure 5.16 –Transcript analysis of lipid handling genes in *Adipo^{CRE}Rev-erbα$^{flox/flox}$* mice. gWAT and liver from male *Adipo^{CRE}Rev-erbα$^{flox/flox}$* mice (n=8 per genotype) was obtained and qPCR analysis carried out at ZT 6. As expected, no difference in gene expression was observed in the liver of *Adipo^{CRE}Rev-erbα$^{flox/flox}$* mice due to the specificity of the genetic targeting. In general, no significant difference was seen in gene expression between genotypes in gWAT of *Adipo^{CRE}Rev-erbα$^{flox/flox}$* mice, but a trend for upregulation of *Fasn* was observed. Data reflect mean ± SEM, unpaired student's t-test, * = $p < 0.05$, ** = $p < 0.005$, *** = $p < 0.005$

5.3.10 Insulin sensitivity in *Adipo^{CRE}Rev-erbα$^{flox/flox}$* mice

Global *Rev-erbα$^{-/-}$* mice showed enhanced insulin sensitivity during an insulin tolerance test. To determine if the role of *Rev-erbα* specifically in adipose tissue may contribute to this phenotype, we performed an insulin tolerance test (0.75 U/kg, I.P) on *Adipo^{CRE}Rev-erbα$^{flox/flox}$* and control animals (n=6 per genotype, male mice). Both targeted and control mice showed a similar decrease in blood glucose in response to insulin administration (Figure 5.17).

5. 4 Summary

Here we targeted *Bmal1* and *Rev-erbα* in adipose to examine differences between loss of clock function (*Bmal1* loss) and clock manipulation (*Rev-erbα* loss) within adipose tissue. *Bmal1* and *Rev-erbα* were selectively deleted in adipose tissue using adiponectin as a driver. *Adipo^{CRE}Bmal1$^{flox/flox}$* mice show no differences in body weight and very subtle differences in adiposity compared to littermate controls. Even when challenged with a positive energy balance they still do not show an increased propensity for weight gain. This contrasts with what was shown by Paschos *et al*., (2012), which demonstrated that adipocyte specific *Bmal1* knockouts using the fatty acid binding protein (aP2) promoter had increased body weights. This may indicate that loss of the clock using adiponectin as a driver has a higher specificity than fatty acid binding protein, which is also expressed in macrophages. This increased specificity of the knockout may pose less of a physiological problem to these animals. Interestingly, no changes in body weight were observed in *Adipo^{CRE}Rev-erbα$^{flox/flox}$* mice compared to littermate controls, which contrasted with global *Rev-erbα* knockout mice, which were an obese phenotype with an increased propensity to gain weight. This may highlight that the metabolic phenotype caused by global *Rev-erbα* knockout mouse is not due to clock manipulation in adipose tissue.

Adipo^{CRE}Bmal1$^{flox/flox}$ and *Adipo^{CRE}Rev-erbα$^{flox/flox}$* mice maintained rhythmicity in metabolism parameters such as VO_2, VCO_2, and RER. Despite this, *Adipo^{CRE}Bmal1$^{flox/flox}$* mice showed attenuated feeding rhythms, which indicates a direct effect of the adipocyte circadian clock on hypothalamic feeding centres. This parallels work by Paschos *et al*., (2012), who showed that disruption of the adipocyte circadian clock resulted in temporal changes in polyunsaturated fatty acids in plasma, which led to corresponding changes in the expression of neurotransmitters responsible for appetite regulation in the hypothalamus, for example Agrp

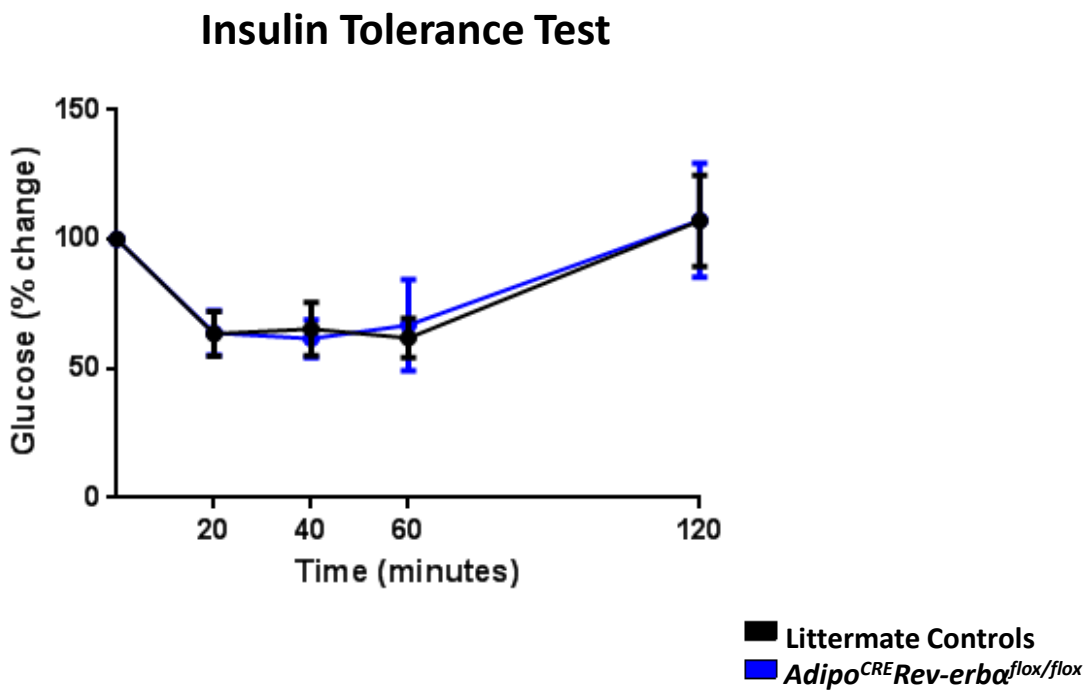

Figure 5.17 –Insulin Tolerance Test of *Adipo^{CRE}Rev-erbα$^{flox/flox}$* mice.
0.75 U/kg insulin was administered I.P. to male *Adipo^{CRE}Rev-erbα$^{flox/flox}$* mice (n = 6 per genotype). Blood glucose was subsequently measured post insulin administration and expressed as a % change. Insulin tolerance was observed to be the same in both genotypes. Data reflect mean ± SEM, 2-way ANOVA, * = $p < 0.05$ compared to control littermates.

and Npy. Work in our lab also shows that global *Rev-erbα* null mice show increased daytime feeding and in both genetic models *Rev-erbα* expression would be low which may suggest that this effect centres on action of *Rev-erbα.*

Severe dysregulation of lipid handling genes was also observed in *Adipo*^{CRE}*Bmal1*$^{flox/flox}$ mice. Lipolytic enzymes such as *Lpl, Atgl and Hsl* are profoundly downregulated in gWAT from *Adipo*^{CRE}*Bmal1*$^{flox\ /flox}$ mice. Reporter gene and ChIP assays indicate that CLOCK/BMAL1 directly and rhythmically bind to E-boxes in the promoters of *Atgl* and *Hsl* (Shostak *et al*., 2013) therefore indicating that *Atgl* and *Hsl* are under clock control. Paschos *et al.* (2012), however, demonstrated normal levels of expression of lipolytic genes and therefore suggested there was no alteration in lipolysis within the adipocytes. There does not, however, seem to be a bias for the lipolytic pathway in these animals as *Dgat2* also shows profound attenuation of expression in gWAT of these animals. *Dgat2* catalyses the formation of triglycerides from diacylglycerol and Acyl-CoA and therefore reduced expression of this would result in less triglyceride formation. This, along with attenuated lipolysis in the *Adipo*^{CRE}*Bmal1*$^{flox/flox}$ animals indicates that there is not a bias towards lipolysis or lipogenesis and therefore fitting with there being no observed differences in body weight compared to control littermates. Conversely, *Fasn* shows profoundly upregulated expression in gWAT of *Adipo*^{CRE}*Bmal1*$^{flox/flox}$ mice. *Fasn* has been shown to be Srebp-1c target, and this transcription factor is temporarily controlled by REV-ERBα (Le Martelot *et al*., 2009). Loss of *Bmal1* results in diminished *Rev-erbα* expression and therefore lack of repression on *Fasn* transcription. This is further supported by increased *Fasn* expression in both global *Rev-erbα* knockout mice and *Adipo*^{CRE}*Rev-erbα*$^{flox/flox}$ mice. Interestingly, however, no other significant differences in lipid handling gene expression were observed in gWAT of *Adipo*^{CRE}*Rev-erbα*$^{flox/flox}$ mice. This was most surprising in the case of *Lpl*, as this was consistently upregulated in all tissues in global *Rev-erbα* knockout mice and downregulated in *Adipo*^{CRE}*Bmal1*$^{flox/flox}$ mice as *Bmal1* is a positive regulator of this gene. These results suggest that other physiological consequences of the loss of *Rev-erbα* throughout the body are responsible for the up-regulation of this gene in gWAT, and it is not a direct transcriptional effect in adipose tissue.

After completion of our studies, Zhang *et al* (2015) reported that the *Rev-erbα*^{flox} model was actually a knock-in of a DBD mutation rather than a complete knockout of the REV-ERBα protein and therefore full-length REV-ERBα is still produced, lacking its DBD domain., which may explain why many of the parameters such as body weight, fasting response, gene

expression that we measured in these mice showed no difference to littermate controls, contrasting with data obtained from global *Rev-erbα* knockouts. Clock control requires *Rev-erbα* to bind directly to the genome at its cognate sites, where it competes with activating ROR transcription factors. Conversely, *Rev-erbα* regulates metabolic genes primarily by recruiting the HDAC3 corepressor to sites which it is tethered by cell-type specific transcription factors. Therefore, direct competition between *Rev-erbα* and *Ror* is responsible for the control of the molecular clock across all tissues, but circadianly expressed *Rev-erbα* uses lineage determination factors such as hepatocyte nuclear factor 6 (HNF6) to convey a tissue specific rhythm, through NCoR and HDAC3, regulating the metabolic needs specific to that tissue. This therefore suggests that the role of *Rev-erbα* in adipose centres on non-DBD dependent actions, and therefore not via RORE elements. Therefore, $Adipo^{CRE}Bmal1^{flox\ /flox}$ mice and $Adipo^{CRE}Rev\text{-}erb\alpha^{flox/flox}$ mice may show such a stark contrast in phenotype compared to global *Rev-erbα* knockout mice, despite both having low *Rev-erbα* expression in adipose tissue, because of the differential role of *Rev-erbα* specifically in this tissue.

Chapter 6 - Discussion

Our knowledge of the relationship between the circadian clock and energy homeostasis is ever increasing. It is important to understand that the coupling between energy metabolism and circadian rhythmicity is reciprocal (i.e. the two systems influence one another). On one hand, the circadian system controls a number of physiological and metabolic processes via circadian oscillators contained within regulatory brain regions and peripheral organs (Hastings, 2007; Schibler *et al.,* 2003). On the other hand, nutritional and hormonal cues are potent synchronizers of oscillators throughout the body, and energy status can influence clock function on a cellular level (Balsalobre *et* al., 2000; Stokkan *et* al., 2001 and Schibler *et* al., 2003). It has been shown that metabolic cues are also capable of altering the master circadian clock, and in doing so shape rhythms in behaviour. This close coupling implies that clock function my play a role in metabolic disease. In line with this epidemiological evidence suggests that disruption of the circadian clock is associated with metabolic complications and obesity (Maury *et al*., 2010; Eckel-Mahan and Sassone Corsi, 2013). A number of studies have now established that shift work, in which the normal synchrony between the light/dark phase, sleeping and eating is significantly disturbed, is a risk factor for obesity and diabetes (Pan *et al*., 2011).

6.1 Diet Induced Obesity disrupts behavioural and molecular circadian rhythms

We therefore wanted to determine the effect of a hypercalorific diet on the circadian clock. Our work showed that robust rhythms in activity and core body temperature are maintained in chronically HFD-fed C57BL6/J mice. However, a reduction in dark phase activity along with reduced amplitude in day/night temperature profiles is observed as well as damped feeding rhythms. Food, temperature and exercise are important zeitgebers and therefore dampening of these zeitgebers may lead to a weakening of synchrony of the clock throughout the body (Stephan, 2002; Atkinson *et* al., 2007; Rensing and Ruoff, 2009). Interestingly, our work demonstrated that chronic HFD leads to altered synchrony amongst different tissue clocks, with the adrenal gland and liver showing a phase advance of clock gene rhythms in HFD-fed mice, whereas other tissues showed virtually no alteration (e.g. muscle and BAT). Kohsaka *et al*. (2007) performed a similar study in which they fed C57BL6/J mice HFD for 10 weeks. Consistent with our findings, the HFD-fed mice maintained robust diurnal rhythms and the amplitude of the circadian rhythm and the overall activity did not differ between NC- and HFD-fed animals. However, these mice showed an increase in the free running period of activity

under DD conditions. Period lengthening occurred within 1 week of HFD-feeding, but differences in body weight did not occur until after 3 weeks of hypercaloric feeding, suggesting that increased period length is independent of body weight and more likely due to impact of the diet itself (Kohsaka *et al.,* 2007). We did not examine free running conditions in our studies.

We also assessed feeding behaviour in the mice on either NC or HFD. The proportion of calories consumed during the light phase was significantly higher in the HFD fed mice, but this was largely due to the decrease in night time feeding rather than an increase in feeding during the day. In turn, this resulted in a blunting of the feeding rhythms and therefore a flattening in the influx of calories to the body. The blunting of the diurnal feeding rhythms means that mice on HFD have a short fasting period and a longer feeding window, which was demonstrated by our temporal feeding profile of mice on NC and HFD. As previously mentioned, food is a potent zeitgeber and therefore metabolic pathways which are entrained by circadian and feeding rhythms become disrupted. This temporal disruption in cellular metabolic processes may predispose the animal to obesity and metabolic disease. In support of this, nocturnal mice fed a HFD only during the 12-h light phase gained significantly more weight than mice fed only during the 12-h dark phase (Arble *et al*., 2009). Our work demonstrated that alterations in nocturnal feeding were apparent within 3 days of the mice being on HFD. This suggests that altered feeding patterns reflect a homeostatic response to increased calorie and fat content, for example, an increase in satiety signals from fat would result in fewer meals during the dark phase, when feeding activity would normally be high.

This data again parallels work done by Kohsaka *et al*. (2007) in which animals on HFD showed diurnal feeding rhythms, which were attenuated in comparison to animals fed NC. In the first week of their 10 week HFD trial, mice consumed a higher percentage of their daily food intake during the light period, which is the same as observed in our studies. This was due to an increased amount of food (g) consumed in the light period and a decrease in the dark period, which again was observed before significant weight gain. Therefore, mice on HFD consume many extra calories during the 12 hour light phase (especially relative to total intake). The altered pattern in food/calorie intake which shifts towards the 'incorrect' time in the light/dark cycle may potentiate the obesogenic effect of a hypercaloric diet (Hatori *et al*., 2012; Garaulet and Gómez-Abellán, 2014). Mice with time-restricted feeding of a HFD in the night phase were found to be protected from DIO. These mice were better able to utilise fat as an energy source,

as reflected in improved RER and energy expenditure. In ad-libitum HFD-fed mice, in which feeding rhythms were dampened, perturbed total and diurnal change in active CREB, mTOR and AMPK either reduced or dampened the oscillations of a range of circadian clock components, such as *Per2, Bmal1* and *Rev-erbα* in the liver. In turn, increased fatty acid synthesis, elongation and desaturation were observed in the mice in comparison to their time restricted counterparts, highlighting the importance of temporal compartmentalisation (Hatori *et al*., 2012, Casiraghi *et al*., 2016).

To specifically address whether HFD feeding would alter clock gene expression/synchrony, we profiled gene expression in central and peripheral tissues in obese and normal weight mice. We found that chronic HFD feeding results in damped rhythms specificially in gWAT. Similar gene expression profiles have been carried out in a number of studies. However, the extent to which HFD-feeding impacts the circadian system varies widely between studies, with minimal effects on clock gene expression reported in some cases (Stavinoha *et al.,* 2004; Sato *et al*., 2006; Yanagihara *et al*., 2006) and a significant damping of circadian rhythm reported in others (Kohsaka *et al*., 2007). The differences in the extent of effect of HFD on clock gene expression is not unexpected as our studies demonstrate that the duration of HFD feeding can have a significant impact, with clock gene disruption being observed only after 16 weeks HFD feeding. Here we provide evidence by profiling clock gene expression in a large number of tissues that chronic HFD feeding results in profound and specific dampening in clock gene rhythms in WAT and most notably in gWAT. In gWAT, *Dbp*, *Per2* and *Rev-erbα* showed the most attenuated rhythms in HFD mice. Interestingly, our study demonstrated that HFD had only a moderate effect on *Bmal1* expression. As BMAL1 activates the transcription of clock genes by heterodimerising with CLOCK and then binding to E-boxes within target genes, it is possible that E-box mediated transcription is affected in DIO. This would explain why diurnal variation of Bmal1 is only mildly affected, yet *Dbp*, *Per2* and *Rev-erbα*, which are strongly E-box regulated, show severe attenuation. This, however, contrasts work done by Prasai *et al*. (2012) which showed that there was a marked and significant attenuation of the cycling of *Bmal1* in adipose tissue of DIO mice after 10 weeks of HFD feeding. Kohsaka *et al*., (2007) also showed clock disruption in adipose tissue, with *Bmal1* expression being reduced in both the light and the dark periods and *Per2* expression decreased selectively during the dark period. Both studies by Prasai *et al*. (2012) and Kohsaka *et al.* (2007) demonstrated a specific dampening of the clock in adipose tissue, which supports our findings. Clock gene rhythms in gWAT are more susceptible to obesity related dysfunction compared to scWAT, likely

representing depot-specific differences in the metabolic and inflammatory response to obesity-related hypertrophy. Clock rhythms persist to the same extent as lean patients in scWAT of patients with obesity and type 2 diabetes maintained under controlled conditions (Otway *et al*., 2011). However, analysis of adipocytes obtained from gWAT of lean and obese patients demonstrated clock gene dysregulation in the obese group, with significant upregulation of *Bmal1*, *Cry1* and *Rev-erbα* over the 24 hour period (Viera *et al*., 2014). This contrasts with our data obtained from a DIO mouse model, specifically in the case of *Rev-erbα*, which is downregulated throughout the circadian series and shows the strongest attenuation of rhythm in the DIO model. This may be an indication that other peripheral factors, such as inflammation, caused by DIO *in vivo* play a role in clock gene dysregulation in gWAT. Severe attenuation of *Rev-erbα* rhythms was also observed in liver and muscle of the DIO muscle, a finding supported by the work of Kohsaka *et al*. (2007). Together, this data may also suggest that attenuation of *Rev-erbα* expression may be a compensatory response *in vivo* to combat the effects of obesity. This is supported by a study which showed that mice lacking *Rev-erbα* had elevated serum adiponectin levels, which acts as an anti-inflammatory cytokine in hypertrophic WAT (Hand *et al*., 2015). Importantly, our study demonstrates that clock gene rhythms are maintained in the hypothalamus in mice on NC and HFD. This is supported by data obtained from Kohsaka *et al*., (2007) in which they show cycling of *Bmal1* and *Per2* RNA in the MBH which was unaffected by HFD, indicating that clock function in the brain is unaffected by HFD. This work is reinforced by data obtained from the *ob/ob* mouse model, in which the leptin gene is disrupted. In this model, peripheral, but not central clocks are impaired. Specifically, mRNA expression profiles of clock and clock controlled genes in the SCN were not affected; however, they were significantly dampened in liver and adipose tissue (Ando *et al*., 2011).

Although amplitude of rhythms is largely unaffected by DIO in the majority of peripheral tissues, chronic HFD feeding did result in tissue desynchrony, for example rhythms are advanced in liver and adrenal gland but not in muscle, BAT or scWAT. Advancement of hepatic clock gene rhythms has been reported previously in HFD-fed mice, in response to acute changes in diet composition (Pendergast*et al*., 2012; Eckel-Mahan *et al*., 2013) suggesting desynchrony may not be due to obesity *per se* but rather in response to altered dietary intake. For example, the shift in feeding pattern towards the inactive phase may result in this desynchrony. Also, metabolites themselves have been shown to affect clock timing. Increased levels of circulating fatty acids result in phase shifts of peripheral clocks (Kim *et al*., 2016).

Eckel-Mahan *et al.,* (2013) suggested that changes in diet composition results in alteration of the clock by impairment of CLOCK:BMAL1 chromatin recruitment. Additionally, insulin resistance can become present as quickly as 3 days into a HFD feeding regime (Lee *et al*., 2011). This results in increased glucose circulation, and glucose is a well-documented circadian clock regulator. *In vivo* glucose administration has effects on both central and peripheral clocks. Glucose infusion during the inactive phase strongly induces expression of *Per2* in the SCN but suppresses *Per2* expression in the liver (Iwanaga *et al*., 2005). This also demonstrates that glucose has tissue specific effects of the clock and may contribute the desynchrony seen in the DIO mice.

The phase of the clock and synchrony between tissues is important as it sets metabolic rhythms. Altered levels as well as rhythm of metabolic gene expression were observed in the DIO model. Mammals show alternating cycles of lipogenesis and lipolysis. During the inactive phase there is an increase in body fat utilisation and therefore lipolysis predominates, reducing the need for food intake. During the active phase, however, the converse is true and lipogenesis predominates in order for energy to be stored to fulfil the energy requirements of the low activity period (Le Magnen, 1988). It is therefore important for adipose tissue to be synchronised with other organs and tissues, for example the liver. In the post-absorptive state, blood glucose levels increase and hepatocytes remove glucose from the blood stream to store it as glycogen or use it to synthesise lipids that can be stored either in the liver or be transported to adipose tissue in the form of VLDLs. Adipose tissue takes up TAG from circulating lipoprotein particles by means of LPL for storage. When lipolysis occurs, FAs are released from adipose tissue in order to be used as an energy source throughout the body, including the liver. In order to ensure tissue homeostasis, these physiological processes must be coordinated. Perturbation of the synchrony of the circadian system throughout the body has been linked to the development of metabolic syndrome (Scheer *et al*., 2009).

My results demonstrate that circadian rhythmicity extends to a selection of genes involved in lipogenesis and lipolysis in gWAT, scWAT and liver, suggesting that the clock is important in the drive of lipid metabolism. Previous evidence has demonstrated that *Atgl* and *Hsl* transcripts show circadian variation in cultured fat pad explants (Shostak *et al*., 2013). As shown by reporter gene and ChIP assays the CLOCK:BMAL1 heterodimer regulates *Atgl* and *Hsl* transcription in adipose tissue by binding to the E-boxes and therefore rhythmicity in these genes is expected (Shostak *et al*., 2013). Circadian variation of lipid gene transcripts has also

been demonstrated previously in the liver, with *Dgat2* (Bhargava *et al*., 2015) and *Lpl* (Ptitsyn *et al*., 2006) showing rhythmicity. A pronounced yet highly tissue-specific alteration in metabolic gene expression was observed in our DIO obesity model. In gWAT, HFD resulted in attenuation of rhythms and downregulation of lipogenic gene expression (*Dgat2, Fasn*) and lipolytic gene expression (*Atgl* and *Hsl*) which contrasts to the upregulation of *Hsl*, *Lpl* and *Dgat2* in scWAT. Interestingly, scWAT has a larger storage capacity for triglyceride than gWAT, as at a certain body weight, gWAT stops expanding because of increased adipocyte death (Strissel *et al*., 2007).Therefore, in a hypercaloric state it would be beneficial for increased lipogenesis within scWAT in order to promote the 'safe' storage of triglyceride rather than the ectopic distribution of fat, for example in the liver. A number of *in vivo* and *in vitro* studies (Reynisdottir *et al*., 1994; Jensen, 1997; Horowitz and Klein, 2000) suggest that there is lipolytic resistance to catecholamines in scWAT in obesity and therefore *Hsl* upregulation in this tissue may be an over-compensatory mechanism, with the aim that enhanced *Hsl* expression would result in increased HSL protein expression to potentially overcome the catecholamine resistance. Increased *Hsl* expression in scWAT of DIO mice may mean increased lipolytic activity within this tissue in comparison to gWAT. It has been previously demonstrated that *Hsl* expression is decreased in mature subcutaneous fat cells of obese subjects (Large *et al*., 1999) but expression increases during adipocyte differentiation (Langin *et al*., 2005). The difference in expression of HSL between the two WAT depots may be due to increased hyperplasia in scWAT under DIO challenge compared to gWAT. It has also been demonstrated that *Hsl* is upregulated by PPARγ (Deng *et al*., 2006). In our DIO mode, *Pparγ* is downregulated in gWAT and upregulated in scWAT and these depot specific expression patterns match those of *Hsl*. It is therefore likely that that *Pparγ* expression is responsible for the differential expression of *Hsl* within the depots. Although HFD-feeding resulted in minimal alterations in expression of genes involved in lipid metabolism in the liver, it induced rhythmic cycling of *Hsl*. Interestingly, Eckel-Mahan (2013) reported that 38% of rhythmic transcripts had an increased amplitude in the liver when mice were subjected to HFD, and this relied on the robust, circadian accumulation in the nucleus and on chromatin of the transcription factor PPARγ. This is in keeping with our data, as HFD-feeding resulted in enhanced PPARγ expression in the liver. As PPARα and PPARγ are direct regulators of the core clock components, *Bmal1* and *Rev-erbα* (Inoue *et al* 2005, Canaple *et al*., 2006), together this data highlights the PPARs are the interface between the clock and metabolism.

Rhythmicity was also observed in genes involved in glucose handling in liver, muscle, gWAT and scWAT with severe downregulation and attenuation of expression particularly observed in gWAT of HFD-fed mice. On normal chow, *Pepck* exhibited robust diurnal variation. *Pepck* codes for an enzyme responsible for gluconeogenesis in the liver and glyceroneogenesis, a process which is critical for the generation of glycerol to support the synthesis of triglyceride, in adipose tissue (Reshef *et al*., 1970). It has been previously demonstrated that PEPCK activity in the liver exhibits a diurnal rhythm (Phillips and Berry, 1970) which in turn contributes to the diurnal rhythm of hepatic glucose production (Kida *et al*., 1980). CREB and FOXO1 are the two major transcription factors that drive *Pepck* expression (Gross *et al.*, 2008; Altarejos and Montminy, 2011). Glucocorticoid hormone is released in a diurnal manner and has been shown to activate transcription of *Pepck*, (Phillips and Berry, 1970; Le Minh *et al*., 2001; Chakravarty *et al*., 2005). The glucocorticoid-dependent interaction between CRYs and the glucocorticoid receptor has been characterised (Lamia *et al*., 2011). CRYs repress both glucagon and glucocorticoid signalling and thus constitute a negative circadian pathway to the transcriptional control of *Pepck.* It was also demonstrated by Yin *et al*., (2007) that the nuclear receptors REV-ERB/ROR also directly regulate PEPCK expression. This data is interesting, as in our studies in DIO mice, we have shown that the circadian clock is disrupted, particularly in gWAT. The effect of HFD on *Pepck* expression in gWAT is profound, with a loss of diurnal variation as well as severely reduced expression. This may indicate that attenuation of clock gene and clock related gene expression in gWAT results in loss of rhythmicity and diminished expression of *Pepck*. It is also important to note that HFD in itself would result in decreased *Pepck* expression, because both the gluconeogenesis and glyceroneogenesis pathways become most prominent in the fasted state, in events of low carbohydrate availability. However, in a positive energy balance state, there is a reduced requirement for these pathways. Out of all tissues examined, rhythmicity of genes in gWAT were most affected, with *Glucokinase* and *Glut4* not only losing diurnal variation but also showing pronounced attenuation of expression. This parallels what was observed in clock gene rhythms as well as lipid handing genes, with gWAT being the most dramatically affected by HFD-feeding. It will be critical to determine whether the clock directly contributes to metabolic gene disruption.

It has previously been demonstrated that PPARγ expression is induced in the liver response to HFD (Vidal-Puig *et al*., 1996) and during the development of diet induced fatty liver disease (Inoue *et al*., 2005). In a study carried out by Eckel-Mahan *et al*., (2013) it was evident that *Pparγ* mRNA expression was robustly oscillatory in the liver of HFD fed animals, whereas levels

of total PPARγ protein were elevated but showed no circadian variation, which correlates to our findings. Moreover, a novel role for PPARγ in reprogramming transcriptional rhythms in the mouse liver in response to HFD was demonstrated (Eckel-Mahan *et al*., 2013). Chromatin-bound PPARγ displayed a robust change at different ZTs only in HFD mice, and it was suggested that transcriptional reprogramming induced by HFD relies on changes in the presence and pattern of oscillation and chromatin recruitment of PPARγ. PPARγ circadian function in HFD-fed mice therefore still relies on the clock-controlled nuclear translocation of the protein and rhythmic chromatin recruitment to target genes. In contrast to this, the profound effect elicited by HFD with regards to dampening rhythms is caused by either phase-shifted or reduced recruitment of the CLOCK:BMAL1 complex to chromatin at the level of target promoters (Eckel-Mahan *et al*., 2013). HFD does not, however, affect CLOCK:BMAL1 nuclear translocation. This may go some way to explain the dampened rhythms and attenuated expression of *Rev-erbα* observed most notably in the liver and gWAT as CLOCK:BMAL1 drives the rhythmic transcription of this gene (Triqueneaux *et al*., 2004). It would be interesting to follow this up with ChIP assays of BMAL1:CLOCK and *Rev-erbα* and Western Blots of REV-ERBα in liver and adipose tissue of DIO mice as it is likely to be gene specific since other E-box driven genes, for example *Dbp* and *Rev-erbβ* were not damped.

Much work has been carried out to establish the close interconnection that exists between the circadian clockwork and cellular metabolism. My work along with the work of others by means of transcriptomic, proteomic and metabolomics studies provides evidence that metabolic processes such as gluconeogenesis and lipid metabolism are highly rhythmic and are either directly or indirectly guided by circadian clockwork (Panda *et al*., 2002; Reddy *et al*., 2006; Eckel-Mahan *et al*., 2012; Zhang *et al*., 2014). Fluctuations in cellular energy balance such as redox state as well as ATP/AMP availability can influence clock function. The activity of energy responsive regulators including SIRT1, AMPK, PGC-1α, and PPARα/γ can also have an impact on the function of the clock (Peek *et al*., 2012). PPARα/γ receptors are both regulated by the clock, yet also feed-back directly onto the clock through transcriptional regulation. This suggests that the alterations to PPAR and clock gene expression observed in gWAT and liver of the obese mice may be causally linked. Based on the liver reprogramming observed by Eckel-Mahan *et al*. (2013) in response to HFD and the dampening of clock gene rhythms observed by our work in adipose tissue, in obesity the temporal relationship between these two tissues may be disrupted. It is uncertain whether clock breakdown drives alterations in *Ppar* expression or vice versa. It can be speculated that as both *Pparα* and *Pparγ* increase *Rev-erbα*

expression (Duez and Staels, 2008), and as expression of the *Ppars* is severely attenuated in gWAT of the DIO model, this may be responsible for the attenuation of *Rev-erbα* expression in this tissue and the subsequent breakdown of the clock.

The contrast between the acute response to HFD in the liver, i.e. advancement of hepatic clock gene rhythms (Pendergast *et* al., 2012; Eckel-Mahan *et al.,* 2013) and the chronic response of dampened rhythms of clock genes (our data) observed in gWAT is particularly interesting. gWAT and liver have previously been shown to have temporally separated development of insulin resistance (Kleemann, 2010). Using radioactive hyperinsulinemic euglycemic clamp analysis, in combination with gene microarray and metabolomic analysis, it was determined that insulin resistance is first observed in the liver after approximately 6 weeks on HFD; whereas, insulin resistance in WAT develops later, after 12 weeks of HFD (Kleemann, 2010). Interestingly, time-dependent and tissue-specific differences in tissue inflammation were also observed in this study, with the liver showing an acute transient increase in inflammation before returning back to normal, whereas gWAT inflammation increased over time up to 12 weeks corresponding to the development of insulin resistance (Kleemann, 2010). Our data, along with others (Prasai *et al.,* 2013) point to the relationship between the increase in inflammation in gWAT and the damping of the circadian clock. Systemic inflammation, such as during endotoxin shock (LPS challenge), has been shown to disrupt clock gene expression and behavioural rhythms (Haimovich *et al.,* 2010; Cermakian *et al.,* 2014; Paladino *et al.*, 2014) Additionally, a wide range proinflammatory cytokines have been shown to have an effect on the circadian system. An example is TNF-α which has been shown to act on the SCN. When injected intracerebroventrically in mice, TNF-α caused a phase delay in locomotor activity rhythms (Leone *et al*. 2012).Therefore it is likely that obesity-related infiltration of pro-inflammatory immune cells into gWAT is a contributing factor to the clock disruption reported in our work. This is also supported by the fact that increased inflammatory marker transcripts, clock disruption and a reduction in *Ppar* expressionwere not present until 16 weeks HFD-feeding.

Given the clear overlap in the timeline between increased inflammation, damping of circadian clock and development of insulin resistance in gWAT during the progression of obesity, it is interesting to spectulate that these processes are dependent upon, or caused by each other. For example, PPAR*γ* is a clear link between the clock, obesity and inflammation. It is involved in governing the inflammatory response by interfering with pro-inflammatory transcription

factors, e.g. NF- κB (Ricote *et al.,* 1998). It also prevents the removal of corepressor complexes from gene promotor regions resulting in suppression of inflammatory gene transcription (Pascual *et al*., 2005). PPARγ also plays a role in determining the fate of preadipocytes to either adipocytes or macrophage type cells. PPARγ activation favours adipocyte differentiation which results in a decreased inflammatory status of adipose tissue during obesity. In our studies, DIO mice show reduced PPARγ expression in gWAT, which may be facilitate the increased inflammatory markers observed in these mice. It is yet to be determined whether loss of robust circadian rhythms in gWAT contributes to obesity related metabolic dysfunction, but interestingly, pharmacological targetting of the circadian clock, by means of synthetic REV-ERBα agaonists has been shown to improve metabolic disturbance in DIO and genetic models of obesity (Solt *et al*., 2011). Our data shows that *Rev-erbα* is the clock related gene most affected by chronic HFD, further strengenthing the possibility of a link between the necessity of robust gWAT clock rhythms to maintain a healthy metabolic state. In fact, our own data suggests that entrainment using daily CK1ε inhibitors can improve glucose homeostasis (Cunningham *et al.,* 2016)..

6.2 Loss of *Rev-erbα* results in severe disruptions to lipid handling

REV-ERBα is a transcription factor involved both in the molecular clockwork and in several metabolic pathways. Therefore, delineating REV-ERBα contribution to energy homeostasis is an important step toward understanding the functional crosstalk between the circadian and metabolic systems. Here we show that loss of *Rev-erb*α in mice, despite maintenance of robust physiological rhythms, results in compromise of the gWAT clock. *Rev-erb*α knockout mice exhibited robust entrainment of wheel-running activity rhythms to a 12:12 LD cycle and displayed a shortened period once released into constant darkness (DD). This confirms previous work carried out by Preitner *et al.* (2002) who showed that under both DD and LL conditions, the average period length was significantly shorter in *Rev-erb*α null mice. Interestingly, transgenic mice overexpressing the *Clock* gene show a similar phenotype, with period shortening beyond the normal WT values observed (Antoch *et al*., 1997). Both transgenic models result in the overexpression of components of the positive limb of the circadian clock and therefore result in more potent activation of *Cry* and *Per* genes, which in turn would reduce the duration required to produce CRY and PER threshold levels sufficient for the downregulation of their own genes. This, however, contrasts our data in which *Per* expression in *Rev-erb*$\alpha^{-/-}$ mice is attenuated. Prietner *et al*., (2002), however, demonstrated

that loss of Rev-erbα in mice resulted in very little alteration in both *Per2* mRNA and PER2 protein expression.

Despite maintaining behavioural rhythms, attenuation of the clock specifically in gWAT of Rev-erbα$^{-/-}$ mice was observed by both *ex vivo* bioluminescence recording or PER2::Luciferase and mRNA expression analyses. *Rev-erb*α is very highly expressed in gWAT (Solt *et al*., 2011) whereas *Rev-erbβ* is expressed at high levels in parts of the brain (pineal and prefrontal cortex), thyroid, uterus and pituitary (Bonnelye *et al*., 1994). Therefore, in gWAT and other metabolic tissues, *Rev-erbβ* is unable to compensate for the lack of *Rev-erbα*, rendering gWAT to be strongly affected. This may also suggest that the clock is more reliant on *Rev-erbα* in adipose tissue. This is interesting, as although *Rev-erb*α knockout mice showed little difference in body weight compared to WT C57BL/6 littermates, they showed significant increase in gWAT weight, resulting in an obese phenotype. This confirms the findings of Delezie *et al*. (2012). It is important to note that the increased adiposity of *Rev-erb*α knockout mice was not due to hyperphagia, as these mice consumed the same amount of calories as WT C57BL/6 littermates. As shown by our DIO studies, HFD-feeding results in a profound and specific dampening of the clock in gWAT, and therefore attenuation of clock gene rhythms in *Rev-erb*α knockout mice may be linked to the increased adiposity. Inflammation was previously suggested as a potential factor of the clock breakdown in gWAT of the DIO model, but *Rev-erb*α knockout mice exhibit an attenuation of typical pro-inflammatory stimuli with enhanced anti-inflammatory signalling (Hand *et al*., 2015). Adiponectin may be responsible for the reduced inflammation observed in *Rev-erb*α null mice as they exhibit elevated serum adiponectin levels and increased adiponectin secretion from WAT. Adiponectin was found to supress primary macrophage responses to lipopolysaccharide and pro-inflammatory fatty acids. This suppression depended on glycogen synthase kinase 3β activation and induction of A20, a cytoplasmic ubiquitin modifying enzyme and therefore the attenuated inflammatory response in mice lacking *Rev-erb*α was also associated with the tonic elevation of A20 (Hand *et* al., 2015). The absence of adipose inflammation in the *Rev-erb*α knockout mice is not a result of general lack of inflammatory response, however, because these animals exhibit robust responses to systemic endotoxin administration (Gibbs *et al.,* 2012). Heme has been shown to have both pro-oxidant (Phumala *et al.,* 2003) and pro-inflammatory effects (Wagener *et al*.,2001) and as this is the natural ligand of *Rev-erb*α, it may be that heme can act via *Rev-erb*α to bring about inflammation, but when *Rev-erb*α is not present, this mechanism cannot be executed. Further supporting reduced inflammation in adipose tissue was reduced circulating FFA and glycerol in *Rev-erb*α knockout mice, which is indicative of reduced lipolysis,

a known inflammatory signal (Zhang *et al*., 2014). Taken together, this suggests an important role for *Rev-erbα* in adipose tissue and may suggest that the increased adiposity in these mice is linked to a less robust clock, but it is unlikely that inflammation is responsible for clock breakdown in gWAT of these animals. PPAR expression was also strongly attenuated specifically in gWAT our C57BL/6J DIO mice. *Rev-erb*α is a target gene of PPARγ and therefore when *Rev-erb*α is absent and adiposity is increased, PPARγ may be unable to exert its circadian effects in gWAT (Gervois *et al*., 1999). Also, *Rev-erb*α is a repressor of PPARγ and therefore loss of this repression may increase PPARγ activity and in turn increase lipogenesis. PPARα is required to maintain the circadian rhythm of *Bmal1* in peripheral tissues via direct binding to a PPARα response element located in the *Bmal1* promotor (Canaple *et al*., 2006). Increased adiposity in *Rev-erb*α knockout mice may therefore result in decreased PPARα expression in gWAT and therefore reduce its ability to maintain circadian rhythms in this tissue, resulting in gWAT being particularly affected by the lack of *Rev-erb*α.

Maintenance of the *Reverbα* knockout mice on HFD resulted in a profound increase in body weight and adiposity compared with HFD-fed control littermates. Interestingly, in contrast to *Rev-erbα*$^{-/-}$ mice on NC, HFD-fed mice were hyperphagic. This hyperphagia may be brought about by a lack of satiety in these animals, but this is unlikely as Delezie *et al*., (2012) showed that leptin levels were increased in *Rev-erbα*$^{-/-}$ mice Characterisation of hypothalamic neurons implicated in feeding and energy balance, for example ARC neurons, which are particularly sensitive to feeding related signals such as leptin and ghrelin may be informative as other clock mutations have been shown to effect the neuropeptides produced by these neurons. For example, the rhythmic pattern of α-MSH, an appetite suppressing peptide, is disrupted in *Per2*$^{-/-}$ mice and peripheral administration of α-MSH induces weight loss (Yang *et al*., 2009). Also, *ClockΔ19* mutation leads to dampening of the rhythms of hypothalamic neuropeptide levels such as CART and orexin (Turek *et al.*, 2005). Rhythms of circulating ghrelin in these mice also become dampened. It is clear that the clock plays a role in satiety signalling. However, in *Rev-erbα-/-* mice subjected to HFD, it is possible that loss of *Rev-erbα,* along with hugely increased adiposity is responsible for the hyperphagia observed, as leptin resistance has been shown to be present in obese animals and human patients (Caro *et al*., 1996; Considine *et al*., 1996; Schwartz *et al*., 1996). It has also been shown that administration of a synthetic REV-ERBα agonist to DIO mice led to a reduction in adipose tissue mass and circulating leptin levels decrease by 80% (Solt *et al*., 2012). It is also possible that there is a defect in energy sensing in *Rev-erbα*$^{-/-}$ mice. It has been shown that in acquired obesity is there is a reduction in the energy sensing NAD^{+}/SIRT pathway (Jukarainen *et al*., 2016). On top of this, *Rev-*

erbα deficiency results in deactivation of the liver kinase B1 (Lkb1)-Ampk-Sirt1–PGC-1α signalling pathway, which is important in detecting and responding to energy status (Woldt *et al*. 2013). *Rev-erbα* also regulates glucagon secretion via AMPK/Nampt/Sirt1 pathway. The catalytic subunits of AMPK are co-localized with NPY in the ARC (Kim *et al*., 2004) and therefore the combined disruption of the AMPK signalling pathway through exaggerated obesity and loss of *Rev-erbα* may be responsible for the hyperphagia seen in *Rev-erbα*$^{-/-}$ mice on HFD. Concentrations of long chain fatty acids (LCFA) in *Rev-erbα*$^{-/-}$ mice on HFD may also explain the hyperphagia observed. Following a bolus administration of the LCFA, oelic acid, in rats, food intake was reduced for 2 days and this was likely mediated by decreased hypothalamic NPY mRNA levels (Obici *et al*., 2002). Paschos *et al*. (2012) demonstrated that disruption to the circadian clock in adipocytes resulted in the reduction in the amount of key enzymes involved in the biosynthesis of polyunsaturated fatty acids (*Elovl6, Scd1*). These polyunsaturated fatty acids are able to cross the blood brain barrier and provide information on the metabolic status of the animal to hypothalamic centres which regulate feeding activity. However, Delezie *et al., (*2012) showed that hepatic expression of *Elovl6* was increased in *Rev-erbα*$^{-/-}$ mice on HFD, suggesting that polyunsaturated fatty acid levels in these mice may not be able to explain the hyperphagia observed.

The hyperphagia observed in the *Rev-erbα*$^{-/-}$ mice, however, does not completely explain the severe obesity observed in these mice. When food intake was restricted in these mice to normalise to WT C57BL/6 mouse intake on HFD, the *Rev-erbα*$^{-/-}$ mice still showed increased adiposity in comparison to the WT C57BL/6 controls (Cunningham, unpublished data). This suggests that there is difference in fat accumulation and storage in these mice. Lower circulating FFAs in *Rev-erbα* knockout mice may reflect the incorporation of lipid into adipose tissue, suggesting that these mice may have an increased storage capability. Decreased expression of the lipolytic genes *Atgl* and *Hsl* is also observed in *Rev-erbα* knockout mice on HFD which may result in decrease circulating FFAs due to decreased lipolysis. This is further supported at a protein level, with ATGL showing reduced expression in *Rev-erbα* knockout mice on HFD compared to WT C57BL/6 controls, showing that even amid adipocyte hypertrophy there is an increased bias for lipid storage. This phenotype was also observed by Delezie *et al*., (2012). This group also observed enhanced hepatic expression of *Acc*, *Fasn* and *Elovl6* in *Rev-erbα* knockout mice maintained on HFD, showing that even when faced with a positive energy balance, there is still an increase in *de novo* lipogenesis in these animals and therefore an increased ability to produce fat. However, despite the fact that *Pparα* and *Pparγ*

are regulated by the clock and our studies showed profound changes in C57BL/6J DIO mice, deletion of *Rev-erbα* did not alter *Ppar* gene expression in gWAT, liver or muscle. *Pparα* and *Pparγ* transcripts were upregulated in the liver of C57BL/6 animals on HFD, however upregulation of *Pparα* in the liver of *Rev-erbα* knockout mice on HFD was not observed. Overall this data would suggest the effect that loss of *Rev-erbα* has on susceptibility to DIO is not due to altered transcription of *Ppars*. Significant downregulation of *Ppar* expression in response to 14 week HFD feeding was also not observed in the gWAT of C57BL/6 or *Rev-erbα* knockout mice in a separate study. This contrast between the different C57BL/6 groups (DIO and *Rev-erbα*$^{+/+}$) may be due to the sex difference and/or the relatively low body weight of the C57BL/6 mice in the *Rev-erbα* trial. Nevertheless, our results suggest that *Pparγ* is protected from the obesity related decrease in *Rev-erbα* knockout mice, because these mice showed extreme adiposity but no change in *Pparγ* expression. Infact, maintenance of *Ppar* levels may contribute to enhanced obesity.

Apolipoprotein C-III (apoC-III), however, may play a role in the increased fat accumulation in *Rev-erbα*$^{-/-}$ mice. It is a major constituent of triglyceride rich remnant lipoproteins that impede triglyceride hydrolysis and remnant clearances. Transient co-transfection experiments in rat hepatocytes in primary culture demonstrated that overexpression of *Rev-erbα* specifically decreases apoC-III promotor activity. On top of this, *Rev-erbα* deficient mice display elevated serum and liver mRNA levels of apoC-III (Raspé *et al*., 2002). It has been demonstrated that apoC-III overexpression exacerbates diet induced obesity by promoting increased availability of NEFA from post-prandial triglyceride-rich lipoproteins combined with greater adipose capacity for lipid uptake and retention as well as reduced adipose tissue lipolysis (Raposo *et al*., 2015). *Rev-erbα* deficient mice on HFD also display increased ketonaemia which is likely as a response to an overload of the citric acid cycle, with blood glucose being converted to acetyl-CoA in parallel to the production of acetyl-CoA from fat breakdown. Although the skeletal muscle has an enhanced oxidative capacity in *Rev-erbα*$^{-/-}$ mice, this is evidence that it is not sufficient to cope with the adverse effects of chronic HFD feeding (Delezie *et al*., 2012). *Rev-erbα* has also been shown to repress PAI-1 gene expression through two *Rev-erbα* binding sites in the PAI-1 promotor and therefore increased expression of PAI-1 would be expected in *Rev-erbα* deficient mice (Wang *et al*., 2006). A variety of studies have been conducted which support the relationship of PAI-1 with the development of obesity. Fat accumulation was prevented in mice lacking PAI-1 in both diet induced and a genetic murine model of obesity (Schafer *et al*., 2001; Ma *et al*., 2004; De Taeye *et al*., 2006).

Daily cycles of lipid and glucose utilisation are observed in animals and therefore it is possible that increased adiposity in the *Rev-erb*α knockout mice may be due to decreased lipid utilisation. However, our studies show that there were no differences seen in the RER values between the control and knockout mice suggesting that there is not a change in fat utilisation. Work by Delezie *et al*. (2012) showed that basal metabolism was not significantly different between genotypes and the daily mean respiratory quotient values did not change between gentotypes. However, Delezie *et al*. (2012) found that *Rev-erb*α null mice showed altered daily variations in respiratory quotient values compared to control mice, with lower, and higher values during the day and night respectively (i.e. there was a larger amplitude compared to control littermates). This group suggested that *Rev-erb*α knockout mice have increased fatty acid utilization during the resting period compared to littermate controls whilst their glucose utilization is delayed and increased during the active period. However, we observed an increase in COX in *Rev-erb*α mice during the light phase, compared to control littermates, which indicated an increased dependency on carbohydrate use during this time. Nonetheless, our work and that of Delezie *et al*., (2012) indicates that no difference in basal metabolism is observed between *Rev-erb*α null mice and control littermates. Administration of a synthetic REV-ERBα agonist has been shown to increase energy expenditure in mice which was not due to increased activity (Solt *et al*., 2012). Administration of this agonist also resulted in a decrease in fat mass in the mice. The increase in metabolic rate in these REV-ERBα agonist treated mice was explained by elevated expression of *Cpt1b,* the rate limiting enzyme for β–oxidation of fatty acids, as well as the increased expression of *Fatp1*, for a protein involved in fatty acid transport into skeletal muscle. Together, this suggested an increase in fatty acid β–oxidation in these mice and it is therefore highly likely that *Rev-erb*α plays a role in the daily cycles of lipid and glucose utilisation, with a possible elevation of fat synthesis from dietary glucose during the active phase.

Our work and the work of others (Ptitsyn *et al*., 2006; Solt *et* al., 2012; Shostak *et al.,* 2013; Bhargava *et al*., 2015) has demonstrated that a variety of genes involved in lipid metabolism show circadian rhythmicity, such as *Dgat2, Fasn, Atgl, Hsl and Lpl*. It would therefore be logical that manipulation of the clock would result in a dysregulation of lipid metabolism. A synthetic REV-ERBα agonist, SR9011, has profound effects on metabolic gene regulation (Solt *et al*., 2012). For example, in the liver, *Fasn* expression is phase shifted around 8 hours, resulting in peak *Fasn* expression occurring at the start of the resting phase, in comparison to peak expression being observed just before the start of the active phase on vehicle treated mice. Our work highlights that *Fasn* expression in the liver of *Rev-erb*α knockouts is downregulated

in comparison to control littermates. However, Fasn expression in gWAT is upregulated in *Rev-erb*α knockouts. *Fasn* also shows profoundly upregulated expression in *Adipo*^{CRE}*Bmal1*$^{flox\ /flox}$ mice and *Adipo*^{CRE}*Rev-erbα*$^{flox/flox}$ mice. *Fasn* has been shown to be Srebp-1c target, and this transcription factor is temporarily controlled by REV-ERBα (Le Martelot *et al*., 2009). Loss of *Bmal1* results in diminished *Rev-erbα* expression, similar to global and adipocyte specific *Rev-erb*α knockout mice and therefore lack of repression on *Fasn* transcription. Both *Hsl* and *Dgat2* were significantly upregulated in gWAT of *Rev-erb*α knockout mice which is interesting as it suggests that there is not a bias for lipogenesis over lipolysis. In the study conducted by Solt *et al*. (2012), administration of SR9011 resulted in the suppression of expression of *Hsl* and *Dgat*2, highlighting *Rev-erb*α as an important regulator of these genes. DGAT2 is an integral membrane protein that catalyses the final enzymatic step in the production of TAGs. It is responsible for transferring an acyl group from acyl-CoA to DAG to form TAG which are stored in either adipocytes or hepatocytes (Lardizabal *et al*., 2001) and so an increase in *Dgat2* would suggest an increase in lipogenesis in the mice. The E-box activators CLOCK and BMAL1 and RRE repressors (REV-ERBs) bind to the *Dgat2* promotor (Tsai *et al*., 2010; Bhargava *et al*., 2015). Upregulation of *Dgat2* in the *Rev-erb*α knockout mouse is therefore logical, as REV-ERBα repression of *Dgat2* is lost. *Dgat2* shows profound attenuation of expression in gWAT of *Adipo*^{CRE}*Bmal1*$^{flox\ /flox}$ mice, likely due to the inability of the CLOCK:BMAL1 heterodimer to bind to the promoter of the gene. However, as there is also an upregulation of *Hsl* transcript in gWAT in *Rev-erb*α knockout mice it would seem that there is no bias towards lipogenesis or lipolysis. The promotor of the *Hsl* gene is associated with *Bmal1* in chromatin immunoprecipitation assays (Koike et al., 2012; Shostak et al., 2013) suggesting it is a direct output gene of the local WAT clock. Given that loss of REV-ERBα results in increased *Bmal1* expression this would cause the subsequent upregulation of *Hsl*. This is further supported by the decrease in *Hsl* expression observed in our studies of the gWAT of adipocyte specific *Bmal1* knockout mice. Shostak *et al*. (2013) also showed that the circadian variation in *Hsl* is lost in *ClockΔ19* mutant mice and global *Bmal1* knockout mice exhibit abolished circadian variation in expression.

Lpl constitutively upregulated in *Rev-erb*α knockout mice which confirms previous studies (Le Martelot *et al*., 2009; Delezie *et al*., 2012). Interestingly, it has been shown previously that overexpression of *Lpl* in either liver or skeletal muscle results in reduced glucose tolerance and tissue specific insulin resistance (Kim *et al*., 2001). However, despite upregulated *Lpl* in adipose tissue, gWAT explants remain insulin sensitive. It would be interesting to explore this further and determine tissue specific insulin sensitivity in the liver and muscle of the *Rev-erb*α

knockout mice. Specific overexpression of *Lpl* in adipose tissue does not lead to increased adiposity (Hensley *et al*., 2003). However, there is evidence that adipocyte-derived LPL is required for efficient fatty acid uptake and storage and that adipocytes express their own source of apoCII and apoCIII for regulating extracellular LPL activity. ApoCII activates LPL activity whereas apoCIII inhibits LPL (Jong *et al*., 1998). As previously mentioned, overexpression of *Rev-erbα* specifically decreases apoC-III promotor activity whereas *Rev-erbα* deficient mice display elevated serum and liver mRNA levels of apoC-III (Raspé *et al*., 2002), resulting in increased LPL activity. This, along with increased *Lpl* transcription in WAT of *Rev-erb*α knockout mice reflects increased activity of LPL, leading to enhanced hydrolysis of circulating triglycerides and facilitated NEFA uptake and storage, resulting in increased adiposity in this mouse. However, it is also possible that high levels of *Lpl* are due to increased fat cell size as LPL activity has been shown to increase as a function of fat cell size (Bessesen *et al*., 1991). *Lpl* contains an E-box in its promotor and it has been suggested that it is a direct target of BMAL1 (Delezie et al., 2012). However, in gWAT explants as well as Western Blot and proteomic analysis, *Lpl* mRNA expression and LPL protein expression is not upregulated in *Rev-erb*α knockout mice.

The upregulation of the lipogenic and lipolytic genes seen in *Rev-erb*α knockout mice was, however, overcome by HFD-feeding, with downregulation of the lipogenic and lipolytic genes (*Fasn* and *Atgl*) observed especially in gWAT. In the *Rev-erbα* knockout mice maintained on HFD *Lpl* was downregulated. Taken together, this would suggest that the clock and metabolic feedback such as increased fatty acid release in HFD have contrasting effects. Interestingly, when *Bmal1* was specifically knocked out in adipose tissue, which resulted in an obese phenotype only on HFD, the expression of *Atgl*, *Hsl* and *Lpl* showed no alteration (Paschos *et al*., 2012). This was an indication of no change in lipolysis in the adipocytes suggesting that the clock itself may have less impact on the lipolytic pathway. This, however, contrasts with our data, in which adipocyte specific *Bmal1* deletion resulted in decreased expression of *Atgl*, *Hsl* and *Lpl.* Taken together, our work demonstrates that it may be *Bmal1* which is important for the regulation of metabolic gene expression, with an upregulation of lipogenic and lipolytic genes observed in *Rev-erb*α knockout mice due to increased *Bmal1* expression. This work also raises the issue of how metabolic pressures (feeding/fasting) interacts with the adipose tissue clock to dictate lipid balance.

During a 24 hour fast, *Rev-erbα* knockout mice lost significantly less weight than control littermates. This may suggest that *Rev-erbα* knockout mice do not 'sense' the fast. However,

the synthesis of heme, the natural ligand for REV-ERBα, is linked to the nutritional status of mammals through the regulation of *ALAS1* by the nuclear receptor coactivator PGC-1α (Wu *et al*., 2009). PGC-1α is induced by fasting and mediates the transition from glucose to fatty acid use as an energy source. Depletion of *Rev-erbα* derepresses *Pgc1-α*, resulting in increased heme levels. *Rev-erbα* is also responsible for heme levels in a negative feedback loop and therefore lack of *Rev-erbα* further exacerbates the increased *Pgc1-α* and therefore heme expression. Increased PGC1-α levels should therefore mean enhanced awareness of the nutritional status of the knockout mice. Biochemical analysis revealed a decreased circulating TAG in C57BL/6 controls but not in *Rev-erbα* knockout mice, with circulating glycerol showing no difference. This raises the possibility of reduced lipolysis within knockout mice. It is also likely that due to excessive TAG accumulation in the liver of *Rev-erbα* knockout mice pre-fast results in it continuing to be liberated into the blood stream during the fast. No difference in RER values, however, were observed during the fast, with reduced RER observed in both genotypes, indicating that fat was the preferential energy source. Previous studies have shown that plasma NEFA and ketone bodies levels in unfed *Rev-erbα* knockout mice are lower than in unfed control mice, possibly reflecting acute utilisation of fatty acids (Delezie *et al*., 2012). However, interestingly, when looking at the profile of lipid-handling transcript in these animals, strikingly, neither 24 nor 48 hours of fasting leads to an upregulation of *Atgl* in adipose tissue or liver, as it does in control animals. This highlights a possible defect in the homeostatic mechanism to upregulate lipolysis during a fast. No post-fast alteration in expression of *Hsl* was observed in either *Rev-erbα* knockout mice or control littermates. It has, however, previously been demonstrated that *Hsl* levels are downregulated during acute fasting and increase only after prolonged food deprivation of between 3-5 days (Sztarlryd and Kraemer, 1994). During fasting, lipolysis is promoted by the combined effects of reduced plasma insulin and increased release of adrenaline and noradrenaline for the adrenal medulla (Jensen *et al*., 1987). Also, it has been demonstrated that lipolysis is further promoted by a combination of increased β-adrenergic sensitivity and decreased insulin sensitivity of adipose tissue during fasting. These fasting-induced changes in hormonal sensitivity are mediated, at least in part, by growth hormone (GH), which is elevated significantly during prolonged fasting (Norrelund *et al*. 2001, 2003; Vendelbo *et al*. 2010). The transcriptional control of *Atgl*, the gene which does not display fasted induced upregulation in *Rev-erbα* knockout mice, is complex. A PPARγ-responsive element has been identified in the promotor sequence of the mouse *Atgl* gene (Kim *et al*., 2006). On top of this, expression of G0/G2 Switch Gene 2 (G0S2), an inhibitor of ATGL, was also found to be regulated by PPARγ (Choi *et al*., 2014) and so given

the strong link between PPARγ and the clock, with *Pparγ* being repressed by *Rev-erbα*, this may be a potential mechanism that renders *Rev-erbα* knockout mice unable to upregulate *Atgl* expression during a fast. In 3T3-L1 adipocytes *Atgl* mRNA expression is negatively regulated by insulin. In humans, ATGL protein is upregulated by fasting (Nielsen *et al*., 2011) and in mice, the mRNA is suppressed by feeding (Kershaw *et al*., 2006) which is again an indication that *Rev-erbα* may not sense the fast. The dysregulation of *Atgl* expression during fasting in *Rev-erbα* knockout mice may also be attributed to the increased levels of *Bmal1* present due to lack of *Rev-erbα* inhibition. *Atgl* expression is also regulated by CLOCK/BMAL1 expression via E-box activation and *Bmal1* expression is constitutively higher in *Rev-erbα* knockout mice (Shostak *et al*., 2013). Our data from $Adipo^{CRE}Bmal1^{flox/flox}$ mice also demonstrates that loss of Bmal1 in adipose tissue results in decreased *Atgl* expression. This is interesting as from *in vitro* experiments in 3T3-L1 adipocytes it has been suggested that glucocorticoids could be responsible for the increase in *Atgl* levels in the fasted state (Villena *et al.,* 2004) and CLOCK/BMAL1 represses glucocorticoid receptor-induced transcriptional activity in a HAT-activity dependent fashion (Nader *et al*., 2009; Kino, 2012). Increased CLOCK/BMAL1 expression could therefore result in more glucocorticoid receptor repression, meaning glucocorticoids may not be able to result in increased *Atgl* expression in the fasted state in *Rev-erbα* knockout mice.

β-adrenergic receptor-stimulated lipolysis is impaired in obesity (Large *et al*., 1999). Adipocytes from obese subjects have lower levels of adenylyl cyclase activity under hormone-stimulated conditions when compared with adipocytes from non-obese controls (Martin *et al*., 1990) and alterations in the adrenergic signalling pathways may contribute to this effect. When this was assessed directly using CL316,243, a β_3 receptor agonist, to stimulate lipolysis in *Rev-erbα* knockout mice and littermate controls, a significant upregulation of *Atgl* was not observed in gWAT. This, however, may be expected due to the time-frame of tissue collection post CL316,243 administration. In a previous study, only a slight, but significant upregulation of *Atgl* was observed in gWAT when 1mg/kg of CL316,243 was administered once a day for 5 consecutive days (Buzelle *et al*., 2015). Interestingly, in scWAT, a pronounced upregulation of *Atgl* was observed in both genotypes after CL316,243 stimulation. In BAT, *Atgl* expression was also enhanced in littermate control mice, but not in *Rev-erbα* knockout mice, suggesting that the influence of REV-ERBα on *Atgl* regulation may be tissue and stimulus specific.

Direct stimulation of lipolysis using CL316,243 did, however, result in upregulation of *Hsl* in gWAT of both *Rev-erbα* knockout mice and littermate controls which contrasts to the results

obtained from fasted *Rev-erbα* knockout mice. This may suggest that the β-adrenergic stimulation is a potent regulator of *Hsl* expression. Post-translational modifications are important for the function of lipase enzymes, and they need to be phosphorylated in order for them to be hydrolytically active. Despite upregulation of *Hsl* mRNA being observed with CL316,243 stimulation in both genotypes, Western Blot analysis showed no increase in total HSL protein expression. However, significant upregulation of phosphorylated HSL at serine563 was observed in C57BL/6 control mice in response to 0.1 mg/kg CL316,243. This was also observed in *Rev-erbα* knockout mice but required a higher concentration of β-adrenergic agonist (1mg/kg) indicating a blunted in the response to this stimulation in these animals. This may relate to the increased adiposity of these animals, as obesity is associated with decreased lipolytic effect of catecholamines in adipose tissue (Large *et al*., 1999). Another possibility is dysfunction of the β_3-adrenoceptor or the β –adrenergic signalling pathways. It has been shown that in almost all animal models of obesity, the β –adrenergic signalling is impaired resulting in decreased ability to stimulate lipolysis or thermogenesis (Collins and Surwit, 2001) and the lack of lipolytic response to fasting in our *Rev-erbα* knockout mice is in-keeping with this.

We did not observe a difference in basal blood glucose levels in *Rev-erbα* knockout mice compared to control littermates. This contrasts with data obtained by Delezie *et al*., (2012), in which mild hyperglycaemia was observed. *Rev-erbα* knockout mice have normal whole-body insulin sensitivity when maintained on both NC and HFD and have an exacerbated response to insulin compared to C57BL/6 control animals. High levels of adiponectin and leptin in both chow and HFD-fed *Rev-erbα* knockout mice has been previously observed (Delezie *et al*., 2012; Hand *et al*., 2014) and it is possible that this contributes to heightened insulin sensitivity within these animals (Yamauchi *et al*., 2001). Insulin regulates energy homeostasis in a variety of ways, one of which is the stimulation of lipogenesis. Insulin also suppresses lipolysis through a signalling cascade involving, Akt, resulting in the inhibition of PKA (Choi *et al*., 2010). After *in vivo* insulin stimulation, *Dgat2* was upregulated in gWAT of control littermates but not in that of *Rev-erbα* knockout mice suggesting that despite normal insulin sensitivity observed with regards to blood glucose regulation, insulin may not be able to promote lipogenesis to the same extent in the knockout animals. Using adipose tissue explants allowed us to specifically assess insulin effects on adipose tissue, removing systemic influences over adipose tissue response. Our studies suggest that gWAT from *Rev-erbα* knockout mice may have enhanced adipose insulin sensitivity, with profound upregulation of both *Fasn* and *Dgat2* being observed. *Lpl* expression was reduced upon insulin stimulation of *Rev-erbα* explants but had no impact

on *Atgl* or *Hsl* expression, further supporting the influence of *Rev-erbα* on *Atgl/Hsl* regulation. Insulin therefore resulted in a pathway bias in *Rev-erbα* knockout explants, enhancing lipogenesis but having no effect on lipolysis. Although the expected response to insulin stimulation is observed in gWAT explants from *Adipo*^{CRE}*Bmal1*$^{flox\ /flox}$ mice (upregulation of lipogenic genes, downregulation of lipolytic genes), no difference in insulin response between the genotypes was present. Also the *in vivo* differences in basal levels of gene expression observed in these mice was not maintained in culture. This may be indicative that systemic factors also play a role in the regulation of metabolic genes in adipose tissue and once these are removed (i.e. in an *ex vivo* situation) the impact of clock loss is less severe.

In general, all insulin dependent responses were maintained in explants derived from HFD fed C57BL/6 control mice, but this was not the case for explant cultures derived from HFD-fed *Rev-erbα* knockout animals, which showed a strongly attenuated transcriptional response to insulin. This may be simply due to their profound adiposity than a genotypic effect. It is however important to note that in obesity, adipocyte hypertrophy occurs and the *Rev-erbα* knockout mice on both NC and HFD are an obese phenotype. This may potentially affect comparisons between the genotypes as larger adipocytes would result in a smaller number of adipocytes per explant, however, this is normalised for mRNA amount.

Global deletion of *Rev-erbα* has pronounced metabolic consequences. The *Rev-erbα* knockout is an obese phenotype with an increased propensity to obesity when faced with HFD-challenge. This can be attributed to a bias towards lipogenesis, with upregulation of *Fasn* observed and an increased susceptibility to insulin-driven upregulation of lipogenic genes in gWAT. On top of this, a defect in lipolysis is observed, with *Atgl* failing to respond normally to negative energy balance, direct β_3-adrenoceptor stimulation or insulin stimulation. Phosphorylation of *Hsl* after direct β_3-adrenoceptor stimulation is also impaired. However, many studies have demonstrated that long term or pronounced obesity is associated with an upregulation in lipolytic drive (Reynisdottir *et al* 1995; Ryden *et al*., 2002; Ryden *et al*., 2004). Despite the obese phenotype and increased susceptibility to weight gain by HFD-feeding of *Rev-erbα* knockout increased lipolytic drive is not observed. This may contribute to the decreased inflammation observed in these mice (Hand *et al*., 2014).

6.3 Adipocyte Specific loss of *Bmal1* causes attenuated feeding rhythms and severe lipid handling gene dysregulation

A further understanding of the role these specific clock components play in adipose physiology was obtained by tissue specific deletion of *Bmal1* and *Rev-erbα* from adipose tissue. Deletion of *Bmal1* renders adipose tissue arrhythmic and results in the profound attenuation of *Rev-erbα* expression (Bunger *et al.,* 2000). *Bmal1* null mice have a higher body weight and greater adipose tissue mass compared to littermate controls (Bunger *et al*., 2005; Lamia *et al*., 2008). Although *Rev-erbα* reinforces the robustness of circadian oscillations, circadian rhythm generation persists in its absence (Preitner *et al*., 2002) and therefore adipose tissue of *Rev-erbα*$^{-/-}$ mice maintain clock functionality, but with a decreased amplitude. *Adipo*^{CRE}*Bmal1*$^{flox/flox}$ mice exhibited no differences in body weight compared to control littermates with only very subtle changes in adiposity. This contrasts to the global *Bmal1* knockout mouse, which, although they had normal body weight by young adulthood, they gained weight more rapidly than littermate controls between weeks 4-8 and have a higher body fat content (Lamia *et al*., 2008). The slight increase in adiposity in *Adipo*^{CRE}*Bmal1*$^{flox/flox}$ and global *Bmal1* knockout mice is interesting as *Bmal1* has been shown to have a positive influence on adipocyte differentiation and BMAL1 in adipocytes increased lipid synthesis activity (Shimba *et al*., 2005) and therefore it may be expected that loss of *Bmal1* would result in a lower body weight. Bunger *et al. (*2005) did, however, show that despite at 12 weeks there being no difference in body weight, past 20 weeks of age progressive weight loss was observed. Even when challenged with a positive energy balance *Adipo*^{CRE}*Bmal1*$^{flox/flox}$ mice did not exhibit an increased propensity for weight gain. This contrasts work undertook by Paschos *et al*. (2012) who showed that *Bmal1* specific deletion from adipocytes using the adipocyte protein 2 (aP2) driver, which is also expressed in macrophages resulted in increased body weight on both NC and HFD. In keeping with our work, their studies on adipocyte specific *Bmal1* knockout mice using the adiponectin driver, the same as our studies, showed that these mice did not have a higher body weight on NC, but they did however on HFD and had increased adiposity. Mice in our study were maintained on HFD from 8 weeks of age, whereas in the experiment conducted by Paschos *et al*. (2012) they were subjected to HFD from 6 weeks of age, which may be the basis for the difference observed. Cell number expansion in adipose tissue does not reach a plateu until 6-10 weeks of age in rodents and during 3-6 weeks of age there is a dramatic increase in the accumulation of adipose tissue in mice (Johnson *et al.*, 1978). Therefore, commencing a HFD challenge before the plateu of cell number expansion has been achieved may result in exacerbated fat accumulation. Strikingly, *Adipo*^{CRE}*Rev-erbα*$^{flox/flox}$ mice also showed no changes in body weight, which was in stark contrast to our studies of the global knockout mouse (Chapter 4) and work carried out by others (Delezie *et al*., 2012). Even when

challenged with HFD no difference in body weight was observed between *Adipo*^{CRE}*Rev-erbα*$^{flox/flox}$ mice and littermate controls. This may highlight that the metabolic phenotype caused by global *Rev-erbα* knockout mouse is not due specifically to clock manipulation in adipose tissue but loss of function at other sites, for example in the brain, where feeding in controlled. Energy expenditure in *Adipo*^{CRE}*Bmal1*$^{flox/flox}$ and *Adipo*^{CRE}*Rev-erbα*$^{flox/flox}$ mice was similar to littermate controls. Global *Bmal1*$^{-/-}$ mice do not have detectable daily rhythms of locomotor activity or feeding behaviour in constant darkness or under a light–dark cycle and instead display ultradian behaviour (Lamia *et al*., 2008). This, along with our adipocyte specific *Bmal1*$^{-/-}$ mouse model displaying the same circadian rhythms in energy expenditure highlights the specificity of the knockouts and the importance of a functional clock in the SCN to coordinate locomotor and metabolic processes. However, the loss of feeding rhythms in *Adipo*^{CRE}*Bmal1*$^{flox/flox}$ mice highlights the importance of the cross-talk between adipose tissue and the SCN. Global *Rev-erbα*$^{-/-}$ mice have been shown to maintain physiological rhythms albeit with a shortened period length which is shorter than control littermates (Preitner *et al*., 2002). No difference in the rhythms of energy expenditure were observed in our *Adipo*^{CRE}*Rev-erbα*$^{flox/flox}$ mice.

No difference was observed in the fasting responses, with regards to temperature regulation and energy expenditure, of *Adipo*^{CRE}*Bmal1*$^{flox/flox}$ and *Adipo*^{CRE}*Rev-erbα*$^{flox/flox}$ mice. Paschos *et al*. (2012) showed that there were no differences in the expression of *Ucp1* or *Pgc-1α* in their targeted *Bmal1* knockouts, which encode key regulators of thermogenesis, in BAT and WAT both in the fed and fasted states. To further support this, there was not a differential response to cold challenge in our *Adipo*^{CRE}*Bmal1*$^{flox/flox}$ mice compared to control littermate which makes compromised thermogenesis in BAT unlikely in these animals. However, previous work has demonstrated that loss of *Rev-erbα* in mice markedly improves cold tolerance (Gerhart-Hines *et al*., 2013) and this was said to be because of the thermogenic regulation that *Rev-erbα* elicits through the active repression of the *Ucp1* gene specifically in BAT and therefore loss of this repression results in increased expression of *Ucp1*. However, in *Adipo*^{CRE}*Bmal1*$^{flox/flox}$ mice *Rev-erbα* expression is also low and therefore in *Rev-erbα* knockout mice it may be high levels of *Bmal1* expression that alter thermogenic regulation, possiblly through changes in the autonomic nervous system.

Lipolysis in WAT releases energy stored in adipocytes. Through this, adipocytes are able to signal the amount of stored energy to the hypothalamus, which is a key input to the centres responsible for energy homeostasis. Alterations in feeding activity, with is a centrally mediated

behaviour, are observed in *Adipo*^{CRE}*Bmal1*$^{flox\ /flox}$ mice, with attenuated day/night rhythms which indicates feedback from the peripheral clock to the central nervous system. Lipidomic analysis in humans has revealed that that a reduction of the amount of polyunsaturated fatty acids in the lipodome is associated with obesity (Pietiläinen *et al*., 2011) and therefore it is possible that the remodelling of the triglyceride pool of the adipocyte by *Bmal1* deletion, leads to attenuated feeding rhythms. In our DIO model, attenuated feeding rhythms were also observed, with a decrease in night-time feeding. However, in the super obese *Rev-erbα* knockout mice on HFD, feeding rhythms were somewhat amplified. Lipolytic enzymes such as *Lpl, Atgl and Hsl* are profoundly downregulated in gWAT from *Adipo*^{CRE}*Bmal1*$^{flox\ /flox}$ mice which may be partially responsible for the attenuation of feeding rhythms, explaining how the adipocyte circadian clock can have a direct effect of hypothalamic feeding centres. This work is paralleled by Paschos *et al*. (2012) who showed that disruption of the adipocyte circadian clock resulted in temporal changes in polyunsaturated fatty acids in plasma which led to corresponding changes in the expression of neurotransmitters responsible for appetite regulation in the hypothalamus, e.g. Agrp and Npy. Lower levels of *Atgl* and *Hsl* expression in *Adipo*^{CRE}*Bmal1*$^{flox\ /flox}$ mice, however, contrasts this study, in which they demonstrated normal levels of expression and therefore suggested there was no alteration in lipolysis within the adipocytes. The adiponectin driver is more adipose tissue specific as it is not expressed in macrophages and therefore the difference observed could be due to the specificity of our adipocyte knockout. Decreased expression of *Atgl* and *Hsl* is logical as reporter gene and ChIP assays indicate that the CLOCK/BMAL1 heterodimer binds to E-boxes in the promoters of *Atgl* and *Hsl*, directly regulating their transcription, and therefore loss of *Bmal1* would result in diminished transcription (Shostak *et al*., 2012).

Interestingly, although severe dysregulation of lipid handling genes is observed in gWAT from both global *Rev-erbα* knockout mice and *Adipo*^{CRE}*Bmal1*$^{flox\ /flox}$ mice, this is not observed in *Adipo*^{CRE}*Rev-erbα*$^{flox/flox}$ mice. This is perhaps most surprising in the case of *Lpl.* An E-box has been found in the mouse *Lpl* promoter (Bey *et al*., 1998) and therefore it is likely that instead of a direct repression by REV-ERBα, activation by CLOCK/BMAL1 could drive the temporal expression of the *Lpl* gene. REV-ERBα expression is crucial for the transcriptional control of *Clock* and *Bmal1*. In the absence of *Rev-erbα*, *Clock* and *Bmal1* mRNA are overexpressed which can affect the expression of CLOCK/BMAL1 target genes. It was shown by Delezie *et al.* (2012) that *Lpl* expression can be elicited by CLOCK alone. Clock control requires *Rev-erbα* to bind directly to the genome at its cognate sites, where it competes with activating ROR transcription factors. Conversely, *Rev-erbα* regulates metabolic genes primarily by recruiting

the HDAC3 corepressor to sites which it is tethered by cell-type specific transcription factors. Therefore, direct competition between *Rev-erbα* and *Ror* is responsible for the control of the molecular clock across all tissues, but circadianly expressed *Rev-erbα* uses lineage determination factors such as hepatocyte nuclear factor 6 (HNF6) to convey a tissue specific rhythm, through NCoR and HDAC3, regulating the metabolic needs specific to that tissue. This therefore suggests that the role of *Rev-erbα* in adipose centres on non-DBD dependent actions, and therefore not via RORE elements. After completion of our studies, Zhang *et al* (2015) reported that the Rev-erbα^{flox} model was actually a knock-in of a DBD mutation rather than a complete knockout of *Rev-erbα* and therefore full-length REV-ERBα is still produced, lacking its DBD domain., which may explain why many of the parameters such as body weight, fasting response, gene expression that we measured in these mice showed no difference to littermate controls, contrasting with data obtained from global *Rev-erbα* knockouts. Therefore, *Adipo^{CRE}Bmal1$^{flox/flox}$* mice and *Adipo^{CRE}Rev-erbα$^{flox/flox}$* mice may show such a stark contrast in phenotype compared to global *Rev-erbα* knockout mice, despite both having low *Rev-erbα* expression in adipose tissue because of the differential role of *Rev-erbα* specifically in this tissue.

6.4 Conclusion

Our work highlights the reciprocal coupling between energy metabolism and circadian rhythmicity. Our studies contribute to the growing evidence that the clockwork is compromised during obesity. Obesity results in desynchrony and pronounced disruption of the circadian clockwork in visceral WAT. This was shown to be due to the increased adiposity of the animals and not due to altered nutritional input (i.e. acute consumption of HFD) as the attenuated clock gene rhythms were associated with chronic HFD feeding and dysregulation of PPARα/γ. Further, more in depth analysis of the temporal changes caused by nutrient excess may provide insight into the progression of diseases such as obesity and diabetes. This work shows that the nuclear receptor *Rev-erbα* is particularly affected by DIO. *Rev-erbα* has previously been shown to fine-tune metabolic pathways by modulating SREBP target genes and recruiting the HDAC3-repressive complex to genes involved in lipid metabolism, thereby providing rhythmic fluctuation in lipid homeostasis (Le Martelot *et al*., 2009; Feng *et al*., 2011). Our results demonstrate that *in vivo* deletion of *Rev-erbα* results in profound metabolic changes, with increased adiposity, lack of lipolysis and enhanced insulin sensitivity. Our data

highlight that *Rev-erbα* plays an important role in the regulation of lipolysis, specifically in the regulation of *Atgl*, *Lpl* and the activation of HSL. Interestingly, our observations suggest that *Rev-erbα* differentially modulates the expression of these genes under basal conditions as well as in response to metabolic challenge. For example, in the *Rev-erbα*$^{-/-}$ mice *Atgl* expression was not profoundly altered under basal condition, yet we observed a profound attenuation in the responsiveness of *Atgl* expression to altered metabolic state (e.g. fasting, HFD). In contrast, constitutive expression of *Lpl* was increased in the *Rev-erbα*$^{-/-}$ mice, yet *Lpl* expression exhibited a normal response to energy challenge.

Mice lacking *Rev-erbα*, despite being an obese phenotype, maintain insulin sensitivity, which may be an indication of 'safe', i.e. not ectopic fat storage in these mice. This may be due to dysregulation of *Atgl* and HSL, resulting in less fatty acid liberation from adipose tissue. In turn, this results in less accumulation of fatty acids in tissues such as liver and skeletal muscle, causing less lipotoxicity and insulin resistance usually associated with obesity. *In vivo* administration of synthetic REV-ERBα agonists have positive effects on lipid and glucose oxidation. These drugs are also effective in reducing lipogenesis and protecting mice from HFD (Solt *et al*., 2012). *Rev-erbα* may therefore be an attractive pharmacological target to confer metabolic benefit. However, loss of *Rev-erbα* specifically in adipocytes of mice does not result in metabolic dysfunction, which may suggest that *Rev-erbα* exerts its main control on lipid metabolism and physiology in tissues distinct to adipose tissue. *Rev-erbα* may play an important role in energy homeostasis by its action in the brain, as hyperphagia is observed in *Rev-erbα*$^{-/-}$ mice on HFD as well as a decreased response to fasting in terms of temperature and metabolic rate. Nutrient-sensitive hypothalamic neurons regulate energy balance and glucose homeostasis and these neurons may become compromised in *Rev-erbα*$^{-/-}$ mice. Complete ablation of the clock specifically in adipocytes of mice by *Bmal1* deletion resulted in an attenuation in feeding rhythm. This is most likely through altered lipolysis in adipose tissue as energy released from lipolysis signals the amount of stored energy to the hypothalamus. This highlights the potential of a peripheral clock to feedback on to the central nervous system.

Taken together, this study shows that *Rev-erbα* and *Bmal1* shape energy homeostasis in a number of ways and across many organ systems (Figure 6.1). *Bmal1* and *Rev-erbα* have a strong influence over *Fasn* highlighting the role the circadian clock plays a pivotal role in *de novo* lipogenesis. Global loss of *Rev-erbα* also results in enhanced insulin sensitivity and insulin-induced *Fasn* expression, therefore increased lipogenesis. However, lipolytic pathways were also strongly influenced by loss of *Rev-erbα* and/or *Bmal1.* Increased action of the

lipolytic pathway, however, results in alterations in energy sensing and feeding in these mice. *Rev-erbα* plays a vital role in the regulation of lipolysis, and loss of *Rev-erbα* results in dysregulation of triglyceride breakdown, potentiating the increased fat storage observed in these mice. An intact circadian clock appears to be vital in the maintenance of energy homeostasis throughout the body. Our work goes to reinforce the circadian clock as a novel avenue which could potentially be pharmacologically targeted to achieve benefit in metabolic diseases.

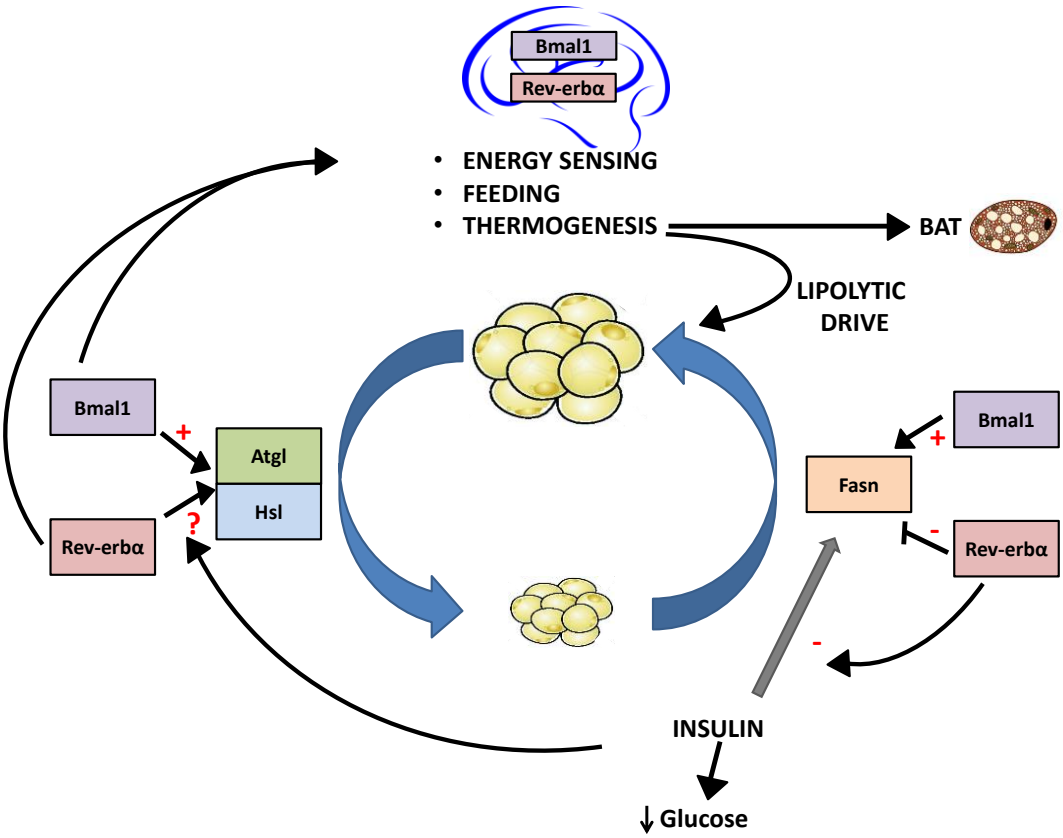

Figure 6.1 - Summary of *Bmal1* and *Rev-erbα* action on energy homeostasis
Both *Bmal1* and *Rev-erbα* are involved in the maintanence of energy balance, playing a role in the regulation of lipogenesis (*Fasn*) and lipolysis (*Atgl/Hsl*). *Bmal1* and *Rev-erbα* are also involved in energy sensing in the brain and feeding behaviour. Disruption of either of these genes results in metabolic dysfunction, highlighting the importance of the circadian clock in energy homeostasis.

References

Abumrad, N. A., M. R. el-Maghrabi, E. Z. Amri, E. Lopez and P. A. Grimaldi (1993). "Cloning of a rat adipocyte membrane protein implicated in binding or transport of long-chain fatty acids that is induced during preadipocyte differentiation. Homology with human CD36." J Biol Chem 268(24): 17665-17668.

Adamovich, Y., L. Rousso-Noori, Z. Zwighaft, A. Neufeld-Cohen, M. Golik, J. Kraut-Cohen, M. Wang, X. Han and G. Asher (2014). "Circadian clocks and feeding time regulate the oscillations and levels of hepatic triglycerides." Cell Metab 19(2): 319-330.

Ahmadian, M., R. E. Duncan, K. Jaworski, E. Sarkadi-Nagy and H. S. Sul (2007). "Triacylglycerol metabolism in adipose tissue." Future Lipidol 2(2): 229-237.

Akashi, M., Y. Tsuchiya, T. Yoshino and E. Nishida (2002). "Control of intracellular dynamics of mammalian period proteins by casein kinase I epsilon (CKIepsilon) and CKIdelta in cultured cells." Mol Cell Biol 22(6): 1693-1703.

Akhtar, R. A., A. B. Reddy, E. S. Maywood, J. D. Clayton, V. M. King, A. G. Smith, T. W. Gant, M. H. Hastings and C. P. Kyriacou (2002). "Circadian cycling of the mouse liver transcriptome, as revealed by cDNA microarray, is driven by the suprachiasmatic nucleus." Curr Biol 12(7): 540-550.

Alenghat, T., K. Meyers, S. E. Mullican, K. Leitner, A. Adeniji-Adele, J. Avila, M. Bucan, R. S. Ahima, K. H. Kaestner and M. A. Lazar (2008). "Nuclear receptor corepressor and histone deacetylase 3 govern circadian metabolic physiology." Nature 456(7224): 997-1000.

Alhadeff, A. L., L. E. Rupprecht and M. R. Hayes (2012). "GLP-1 neurons in the nucleus of the solitary tract project directly to the ventral tegmental area and nucleus accumbens to control for food intake." Endocrinology 153(2): 647-658.

Ali, Y. B., F. Carriere, R. Verger, S. Petry, G. Muller and A. Abousalham (2005). "Continuous monitoring of cholesterol oleate hydrolysis by hormone-sensitive lipase and other cholesterol esterases." J Lipid Res 46(5): 994-1000.

Allison, K. C., S. J. Crow, R. R. Reeves, D. S. West, J. P. Foreyt, V. G. Dilillo, T. A. Wadden, R. W. Jeffery, B. Van Dorsten and A. J. Stunkard (2007). "Binge eating disorder and night eating syndrome in adults with type 2 diabetes." Obesity (Silver Spring) 15(5): 1287-1293.

Altarejos, J. Y. and M. Montminy (2011). "CREB and the CRTC co-activators: sensors for hormonal and metabolic signals." Nat Rev Mol Cell Biol 12(3): 141-151.

Andersson, U., K. Filipsson, C. R. Abbott, A. Woods, K. Smith, S. R. Bloom, D. Carling and C. J. Small (2004). "AMP-activated protein kinase plays a role in the control of food intake." J Biol Chem 279(13): 12005-12008.

Ando, H., M. Kumazaki, Y. Motosugi, K. Ushijima, T. Maekawa, E. Ishikawa and A. Fujimura (2011). "Impairment of peripheral circadian clocks precedes metabolic abnormalities in ob/ob mice." Endocrinology 152(4): 1347-1354.

Ando, H., H. Yanagihara, Y. Hayashi, Y. Obi, S. Tsuruoka, T. Takamura, S. Kaneko and A. Fujimura (2005). "Rhythmic messenger ribonucleic acid expression of clock genes and adipocytokines in mouse visceral adipose tissue." Endocrinology 146(12): 5631-5636.

Anea, C. B., M. Zhang, D. W. Stepp, G. B. Simkins, G. Reed, D. J. Fulton and R. D. Rudic (2009). "Vascular disease in mice with a dysfunctional circadian clock." Circulation 119(11): 1510-1517.

Antin, J., J. Gibbs, J. Holt, R. C. Young and G. P. Smith (1975). "Cholecystokinin elicits the complete behavioral sequence of satiety in rats." J Comp Physiol Psychol 89(7): 784-790.

Antoch, M. P., E. J. Song, A. M. Chang, M. H. Vitaterna, Y. Zhao, L. D. Wilsbacher, A. M. Sangoram, D. P. King, L. H. Pinto and J. S. Takahashi (1997). "Functional identification of the mouse circadian Clock gene by transgenic BAC rescue." Cell 89(4): 655-667.

Anzulovich, A., A. Mir, M. Brewer, G. Ferreyra, C. Vinson and R. Baler (2006). "Elovl3: a model gene to dissect homeostatic links between the circadian clock and nutritional status." J Lipid Res 47(12): 2690-2700.

Aponte, Y., D. Atasoy and S. M. Sternson (2011). "AGRP neurons are sufficient to orchestrate feeding behavior rapidly and without training." Nat Neurosci 14(3): 351-355.

Arble, D. M., J. Bass, A. D. Laposky, M. H. Vitaterna and F. W. Turek (2009). "Circadian timing of food intake contributes to weight gain." Obesity (Silver Spring) 17(11): 2100-2102.

Arita, Y., S. Kihara, N. Ouchi, M. Takahashi, K. Maeda, J. Miyagawa, K. Hotta, I. Shimomura, T. Nakamura, K. Miyaoka, H. Kuriyama, M. Nishida, S. Yamashita, K. Okubo, K. Matsubara, M. Muraguchi, Y. Ohmoto, T. Funahashi and Y. Matsuzawa (1999). "Paradoxical decrease of an adipose-specific protein, adiponectin, in obesity." Biochem Biophys Res Commun 257(1): 79-83.

Asterholm, I. W. and P. E. Scherer (2010). "Enhanced metabolic flexibility associated with elevated adiponectin levels." Am J Pathol 176(3): 1364-1376.

Astrup, A., J. Bulow, J. Madsen and N. J. Christensen (1985). "Contribution of BAT and skeletal muscle to thermogenesis induced by ephedrine in man." Am J Physiol 248(5 Pt 1): E507-515.

Atkinson, G., B. Edwards, T. Reilly and J. Waterhouse (2007). "Exercise as a synchroniser of human circadian rhythms: an update and discussion of the methodological problems." Eur J Appl Physiol 99(4): 331-341.

Aton, S. J. and E. D. Herzog (2005). "Come together, right...now: synchronization of rhythms in a mammalian circadian clock." Neuron 48(4): 531-534.

Back, P., B. Hamprecht and F. Lynen (1969). "Regulation of cholesterol biosynthesis in rat liver: diurnal changes of activity and influence of bile acids." Arch Biochem Biophys 133(1): 11-21.

Bado, A., S. Levasseur, S. Attoub, S. Kermorgant, J. P. Laigneau, M. N. Bortoluzzi, L. Moizo, T. Lehy, M. Guerre-Millo, Y. Le Marchand-Brustel and M. J. Lewin (1998). "The stomach is a source of leptin." Nature 394(6695): 790-793.

Bae, K., X. Jin, E. S. Maywood, M. H. Hastings, S. M. Reppert and D. R. Weaver (2001). "Differential functions of mPer1, mPer2, and mPer3 in the SCN circadian clock." Neuron 30(2): 525-536.

Bahr, I., E. Muhlbauer, H. Schucht and E. Peschke (2011). "Melatonin stimulates glucagon secretion in vitro and in vivo." J Pineal Res 50(3): 336-344.

Balsalobre, A., S. A. Brown, L. Marcacci, F. Tronche, C. Kellendonk, H. M. Reichardt, G. Schutz and U. Schibler (2000). "Resetting of circadian time in peripheral tissues by glucocorticoid signaling." Science 289(5488): 2344-2347.

Balsalobre, A., F. Damiola and U. Schibler (1998). "A serum shock induces circadian gene expression in mammalian tissue culture cells." Cell 93(6): 929-937.

Barbadoro, P., L. Santarelli, N. Croce, M. Bracci, D. Vincitorio, E. Prospero and A. Minelli (2013). "Rotating shift-work as an independent risk factor for overweight Italian workers: a cross-sectional study." PLoS One 8(5): e63289.

Barbera, M. J., A. Schluter, N. Pedraza, R. Iglesias, F. Villarroya and M. Giralt (2001). "Peroxisome proliferator-activated receptor alpha activates transcription of the brown fat uncoupling protein-1 gene. A link between regulation of the thermogenic and lipid oxidation pathways in the brown fat cell." J Biol Chem 276(2): 1486-1493.

Barish, G. D., V. A. Narkar and R. M. Evans (2006). "PPAR delta: a dagger in the heart of the metabolic syndrome." J Clin Invest 116(3): 590-597.

Barsh, G. S., I. S. Farooqi and S. O'Rahilly (2000). "Genetics of body-weight regulation." Nature 404(6778): 644-651.

Bassareo, V. and G. Di Chiara (1999). "Modulation of feeding-induced activation of mesolimbic dopamine transmission by appetitive stimuli and its relation to motivational state." Eur J Neurosci 11(12): 4389-4397.

Behall, K. M. and J. C. Howe (1995). "Contribution of fiber and resistant starch to metabolizable energy." Am J Clin Nutr 62(5 Suppl): 1158S-1160S.

Belgardt, B. F. and J. C. Bruning (2010). "CNS leptin and insulin action in the control of energy homeostasis." Ann N Y Acad Sci 1212: 97-113.

Bell-Pedersen, D., V. M. Cassone, D. J. Earnest, S. S. Golden, P. E. Hardin, T. L. Thomas and M. J. Zoran (2005). "Circadian rhythms from multiple oscillators: lessons from diverse organisms." Nat Rev Genet 6(7): 544-556.

Berg, J. M., Tymoczko, J. L. and Stryer L. (2002). *Biochemistry.* 5th ed. New York: W H Freeman.

Berglund, E. D., R. S. Lee-Young, D. G. Lustig, S. E. Lynes, E. P. Donahue, R. C. Camacho, M. E. Meredith, M. A. Magnuson, M. J. Charron and D. H. Wasserman (2009). "Hepatic energy state is regulated by glucagon receptor signaling in mice." J Clin Invest 119(8): 2412-2422.

Bernlohr, D. A., Jenkins, A. E. & Bennaars, A. A. (2002). *New Comprehensive Biochemistry.* vol. 36, pp. 263-289.

Bertrand, R. L., S. Senadheera, I. Markus, L. Liu, L. Howitt, H. Chen, T. V. Murphy, S. L. Sandow and P. P. Bertrand (2011). "A Western diet increases serotonin availability in rat small intestine." Endocrinology 152(1): 36-47.

Bessesen, D. H., A. D. Robertson and R. H. Eckel (1991). "Weight reduction increases adipose but decreases cardiac LPL in reduced-obese Zucker rats." Am J Physiol 261(2 Pt 1): E246-251.

Bey, L., J. Etienne, C. Tse, D. Brault, L. Noe, A. Raisonnier, F. Arnault, M. T. Hamilton and F. Galibert (1998). "Cloning, sequencing and structural analysis of 976 base pairs of the promoter sequence for the rat lipoprotein lipase gene. Comparison with the mouse and human sequences." Gene 209(1-2): 31-38.

Bhargava, A., H. Herzel and B. Ananthasubramaniam (2015). "Mining for novel candidate clock genes in the circadian regulatory network." BMC Syst Biol 9: 78.

Biddinger, S. B., K. Almind, M. Miyazaki, E. Kokkotou, J. M. Ntambi and C. R. Kahn (2005). "Effects of diet and genetic background on sterol regulatory element-binding protein-1c, stearoyl-CoA desaturase 1, and the development of the metabolic syndrome." Diabetes 54(5): 1314-1323.

Block, B. A. (1994). "Thermogenesis in muscle." Annu Rev Physiol 56: 535-577.

Bodosi, B., J. Gardi, I. Hajdu, E. Szentirmai, F. Obal, Jr. and J. M. Krueger (2004). "Rhythms of ghrelin, leptin, and sleep in rats: effects of the normal diurnal cycle, restricted feeding, and sleep deprivation." Am J Physiol Regul Integr Comp Physiol 287(5): R1071-1079.

Bolli, G. B., P. De Feo, S. De Cosmo, G. Perriello, M. M. Ventura, F. Calcinaro, C. Lolli, P. Campbell, P. Brunetti and J. E. Gerich (1984). "Demonstration of a dawn phenomenon in normal human volunteers." Diabetes 33(12): 1150-1153.

Bonnelye, E., J. M. Vanacker, X. Desbiens, A. Begue, D. Stehelin and V. Laudet (1994). "Rev-erb beta, a new member of the nuclear receptor superfamily, is expressed in the nervous system during chicken development." Cell Growth Differ 5(12): 1357-1365.

Bonnet, M. H. and D. L. Arand (1995). "We are chronically sleep deprived." Sleep 18(10): 908-911.

Borgland, S. L., M. A. Ungless and A. Bonci (2010). "Convergent actions of orexin/hypocretin and CRF on dopamine neurons: Emerging players in addiction." Brain Res 1314: 139-144.

Boss, O., S. Samec, F. Kuhne, P. Bijlenga, F. Assimacopoulos-Jeannet, J. Seydoux, J. P. Giacobino and P. Muzzin (1998). "Uncoupling protein-3 expression in rodent skeletal muscle is modulated by food intake but not by changes in environmental temperature." J Biol Chem 273(1): 5-8.

Branson, R. D. and J. A. Johannigman (2004). "The measurement of energy expenditure." Nutr Clin Pract 19(6): 622-636.

Brasaemle, D. L., G. Dolios, L. Shapiro and R. Wang (2004). "Proteomic analysis of proteins associated with lipid droplets of basal and lipolytically stimulated 3T3-L1 adipocytes." J Biol Chem 279(45): 46835-46842.

Bray, G. A., B. J. Whipp and S. N. Koyal (1974). "The acute effects of food intake on energy expenditure during cycle ergometry." Am J Clin Nutr 27(3): 254-259.

Bray, M. S. and M. E. Young (2007). "Circadian rhythms in the development of obesity: potential role for the circadian clock within the adipocyte." Obes Rev 8(2): 169-181.

Brody, S. (1945). *Bioenergetics and Growth*. New York: Reinhold Publishing Corporation.

Brown, J. E., A. C. Conner, J. E. Digby, K. L. Ward, M. Ramanjaneya, H. S. Randeva and S. J. Dunmore (2010). "Regulation of beta-cell viability and gene expression by distinct agonist fragments of adiponectin." Peptides 31(5): 944-949.

Brown, L. M., D. J. Clegg, S. C. Benoit and S. C. Woods (2006). "Intraventricular insulin and leptin reduce food intake and body weight in C57BL/6J mice." Physiol Behav 89(5): 687-691.

Brown, S. A., E. Kowalska and R. Dallmann (2012). "(Re)inventing the circadian feedback loop." Dev Cell 22(3): 477-487.

Bruning, J. C., D. Gautam, D. J. Burks, J. Gillette, M. Schubert, P. C. Orban, R. Klein, W. Krone, D. Muller-Wieland and C. R. Kahn (2000). "Role of brain insulin receptor in control of body weight and reproduction." Science 289(5487): 2122-2125.

Bugge, A., D. Feng, L. J. Everett, E. R. Briggs, S. E. Mullican, F. Wang, J. Jager and M. A. Lazar (2012). "Rev-erbalpha and Rev-erbbeta coordinately protect the circadian clock and normal metabolic function." Genes Dev 26(7): 657-667.

Buhman, K. F., M. Accad and R. V. Farese (2000). "Mammalian acyl-CoA:cholesterol acyltransferases." Biochim Biophys Acta 1529(1-3): 142-154.

Buijs, R. M., J. Wortel and Y. X. Hou (1995). "Colocalization of gamma-aminobutyric acid with vasopressin, vasoactive intestinal peptide, and somatostatin in the rat suprachiasmatic nucleus." J Comp Neurol 358(3): 343-352.

Buijs, R. M., J. Wortel, J. J. Van Heerikhuize, M. G. Feenstra, G. J. Ter Horst, H. J. Romijn and A. Kalsbeek (1999). "Anatomical and functional demonstration of a multisynaptic suprachiasmatic nucleus adrenal (cortex) pathway." Eur J Neurosci 11(5): 1535-1544.

Bunger, M. K., J. A. Walisser, R. Sullivan, P. A. Manley, S. M. Moran, V. L. Kalscheur, R. J. Colman and C. A. Bradfield (2005). "Progressive arthropathy in mice with a targeted disruption of the Mop3/Bmal-1 locus." Genesis 41(3): 122-132.

Bunger, M. K., L. D. Wilsbacher, S. M. Moran, C. Clendenin, L. A. Radcliffe, J. B. Hogenesch, M. C. Simon, J. S. Takahashi and C. A. Bradfield (2000). "Mop3 is an essential component of the master circadian pacemaker in mammals." Cell 103(7): 1009-1017.

Burks, D. J., J. Font de Mora, M. Schubert, D. J. Withers, M. G. Myers, H. H. Towery, S. L. Altamuro, C. L. Flint and M. F. White (2000). "IRS-2 pathways integrate female reproduction and energy homeostasis." Nature 407(6802): 377-382.

Butler, A. A. and R. D. Cone (2001). "Knockout models resulting in the development of obesity." Trends Genet 17(10): S50-54.

Buzelle, S. L., R. E. MacPherson, W. T. Peppler, L. Castellani and D. C. Wright (2015). "The contribution of IL-6 to beta 3 adrenergic receptor mediated adipose tissue remodeling." Physiol Rep 3(2).

Byku, M. and R. L. Gannon (2000). "Opioid induced non-photic phase shifts of hamster circadian activity rhythms." Brain Res 873(2): 189-196.

Cailotto, C., J. Lei, J. van der Vliet, C. van Heijningen, C. G. van Eden, A. Kalsbeek, P. Pevet and R. M. Buijs (2009). "Effects of nocturnal light on (clock) gene expression in peripheral organs: a role for the autonomic innervation of the liver." PLoS One 4(5): e5650.

Campos, H., C. Khoo and F. M. Sacks (2005). "Diurnal and acute patterns of postprandial apolipoprotein B-48 in VLDL, IDL, and LDL from normolipidemic humans." Atherosclerosis 181(2): 345-351.

Campos, H., D. Perlov, C. Khoo and F. M. Sacks (2001). "Distinct patterns of lipoproteins with apoB defined by presence of apoE or apoC-III in hypercholesterolemia and hypertriglyceridemia." J Lipid Res 42(8): 1239-1249.

Canaple, L., J. Rambaud, O. Dkhissi-Benyahya, B. Rayet, N. S. Tan, L. Michalik, F. Delaunay, W. Wahli and V. Laudet (2006). "Reciprocal regulation of brain and muscle Arnt-like protein 1 and

peroxisome proliferator-activated receptor alpha defines a novel positive feedback loop in the rodent liver circadian clock." Mol Endocrinol 20(8): 1715-1727.

Cannon, B. and J. Nedergaard (2004). "Brown adipose tissue: function and physiological significance." Physiol Rev 84(1): 277-359.

Cannon, B. and J. Nedergaard (2009). "Thermogenesis challenges the adipostat hypothesis for body-weight control." Proc Nutr Soc 68(4): 401-407.

Cannon, B. and J. Nedergaard (2010). "Metabolic consequences of the presence or absence of the thermogenic capacity of brown adipose tissue in mice (and probably in humans)." Int J Obes (Lond) 34 Suppl 1: S7-16.

Canto, C., Z. Gerhart-Hines, J. N. Feige, M. Lagouge, L. Noriega, J. C. Milne, P. J. Elliott, P. Puigserver and J. Auwerx (2009). "AMPK regulates energy expenditure by modulating NAD+ metabolism and SIRT1 activity." Nature 458(7241): 1056-1060.

Cao, W., K. W. Daniel, J. Robidoux, P. Puigserver, A. V. Medvedev, X. Bai, L. M. Floering, B. M. Spiegelman and S. Collins (2004). "p38 mitogen-activated protein kinase is the central regulator of cyclic AMP-dependent transcription of the brown fat uncoupling protein 1 gene." Mol Cell Biol 24(7): 3057-3067.

Carey, M. C., D. M. Small, et al. (1983). "Lipid digestion and absorption." Annu Rev Physiol 45: 651-677.

Caro, J. F., J. W. Kolaczynski, M. R. Nyce, J. P. Ohannesian, I. Opentanova, W. H. Goldman, R. B. Lynn, P. L. Zhang, M. K. Sinha and R. V. Considine (1996). "Decreased cerebrospinal-fluid/serum leptin ratio in obesity: a possible mechanism for leptin resistance." Lancet 348(9021): 159-161.

Carpenter, W. H., E. T. Poehlman, M. O'Connell and M. I. Goran (1995). "Influence of body composition and resting metabolic rate on variation in total energy expenditure: a meta-analysis." Am J Clin Nutr 61(1): 4-10.

Casiraghi, L. P., A. Alzamendi, A. Giovambattista, J. J. Chiesa and D. A. Golombek (2016). "Effects of chronic forced circadian desynchronization on body weight and metabolism in male mice." Physiol Rep 4(8).

Caspersen, C. J., K. E. Powell and G. M. Christenson (1985). "Physical activity, exercise, and physical fitness: definitions and distinctions for health-related research." Public Health Rep 100(2): 126-131.

Castanon-Cervantes, O., M. Wu, J. C. Ehlen, K. Paul, K. L. Gamble, R. L. Johnson, R. C. Besing, M. Menaker, A. T. Gewirtz and A. J. Davidson (2010). "Dysregulation of inflammatory responses by chronic circadian disruption." J Immunol 185(10): 5796-5805.

Castel, M. and J. F. Morris (2000). "Morphological heterogeneity of the GABAergic network in the suprachiasmatic nucleus, the brain's circadian pacemaker." J Anat 196 (Pt 1): 1-13.

Cermakian, N., S. Westfall and S. Kiessling (2014). "Circadian clocks and inflammation: reciprocal regulation and shared mediators." Arch Immunol Ther Exp (Warsz) 62(4): 303-318.

Chakravarty, K., H. Cassuto, L. Reshef and R. W. Hanson (2005). "Factors that control the tissue-specific transcription of the gene for phosphoenolpyruvate carboxykinase-C." Crit Rev Biochem Mol Biol 40(3): 129-154.

Champigny, O. and D. Ricquier (1990). "Effects of fasting and refeeding on the level of uncoupling protein mRNA in rat brown adipose tissue: evidence for diet-induced and cold-induced responses." J Nutr 120(12): 1730-1736.

Chan, J. L., K. Heist, A. M. DePaoli, J. D. Veldhuis and C. S. Mantzoros (2003). "The role of falling leptin levels in the neuroendocrine and metabolic adaptation to short-term starvation in healthy men." J Clin Invest 111(9): 1409-1421.

Chang, T. Y., B. L. Li, et al. (2009). "Acyl-coenzyme A:cholesterol acyltransferases." Am J Physiol Endocrinol Metab 297(1): E1-9.

Chao, F. F., D. L. Stiers and J. A. Ontko (1986). "Hepatocellular triglyceride synthesis and transfer to lipid droplets and nascent very low density lipoproteins." J Lipid Res 27(11): 1174-1181.

Chavez, M., K. Kaiyala, L. J. Madden, M. W. Schwartz and S. C. Woods (1995). "Intraventricular insulin and the level of maintained body weight in rats." Behav Neurosci 109(3): 528-531.

Chawla, A. and M. A. Lazar (1993). "Induction of Rev-ErbA alpha, an orphan receptor encoded on the opposite strand of the alpha-thyroid hormone receptor gene, during adipocyte differentiation." J Biol Chem 268(22): 16265-16269.

Chawla, A., C. H. Lee, Y. Barak, W. He, J. Rosenfeld, D. Liao, J. Han, H. Kang and R. M. Evans (2003). "PPARdelta is a very low-density lipoprotein sensor in macrophages." Proc Natl Acad Sci U S A 100(3): 1268-1273.

Chee, M. J. and W. F. Colmers (2008). "Y eat?" Nutrition 24(9): 869-877.

Chen, J. J. and I. M. London (1981). "Hemin enhances the differentiation of mouse 3T3 cells to adipocytes." Cell 26(1 Pt 1): 117-122.

Chen, L. and G. Yang (2014). "PPARs Integrate the Mammalian Clock and Energy Metabolism." PPAR Res 2014: 653017.

Chiang, J. Y., W. F. Miller and G. M. Lin (1990). "Regulation of cholesterol 7 alpha-hydroxylase in the liver. Purification of cholesterol 7 alpha-hydroxylase and the immunochemical evidence for the induction of cholesterol 7 alpha-hydroxylase by cholestyramine and circadian rhythm." J Biol Chem 265(7): 3889-3897.

Chin-Chance, C., K. S. Polonsky and D. A. Schoeller (2000). "Twenty-four-hour leptin levels respond to cumulative short-term energy imbalance and predict subsequent intake." J Clin Endocrinol Metab 85(8): 2685-2691.

Cho, H., X. Zhao, M. Hatori, R. T. Yu, G. D. Barish, M. T. Lam, L. W. Chong, L. DiTacchio, A. R. Atkins, C. K. Glass, C. Liddle, J. Auwerx, M. Downes, S. Panda and R. M. Evans (2012). "Regulation of circadian behaviour and metabolism by REV-ERB-alpha and REV-ERB-beta." Nature 485(7396): 123-127.

Choi, H., H. Lee, T. H. Kim, H. J. Kim, Y. J. Lee, S. J. Lee, J. H. Yu, D. Kim, K. S. Kim, S. W. Park and J. W. Kim (2014). "G0/G1 switch gene 2 has a critical role in adipocyte differentiation." Cell Death Differ 21(7): 1071-1080.

Choi, J. K., Y. I. Chen, E. Hamel and B. G. Jenkins (2006). "Brain hemodynamic changes mediated by dopamine receptors: Role of the cerebral microvasculature in dopamine-mediated neurovascular coupling." Neuroimage 30(3): 700-712.

Choi, S. M., D. F. Tucker, D. N. Gross, R. M. Easton, L. M. DiPilato, A. S. Dean, B. R. Monks and M. J. Birnbaum (2010). "Insulin regulates adipocyte lipolysis via an Akt-independent signaling pathway." Mol Cell Biol 30(21): 5009-5020.

Chomez, P., I. Neveu, A. Mansen, E. Kiesler, L. Larsson, B. Vennstrom and E. Arenas (2000). "Increased cell death and delayed development in the cerebellum of mice lacking the rev-erbA(alpha) orphan receptor." Development 127(7): 1489-1498.

Chua, E. C., G. Shui, I. T. Lee, P. Lau, L. C. Tan, S. C. Yeo, B. D. Lam, S. Bulchand, S. A. Summers, K. Puvanendran, S. G. Rozen, M. R. Wenk and J. J. Gooley (2013). "Extensive diversity in circadian regulation of plasma lipids and evidence for different circadian metabolic phenotypes in humans." Proc Natl Acad Sci U S A 110(35): 14468-14473.

Chung, S., E. J. Lee, S. Yun, H. K. Choe, S. B. Park, H. J. Son, K. S. Kim, D. E. Dluzen, I. Lee, O. Hwang, G. H. Son and K. Kim (2014). "Impact of circadian nuclear receptor REV-ERBalpha on midbrain dopamine production and mood regulation." Cell 157(4): 858-868.

Cinti, S. (2005). "The adipose organ." Prostaglandins Leukot Essent Fatty Acids 73(1): 9-15.

Civitarese, A. E., B. Ukropcova, S. Carling, M. Hulver, R. A. DeFronzo, L. Mandarino, E. Ravussin and S. R. Smith (2006). "Role of adiponectin in human skeletal muscle bioenergetics." Cell Metab 4(1): 75-87.

Cohen, P., H. G. Nimmo, et al. (1978). "How does insulin stimulate glycogen synthesis?" Biochem Soc Symp(43): 69-95.

Collins, S. and R. S. Surwit (2001). "The beta-adrenergic receptors and the control of adipose tissue metabolism and thermogenesis." Recent Prog Horm Res 56: 309-328.

Considine, R. V., M. K. Sinha, M. L. Heiman, A. Kriauciunas, T. W. Stephens, M. R. Nyce, J. P. Ohannesian, C. C. Marco, L. J. McKee, T. L. Bauer and et al. (1996). "Serum immunoreactive-leptin concentrations in normal-weight and obese humans." N Engl J Med 334(5): 292-295.

Costet, P., C. Legendre, J. More, A. Edgar, P. Galtier and T. Pineau (1998). "Peroxisome proliferator-activated receptor alpha-isoform deficiency leads to progressive dyslipidemia with sexually dimorphic obesity and steatosis." J Biol Chem 273(45): 29577-29585.

Cowley, M. A., J. L. Smart, M. Rubinstein, M. G. Cerdan, S. Diano, T. L. Horvath, R. D. Cone and M. J. Low (2001). "Leptin activates anorexigenic POMC neurons through a neural network in the arcuate nucleus." Nature 411(6836): 480-484.

Crosio, C., N. Cermakian, C. D. Allis and P. Sassone-Corsi (2000). "Light induces chromatin modification in cells of the mammalian circadian clock." Nat Neurosci 3(12): 1241-1247.

Cummings, D. E. and J. Overduin (2007). "Gastrointestinal regulation of food intake." J Clin Invest 117(1): 13-23.

Cummings, D. E., J. Q. Purnell, R. S. Frayo, K. Schmidova, B. E. Wisse and D. S. Weigle (2001). "A preprandial rise in plasma ghrelin levels suggests a role in meal initiation in humans." Diabetes 50(8): 1714-1719.

Cunningham, P. S., S. A. Ahern, L. C. Smith, C. S. da Silva Santos, T. T. Wager and D. A. Bechtold (2016). "Targeting of the circadian clock via CK1delta/epsilon to improve glucose homeostasis in obesity." Sci Rep 6: 29983.

Curtis, R., B. J. Geesaman and P. S. DiStefano (2005). "Ageing and metabolism: drug discovery opportunities." Nat Rev Drug Discov 4(7): 569-580.

Czeisler, C. A. (2013). "Perspective: casting light on sleep deficiency." Nature 497(7450): S13.

Dallmann, R., A. U. Viola, L. Tarokh, C. Cajochen and S. A. Brown (2012). "The human circadian metabolome." Proc Natl Acad Sci U S A 109(7): 2625-2629.

Damiola, F., N. Le Minh, N. Preitner, B. Kornmann, F. Fleury-Olela and U. Schibler (2000). "Restricted feeding uncouples circadian oscillators in peripheral tissues from the central pacemaker in the suprachiasmatic nucleus." Genes Dev 14(23): 2950-2961.

Dashty, M. (2013). "A quick look at biochemistry: carbohydrate metabolism." Clin Biochem 46(15): 1339-1352.

Daval, M., F. Foufelle and P. Ferre (2006). "Functions of AMP-activated protein kinase in adipose tissue." J Physiol 574(Pt 1): 55-62.

De Taeye, B. M., T. Novitskaya, L. Gleaves, J. W. Covington and D. E. Vaughan (2006). "Bone marrow plasminogen activator inhibitor-1 influences the development of obesity." J Biol Chem 281(43): 32796-32805.

Delezie, J., S. Dumont, H. Dardente, H. Oudart, A. Grechez-Cassiau, P. Klosen, M. Teboul, F. Delaunay, P. Pevet and E. Challet (2012). "The nuclear receptor REV-ERBalpha is required for the daily balance of carbohydrate and lipid metabolism." FASEB J 26(8): 3321-3335.

Deng, J., S. Liu, L. Zou, C. Xu, B. Geng and G. Xu (2012). "Lipolysis response to endoplasmic reticulum stress in adipose cells." J Biol Chem 287(9): 6240-6249.

Deng, T., S. Shan, P. P. Li, Z. F. Shen, X. P. Lu, J. Cheng and Z. Q. Ning (2006). "Peroxisome proliferator-activated receptor-gamma transcriptionally up-regulates hormone-sensitive lipase via the involvement of specificity protein-1." Endocrinology 147(2): 875-884.

Di Lorenzo, L., G. De Pergola, C. Zocchetti, N. L'Abbate, A. Basso, N. Pannacciulli, M. Cignarelli, R. Giorgino and L. Soleo (2003). "Effect of shift work on body mass index: results of a study performed in 319 glucose-tolerant men working in a Southern Italian industry." Int J Obes Relat Metab Disord 27(11): 1353-1358.

Digel, M., R. Ehehalt and J. Fullekrug (2010). "Lipid droplets lighting up: insights from live microscopy." FEBS Lett 584(11): 2168-2175.

Ding, J. M., G. F. Buchanan, S. A. Tischkau, D. Chen, L. Kuriashkina, L. E. Faiman, J. M. Alster, P. S. McPherson, K. P. Campbell and M. U. Gillette (1998). "A neuronal ryanodine receptor mediates light-induced phase delays of the circadian clock." Nature 394(6691): 381-384.

Dohm, G. L., P. L. Dolan, W. R. Frisell and R. W. Dudek (1993). "Role of transverse tubules in insulin stimulated muscle glucose transport." J Cell Biochem 52(1): 1-7.

Doi, R., K. Oishi and N. Ishida (2010). "CLOCK regulates circadian rhythms of hepatic glycogen synthesis through transcriptional activation of Gys2." J Biol Chem 285(29): 22114-22121.

Donsmark, M., J. Langfort, C. Holm, T. Ploug and H. Galbo (2003). "Contractions activate hormone-sensitive lipase in rat muscle by protein kinase C and mitogen-activated protein kinase." J Physiol 550(Pt 3): 845-854.

Donsmark, M., J. Langfort, C. Holm, T. Ploug and H. Galbo (2004). "Regulation and role of hormone-sensitive lipase in rat skeletal muscle." Proc Nutr Soc 63(2): 309-314.

Druce, M. R., N. M. Neary, C. J. Small, J. Milton, M. Monteiro, M. Patterson, M. A. Ghatei and S. R. Bloom (2006). "Subcutaneous administration of ghrelin stimulates energy intake in healthy lean human volunteers." Int J Obes (Lond) 30(2): 293-296.

Druce, M. R., A. M. Wren, A. J. Park, J. E. Milton, M. Patterson, G. Frost, M. A. Ghatei, C. Small and S. R. Bloom (2005). "Ghrelin increases food intake in obese as well as lean subjects." Int J Obes (Lond) 29(9): 1130-1136.

Duez, H. and B. Staels (2008). "The nuclear receptors Rev-erbs and RORs integrate circadian rhythms and metabolism." Diab Vasc Dis Res 5(2): 82-88.

Duez, H., J. N. van der Veen, C. Duhem, B. Pourcet, T. Touvier, C. Fontaine, B. Derudas, E. Bauge, R. Havinga, V. W. Bloks, H. Wolters, F. H. van der Sluijs, B. Vennstrom, F. Kuipers and B. Staels (2008). "Regulation of bile acid synthesis by the nuclear receptor Rev-erbalpha." Gastroenterology 135(2): 689-698.

Duffield, G. E., J. D. Best, B. H. Meurers, A. Bittner, J. J. Loros and J. C. Dunlap (2002). "Circadian programs of transcriptional activation, signaling, and protein turnover revealed by microarray analysis of mammalian cells." Curr Biol 12(7): 551-557.

Duncan, R. E., M. Ahmadian, K. Jaworski, E. Sarkadi-Nagy and H. S. Sul (2007). "Regulation of lipolysis in adipocytes." Annu Rev Nutr 27: 79-101.

Durgan, D. J. and M. E. Young (2010). "The cardiomyocyte circadian clock: emerging roles in health and disease." Circ Res 106(4): 647-658.

Eberle, D., B. Hegarty, P. Bossard, P. Ferre and F. Foufelle (2004). "SREBP transcription factors: master regulators of lipid homeostasis." Biochimie 86(11): 839-848.

Eckel-Mahan, K. L., V. R. Patel, et al. (2013). "Reprogramming of the circadian clock by nutritional challenge." Cell 155(7): 1464-1478.

Eckel-Mahan, K. and P. Sassone-Corsi (2013). "Metabolism and the circadian clock converge." Physiol Rev 93(1): 107-135.

Eckel-Mahan, K. L., V. R. Patel, R. P. Mohney, K. S. Vignola, P. Baldi and P. Sassone-Corsi (2012). "Coordination of the transcriptome and metabolome by the circadian clock." Proc Natl Acad Sci U S A 109(14): 5541-5546.

Edwards, P. A., H. Muroya and R. G. Gould (1972). "In vivo demonstration of the circadian thythm of cholesterol biosynthesis in the liver and intestine of the rat." J Lipid Res 13(3): 396-401.

Eguchi, J., X. Wang, S. Yu, E. E. Kershaw, P. C. Chiu, J. Dushay, J. L. Estall, U. Klein, E. Maratos-Flier and E. D. Rosen (2011). "Transcriptional control of adipose lipid handling by IRF4." Cell Metab 13(3): 249-259.

Eide, E. J., E. L. Vielhaber, W. A. Hinz and D. M. Virshup (2002). "The circadian regulatory proteins BMAL1 and cryptochromes are substrates of casein kinase Iepsilon." J Biol Chem 277(19): 17248-17254.

Eide, E. J., M. F. Woolf, H. Kang, P. Woolf, W. Hurst, F. Camacho, E. L. Vielhaber, A. Giovanni and D. M. Virshup (2005). "Control of mammalian circadian rhythm by CKIepsilon-regulated proteasome-mediated PER2 degradation." Mol Cell Biol 25(7): 2795-2807.

Elks, M. L. and V. C. Manganiello (1985). "Antilipolytic action of insulin: role of cAMP phosphodiesterase activation." Endocrinology 116(5): 2119-2121.

Enerback, S., A. Jacobsson, E. M. Simpson, C. Guerra, H. Yamashita, M. E. Harper and L. P. Kozak (1997). "Mice lacking mitochondrial uncoupling protein are cold-sensitive but not obese." Nature 387(6628): 90-94.

Espenshade, P. J. and A. L. Hughes (2007). "Regulation of sterol synthesis in eukaryotes." Annu Rev Genet 41: 401-427.

Etchegaray, J. P., C. Lee, P. A. Wade and S. M. Reppert (2003). "Rhythmic histone acetylation underlies transcription in the mammalian circadian clock." Nature 421(6919): 177-182.

Even, P. C. and S. Nicolaidis (1993). "Adaptive changes in energy expenditure during mild and severe feed restriction in the rat." Br J Nutr 70(2): 421-431.

Exley, M. A., L. Hand, D. O'Shea and L. Lynch (2014). "Interplay between the immune system and adipose tissue in obesity." J Endocrinol 223(2): R41-48.

Fahy, E., S. Subramaniam, H. A. Brown, C. K. Glass, A. H. Merrill, Jr., R. C. Murphy, C. R. Raetz, D. W. Russell, Y. Seyama, W. Shaw, T. Shimizu, F. Spener, G. van Meer, M. S. VanNieuwenhze, S. H. White, J. L. Witztum and E. A. Dennis (2005). "A comprehensive classification system for lipids." J Lipid Res 46(5): 839-861.

Fang, X., S. X. Yu, et al. (2000). "Phosphorylation and inactivation of glycogen synthase kinase 3 by protein kinase A." Proc Natl Acad Sci U S A 97(22): 11960-11965.

Feldmann, H. M., V. Golozoubova, B. Cannon and J. Nedergaard (2009). "UCP1 ablation induces obesity and abolishes diet-induced thermogenesis in mice exempt from thermal stress by living at thermoneutrality." Cell Metab 9(2): 203-209.

Feng, D., T. Liu, Z. Sun, A. Bugge, S. E. Mullican, T. Alenghat, X. S. Liu and M. A. Lazar (2011). "A circadian rhythm orchestrated by histone deacetylase 3 controls hepatic lipid metabolism." Science 331(6022): 1315-1319.

Ferrannini, E. (1988). "The theoretical bases of indirect calorimetry: a review." Metabolism 37(3): 287-301.

Ferraris, R. P. (2001). "Dietary and developmental regulation of intestinal sugar transport." Biochem J 360(Pt 2): 265-276.

Feuerer, M., L. Herrero, D. Cipolletta, A. Naaz, J. Wong, A. Nayer, J. Lee, A. B. Goldfine, C. Benoist, S. Shoelson and D. Mathis (2009). "Lean, but not obese, fat is enriched for a unique population of regulatory T cells that affect metabolic parameters." Nat Med 15(8): 930-939.

Figlewicz, D. P. and A. J. Sipols (2010). "Energy regulatory signals and food reward." Pharmacol Biochem Behav 97(1): 15-24.

Flier, J. S. and J. K. Elmquist (2004). "A good night's sleep: future antidote to the obesity epidemic?" Ann Intern Med 141(11): 885-886.

Fontaine, C., G. Dubois, Y. Duguay, T. Helledie, N. Vu-Dac, P. Gervois, F. Soncin, S. Mandrup, J. C. Fruchart, J. Fruchart-Najib and B. Staels (2003). "The orphan nuclear receptor Rev-Erbalpha is a peroxisome proliferator-activated receptor (PPAR) gamma target gene and promotes PPARgamma-induced adipocyte differentiation." J Biol Chem 278(39): 37672-37680.

Foster, D. W. (2012). "Malonyl-CoA: the regulator of fatty acid synthesis and oxidation." J Clin Invest 122(6): 1958-1959.

Foufelle, F. and P. Ferre (2002). "New perspectives in the regulation of hepatic glycolytic and lipogenic genes by insulin and glucose: a role for the transcription factor sterol regulatory element binding protein-1c." Biochem J 366(Pt 2): 377-391.

Franckhauser, S., S. Munoz, A. Pujol, A. Casellas, E. Riu, P. Otaegui, B. Su and F. Bosch (2002). "Increased fatty acid re-esterification by PEPCK overexpression in adipose tissue leads to obesity without insulin resistance." Diabetes 51(3): 624-630.

Frayling, T. M., N. J. Timpson, M. N. Weedon, E. Zeggini, R. M. Freathy, C. M. Lindgren, J. R. Perry, K. S. Elliott, H. Lango, N. W. Rayner, B. Shields, L. W. Harries, J. C. Barrett, S. Ellard, C. J. Groves, B. Knight, A. M. Patch, A. R. Ness, S. Ebrahim, D. A. Lawlor, S. M. Ring, Y. Ben-Shlomo, M. R. Jarvelin, U. Sovio, A. J. Bennett, D. Melzer, L. Ferrucci, R. J. Loos, I. Barroso, N. J. Wareham, F. Karpe, K. R. Owen, L. R. Cardon, M. Walker, G. A. Hitman, C. N. Palmer, A. S. Doney, A. D. Morris, G. D. Smith, A. T. Hattersley and M. I. McCarthy (2007). "A common variant in the FTO gene is associated with body mass index and predisposes to childhood and adult obesity." Science 316(5826): 889-894.

Frayn, K. N. (1983). "Calculation of substrate oxidation rates in vivo from gaseous exchange." J Appl Physiol Respir Environ Exerc Physiol 55(2): 628-634.

Frayn, K. N. (1998). "Regulation of fatty acid delivery in vivo." Adv Exp Med Biol 441: 171-179.

Frayn, K. N. (2002). "Adipose tissue as a buffer for daily lipid flux." Diabetologia 45(9): 1201-1210.

Frayn, K. N., P. Arner and H. Yki-Jarvinen (2006). "Fatty acid metabolism in adipose tissue, muscle and liver in health and disease." Essays Biochem 42: 89-103.

Fried, S. K., D. A. Bunkin and A. S. Greenberg (1998). "Omental and subcutaneous adipose tissues of obese subjects release interleukin-6: depot difference and regulation by glucocorticoid." J Clin Endocrinol Metab 83(3): 847-850.

Friedman, J. M. and J. L. Halaas (1998). "Leptin and the regulation of body weight in mammals." Nature 395(6704): 763-770.

Fruebis, J., T. S. Tsao, S. Javorschi, D. Ebbets-Reed, M. R. Erickson, F. T. Yen, B. E. Bihain and H. F. Lodish (2001). "Proteolytic cleavage product of 30-kDa adipocyte complement-related protein increases fatty acid oxidation in muscle and causes weight loss in mice." Proc Natl Acad Sci U S A 98(4): 2005-2010.

Fruhbeck, G., J. Gomez-Ambrosi, F. J. Muruzabal and M. A. Burrell (2001). "The adipocyte: a model for integration of endocrine and metabolic signaling in energy metabolism regulation." Am J Physiol Endocrinol Metab 280(6): E827-847.

Fukagawa, K., H. M. Gou, R. Wolf and P. Tso (1994). "Circadian rhythm of serum and lymph apolipoprotein AIV in ad libitum-fed and fasted rats." Am J Physiol 267(5 Pt 2): R1385-1390.

Gachon, F. (2007). "Physiological function of PARbZip circadian clock-controlled transcription factors." Ann Med 39(8): 562-571.

Gachon, F., E. Nagoshi, S. A. Brown, J. Ripperger and U. Schibler (2004). "The mammalian circadian timing system: from gene expression to physiology." Chromosoma 113(3): 103-112.

Gachon, F., F. F. Olela, O. Schaad, P. Descombes and U. Schibler (2006). "The circadian PAR-domain basic leucine zipper transcription factors DBP, TEF, and HLF modulate basal and inducible xenobiotic detoxification." Cell Metab 4(1): 25-36.

Gao, X., M. Qian, J. L. Campian, J. Marshall, Z. Zhou, A. M. Roberts, Y. J. Kang, S. D. Prabhu, X. F. Sun and J. W. Eaton (2010). "Mitochondrial dysfunction may explain the cardiomyopathy of chronic iron overload." Free Radic Biol Med 49(3): 401-407.

Garaulet, M. and P. Gomez-Abellan (2014). "Timing of food intake and obesity: a novel association." Physiol Behav 134: 44-50.

Garofalo, M. A., I. C. Kettelhut, J. E. Roselino and R. H. Migliorini (1996). "Effect of acute cold exposure on norepinephrine turnover rates in rat white adipose tissue." J Auton Nerv Syst 60(3): 206-208.

Gerber, A., C. Saini, T. Curie, Y. Emmenegger, G. Rando, P. Gosselin, I. Gotic, P. Gos, P. Franken and U. Schibler (2015). "The systemic control of circadian gene expression." Diabetes Obes Metab 17 Suppl 1: 23-32.

Gerhart-Hines, Z., D. Feng, M. J. Emmett, L. J. Everett, E. Loro, E. R. Briggs, A. Bugge, C. Hou, C. Ferrara, P. Seale, D. A. Pryma, T. S. Khurana and M. A. Lazar (2013). "The nuclear receptor Rev-erbalpha controls circadian thermogenic plasticity." Nature 503(7476): 410-413.

Gerhold, D. L., F. Liu, G. Jiang, Z. Li, J. Xu, M. Lu, J. R. Sachs, A. Bagchi, A. Fridman, D. J. Holder, T. W. Doebber, J. Berger, A. Elbrecht, D. E. Moller and B. B. Zhang (2002). "Gene expression profile of adipocyte differentiation and its regulation by peroxisome proliferator-activated receptor-gamma agonists." Endocrinology 143(6): 2106-2118.

Gervois, P., S. Chopin-Delannoy, A. Fadel, G. Dubois, V. Kosykh, J. C. Fruchart, J. Najib, V. Laudet and B. Staels (1999). "Fibrates increase human REV-ERBalpha expression in liver via a novel peroxisome proliferator-activated receptor response element." Mol Endocrinol 13(3): 400-409.

Gibbs, J., R. C. Young and G. P. Smith (1973). "Cholecystokinin decreases food intake in rats." J Comp Physiol Psychol 84(3): 488-495.

Gibbs, J. E., J. Blaikley, S. Beesley, L. Matthews, K. D. Simpson, S. H. Boyce, S. N. Farrow, K. J. Else, D. Singh, D. W. Ray and A. S. Loudon (2012). "The nuclear receptor REV-ERBalpha mediates circadian regulation of innate immunity through selective regulation of inflammatory cytokines." Proc Natl Acad Sci U S A 109(2): 582-587.

Gimble, J. M. and Z. E. Floyd (2009). "Fat circadian biology." J Appl Physiol (1985) 107(5): 1629-1637.

Glatz, J. F., J. J. Luiken and A. Bonen (2010). "Membrane fatty acid transporters as regulators of lipid metabolism: implications for metabolic disease." Physiol Rev 90(1): 367-417.

Gong, D. W., Y. He, M. Karas and M. Reitman (1997). "Uncoupling protein-3 is a mediator of thermogenesis regulated by thyroid hormone, beta3-adrenergic agonists, and leptin." J Biol Chem 272(39): 24129-24132.

Gong, D. W., Y. He and M. L. Reitman (1999). "Genomic organization and regulation by dietary fat of the uncoupling protein 3 and 2 genes." Biochem Biophys Res Commun 256(1): 27-32.

Gottlieb, D. J., N. M. Punjabi, A. B. Newman, H. E. Resnick, S. Redline, C. M. Baldwin and F. J. Nieto (2005). "Association of sleep time with diabetes mellitus and impaired glucose tolerance." Arch Intern Med 165(8): 863-867.

Green, D. J. and R. Gillette (1982). "Circadian rhythm of firing rate recorded from single cells in the rat suprachiasmatic brain slice." Brain Res 245(1): 198-200.

Grewal, S. S., R. D. York and P. J. Stork (1999). "Extracellular-signal-regulated kinase signalling in neurons." Curr Opin Neurobiol 9(5): 544-553.

Grill, H. J. and R. Norgren (1978). "The taste reactivity test. II. Mimetic responses to gustatory stimuli in chronic thalamic and chronic decerebrate rats." Brain Res 143(2): 281-297.

Grill, H. J. and G. P. Smith (1988). "Cholecystokinin decreases sucrose intake in chronic decerebrate rats." Am J Physiol 254(6 Pt 2): R853-856.

Grimaldi, B., M. M. Bellet, S. Katada, G. Astarita, J. Hirayama, R. H. Amin, J. G. Granneman, D. Piomelli, T. Leff and P. Sassone-Corsi (2010). "PER2 controls lipid metabolism by direct regulation of PPARgamma." Cell Metab 12(5): 509-520.

Groos, G. and J. Hendriks (1982). "Circadian rhythms in electrical discharge of rat suprachiasmatic neurones recorded in vitro." Neurosci Lett 34(3): 283-288.

Gross, D. N., A. P. van den Heuvel and M. J. Birnbaum (2008). "The role of FoxO in the regulation of metabolism." Oncogene 27(16): 2320-2336.

Grunfeld, C., C. Zhao, J. Fuller, A. Pollack, A. Moser, J. Friedman and K. R. Feingold (1996). "Endotoxin and cytokines induce expression of leptin, the ob gene product, in hamsters." J Clin Invest 97(9): 2152-2157.

Guerre-Millo, M., P. Gervois, E. Raspe, L. Madsen, P. Poulain, B. Derudas, J. M. Herbert, D. A. Winegar, T. M. Willson, J. C. Fruchart, R. K. Berge and B. Staels (2000). "Peroxisome proliferator-activated receptor alpha activators improve insulin sensitivity and reduce adiposity." J Biol Chem 275(22): 16638-16642.

Guilding, C. and H. D. Piggins (2007). "Challenging the omnipotence of the suprachiasmatic timekeeper: are circadian oscillators present throughout the mammalian brain?" Eur J Neurosci 25(11): 3195-3216.

Guilherme, A., J. V. Virbasius, V. Puri and M. P. Czech (2008). "Adipocyte dysfunctions linking obesity to insulin resistance and type 2 diabetes." Nat Rev Mol Cell Biol 9(5): 367-377.

Guillaumond, F., H. Dardente, V. Giguere and N. Cermakian (2005). "Differential control of Bmal1 circadian transcription by REV-ERB and ROR nuclear receptors." J Biol Rhythms 20(5): 391-403.

Guo, H., J. M. Brewer, M. N. Lehman and E. L. Bittman (2006). "Suprachiasmatic regulation of circadian rhythms of gene expression in hamster peripheral organs: effects of transplanting the pacemaker." J Neurosci 26(24): 6406-6412.

Guo, Y., K. R. Cordes, R. V. Farese, Jr. and T. C. Walther (2009). "Lipid droplets at a glance." J Cell Sci 122(Pt 6): 749-752.

Gupta, R. K., R. J. Mepani, S. Kleiner, J. C. Lo, M. J. Khandekar, P. Cohen, A. Frontini, D. C. Bhowmick, L. Ye, S. Cinti and B. M. Spiegelman (2012). "Zfp423 expression identifies committed preadipocytes and localizes to adipose endothelial and perivascular cells." Cell Metab 15(2): 230-239.

Haigis, M. C. and D. A. Sinclair (2010). "Mammalian sirtuins: biological insights and disease relevance." Annu Rev Pathol 5: 253-295.

Haimovich, B., J. Calvano, A. D. Haimovich, S. E. Calvano, S. M. Coyle and S. F. Lowry (2010). "In vivo endotoxin synchronizes and suppresses clock gene expression in human peripheral blood leukocytes." Crit Care Med 38(3): 751-758.

Hajnal, A., G. P. Smith and R. Norgren (2004). "Oral sucrose stimulation increases accumbens dopamine in the rat." Am J Physiol Regul Integr Comp Physiol 286(1): R31-37.

Halberg, N., T. Khan, M. E. Trujillo, I. Wernstedt-Asterholm, A. D. Attie, S. Sherwani, Z. V. Wang, S. Landskroner-Eiger, S. Dineen, U. J. Magalang, R. A. Brekken and P. E. Scherer (2009). "Hypoxia-inducible factor 1alpha induces fibrosis and insulin resistance in white adipose tissue." Mol Cell Biol 29(16): 4467-4483.

Hales, C. N., J. P. Luzio and K. Siddle (1978). "Hormonal control of adipose-tissue lipolysis." Biochem Soc Symp(43): 97-135.

Hall, K. D., S. B. Heymsfield, J. W. Kemnitz, S. Klein, D. A. Schoeller and J. R. Speakman (2012). "Energy balance and its components: implications for body weight regulation." Am J Clin Nutr 95(4): 989-994.

Hallschmid, M., C. Benedict, B. Schultes, H. L. Fehm, J. Born and W. Kern (2004). "Intranasal insulin reduces body fat in men but not in women." Diabetes 53(11): 3024-3029.

Halton, T. L. and F. B. Hu (2004). "The effects of high protein diets on thermogenesis, satiety and weight loss: a critical review." J Am Coll Nutr 23(5): 373-385.

Hand, L. E., P. Usan, G. J. Cooper, L. Y. Xu, B. Ammori, P. S. Cunningham, R. Aghamohammadzadeh, H. Soran, A. Greenstein, A. S. Loudon, D. A. Bechtold and D. W. Ray (2015). "Adiponectin induces A20 expression in adipose tissue to confer metabolic benefit." Diabetes 64(1): 128-136.

Harada, Y., M. Sakai, N. Kurabayashi, T. Hirota and Y. Fukada (2005). "Ser-557-phosphorylated mCRY2 is degraded upon synergistic phosphorylation by glycogen synthase kinase-3 beta." J Biol Chem 280(36): 31714-31721.

Hastings, M., J. S. O'Neill and E. S. Maywood (2007). "Circadian clocks: regulators of endocrine and metabolic rhythms." J Endocrinol 195(2): 187-198.

Hastings, M. H., M. D. Field, E. S. Maywood, D. R. Weaver and S. M. Reppert (1999). "Differential regulation of mPER1 and mTIM proteins in the mouse suprachiasmatic nuclei: new insights into a core clock mechanism." J Neurosci 19(12): RC11.

Hatori, M., C. Vollmers, A. Zarrinpar, L. DiTacchio, E. A. Bushong, S. Gill, M. Leblanc, A. Chaix, M. Joens, J. A. Fitzpatrick, M. H. Ellisman and S. Panda (2012). "Time-restricted feeding without reducing caloric intake prevents metabolic diseases in mice fed a high-fat diet." Cell Metab 15(6): 848-860.

He, W., T. K. Lam, S. Obici and L. Rossetti (2006). "Molecular disruption of hypothalamic nutrient sensing induces obesity." Nat Neurosci 9(2): 227-233.

Health and Social Care Information Centre 2015 (England) *Statistics on Obesity, Physical Activity and Diet,* viewed 6TH June 2016. Available at: < http://digital.nhs.uk/catalogue/PUB16988/obes-phys-acti-diet-eng-2015.pdf>

Hensley, L. L., G. Ranganathan, E. M. Wagner, B. D. Wells, J. C. Daniel, D. Vu, C. F. Semenkovich, R. Zechner and P. A. Kern (2003). "Transgenic mice expressing lipoprotein lipase in adipose tissue. Absence of the proximal 3'-untranslated region causes translational upregulation." J Biol Chem 278(35): 32702-32709.

Hinney, A., A. Schmidt, K. Nottebom, O. Heibult, I. Becker, A. Ziegler, G. Gerber, M. Sina, T. Gorg, H. Mayer, W. Siegfried, M. Fichter, H. Remschmidt and J. Hebebrand (1999). "Several mutations in the melanocortin-4 receptor gene including a nonsense and a frameshift mutation associated with dominantly inherited obesity in humans." J Clin Endocrinol Metab 84(4): 1483-1486.

Hirano, A., K. Yumimoto, R. Tsunematsu, M. Matsumoto, M. Oyama, H. Kozuka-Hata, T. Nakagawa, D. Lanjakornsiripan, K. I. Nakayama and Y. Fukada (2013). "FBXL21 regulates oscillation of the circadian clock through ubiquitination and stabilization of cryptochromes." Cell 152(5): 1106-1118.

Hirayama, J., S. Sahar, B. Grimaldi, T. Tamaru, K. Takamatsu, Y. Nakahata and P. Sassone-Corsi (2007). "CLOCK-mediated acetylation of BMAL1 controls circadian function." Nature 450(7172): 1086-1090.

Ho, K. J. (1976). "Circadian distribution of bile acids in the enterohepatic circulatory system in rats." Am J Physiol 230(5): 1331-1335.

Holland, W. L., R. A. Miller, Z. V. Wang, K. Sun, B. M. Barth, H. H. Bui, K. E. Davis, B. T. Bikman, N. Halberg, J. M. Rutkowski, M. R. Wade, V. M. Tenorio, M. S. Kuo, J. T. Brozinick, B. B. Zhang, M. J. Birnbaum, S. A. Summers and P. E. Scherer (2011). "Receptor-mediated activation of ceramidase activity initiates the pleiotropic actions of adiponectin." Nat Med 17(1): 55-63.

Hoofnagle, A. N. and J. W. Heinecke (2009). "Lipoproteomics: using mass spectrometry-based proteomics to explore the assembly, structure, and function of lipoproteins." J Lipid Res 50(10): 1967-1975.

Horowitz, J. F. and S. Klein (2000). "Lipid metabolism during endurance exercise." Am J Clin Nutr 72(2 Suppl): 558S-563S.

Hosokawa, M. and B. Thorens (2002). "Glucose release from GLUT2-null hepatocytes: characterization of a major and a minor pathway." Am J Physiol Endocrinol Metab 282(4): E794-801.

Hotamisligil, G. S., N. S. Shargill and B. M. Spiegelman (1993). "Adipose expression of tumor necrosis factor-alpha: direct role in obesity-linked insulin resistance." Science 259(5091): 87-91.

Hue, L. and H. Taegtmeyer (2009). "The Randle cycle revisited: a new head for an old hat." Am J Physiol Endocrinol Metab 297(3): E578-591.

Hughes, M. E., L. DiTacchio, K. R. Hayes, C. Vollmers, S. Pulivarthy, J. E. Baggs, S. Panda and J. B. Hogenesch (2009). "Harmonics of circadian gene transcription in mammals." PLoS Genet 5(4): e1000442.

Huh, J. Y., E. Y. Seo, H. B. Lee and H. Ha (2012). "Glucose-based peritoneal dialysis solution suppresses adiponectin synthesis through oxidative stress in an experimental model of peritoneal dialysis." Perit Dial Int 32(1): 20-28.

Huypens, P., K. Moens, H. Heimberg, Z. Ling, D. Pipeleers and M. Van de Casteele (2005). "Adiponectin-mediated stimulation of AMP-activated protein kinase (AMPK) in pancreatic beta cells." Life Sci 77(11): 1273-1282.

Iitaka, C., K. Miyazaki, T. Akaike and N. Ishida (2005). "A role for glycogen synthase kinase-3beta in the mammalian circadian clock." J Biol Chem 280(33): 29397-29402.

Imai, T., R. Takakuwa, S. Marchand, E. Dentz, J. M. Bornert, N. Messaddeq, O. Wendling, M. Mark, B. Desvergne, W. Wahli, P. Chambon and D. Metzger (2004). "Peroxisome proliferator-activated receptor gamma is required in mature white and brown adipocytes for their survival in the mouse." Proc Natl Acad Sci U S A 101(13): 4543-4547.

Inoue, I., Y. Shinoda, M. Ikeda, K. Hayashi, K. Kanazawa, M. Nomura, T. Matsunaga, H. Xu, S. Kawai, T. Awata, T. Komoda and S. Katayama (2005). "CLOCK/BMAL1 is involved in lipid metabolism via transactivation of the peroxisome proliferator-activated receptor (PPAR) response element." J Atheroscler Thromb 12(3): 169-174.

Inouye, S. T. and H. Kawamura (1979). "Persistence of circadian rhythmicity in a mammalian hypothalamic "island" containing the suprachiasmatic nucleus." Proc Natl Acad Sci U S A 76(11): 5962-5966.

Ip, E., G. Farrell, P. Hall, G. Robertson and I. Leclercq (2004). "Administration of the potent PPARalpha agonist, Wy-14,643, reverses nutritional fibrosis and steatohepatitis in mice." Hepatology 39(5): 1286-1296.

Isenman, L., C. Liebow and S. Rothman (1999). "The endocrine secretion of mammalian digestive enzymes by exocrine glands." Am J Physiol 276(2 Pt 1): E223-232.

Ishikawa, K. and T. Shimazu (1976). "Daily rhythms of glycogen synthetase and phosphorylase activities in rat liver: influence of food and light." Life Sci 19(12): 1873-1878.

Ishikawa, K. and T. Shimazu (1980). "Circadian rhythm of liver glycogen metabolism in rats: effects of hypothalamic lesions." Am J Physiol 238(1): E21-25.

Isola, L. M., S. L. Zhou, C. L. Kiang, D. D. Stump, M. W. Bradbury and P. D. Berk (1995). "3T3 fibroblasts transfected with a cDNA for mitochondrial aspartate aminotransferase express plasma membrane fatty acid-binding protein and saturable fatty acid uptake." Proc Natl Acad Sci U S A 92(21): 9866-9870.

Iwanaga, H., M. Yano, H. Miki, K. Okada, T. Azama, S. Takiguchi, Y. Fujiwara, T. Yasuda, M. Nakayama, M. Kobayashi, K. Oishi, N. Ishida, K. Nagai and M. Monden (2005). "Per2 gene expressions in the suprachiasmatic nucleus and liver differentially respond to nutrition factors in rats." JPEN J Parenter Enteral Nutr 29(3): 157-161.

Javed, F., Q. He, L. E. Davidson, J. C. Thornton, J. Albu, L. Boxt, N. Krasnow, M. Elia, P. Kang, S. Heshka and D. Gallagher (2010). "Brain and high metabolic rate organ mass: contributions to resting energy expenditure beyond fat-free mass." Am J Clin Nutr 91(4): 907-912.

Jaworski, K., E. Sarkadi-Nagy, R. E. Duncan, M. Ahmadian and H. S. Sul (2007). "Regulation of triglyceride metabolism. IV. Hormonal regulation of lipolysis in adipose tissue." Am J Physiol Gastrointest Liver Physiol 293(1): G1-4.

Jensen, M. D. (1997). "Lipolysis: contribution from regional fat." Annu Rev Nutr 17: 127-139.

Jensen, M. D. (2003). "Fate of fatty acids at rest and during exercise: regulatory mechanisms." Acta Physiol Scand 178(4): 385-390.

Jensen, M. D., M. W. Haymond, J. E. Gerich, P. E. Cryer and J. M. Miles (1987). "Lipolysis during fasting. Decreased suppression by insulin and increased stimulation by epinephrine." J Clin Invest 79(1): 207-213.

Jequier, E. (1985). "[Thermogenesis induced by nutrients in man: its role in weight regulation]." J Physiol (Paris) 80(2): 129-140.

Jiang, G. and B. B. Zhang (2003). "Glucagon and regulation of glucose metabolism." Am J Physiol Endocrinol Metab 284(4): E671-678.

Jo, J., O. Gavrilova, S. Pack, W. Jou, S. Mullen, A. E. Sumner, S. W. Cushman and V. Periwal (2009). "Hypertrophy and/or Hyperplasia: Dynamics of Adipose Tissue Growth." PLoS Comput Biol 5(3): e1000324.

Johansson, C., H. O. Lagerlof, et al. (1972). "Studies of gastrointestinal interactions. 3. Determination of gastric secretion and evacuation, biliary and pancreactic secretion, intestinal absorption, intestinal transit time and flow of water in man." Scand J Gastroenterol 7(5): 489-499.

Johnson, P. R., J. S. Stern, M. R. Greenwood and J. Hirsch (1978). "Adipose tissue hyperplasia and hyperinsulinemia on Zucker obese female rats: a developmental study." Metabolism 27(12 Suppl 2): 1941-1954.

Johnston, J. D., G. Frost and D. T. Otway (2009). "Adipose tissue, adipocytes and the circadian timing system." Obes Rev 10 Suppl 2: 52-60.

Johnstone, A. M., S. D. Murison, J. S. Duncan, K. A. Rance and J. R. Speakman (2005). "Factors influencing variation in basal metabolic rate include fat-free mass, fat mass, age, and circulating thyroxine but not sex, circulating leptin, or triiodothyronine." Am J Clin Nutr 82(5): 941-948.

Jong, M. C., V. E. Dahlmans, H. M. Princen, M. H. Hofker and L. M. Havekes (1998). "Effects of fenofibrate on hyperlipidemia and postprandial triglyceride metabolism in human apolipoprotein C1 transgenic mice." Atherosclerosis 141 Suppl 1: S77-80.

Jukarainen, S., S. Heinonen, J. T. Ramo, R. Rinnankoski-Tuikka, E. Rappou, M. Tummers, M. Muniandy, A. Hakkarainen, J. Lundbom, N. Lundbom, J. Kaprio, A. Rissanen, E. Pirinen and K. H. Pietilainen (2016). "Obesity Is Associated With Low NAD(+)/SIRT Pathway Expression in Adipose Tissue of BMI-Discordant Monozygotic Twins." J Clin Endocrinol Metab 101(1): 275-283.

Jumpertz, R., D. S. Le, P. J. Turnbaugh, C. Trinidad, C. Bogardus, J. I. Gordon and J. Krakoff (2011). "Energy-balance studies reveal associations between gut microbes, caloric load, and nutrient absorption in humans." Am J Clin Nutr 94(1): 58-65.

Kaasik, K. and C. C. Lee (2004). "Reciprocal regulation of haem biosynthesis and the circadian clock in mammals." Nature 430(6998): 467-471.

Kalsbeek, A. and J. H. Strubbe (1998). "Circadian control of insulin secretion is independent of the temporal distribution of feeding." Physiol Behav 63(4): 553-558.

Kalsbeek, A., J. J. van Heerikhuize, J. Wortel and R. M. Buijs (1996). "A diurnal rhythm of stimulatory input to the hypothalamo-pituitary-adrenal system as revealed by timed intrahypothalamic administration of the vasopressin V1 antagonist." J Neurosci 16(17): 5555-5565.

Kaplan, J. M., R. J. Seeley and H. J. Grill (1993). "Daily caloric intake in intact and chronic decerebrate rats." Behav Neurosci 107(5): 876-881.

Karlsson, B., A. Knutsson and B. Lindahl (2001). "Is there an association between shift work and having a metabolic syndrome? Results from a population based study of 27,485 people." Occup Environ Med 58(11): 747-752.

Karlsson, B. H., A. K. Knutsson, B. O. Lindahl and L. S. Alfredsson (2003). "Metabolic disturbances in male workers with rotating three-shift work. Results of the WOLF study." Int Arch Occup Environ Health 76(6): 424-430.

Kaser, S., A. Kaser, A. Sandhofer, C. F. Ebenbichler, H. Tilg and J. R. Patsch (2003). "Resistin messenger-RNA expression is increased by proinflammatory cytokines in vitro." Biochem Biophys Res Commun 309(2): 286-290.

Kasukawa, T., M. Sugimoto, A. Hida, Y. Minami, M. Mori, S. Honma, K. Honma, K. Mishima, T. Soga and H. R. Ueda (2012). "Human blood metabolite timetable indicates internal body time." Proc Natl Acad Sci U S A 109(37): 15036-15041.

Kern, P. A., S. Ranganathan, C. Li, L. Wood and G. Ranganathan (2001). "Adipose tissue tumor necrosis factor and interleukin-6 expression in human obesity and insulin resistance." Am J Physiol Endocrinol Metab 280(5): E745-751.

Kern, P. A., M. Saghizadeh, J. M. Ong, R. J. Bosch, R. Deem and R. B. Simsolo (1995). "The expression of tumor necrosis factor in human adipose tissue. Regulation by obesity, weight loss, and relationship to lipoprotein lipase." J Clin Invest 95(5): 2111-2119.

Kershaw, E. E., J. K. Hamm, L. A. Verhagen, O. Peroni, M. Katic and J. S. Flier (2006). "Adipose triglyceride lipase: function, regulation by insulin, and comparison with adiponutrin." Diabetes 55(1): 148-157.

Kharroubi, I., J. Rasschaert, D. L. Eizirik and M. Cnop (2003). "Expression of adiponectin receptors in pancreatic beta cells." Biochem Biophys Res Commun 312(4): 1118-1122.

Kida, K., T. Nishio, T. Yokozawa, K. Nagai, H. Matsuda and H. Nakagawa (1980). "The circadian change of gluconeogenesis in the liver in vivo in fed rats." J Biochem 88(4): 1009-1013.

Kiguchi, N., T. Maeda, Y. Kobayashi, Y. Fukazawa and S. Kishioka (2009). "Leptin enhances CC-chemokine ligand expression in cultured murine macrophage." Biochem Biophys Res Commun 384(3): 311-315.

Kim, J. K., J. J. Fillmore, Y. Chen, C. Yu, I. K. Moore, M. Pypaert, E. P. Lutz, Y. Kako, W. Velez-Carrasco, I. J. Goldberg, J. L. Breslow and G. I. Shulman (2001). "Tissue-specific overexpression of lipoprotein lipase causes tissue-specific insulin resistance." Proc Natl Acad Sci U S A 98(13): 7522-7527.

Kim, J. Y., E. van de Wall, M. Laplante, A. Azzara, M. E. Trujillo, S. M. Hofmann, T. Schraw, J. L. Durand, H. Li, G. Li, L. A. Jelicks, M. F. Mehler, D. Y. Hui, Y. Deshaies, G. I. Shulman, G. J. Schwartz and P. E. Scherer (2007). "Obesity-associated improvements in metabolic profile through expansion of adipose tissue." J Clin Invest 117(9): 2621-2637.

Kim, S. M., N. Neuendorff, R. S. Chapkin and D. J. Earnest (2016). "Role of Inflammatory Signaling in the Differential Effects of Saturated and Poly-unsaturated Fatty Acids on Peripheral Circadian Clocks." EBioMedicine 7: 100-111.

Kino, T. (2012). "Circadian rhythms of glucocorticoid hormone actions in target tissues: potential clinical implications." Sci Signal 5(244): pt4.

Kissileff, H. R., F. X. Pi-Sunyer, J. Thornton and G. P. Smith (1981). "C-terminal octapeptide of cholecystokinin decreases food intake in man." Am J Clin Nutr 34(2): 154-160.

Kleemann, R., M. van Erk, L. Verschuren, A. M. van den Hoek, M. Koek, P. Y. Wielinga, A. Jie, L. Pellis, I. Bobeldijk-Pastorova, T. Kelder, K. Toet, S. Wopereis, N. Cnubben, C. Evelo, B. van Ommen and T. Kooistra (2010). "Time-resolved and tissue-specific systems analysis of the pathogenesis of insulin resistance." PLoS One 5(1): e8817.

Kleiber, M. (1947). "Body size and metabolic rate." Physiol Rev 27(4): 511-541.

Klein, S., J. F. Horowitz, M. Landt, S. J. Goodrick, V. Mohamed-Ali and S. W. Coppack (2000). "Leptin production during early starvation in lean and obese women." Am J Physiol Endocrinol Metab 278(2): E280-284.

Knutson, K. L. and E. Van Cauter (2008). "Associations between sleep loss and increased risk of obesity and diabetes." Ann N Y Acad Sci 1129: 287-304.

Kohlwein, S. D., M. Veenhuis and I. J. van der Klei (2013). "Lipid droplets and peroxisomes: key players in cellular lipid homeostasis or a matter of fat--store 'em up or burn 'em down." Genetics 193(1): 1-50.

Kohsaka, A., A. D. Laposky, K. M. Ramsey, C. Estrada, C. Joshu, Y. Kobayashi, F. W. Turek and J. Bass (2007). "High-fat diet disrupts behavioral and molecular circadian rhythms in mice." Cell Metab 6(5): 414-421.

Koike, N., S. H. Yoo, H. C. Huang, V. Kumar, C. Lee, T. K. Kim and J. S. Takahashi (2012). "Transcriptional architecture and chromatin landscape of the core circadian clock in mammals." Science 338(6105): 349-354.

Kojima, S., M. Hirose, K. Tokunaga, Y. Sakaki and H. Tei (2003). "Structural and functional analysis of 3' untranslated region of mouse Period1 mRNA." Biochem Biophys Res Commun 301(1): 1-7.

Kondratov, R. V., A. A. Kondratova, V. Y. Gorbacheva, O. V. Vykhovanets and M. P. Antoch (2006). "Early aging and age-related pathologies in mice deficient in BMAL1, the core componentof the circadian clock." Genes Dev 20(14): 1868-1873.

Konturek, S. J., J. W. Konturek, T. Pawlik and T. Brzozowski (2004). "Brain-gut axis and its role in the control of food intake." J Physiol Pharmacol 55(1 Pt 2): 137-154.

Kornmann, B., O. Schaad, H. Reinke, C. Saini and U. Schibler (2007). "Regulation of circadian gene expression in liver by systemic signals and hepatocyte oscillators." Cold Spring Harb Symp Quant Biol 72: 319-330.

Koves, T. R., J. R. Ussher, R. C. Noland, D. Slentz, M. Mosedale, O. Ilkayeva, J. Bain, R. Stevens, J. R. Dyck, C. B. Newgard, G. D. Lopaschuk and D. M. Muoio (2008). "Mitochondrial overload and incomplete fatty acid oxidation contribute to skeletal muscle insulin resistance." Cell Metab 7(1): 45-56.

Krude, H., H. Biebermann, W. Luck, R. Horn, G. Brabant and A. Gruters (1998). "Severe early-onset obesity, adrenal insufficiency and red hair pigmentation caused by POMC mutations in humans." Nat Genet 19(2): 155-157.

Krude, H. and A. Gruters (2000). "Implications of proopiomelanocortin (POMC) mutations in humans: the POMC deficiency syndrome." Trends Endocrinol Metab 11(1): 15-22.

Kudo, T., K. Horikawa and S. Shibata (2007). "Circadian rhythms in the CNS and peripheral clock disorders: the circadian clock and hyperlipidemia." J Pharmacol Sci 103(2): 139-143.

Kumada, M., S. Kihara, N. Ouchi, H. Kobayashi, Y. Okamoto, K. Ohashi, K. Maeda, H. Nagaretani, K. Kishida, N. Maeda, A. Nagasawa, T. Funahashi and Y. Matsuzawa (2004). "Adiponectin specifically increased tissue inhibitor of metalloproteinase-1 through interleukin-10 expression in human macrophages." Circulation 109(17): 2046-2049.

Kumar, N., L. A. Solt, Y. Wang, P. M. Rogers, G. Bhattacharyya, T. M. Kamenecka, K. R. Stayrook, C. Crumbley, Z. E. Floyd, J. M. Gimble, P. R. Griffin and T. P. Burris (2010). "Regulation of adipogenesis by natural and synthetic REV-ERB ligands." Endocrinology 151(7): 3015-3025.

Kusminski, C. M., W. L. Holland, K. Sun, J. Park, S. B. Spurgin, Y. Lin, G. R. Askew, J. A. Simcox, D. A. McClain, C. Li and P. E. Scherer (2012). "MitoNEET-driven alterations in adipocyte mitochondrial activity reveal a crucial adaptive process that preserves insulin sensitivity in obesity." Nat Med 18(10): 1539-1549.

Kwak, E., T. D. Kim and K. T. Kim (2006). "Essential role of 3'-untranslated region-mediated mRNA decay in circadian oscillations of mouse Period3 mRNA." J Biol Chem 281(28): 19100-19106.

La Fleur, S. E., A. Kalsbeek, J. Wortel and R. M. Buijs (1999). "A suprachiasmatic nucleus generated rhythm in basal glucose concentrations." J Neuroendocrinol 11(8): 643-652.

la Fleur, S. E., A. Kalsbeek, J. Wortel, M. L. Fekkes and R. M. Buijs (2001). "A daily rhythm in glucose tolerance: a role for the suprachiasmatic nucleus." Diabetes 50(6): 1237-1243.

Labouebe, G., S. Liu, C. Dias, H. Zou, J. C. Wong, S. Karunakaran, S. M. Clee, A. G. Phillips, B. Boutrel and S. L. Borgland (2013). "Insulin induces long-term depression of ventral tegmental area dopamine neurons via endocannabinoids." Nat Neurosci 16(3): 300-308.

Lafontan, M., C. Moro, C. Sengenes, J. Galitzky, F. Crampes and M. Berlan (2005). "An unsuspected metabolic role for atrial natriuretic peptides: the control of lipolysis, lipid mobilization, and systemic nonesterified fatty acids levels in humans." Arterioscler Thromb Vasc Biol 25(10): 2032-2042.

Laforgia, J., R. T. Withers, N. J. Shipp and C. J. Gore (1997). "Comparison of energy expenditure elevations after submaximal and supramaximal running." J Appl Physiol (1985) 82(2): 661-666.

Lamia, K. A., S. J. Papp, R. T. Yu, G. D. Barish, N. H. Uhlenhaut, J. W. Jonker, M. Downes and R. M. Evans (2011). "Cryptochromes mediate rhythmic repression of the glucocorticoid receptor." Nature 480(7378): 552-556.

Lamia, K. A., U. M. Sachdeva, L. DiTacchio, E. C. Williams, J. G. Alvarez, D. F. Egan, D. S. Vasquez, H. Juguilon, S. Panda, R. J. Shaw, C. B. Thompson and R. M. Evans (2009). "AMPK regulates the circadian clock by cryptochrome phosphorylation and degradation." Science 326(5951): 437-440.

Lamia, K. A., K. F. Storch and C. J. Weitz (2008). "Physiological significance of a peripheral tissue circadian clock." Proc Natl Acad Sci U S A 105(39): 15172-15177.

Landau, B. R., J. Wahren, et al. (1996). "Contributions of gluconeogenesis to glucose production in the fasted state." J Clin Invest 98(2): 378-385.

Langin, D., A. Dicker, G. Tavernier, J. Hoffstedt, A. Mairal, M. Ryden, E. Arner, A. Sicard, C. M. Jenkins, N. Viguerie, V. van Harmelen, R. W. Gross, C. Holm and P. Arner (2005). "Adipocyte lipases and defect of lipolysis in human obesity." Diabetes 54(11): 3190-3197.

Lardizabal, K. D., J. T. Mai, N. W. Wagner, A. Wyrick, T. Voelker and D. J. Hawkins (2001). "DGAT2 is a new diacylglycerol acyltransferase gene family: purification, cloning, and expression in insect cells of two polypeptides from Mortierella ramanniana with diacylglycerol acyltransferase activity." J Biol Chem 276(42): 38862-38869.

Large, V., S. Reynisdottir, D. Langin, K. Fredby, M. Klannemark, C. Holm and P. Arner (1999). "Decreased expression and function of adipocyte hormone-sensitive lipase in subcutaneous fat cells of obese subjects." J Lipid Res 40(11): 2059-2066.

Le Magnen, J. (1988). "[Lipogenesis, lipolysis and feeding rhythms]." Ann Endocrinol (Paris) 49(2): 98-104.

Le Martelot, G., T. Claudel, D. Gatfield, O. Schaad, B. Kornmann, G. Lo Sasso, A. Moschetta and U. Schibler (2009). "REV-ERBalpha participates in circadian SREBP signaling and bile acid homeostasis." PLoS Biol 7(9): e1000181.

Le Minh, N., F. Damiola, F. Tronche, G. Schutz and U. Schibler (2001). "Glucocorticoid hormones inhibit food-induced phase-shifting of peripheral circadian oscillators." EMBO J 20(24): 7128-7136.

Le Roith, D. and Y. Zick (2001). "Recent advances in our understanding of insulin action and insulin resistance." Diabetes Care 24(3): 588-597.

Le Stunff, C., C. Le Bihan, N. J. Schork and P. Bougneres (2000). "A common promoter variant of the leptin gene is associated with changes in the relationship between serum leptin and fat mass in obese girls." Diabetes 49(12): 2196-2200.

Leak, R. K. and R. Y. Moore (2001). "Topographic organization of suprachiasmatic nucleus projection neurons." J Comp Neurol 433(3): 312-334.

Lee, A., M. Ader, G. A. Bray and R. N. Bergman (1992). "Diurnal variation in glucose tolerance. Cyclic suppression of insulin action and insulin secretion in normal-weight, but not obese, subjects." Diabetes 41(6): 750-759.

Lee, C., J. P. Etchegaray, F. R. Cagampang, A. S. Loudon and S. M. Reppert (2001). "Posttranslational mechanisms regulate the mammalian circadian clock." Cell 107(7): 855-867.

Lee, H. M., R. Chen, H. Kim, J. P. Etchegaray, D. R. Weaver and C. Lee (2011). "The period of the circadian oscillator is primarily determined by the balance between casein kinase 1 and protein phosphatase 1." Proc Natl Acad Sci U S A 108(39): 16451-16456.

Lee, Y. S., J. W. Kim, O. Osborne, D. Y. Oh, R. Sasik, S. Schenk, A. Chen, H. Chung, A. Murphy, S. M. Watkins, O. Quehenberger, R. S. Johnson and J. M. Olefsky (2014). "Increased adipocyte O2 consumption triggers HIF-1alpha, causing inflammation and insulin resistance in obesity." Cell 157(6): 1339-1352.

Lehman, M. N., R. Silver, W. R. Gladstone, R. M. Kahn, M. Gibson and E. L. Bittman (1987). "Circadian rhythmicity restored by neural transplant. Immunocytochemical characterization of the graft and its integration with the host brain." J Neurosci 7(6): 1626-1638.

Leone, M. J., L. Marpegan, J. M. Duhart and D. A. Golombek (2012). "Role of proinflammatory cytokines on lipopolysaccharide-induced phase shifts in locomotor activity circadian rhythm." Chronobiol Int 29(6): 715-723.

Levine, J. A., N. L. Eberhardt and M. D. Jensen (1999). "Role of nonexercise activity thermogenesis in resistance to fat gain in humans." Science 283(5399): 212-214.

Li, S., Q. Yu, G. X. Wang and J. D. Lin (2013). "The biological clock is regulated by adrenergic signaling in brown fat but is dispensable for cold-induced thermogenesis." PLoS One 8(8): e70109.

Lieverse, R. J., A. A. Masclee, J. B. Jansen, L. C. Rovati and C. B. Lamers (1995). "Satiety effects of the type A CCK receptor antagonist loxiglumide in lean and obese women." Biol Psychiatry 37(5): 331-335.

Lin, F. T. and M. D. Lane (1994). "CCAAT/enhancer binding protein alpha is sufficient to initiate the 3T3-L1 adipocyte differentiation program." Proc Natl Acad Sci U S A 91(19): 8757-8761.

Lin, J., P. H. Wu, P. T. Tarr, K. S. Lindenberg, J. St-Pierre, C. Y. Zhang, V. K. Mootha, S. Jager, C. R. Vianna, R. M. Reznick, L. Cui, M. Manieri, M. X. Donovan, Z. Wu, M. P. Cooper, M. C. Fan, L. M. Rohas, A. M. Zavacki, S. Cinti, G. I. Shulman, B. B. Lowell, D. Krainc and B. M. Spiegelman (2004). "Defects in adaptive energy metabolism with CNS-linked hyperactivity in PGC-1alpha null mice." Cell 119(1): 121-135.

Liu, C., S. Li, T. Liu, J. Borjigin and J. D. Lin (2007). "Transcriptional coactivator PGC-1alpha integrates the mammalian clock and energy metabolism." Nature 447(7143): 477-481.

Liu, C., D. R. Weaver, X. Jin, L. P. Shearman, R. L. Pieschl, V. K. Gribkoff and S. M. Reppert (1997). "Molecular dissection of two distinct actions of melatonin on the suprachiasmatic circadian clock." Neuron 19(1): 91-102.

Lodish, H., Berk A. and Kaiser C. (2007). *Molecular Cell Biology*. 6th Ed. New York: W.H.Freeman.

Loftus, T. M., D. E. Jaworsky, G. L. Frehywot, C. A. Townsend, G. V. Ronnett, M. D. Lane and F. P. Kuhajda (2000). "Reduced food intake and body weight in mice treated with fatty acid synthase inhibitors." Science 288(5475): 2379-2381.

Lorente-Cebrian, S., A. Kulyte, P. Heden, E. Naslund, P. Arner and M. Ryden (2011). "Relationship between site-specific HSL phosphorylation and adipocyte lipolysis in obese women." Obes Facts 4(5): 365-371.

Lowrey, P. L., K. Shimomura, M. P. Antoch, S. Yamazaki, P. D. Zemenides, M. R. Ralph, M. Menaker and J. S. Takahashi (2000). "Positional syntenic cloning and functional characterization of the mammalian circadian mutation tau." Science 288(5465): 483-492.

Lowe, M. E. (1994). "Pancreatic triglyceride lipase and colipase: insights into dietary fat digestion." Gastroenterology 107(5): 1524-1536.

Lowrey, P. L. and J. S. Takahashi (2004). "Mammalian circadian biology: elucidating genome-wide levels of temporal organization." Annu Rev Genomics Hum Genet 5: 407-441.

Lumeng, C. N., J. L. Bodzin and A. R. Saltiel (2007). "Obesity induces a phenotypic switch in adipose tissue macrophage polarization." J Clin Invest 117(1): 175-184.

Ma, L. J., S. L. Mao, K. L. Taylor, T. Kanjanabuch, Y. Guan, Y. Zhang, N. J. Brown, L. L. Swift, O. P. McGuinness, D. H. Wasserman, D. E. Vaughan and A. B. Fogo (2004). "Prevention of obesity and insulin resistance in mice lacking plasminogen activator inhibitor 1." Diabetes 53(2): 336-346.

Maeda, K., K. Okubo, I. Shimomura, K. Mizuno, Y. Matsuzawa and K. Matsubara (1997). "Analysis of an expression profile of genes in the human adipose tissue." Gene 190(2): 227-235.

Maeda, N., I. Shimomura, K. Kishida, H. Nishizawa, M. Matsuda, H. Nagaretani, N. Furuyama, H. Kondo, M. Takahashi, Y. Arita, R. Komuro, N. Ouchi, S. Kihara, Y. Tochino, K. Okutomi, M. Horie, S. Takeda, T. Aoyama, T. Funahashi and Y. Matsuzawa (2002). "Diet-induced insulin resistance in mice lacking adiponectin/ACRP30." Nat Med 8(7): 731-737.

Maffei, M., J. Halaas, E. Ravussin, R. E. Pratley, G. H. Lee, Y. Zhang, H. Fei, S. Kim, R. Lallone, S. Ranganathan and et al. (1995). "Leptin levels in human and rodent: measurement of plasma leptin and ob RNA in obese and weight-reduced subjects." Nat Med 1(11): 1155-1161.

Mahley, R. W., T. L. Innerarity, S. C. Rall, Jr. and K. H. Weisgraber (1984). "Plasma lipoproteins: apolipoprotein structure and function." J Lipid Res 25(12): 1277-1294.

Mancini, F. P., A. Lanni, L. Sabatino, M. Moreno, A. Giannino, F. Contaldo, V. Colantuoni and F. Goglia (2001). "Fenofibrate prevents and reduces body weight gain and adiposity in diet-induced obese rats." FEBS Lett 491(1-2): 154-158.

Mansbach, C. M., 2nd and S. Siddiqi (2016). "Control of chylomicron export from the intestine." Am J Physiol Gastrointest Liver Physiol 310(9): G659-668.

Marcheva, B., K. M. Ramsey, E. D. Buhr, Y. Kobayashi, H. Su, C. H. Ko, G. Ivanova, C. Omura, S. Mo, M. H. Vitaterna, J. P. Lopez, L. H. Philipson, C. A. Bradfield, S. D. Crosby, L. JeBailey, X. Wang, J. S. Takahashi and J. Bass (2010). "Disruption of the clock components CLOCK and BMAL1 leads to hypoinsulinaemia and diabetes." Nature 466(7306): 627-631.

Markwald, R. R., E. L. Melanson, M. R. Smith, J. Higgins, L. Perreault, R. H. Eckel and K. P. Wright, Jr. (2013). "Impact of insufficient sleep on total daily energy expenditure, food intake, and weight gain." Proc Natl Acad Sci U S A 110(14): 5695-5700.

Martin, L. F., C. M. Klim, S. J. Vannucci, L. B. Dixon, J. R. Landis and K. F. LaNoue (1990). "Alterations in adipocyte adenylate cyclase activity in morbidly obese and formerly morbidly obese humans." Surgery 108(2): 228-234; discussion 234-225.

Masri, S. and P. Sassone-Corsi (2010). "Plasticity and specificity of the circadian epigenome." Nat Neurosci 13(11): 1324-1329.

Matamala, J. C., M. Gianotti, J. Pericas, S. Quevedo, P. Roca, A. Palou and F. J. Garcia-Palmer (1996). "Changes induced by fasting and dietetic obesity in thermogenic parameters of rat brown adipose tissue mitochondrial subpopulations." Biochem J 319 (Pt 2): 529-534.

Maury, E., K. M. Ramsey and J. Bass (2010). "Circadian rhythms and metabolic syndrome: from experimental genetics to human disease." Circ Res 106(3): 447-462.

Maywood, E. S., J. E. Chesham, J. A. O'Brien and M. H. Hastings (2011). "A diversity of paracrine signals sustains molecular circadian cycling in suprachiasmatic nucleus circuits." Proc Natl Acad Sci U S A 108(34): 14306-14311.

McHill, A. W., E. L. Melanson, J. Higgins, E. Connick, T. M. Moehlman, E. R. Stothard and K. P. Wright, Jr. (2014). "Impact of circadian misalignment on energy metabolism during simulated nightshift work." Proc Natl Acad Sci U S A 111(48): 17302-17307.

Mead, J. R., S. A. Irvine and D. P. Ramji (2002). "Lipoprotein lipase: structure, function, regulation, and role in disease." J Mol Med (Berl) 80(12): 753-769.

Mebel, D. M., J. C. Wong, Y. J. Dong and S. L. Borgland (2012). "Insulin in the ventral tegmental area reduces hedonic feeding and suppresses dopamine concentration via increased reuptake." Eur J Neurosci 36(3): 2336-2346.

Meister, B. (2000). "Control of food intake via leptin receptors in the hypothalamus." Vitam Horm 59: 265-304.

Mertens, I. and L. F. Van Gaal (2002). "Obesity, haemostasis and the fibrinolytic system." Obes Rev 3(2): 85-101.

Meyer-Bernstein, E. L. and L. P. Morin (1999). "Electrical stimulation of the median or dorsal raphe nuclei reduces light-induced FOS protein in the suprachiasmatic nucleus and causes circadian activity rhythm phase shifts." Neuroscience 92(1): 267-279.

Migliorini, R. H., M. A. Garofalo and I. C. Kettelhut (1997). "Increased sympathetic activity in rat white adipose tissue during prolonged fasting." Am J Physiol 272(2 Pt 2): R656-661.

Miles, J. M. and M. D. Jensen (1993). "Does glucagon regulate adipose tissue lipolysis?" J Clin Endocrinol Metab 77(1): 5A-5B.

Minokoshi, Y., T. Alquier, N. Furukawa, Y. B. Kim, A. Lee, B. Xue, J. Mu, F. Foufelle, P. Ferre, M. J. Birnbaum, B. J. Stuck and B. B. Kahn (2004). "AMP-kinase regulates food intake by responding to hormonal and nutrient signals in the hypothalamus." Nature 428(6982): 569-574.

Minokoshi, Y., T. Shiuchi, S. Lee, A. Suzuki and S. Okamoto (2008). "Role of hypothalamic AMP-kinase in food intake regulation." Nutrition 24(9): 786-790.

Mirani-Oostdijk, C. P., L. Havekes, C. M. Van Gent, M. Frolich, H. Jansen and J. Terpstra (1985). "Diurnal changes in serum triglycerides as related to changes in lipolytic enzymes, lipoproteins

and hormones in patients with primary endogenous hypertriglyceridaemia on a carbohydrate-rich diet." Atherosclerosis 57(2-3): 129-137.

Mistlberger, R. E. (1994). "Circadian food-anticipatory activity: formal models and physiological mechanisms." Neurosci Biobehav Rev 18(2): 171-195.

Montague, C. T., I. S. Farooqi, J. P. Whitehead, M. A. Soos, H. Rau, N. J. Wareham, C. P. Sewter, J. E. Digby, S. N. Mohammed, J. A. Hurst, C. H. Cheetham, A. R. Earley, A. H. Barnett, J. B. Prins and S. O'Rahilly (1997). "Congenital leptin deficiency is associated with severe early-onset obesity in humans." Nature 387(6636): 903-908.

Montague, C. T. and S. O'Rahilly (2000). "The perils of portliness: causes and consequences of visceral adiposity." Diabetes 49(6): 883-888.

Mooney, R. A., J. Senn, S. Cameron, N. Inamdar, L. M. Boivin, Y. Shang and R. W. Furlanetto (2001). "Suppressors of cytokine signaling-1 and -6 associate with and inhibit the insulin receptor. A potential mechanism for cytokine-mediated insulin resistance." J Biol Chem 276(28): 25889-25893.

Moore, R. Y. and V. B. Eichler (1972). "Loss of a circadian adrenal corticosterone rhythm following suprachiasmatic lesions in the rat." Brain Res 42(1): 201-206.

Moore, R. Y., J. C. Speh and J. P. Card (1995). "The retinohypothalamic tract originates from a distinct subset of retinal ganglion cells." J Comp Neurol 352(3): 351-366.

Moran, T. H., P. Lee, E. E. Ladenheim and G. J. Schwartz (2002). "Responsivity to NPY and melanocortins in obese OLETF rats lacking CCK-A receptors." Physiol Behav 75(3): 397-402.

Morgan, L., J. Arendt, D. Owens, S. Folkard, S. Hampton, S. Deacon, J. English, D. Ribeiro and K. Taylor (1998). "Effects of the endogenous clock and sleep time on melatonin, insulin, glucose and lipid metabolism." J Endocrinol 157(3): 443-451.

Morin, L. P. (1994). "The circadian visual system." Brain Res Brain Res Rev 19(1): 102-127.

Morris, C. J., J. N. Yang and F. A. Scheer (2012). "The impact of the circadian timing system on cardiovascular and metabolic function." Prog Brain Res 199: 337-358.

Mortimer, B. C., D. J. Beveridge, C. T. Phan, C. Lutton and T. G. Redgrave (1998). "The diurnal rhythms of cholesterol metabolism and plasma clearance of model chylomicrons: comparison of normal and genetically hypercholesterolemic rats (RICO)." Comp Biochem Physiol A Mol Integr Physiol 120(4): 671-680.

Morton, G. J., D. E. Cummings, D. G. Baskin, G. S. Barsh and M. W. Schwartz (2006). "Central nervous system control of food intake and body weight." Nature 443(7109): 289-295.

Mukherji, A., A. Kobiita, M. Damara, N. Misra, H. Meziane, M. F. Champy and P. Chambon (2015). "Shifting eating to the circadian rest phase misaligns the peripheral clocks with the master SCN clock and leads to a metabolic syndrome." Proc Natl Acad Sci U S A 112(48): E6691-6698.

Mukherji, A., A. Kobiita, T. Ye and P. Chambon (2013). "Homeostasis in intestinal epithelium is orchestrated by the circadian clock and microbiota cues transduced by TLRs." Cell 153(4): 812-827.

Murdoch, S. J. and W. C. Breckenridge (1995). "Influence of lipoprotein lipase and hepatic lipase on the transformation of VLDL and HDL during lipolysis of VLDL." Atherosclerosis 118(2): 193-212.

Myers, M. G., M. A. Cowley and H. Munzberg (2008). "Mechanisms of leptin action and leptin resistance." Annu Rev Physiol 70: 537-556.

Nader, N., G. P. Chrousos and T. Kino (2009). "Circadian rhythm transcription factor CLOCK regulates the transcriptional activity of the glucocorticoid receptor by acetylating its hinge region lysine cluster: potential physiological implications." FASEB J 23(5): 1572-1583.

Nakahata, Y., S. Sahar, G. Astarita, M. Kaluzova and P. Sassone-Corsi (2009). "Circadian control of the NAD+ salvage pathway by CLOCK-SIRT1." Science 324(5927): 654-657.

Nallamshetty, S., S. Y. Chan and J. Loscalzo (2013). "Hypoxia: a master regulator of microRNA biogenesis and activity." Free Radic Biol Med 64: 20-30.

National Health Service 2012 (England), *National Diabetes Audit*, viewed 6th June 2016. Available at: < http://digital.nhs.uk/catalogue/PUB12421/nati-diab-audi-11-12-summ-rep.pdf>

Nielsen, T. S., M. H. Vendelbo, N. Jessen, S. B. Pedersen, J. O. Jorgensen, S. Lund and N. Moller (2011). "Fasting, but not exercise, increases adipose triglyceride lipase (ATGL) protein and reduces G(0)/G(1) switch gene 2 (G0S2) protein and mRNA content in human adipose tissue." J Clin Endocrinol Metab 96(8): E1293-1297.

Norrelund, H., C. Djurhuus, J. O. Jorgensen, S. Nielsen, K. S. Nair, O. Schmitz, J. S. Christiansen and N. Moller (2003). "Effects of GH on urea, glucose and lipid metabolism, and insulin sensitivity during fasting in GH-deficient patients." Am J Physiol Endocrinol Metab 285(4): E737-743.

Norrelund, H., N. Moller, K. S. Nair, J. S. Christiansen and J. O. Jorgensen (2001). "Continuation of growth hormone (GH) substitution during fasting in GH-deficient patients decreases urea excretion and conserves protein synthesis." J Clin Endocrinol Metab 86(7): 3120-3129.

Obici, S., Z. Feng, K. Morgan, D. Stein, G. Karkanias and L. Rossetti (2002). "Central administration of oleic acid inhibits glucose production and food intake." Diabetes 51(2): 271-275.

Oishi, K., N. Amagai, H. Shirai, K. Kadota, N. Ohkura and N. Ishida (2005). "Genome-wide expression analysis reveals 100 adrenal gland-dependent circadian genes in the mouse liver." DNA Res 12(3): 191-202.

Oishi, K., G. Atsumi, S. Sugiyama, I. Kodomari, M. Kasamatsu, K. Machida and N. Ishida (2006). "Disrupted fat absorption attenuates obesity induced by a high-fat diet in Clock mutant mice." FEBS Lett 580(1): 127-130.

Oishi, K., K. Miyazaki, K. Kadota, R. Kikuno, T. Nagase, G. Atsumi, N. Ohkura, T. Azama, M. Mesaki, S. Yukimasa, H. Kobayashi, C. Iitaka, T. Umehara, M. Horikoshi, T. Kudo, Y. Shimizu, M. Yano, M. Monden, K. Machida, J. Matsuda, S. Horie, T. Todo and N. Ishida (2003). "Genome-wide expression analysis of mouse liver reveals CLOCK-regulated circadian output genes." J Biol Chem 278(42): 41519-41527.

Okuno, A., H. Tamemoto, K. Tobe, K. Ueki, Y. Mori, K. Iwamoto, K. Umesono, Y. Akanuma, T. Fujiwara, H. Horikoshi, Y. Yazaki and T. Kadowaki (1998). "Troglitazone increases the number of

small adipocytes without the change of white adipose tissue mass in obese Zucker rats." J Clin Invest 101(6): 1354-1361.

Oster, H., S. Damerow, S. Kiessling, V. Jakubcakova, D. Abraham, J. Tian, M. W. Hoffmann and G. Eichele (2006). "The circadian rhythm of glucocorticoids is regulated by a gating mechanism residing in the adrenal cortical clock." Cell Metab 4(2): 163-173.

Otway, D. T., S. Mantele, S. Bretschneider, J. Wright, P. Trayhurn, D. J. Skene, M. D. Robertson and J. D. Johnston (2011). "Rhythmic diurnal gene expression in human adipose tissue from individuals who are lean, overweight, and type 2 diabetic." Diabetes 60(5): 1577-1581.

Ouchi, N., S. Kihara, Y. Arita, M. Nishida, A. Matsuyama, Y. Okamoto, M. Ishigami, H. Kuriyama, K. Kishida, H. Nishizawa, K. Hotta, M. Muraguchi, Y. Ohmoto, S. Yamashita, T. Funahashi and Y. Matsuzawa (2001). "Adipocyte-derived plasma protein, adiponectin, suppresses lipid accumulation and class A scavenger receptor expression in human monocyte-derived macrophages." Circulation 103(8): 1057-1063.

Paladino, N., M. L. Mul Fedele, J. M. Duhart, L. Marpegan and D. A. Golombek (2014). "Modulation of mammalian circadian rhythms by tumor necrosis factor-alpha." Chronobiol Int 31(5): 668-679.

Pan, A., E. S. Schernhammer, Q. Sun and F. B. Hu (2011). "Rotating night shift work and risk of type 2 diabetes: two prospective cohort studies in women." PLoS Med 8(12): e1001141.

Pan, X. and M. M. Hussain (2009). "Clock is important for food and circadian regulation of macronutrient absorption in mice." J Lipid Res 50(9): 1800-1813.

Pan, X., Y. Zhang, L. Wang and M. M. Hussain (2010). "Diurnal regulation of MTP and plasma triglyceride by CLOCK is mediated by SHP." Cell Metab 12(2): 174-186.

Panda, S., M. P. Antoch, B. H. Miller, A. I. Su, A. B. Schook, M. Straume, P. G. Schultz, S. A. Kay, J. S. Takahashi and J. B. Hogenesch (2002). "Coordinated transcription of key pathways in the mouse by the circadian clock." Cell 109(3): 307-320.

Partch, C. L., K. F. Shields, C. L. Thompson, C. P. Selby and A. Sancar (2006). "Posttranslational regulation of the mammalian circadian clock by cryptochrome and protein phosphatase 5." Proc Natl Acad Sci U S A 103(27): 10467-10472.

Paschos, G. K., S. Ibrahim, W. L. Song, T. Kunieda, G. Grant, T. M. Reyes, C. A. Bradfield, C. H. Vaughan, M. Eiden, M. Masoodi, J. L. Griffin, F. Wang, J. A. Lawson and G. A. Fitzgerald (2012). "Obesity in mice with adipocyte-specific deletion of clock component Arntl." Nat Med 18(12): 1768-1777.

Pascual, G., A. L. Fong, S. Ogawa, A. Gamliel, A. C. Li, V. Perissi, D. W. Rose, T. M. Willson, M. G. Rosenfeld and C. K. Glass (2005). "A SUMOylation-dependent pathway mediates transrepression of inflammatory response genes by PPAR-gamma." Nature 437(7059): 759-763.

Patsouris, D., J. K. Reddy, M. Muller and S. Kersten (2006). "Peroxisome proliferator-activated receptor alpha mediates the effects of high-fat diet on hepatic gene expression." Endocrinology 147(3): 1508-1516.

Peek, C. B., K. M. Ramsey, B. Marcheva and J. Bass (2012). "Nutrient sensing and the circadian clock." Trends Endocrinol Metab 23(7): 312-318.

Pendergast, J. S., G. A. Oda, K. D. Niswender and S. Yamazaki (2012). "Period determination in the food-entrainable and methamphetamine-sensitive circadian oscillator(s)." Proc Natl Acad Sci U S A 109(35): 14218-14223.

Peret, J., M. Chanez and G. Pascal (1976). "Schedule of protein ingestion and circadian rhythm of certain hepatic enzyme activities involved in glucose metabolism in the rat." Nutr Metab 20(2): 143-157.

Perreault, M. and A. Marette (2001). "Targeted disruption of inducible nitric oxide synthase protects against obesity-linked insulin resistance in muscle." Nat Med 7(10): 1138-1143.

Petrovic, N., T. B. Walden, I. G. Shabalina, J. A. Timmons, B. Cannon and J. Nedergaard (2010). "Chronic peroxisome proliferator-activated receptor gamma (PPARgamma) activation of epididymally derived white adipocyte cultures reveals a population of thermogenically competent, UCP1-containing adipocytes molecularly distinct from classic brown adipocytes." J Biol Chem 285(10): 7153-7164.

Phillips, L. J. and L. J. Berry (1970). "Circadian rhythm of mouse liver phosphoenolpyruvate carboxykinase." Am J Physiol 218(5): 1440-1444.

Phumala, N., S. Porasuphatana, S. Unchern, P. Pootrakul, S. Fucharoen and U. Chantharaksri (2003). "Hemin: a possible cause of oxidative stress in blood circulation of beta-thalassemia/hemoglobin E disease." Free Radic Res 37(2): 129-135.

Pickard, G. E. (1985). "Bifurcating axons of retinal ganglion cells terminate in the hypothalamic suprachiasmatic nucleus and the intergeniculate leaflet of the thalamus." Neurosci Lett 55(2): 211-217.

Pietilainen, K. H., T. Rog, T. Seppanen-Laakso, S. Virtue, P. Gopalacharyulu, J. Tang, S. Rodriguez-Cuenca, A. Maciejewski, J. Naukkarinen, A. L. Ruskeepaa, P. S. Niemela, L. Yetukuri, C. Y. Tan, V. Velagapudi, S. Castillo, H. Nygren, T. Hyotylainen, A. Rissanen, J. Kaprio, H. Yki-Jarvinen, I. Vattulainen, A. Vidal-Puig and M. Oresic (2011). "Association of lipidome remodeling in the adipocyte membrane with acquired obesity in humans." PLoS Biol 9(6): e1000623.

Ponka, P. and C. N. Lok (1999). "The transferrin receptor: role in health and disease." Int J Biochem Cell Biol 31(10): 1111-1137.

Prasai, M. J., R. S. Mughal, S. B. Wheatcroft, M. T. Kearney, P. J. Grant and E. M. Scott (2013). "Diurnal variation in vascular and metabolic function in diet-induced obesity: divergence of insulin resistance and loss of clock rhythm." Diabetes 62(6): 1981-1989.

Preitner, N., F. Damiola, L. Lopez-Molina, J. Zakany, D. Duboule, U. Albrecht and U. Schibler (2002). "The orphan nuclear receptor REV-ERBalpha controls circadian transcription within the positive limb of the mammalian circadian oscillator." Cell 110(2): 251-260.

Ptitsyn, A. A., S. Zvonic, S. A. Conrad, L. K. Scott, R. L. Mynatt and J. M. Gimble (2006). "Circadian clocks are resounding in peripheral tissues." PLoS Comput Biol 2(3): e16.

Puigserver, P., Z. Wu, C. W. Park, R. Graves, M. Wright and B. M. Spiegelman (1998). "A cold-inducible coactivator of nuclear receptors linked to adaptive thermogenesis." Cell 92(6): 829-839.

Puri, V., S. Konda, S. Ranjit, M. Aouadi, A. Chawla, M. Chouinard, A. Chakladar and M. P. Czech (2007). "Fat-specific protein 27, a novel lipid droplet protein that enhances triglyceride storage." J Biol Chem 282(47): 34213-34218.

Raghuram, S., K. R. Stayrook, P. Huang, P. M. Rogers, A. K. Nosie, D. B. McClure, L. L. Burris, S. Khorasanizadeh, T. P. Burris and F. Rastinejad (2007). "Identification of heme as the ligand for the orphan nuclear receptors REV-ERBalpha and REV-ERBbeta." Nat Struct Mol Biol 14(12): 1207-1213.

Rakatzi, I., H. Mueller, O. Ritzeler, N. Tennagels and J. Eckel (2004). "Adiponectin counteracts cytokine- and fatty acid-induced apoptosis in the pancreatic beta-cell line INS-1." Diabetologia 47(2): 249-258.

Rankinen, T., L. Perusse, R. Rauramaa, M. A. Rivera, B. Wolfarth and C. Bouchard (2001). "The human gene map for performance and health-related fitness phenotypes." Med Sci Sports Exerc 33(6): 855-867.

Rankinen, T., L. Perusse, S. J. Weisnagel, E. E. Snyder, Y. C. Chagnon and C. Bouchard (2002). "The human obesity gene map: the 2001 update." Obes Res 10(3): 196-243.

Raposo, H. F., A. A. Paiva, L. S. Kato and H. C. de Oliveira (2015). "Apolipoprotein CIII overexpression exacerbates diet-induced obesity due to adipose tissue higher exogenous lipid uptake and retention and lower lipolysis rates." Nutr Metab (Lond) 12: 61.

Raspe, E., G. Mautino, C. Duval, C. Fontaine, H. Duez, O. Barbier, D. Monte, J. Fruchart, J. C. Fruchart and B. Staels (2002). "Transcriptional regulation of human Rev-erbalpha gene expression by the orphan nuclear receptor retinoic acid-related orphan receptor alpha." J Biol Chem 277(51): 49275-49281.

Ravussin, E., B. Burnand, Y. Schutz and E. Jequier (1982). "Twenty-four-hour energy expenditure and resting metabolic rate in obese, moderately obese, and control subjects." Am J Clin Nutr 35(3): 566-573.

Reddy, A. B., N. A. Karp, E. S. Maywood, E. A. Sage, M. Deery, J. S. O'Neill, G. K. Wong, J. Chesham, M. Odell, K. S. Lilley, C. P. Kyriacou and M. H. Hastings (2006). "Circadian orchestration of the hepatic proteome." Curr Biol 16(11): 1107-1115.

Redlin, U., B. Nuesslein and I. Schmidt (1992). "Circadian changes of brown adipose tissue thermogenesis in juvenile rats." Am J Physiol 262(3 Pt 2): R504-508.

Rensing, L. and P. Ruoff (2009). "How can yeast cells decide between three activated MAP kinase pathways? A model approach." J Theor Biol 257(4): 578-587.

Reppert, S. M. and D. R. Weaver (2001). "Molecular analysis of mammalian circadian rhythms." Annu Rev Physiol 63: 647-676.

Reshef, L., R. W. Hanson and F. J. Ballard (1970). "A possible physiological role for glyceroneogenesis in rat adipose tissue." J Biol Chem 245(22): 5979-5984.

Resnick, H. E., S. Redline, E. Shahar, A. Gilpin, A. Newman, R. Walter, G. A. Ewy, B. V. Howard, N. M. Punjabi and S. Sleep Heart Health (2003). "Diabetes and sleep disturbances: findings from the Sleep Heart Health Study." Diabetes Care 26(3): 702-709.

Reynisdottir, S., D. Langin, K. Carlstrom, C. Holm, S. Rossner and P. Arner (1995). "Effects of weight reduction on the regulation of lipolysis in adipocytes of women with upper-body obesity." Clin Sci (Lond) 89(4): 421-429.

Reynisdottir, S., H. Wahrenberg, K. Carlstrom, S. Rossner and P. Arner (1994). "Catecholamine resistance in fat cells of women with upper-body obesity due to decreased expression of beta 2-adrenoceptors." Diabetologia 37(4): 428-435.

Ricote, M., A. C. Li, T. M. Willson, C. J. Kelly and C. K. Glass (1998). "The peroxisome proliferator-activated receptor-gamma is a negative regulator of macrophage activation." Nature 391(6662): 79-82.

Ripperger, J. A. and U. Schibler (2006). "Rhythmic CLOCK-BMAL1 binding to multiple E-box motifs drives circadian Dbp transcription and chromatin transitions." Nat Genet 38(3): 369-374.

Ritter, R. C. (2004). "Gastrointestinal mechanisms of satiation for food." Physiol Behav 81(2): 249-273.

Rivellese, A. A., C. De Natale, L. Di Marino, L. Patti, C. Iovine, S. Coppola, S. Del Prato, G. Riccardi and G. Annuzzi (2004). "Exogenous and endogenous postprandial lipid abnormalities in type 2 diabetic patients with optimal blood glucose control and optimal fasting triglyceride levels." J Clin Endocrinol Metab 89(5): 2153-2159.

Roberts, S. B. and V. R. Young (1988). "Energy costs of fat and protein deposition in the human infant." Am J Clin Nutr 48(4): 951-955.

Rodeheffer, M. S., K. Birsoy and J. M. Friedman (2008). "Identification of white adipocyte progenitor cells in vivo." Cell 135(2): 240-249.

Roden, M., T. B. Price, G. Perseghin, K. F. Petersen, D. L. Rothman, G. W. Cline and G. I. Shulman (1996). "Mechanism of free fatty acid-induced insulin resistance in humans." J Clin Invest 97(12): 2859-2865.

Ronti, T., G. Lupattelli and E. Mannarino (2006). "The endocrine function of adipose tissue: an update." Clin Endocrinol (Oxf) 64(4): 355-365.

Rosen, E. D. and B. M. Spiegelman (2000). "Peroxisome proliferator-activated receptor gamma ligands and atherosclerosis: ending the heartache." J Clin Invest 106(5): 629-631.

Rothwell, N. J. and M. J. Stock (1997). "A role for brown adipose tissue in diet-induced thermogenesis." Obes Res 5(6): 650-656.

Royo, T., M. J. Pedragosa, J. Ayte, G. Gil-Gomez, S. Vilaro and F. G. Hegardt (1993). "Testis and ovary express the gene for the ketogenic mitochondrial 3- hydroxy-3-methylglutaryl-CoA synthase." J Lipid Res 34(9): 1636.

Rudic, R. D., P. McNamara, A. M. Curtis, R. C. Boston, S. Panda, J. B. Hogenesch and G. A. Fitzgerald (2004). "BMAL1 and CLOCK, two essential components of the circadian clock, are involved in glucose homeostasis." PLoS Biol 2(11): e377.

Rui, L. (2014). "Energy metabolism in the liver." Compr Physiol 4(1): 177-197.

Ruiter, M., S. E. La Fleur, C. van Heijningen, J. van der Vliet, A. Kalsbeek and R. M. Buijs (2003). "The daily rhythm in plasma glucagon concentrations in the rat is modulated by the biological clock and by feeding behavior." Diabetes 52(7): 1709-1715.

Ryden, M., E. Arvidsson, L. Blomqvist, L. Perbeck, A. Dicker and P. Arner (2004). "Targets for TNF-alpha-induced lipolysis in human adipocytes." Biochem Biophys Res Commun 318(1): 168-175.

Ryden, M., G. Faulds, J. Hoffstedt, A. Wennlund and P. Arner (2002). "Effect of the (C825T) Gbeta(3) polymorphism on adrenoceptor-mediated lipolysis in human fat cells." Diabetes 51(5): 1601-1608.

Sakayama, K., T. Kidani, N. Tanji, H. Yamamoto and H. Masuno (2008). "The synthesis and activity of lipoprotein lipase in the subcutaneous adipose tissue of patients with musculoskeletal sarcomas." Anticancer Res 28(4B): 2081-2086.

Salamone, J. D. and M. Correa (2012). "The mysterious motivational functions of mesolimbic dopamine." Neuron 76(3): 470-485.

Samuel, V. T., Z. X. Liu, X. Qu, B. D. Elder, S. Bilz, D. Befroy, A. J. Romanelli and G. I. Shulman (2004). "Mechanism of hepatic insulin resistance in non-alcoholic fatty liver disease." J Biol Chem 279(31): 32345-32353.

Santomauro, A. T., G. Boden, M. E. Silva, D. M. Rocha, R. F. Santos, M. J. Ursich, P. G. Strassmann and B. L. Wajchenberg (1999). "Overnight lowering of free fatty acids with Acipimox improves insulin resistance and glucose tolerance in obese diabetic and nondiabetic subjects." Diabetes 48(9): 1836-1841.

Saper, C. B., T. C. Chou and J. K. Elmquist (2002). "The need to feed: homeostatic and hedonic control of eating." Neuron 36(2): 199-211.

Saper, C. B., J. Lu, T. C. Chou and J. Gooley (2005). "The hypothalamic integrator for circadian rhythms." Trends Neurosci 28(3): 152-157.

Sato, T. K., S. Panda, L. J. Miraglia, T. M. Reyes, R. D. Rudic, P. McNamara, K. A. Naik, G. A. FitzGerald, S. A. Kay and J. B. Hogenesch (2004). "A functional genomics strategy reveals Rora as a component of the mammalian circadian clock." Neuron 43(4): 527-537.

Sato, T. K., R. G. Yamada, H. Ukai, J. E. Baggs, L. J. Miraglia, T. J. Kobayashi, D. K. Welsh, S. A. Kay, H. R. Ueda and J. B. Hogenesch (2006). "Feedback repression is required for mammalian circadian clock function." Nat Genet 38(3): 312-319.

Savage, D. B., C. P. Sewter, E. S. Klenk, D. G. Segal, A. Vidal-Puig, R. V. Considine and S. O'Rahilly (2001). "Resistin / Fizz3 expression in relation to obesity and peroxisome proliferator-activated receptor-gamma action in humans." Diabetes 50(10): 2199-2202.

Schafer, K., K. Fujisawa, S. Konstantinides and D. J. Loskutoff (2001). "Disruption of the plasminogen activator inhibitor 1 gene reduces the adiposity and improves the metabolic profile of genetically obese and diabetic ob/ob mice." FASEB J 15(10): 1840-1842.

Schaffer, J. E. and H. F. Lodish (1994). "Expression cloning and characterization of a novel adipocyte long chain fatty acid transport protein." Cell 79(3): 427-436.

Scheer, F. A., M. F. Hilton, C. S. Mantzoros and S. A. Shea (2009). "Adverse metabolic and cardiovascular consequences of circadian misalignment." Proc Natl Acad Sci U S A 106(11): 4453-4458.

Schibler, U. (2009). "The 2008 Pittendrigh/Aschoff lecture: peripheral phase coordination in the mammalian circadian timing system." J Biol Rhythms 24(1): 3-15.

Schlierf, G. and E. Dorow (1973). "Diurnal patterns of triglycerides, free fatty acids, blood sugar, and insulin during carbohydrate-induction in man and their modification by nocturnal suppression of lipolysis." J Clin Invest 52(3): 732-740.

Schrauwen, P., H. Hoppeler, R. Billeter, A. H. Bakker and D. R. Pendergast (2001). "Fiber type dependent upregulation of human skeletal muscle UCP2 and UCP3 mRNA expression by high-fat diet." Int J Obes Relat Metab Disord 25(4): 449-456.

Schreurs, M., F. Kuipers, et al. (2010). "Regulatory enzymes of mitochondrial beta-oxidation as targets for treatment of the metabolic syndrome." Obes Rev 11(5): 380-388.

Schulz, H. (1991). "Beta oxidation of fatty acids." Biochim Biophys Acta 1081(2): 109-120.

Schutz, Y. (2004). "Dietary fat, lipogenesis and energy balance." Physiol Behav 83(4): 557-564.

Schwartz, M. W., E. Peskind, M. Raskind, E. J. Boyko and D. Porte, Jr. (1996). "Cerebrospinal fluid leptin levels: relationship to plasma levels and to adiposity in humans." Nat Med 2(5): 589-593.

Schwartz, W. J. and H. Gainer (1977). "Suprachiasmatic nucleus: use of 14C-labeled deoxyglucose uptake as a functional marker." Science 197(4308): 1089-1091.

Scott, E. M., A. M. Carter and P. J. Grant (2008). "Association between polymorphisms in the Clock gene, obesity and the metabolic syndrome in man." Int J Obes (Lond) 32(4): 658-662.

Seale, P., B. Bjork, W. Yang, S. Kajimura, S. Chin, S. Kuang, A. Scime, S. Devarakonda, H. M. Conroe, H. Erdjument-Bromage, P. Tempst, M. A. Rudnicki, D. R. Beier and B. M. Spiegelman (2008). "PRDM16 controls a brown fat/skeletal muscle switch." Nature 454(7207): 961-967.

Sears, I. B., M. A. MacGinnitie, L. G. Kovacs and R. A. Graves (1996). "Differentiation-dependent expression of the brown adipocyte uncoupling protein gene: regulation by peroxisome proliferator-activated receptor gamma." Mol Cell Biol 16(7): 3410-3419.

Shachter, N. S. (2001). "Apolipoproteins C-I and C-III as important modulators of lipoprotein metabolism." Curr Opin Lipidol 12(3): 297-304.

Shibata, S., Y. Oomura, H. Kita and K. Hattori (1982). "Circadian rhythmic changes of neuronal activity in the suprachiasmatic nucleus of the rat hypothalamic slice." Brain Res 247(1): 154-158.

Shimba, S., N. Ishii, Y. Ohta, T. Ohno, Y. Watabe, M. Hayashi, T. Wada, T. Aoyagi and M. Tezuka (2005). "Brain and muscle Arnt-like protein-1 (BMAL1), a component of the molecular clock, regulates adipogenesis." Proc Natl Acad Sci U S A 102(34): 12071-12076.

Shirogane, T., J. Jin, X. L. Ang and J. W. Harper (2005). "SCFbeta-TRCP controls clock-dependent transcription via casein kinase 1-dependent degradation of the mammalian period-1 (Per1) protein." J Biol Chem 280(29): 26863-26872.

Shostak, A., J. Meyer-Kovac and H. Oster (2013). "Circadian regulation of lipid mobilization in white adipose tissues." Diabetes 62(7): 2195-2203.

Shu, Y. and L. Hong-Hui (2004). "Transcription, translation, degradation, and circadian clock." Biochem Biophys Res Commun 321(1): 1-6.

Shulman, G. I. (2000). "Cellular mechanisms of insulin resistance." J Clin Invest 106(2): 171-176.

Silva, J. E. (2011). "Physiological importance and control of non-shivering facultative thermogenesis." Front Biosci (Schol Ed) 3: 352-371.

Simonsen, L., B. Stallknecht and J. Bulow (1993). "Contribution of skeletal muscle and adipose tissue to adrenaline-induced thermogenesis in man." Int J Obes Relat Metab Disord 17 Suppl 3: S47-51; discussion S68.

Skibicka, K. P. and S. L. Dickson (2011). "Ghrelin and food reward: the story of potential underlying substrates." Peptides 32(11): 2265-2273.

Skibicka, K. P., C. Hansson, E. Egecioglu and S. L. Dickson (2012). "Role of ghrelin in food reward: impact of ghrelin on sucrose self-administration and mesolimbic dopamine and acetylcholine receptor gene expression." Addict Biol 17(1): 95-107.

Smith, J. J., Y. Sydorskyy, M. Marelli, D. Hwang, H. Bolouri, R. A. Rachubinski and J. D. Aitchison (2006). "Expression and functional profiling reveal distinct gene classes involved in fatty acid metabolism." Mol Syst Biol 2: 2006 0009.

Solt, L. A., D. J. Kojetin and T. P. Burris (2011). "The REV-ERBs and RORs: molecular links between circadian rhythms and lipid homeostasis." Future Med Chem 3(5): 623-638.

Solt, L. A., Y. Wang, S. Banerjee, T. Hughes, D. J. Kojetin, T. Lundasen, Y. Shin, J. Liu, M. D. Cameron, R. Noel, S. H. Yoo, J. S. Takahashi, A. A. Butler, T. M. Kamenecka and T. P. Burris (2012). "Regulation of circadian behaviour and metabolism by synthetic REV-ERB agonists." Nature 485(7396): 62-68.

Sorensen, G., G. Wegener, J. Hasselstrom, T. V. Hansen, G. Wortwein, A. Fink-Jensen and D. P. Woldbye (2009). "Neuropeptide Y infusion into the shell region of the rat nucleus accumbens increases extracellular levels of dopamine." Neuroreport 20(11): 1023-1026.

Southgate, D. A. and J. V. Durnin (1970). "Calorie conversion factors. An experimental reassessment of the factors used in the calculation of the energy value of human diets." Br J Nutr 24(2): 517-535.

Spiegel, K., E. Tasali, P. Penev and E. Van Cauter (2004). "Brief communication: Sleep curtailment in healthy young men is associated with decreased leptin levels, elevated ghrelin levels, and increased hunger and appetite." Ann Intern Med 141(11): 846-850.

Stacher, G., H. Steinringer, G. Schmierer, C. Schneider and S. Winklehner (1982). "Cholecystokinin octapeptide decreases intake of solid food in man." Peptides 3(2): 133-136.

Staels, B. and J. Auwerx (1992). "Perturbation of developmental gene expression in rat liver by fibric acid derivatives: lipoprotein lipase and alpha-fetoprotein as models." Development 115(4): 1035-1043.

Stahl, A., R. E. Gimeno, L. A. Tartaglia and H. F. Lodish (2001). "Fatty acid transport proteins: a current view of a growing family." Trends Endocrinol Metab 12(6): 266-273.

Stanley, S., S. Pinto, J. Segal, C. A. Perez, A. Viale, J. DeFalco, X. Cai, L. K. Heisler and J. M. Friedman (2010). "Identification of neuronal subpopulations that project from hypothalamus to both liver and adipose tissue polysynaptically." Proc Natl Acad Sci U S A 107(15): 7024-7029.

Stavinoha, M. A., J. W. Rayspellicy, M. L. Hart-Sailors, H. J. Mersmann, M. S. Bray and M. E. Young (2004). "Diurnal variations in the responsiveness of cardiac and skeletal muscle to fatty acids." Am J Physiol Endocrinol Metab 287(5): E878-887.

Stephan, F. K. (2002). "The "other" circadian system: food as a Zeitgeber." J Biol Rhythms 17(4): 284-292.

Stephan, F. K. and I. Zucker (1972). "Circadian rhythms in drinking behavior and locomotor activity of rats are eliminated by hypothalamic lesions." Proc Natl Acad Sci U S A 69(6): 1583-1586.

Steppan, C. M., S. T. Bailey, S. Bhat, E. J. Brown, R. R. Banerjee, C. M. Wright, H. R. Patel, R. S. Ahima and M. A. Lazar (2001). "The hormone resistin links obesity to diabetes." Nature 409(6818): 307-312.

Stokkan, K. A., S. Yamazaki, H. Tei, Y. Sakaki and M. Menaker (2001). "Entrainment of the circadian clock in the liver by feeding." Science 291(5503): 490-493.

Storch, K. F., C. Paz, J. Signorovitch, E. Raviola, B. Pawlyk, T. Li and C. J. Weitz (2007). "Intrinsic circadian clock of the mammalian retina: importance for retinal processing of visual information." Cell 130(4): 730-741.

Stralfors, P. and P. Belfrage (1985). "Phosphorylation of hormone-sensitive lipase by cyclic GMP-dependent protein kinase." FEBS Lett 180(2): 280-284.

Stratmann, M. and U. Schibler (2006). "Properties, entrainment, and physiological functions of mammalian peripheral oscillators." J Biol Rhythms 21(6): 494-506.

Strissel, K. J., Z. Stancheva, H. Miyoshi, J. W. Perfield, 2nd, J. DeFuria, Z. Jick, A. S. Greenberg and M. S. Obin (2007). "Adipocyte death, adipose tissue remodeling, and obesity complications." Diabetes 56(12): 2910-2918.

Sturley, S. L. and M. M. Hussain (2012). "Lipid droplet formation on opposing sides of the endoplasmic reticulum." J Lipid Res 53(9): 1800-1810.

Sujino, M., K. H. Masumoto, S. Yamaguchi, G. T. van der Horst, H. Okamura and S. T. Inouye (2003). "Suprachiasmatic nucleus grafts restore circadian behavioral rhythms of genetically arrhythmic mice." Curr Biol 13(8): 664-668.

Sun, K., N. Halberg, M. Khan, U. J. Magalang and P. E. Scherer (2013). "Selective inhibition of hypoxia-inducible factor 1alpha ameliorates adipose tissue dysfunction." Mol Cell Biol 33(5): 904-917.

Sun, Z., R. A. Miller, R. T. Patel, J. Chen, R. Dhir, H. Wang, D. Zhang, M. J. Graham, T. G. Unterman, G. I. Shulman, C. Sztalryd, M. J. Bennett, R. S. Ahima, M. J. Birnbaum and M. A. Lazar (2012). "Hepatic Hdac3 promotes gluconeogenesis by repressing lipid synthesis and sequestration." Nat Med 18(6): 934-942.

Sun, Z. S., U. Albrecht, O. Zhuchenko, J. Bailey, G. Eichele and C. C. Lee (1997). "RIGUI, a putative mammalian ortholog of the Drosophila period gene." Cell 90(6): 1003-1011.

Sztalryd, C. and F. B. Kraemer (1994). "Regulation of hormone-sensitive lipase during fasting." Am J Physiol 266(2 Pt 1): E179-185.

Tanaka, N., S. Takahashi, T. Matsubara, C. Jiang, W. Sakamoto, T. Chanturiya, R. Teng, O. Gavrilova and F. J. Gonzalez (2015). "Adipocyte-specific disruption of fat-specific protein 27 causes hepatosteatosis and insulin resistance in high-fat diet-fed mice." J Biol Chem 290(5): 3092-3105.

Tang, W., D. Zeve, J. M. Suh, D. Bosnakovski, M. Kyba, R. E. Hammer, M. D. Tallquist and J. M. Graff (2008). "White fat progenitor cells reside in the adipose vasculature." Science 322(5901): 583-586.

Tansey, J. T., C. Sztalryd, E. M. Hlavin, A. R. Kimmel and C. Londos (2004). "The central role of perilipin a in lipid metabolism and adipocyte lipolysis." IUBMB Life 56(7): 379-385.

Tasaka, Y., S. Inoue, K. Maruno and Y. Hirata (1980). "Twenty-four-hour variations of plasma pancreatic polypeptide, insulin and glucagon in normal human subjects." Endocrinol Jpn 27(4): 495-498.

Tei, H., H. Okamura, Y. Shigeyoshi, C. Fukuhara, R. Ozawa, M. Hirose and Y. Sakaki (1997). "Circadian oscillation of a mammalian homologue of the Drosophila period gene." Nature 389(6650): 512-516.

Thomasson, H. J. (1962). "Essential fatty acids." Nature 194: 973.

Tilg, H. and A. R. Moschen (2006). "Adipocytokines: mediators linking adipose tissue, inflammation and immunity." Nat Rev Immunol 6(10): 772-783.

Timmons, J. A., K. Wennmalm, O. Larsson, T. B. Walden, T. Lassmann, N. Petrovic, D. L. Hamilton, R. E. Gimeno, C. Wahlestedt, K. Baar, J. Nedergaard and B. Cannon (2007). "Myogenic gene expression signature establishes that brown and white adipocytes originate from distinct cell lineages." Proc Natl Acad Sci U S A 104(11): 4401-4406.

Tomas, E., T. S. Tsao, A. K. Saha, H. E. Murrey, C. Zhang Cc, S. I. Itani, H. F. Lodish and N. B. Ruderman (2002). "Enhanced muscle fat oxidation and glucose transport by ACRP30 globular domain: acetyl-CoA carboxylase inhibition and AMP-activated protein kinase activation." Proc Natl Acad Sci U S A 99(25): 16309-16313.

Tong, Q., G. Dalgin, H. Xu, C. N. Ting, J. M. Leiden and G. S. Hotamisligil (2000). "Function of GATA transcription factors in preadipocyte-adipocyte transition." Science 290(5489): 134-138.

Tordjman, J., G. Chauvet, J. Quette, E. G. Beale, C. Forest and B. Antoine (2003). "Thiazolidinediones block fatty acid release by inducing glyceroneogenesis in fat cells." J Biol Chem 278(21): 18785-18790.

Triqueneaux, G., S. Thenot, T. Kakizawa, M. P. Antoch, R. Safi, J. S. Takahashi, F. Delaunay and V. Laudet (2004). "The orphan receptor Rev-erbalpha gene is a target of the circadian clock pacemaker." J Mol Endocrinol 33(3): 585-608.

Tsai, J. Y., P. C. Kienesberger, T. Pulinilkunnil, M. H. Sailors, D. J. Durgan, C. Villegas-Montoya, A. Jahoor, R. Gonzalez, M. E. Garvey, B. Boland, Z. Blasier, T. A. McElfresh, V. Nannegari, C. W. Chow, W. C. Heird, M. P. Chandler, J. R. Dyck, M. S. Bray and M. E. Young (2010). "Direct regulation of myocardial triglyceride metabolism by the cardiomyocyte circadian clock." J Biol Chem 285(5): 2918-2929.

Tschop, M., D. L. Smiley and M. L. Heiman (2000). "Ghrelin induces adiposity in rodents." Nature 407(6806): 908-913.

Tsuchida, A., T. Yamauchi, S. Takekawa, Y. Hada, Y. Ito, T. Maki and T. Kadowaki (2005). "Peroxisome proliferator-activated receptor (PPAR)alpha activation increases adiponectin receptors and reduces obesity-related inflammation in adipose tissue: comparison of activation of PPARalpha, PPARgamma, and their combination." Diabetes 54(12): 3358-3370.

Turek, F. W., C. Joshu, A. Kohsaka, E. Lin, G. Ivanova, E. McDearmon, A. Laposky, S. Losee-Olson, A. Easton, D. R. Jensen, R. H. Eckel, J. S. Takahashi and J. Bass (2005). "Obesity and metabolic syndrome in circadian Clock mutant mice." Science 308(5724): 1043-1045.

Turer, A. T., A. Khera, C. R. Ayers, C. B. Turer, S. M. Grundy, G. L. Vega and P. E. Scherer (2011). "Adipose tissue mass and location affect circulating adiponectin levels." Diabetologia 54(10): 2515-2524.

Tyagi, S., P. Gupta, A. S. Saini, C. Kaushal and S. Sharma (2011). "The peroxisome proliferator-activated receptor: A family of nuclear receptors role in various diseases." J Adv Pharm Technol Res 2(4): 236-240.

Tzen, J. T., G. C. Lie and A. H. Huang (1992). "Characterization of the charged components and their topology on the surface of plant seed oil bodies." J Biol Chem 267(22): 15626-15634.

Ueda, H. R., S. Hayashi, W. Chen, M. Sano, M. Machida, Y. Shigeyoshi, M. Iino and S. Hashimoto (2005). "System-level identification of transcriptional circuits underlying mammalian circadian clocks." Nat Genet 37(2): 187-192.

Ukai-Tadenuma, M., R. G. Yamada, H. Xu, J. A. Ripperger, A. C. Liu and H. R. Ueda (2011). "Delay in feedback repression by cryptochrome 1 is required for circadian clock function." Cell 144(2): 268-281.

Uldry, M., W. Yang, J. St-Pierre, J. Lin, P. Seale and B. M. Spiegelman (2006). "Complementary action of the PGC-1 coactivators in mitochondrial biogenesis and brown fat differentiation." Cell Metab 3(5): 333-341.

Um, J. H., J. S. Pendergast, D. A. Springer, M. Foretz, B. Viollet, A. Brown, M. K. Kim, S. Yamazaki and J. H. Chung (2011). "AMPK regulates circadian rhythms in a tissue- and isoform-specific manner." PLoS One 6(3): e18450.

Um, J. H., S. Yang, S. Yamazaki, H. Kang, B. Viollet, M. Foretz and J. H. Chung (2007). "Activation of 5'-AMP-activated kinase with diabetes drug metformin induces casein kinase Iepsilon (CKIepsilon)-dependent degradation of clock protein mPer2." J Biol Chem 282(29): 20794-20798.

Vaisse, C., K. Clement, E. Durand, S. Hercberg, B. Guy-Grand and P. Froguel (2000). "Melanocortin-4 receptor mutations are a frequent and heterogeneous cause of morbid obesity." J Clin Invest 106(2): 253-262.

van Amelsvoort, L. G., E. G. Schouten and F. J. Kok (1999). "Duration of shiftwork related to body mass index and waist to hip ratio." Int J Obes Relat Metab Disord 23(9): 973-978.

Van Cauter, E., K. S. Polonsky and A. J. Scheen (1997). "Roles of circadian rhythmicity and sleep in human glucose regulation." Endocr Rev 18(5): 716-738.

van Marken Lichtenbelt, W. D. and P. Schrauwen (2011). "Implications of nonshivering thermogenesis for energy balance regulation in humans." Am J Physiol Regul Integr Comp Physiol 301(2): R285-296.

Vanselow, K., J. T. Vanselow, P. O. Westermark, S. Reischl, B. Maier, T. Korte, A. Herrmann, H. Herzel, A. Schlosser and A. Kramer (2006). "Differential effects of PER2 phosphorylation: molecular basis for the human familial advanced sleep phase syndrome (FASPS)." Genes Dev 20(19): 2660-2672.

Vazquez, M., N. Roglans, A. Cabrero, C. Rodriguez, T. Adzet, M. Alegret, R. M. Sanchez and J. C. Laguna (2001). "Bezafibrate induces acyl-CoA oxidase mRNA levels and fatty acid peroxisomal beta-oxidation in rat white adipose tissue." Mol Cell Biochem 216(1-2): 71-78.

Vendelbo, M. H., J. O. Jorgensen, S. B. Pedersen, L. C. Gormsen, S. Lund, O. Schmitz, N. Jessen and N. Moller (2010). "Exercise and fasting activate growth hormone-dependent myocellular signal transducer and activator of transcription-5b phosphorylation and insulin-like growth factor-I messenger ribonucleic acid expression in humans." J Clin Endocrinol Metab 95(9): E64-68.

Vgontzas, A. N., D. A. Papanicolaou, E. O. Bixler, A. Lotsikas, K. Zachman, A. Kales, P. Prolo, M. L. Wong, J. Licinio, P. W. Gold, R. C. Hermida, G. Mastorakos and G. P. Chrousos (1999). "Circadian interleukin-6 secretion and quantity and depth of sleep." J Clin Endocrinol Metab 84(8): 2603-2607.

Vgontzas, A. N., M. Zoumakis, D. A. Papanicolaou, E. O. Bixler, P. Prolo, H. M. Lin, A. Vela-Bueno, A. Kales and G. P. Chrousos (2002). "Chronic insomnia is associated with a shift of interleukin-6 and tumor necrosis factor secretion from nighttime to daytime." Metabolism 51(7): 887-892.

Vidal-Puig, A., M. Jimenez-Linan, B. B. Lowell, A. Hamann, E. Hu, B. Spiegelman, J. S. Flier and D. E. Moller (1996). "Regulation of PPAR gamma gene expression by nutrition and obesity in rodents." J Clin Invest 97(11): 2553-2561.

Vieira, E., L. Marroqui, A. L. Figueroa, B. Merino, R. Fernandez-Ruiz, A. Nadal, T. P. Burris, R. Gomis and I. Quesada (2013). "Involvement of the clock gene Rev-erb alpha in the regulation of glucagon secretion in pancreatic alpha-cells." PLoS One 8(7): e69939.

Vieira, E., E. Ruano, A. L. Figueroa, G. Aranda, D. Momblan, F. Carmona, R. Gomis, J. Vidal and F. A. Hanzu (2014). "Altered clock gene expression in obese visceral adipose tissue is associated with metabolic syndrome." PLoS One 9(11): e111678.

Villar-Palasi, C. and J. J. Guinovart (1997). "The role of glucose 6-phosphate in the control of glycogen synthase." FASEB J 11(7): 544-558.

Villena, J. A., S. Roy, E. Sarkadi-Nagy, K. H. Kim and H. S. Sul (2004). "Desnutrin, an adipocyte gene encoding a novel patatin domain-containing protein, is induced by fasting and glucocorticoids: ectopic expression of desnutrin increases triglyceride hydrolysis." J Biol Chem 279(45): 47066-47075.

Viswanathan, N. and F. C. Davis (1997). "Single prenatal injections of melatonin or the D1-dopamine receptor agonist SKF 38393 to pregnant hamsters sets the offsprings' circadian rhythms to phases 180 degrees apart." J Comp Physiol A 180(4): 339-346.

Volkow, N. D., G. J. Wang and R. D. Baler (2011). "Reward, dopamine and the control of food intake: implications for obesity." Trends Cogn Sci 15(1): 37-46.

Wagener, F. A., A. Eggert, O. C. Boerman, W. J. Oyen, A. Verhofstad, N. G. Abraham, G. Adema, Y. van Kooyk, T. de Witte and C. G. Figdor (2001). "Heme is a potent inducer of inflammation in mice and is counteracted by heme oxygenase." Blood 98(6): 1802-1811.

Waki, H., T. Yamauchi, J. Kamon, Y. Ito, S. Uchida, S. Kita, K. Hara, Y. Hada, F. Vasseur, P. Froguel, S. Kimura, R. Nagai and T. Kadowaki (2003). "Impaired multimerization of human adiponectin mutants associated with diabetes. Molecular structure and multimer formation of adiponectin." J Biol Chem 278(41): 40352-40363.

Wang, G. Z., S. L. Hickey, L. Shi, H. C. Huang, P. Nakashe, N. Koike, B. P. Tu, J. S. Takahashi and G. Konopka (2015). "Cycling Transcriptional Networks Optimize Energy Utilization on a Genome Scale." Cell Rep 13(9): 1868-1880.

Wang, H. and R. H. Eckel (2009). "Lipoprotein lipase: from gene to obesity." Am J Physiol Endocrinol Metab 297(2): E271-288.

Wang, J. and M. A. Lazar (2008). "Bifunctional role of Rev-erbalpha in adipocyte differentiation." Mol Cell Biol 28(7): 2213-2220.

Wang, J., L. Yin and M. A. Lazar (2006). "The orphan nuclear receptor Rev-erb alpha regulates circadian expression of plasminogen activator inhibitor type 1." J Biol Chem 281(45): 33842-33848.

Wang, Y. X., C. H. Lee, S. Tiep, R. T. Yu, J. Ham, H. Kang and R. M. Evans (2003). "Peroxisome-proliferator-activated receptor delta activates fat metabolism to prevent obesity." Cell 113(2): 159-170.

Wang, C. S., W. J. McConathy, et al. (1985). "Modulation of lipoprotein lipase activity by apolipoproteins. Effect of apolipoprotein C-III." J Clin Invest 75(2): 384-390.

Watt, M. J., G. R. Steinberg, S. Chan, A. Garnham, B. E. Kemp and M. A. Febbraio (2004). "Beta-adrenergic stimulation of skeletal muscle HSL can be overridden by AMPK signaling." FASEB J 18(12): 1445-1446.

Weaver, D. R. (1999). "The roles of melatonin in development." Adv Exp Med Biol 460: 199-214.

Weisberg, S. P., D. McCann, M. Desai, M. Rosenbaum, R. L. Leibel and A. W. Ferrante, Jr. (2003). "Obesity is associated with macrophage accumulation in adipose tissue." J Clin Invest 112(12): 1796-1808.

Wellen, K. E. and G. S. Hotamisligil (2005). "Inflammation, stress, and diabetes." J Clin Invest 115(5): 1111-1119.

Welsh, D. K., D. E. Logothetis, M. Meister and S. M. Reppert (1995). "Individual neurons dissociated from rat suprachiasmatic nucleus express independently phased circadian firing rhythms." Neuron 14(4): 697-706.

Westenskow, D. R., C. A. Schipke, J. L. Raymond, J. R. Saffle, J. M. Becker, E. W. Young and C. A. Cutler (1988). "Calculation of metabolic expenditure and substrate utilization from gas exchange measurements." JPEN J Parenter Enteral Nutr 12(1): 20-24.

Westerterp, K. R. (2003). "Impacts of vigorous and non-vigorous activity on daily energy expenditure." Proc Nutr Soc 62(3): 645-650.

Whichelow, M. J., R. A. Sturge, H. Keen, R. J. Jarrett, L. Stimmler and S. Grainger (1974). "Diurnal variation in response to intravenous glucose." Br Med J 1(5906): 488-491.

Wijesekara, N., M. Krishnamurthy, A. Bhattacharjee, A. Suhail, G. Sweeney and M. B. Wheeler (2010). "Adiponectin-induced ERK and Akt phosphorylation protects against pancreatic beta cell apoptosis and increases insulin gene expression and secretion." J Biol Chem 285(44): 33623-33631.

Wilsbacher, L. D., S. Yamazaki, E. D. Herzog, E. J. Song, L. A. Radcliffe, M. Abe, G. Block, E. Spitznagel, M. Menaker and J. S. Takahashi (2002). "Photic and circadian expression of luciferase in mPeriod1-luc transgenic mice invivo." Proc Natl Acad Sci U S A 99(1): 489-494.

Woldt, E., Y. Sebti, L. A. Solt, C. Duhem, S. Lancel, J. Eeckhoute, M. K. Hesselink, C. Paquet, S. Delhaye, Y. Shin, T. M. Kamenecka, G. Schaart, P. Lefebvre, R. Neviere, T. P. Burris, P. Schrauwen, B. Staels and H. Duez (2013). "Rev-erb-alpha modulates skeletal muscle oxidative capacity by regulating mitochondrial biogenesis and autophagy." Nat Med 19(8): 1039-1046.

Woods, S. C., R. J. Seeley, D. Porte, Jr. and M. W. Schwartz (1998). "Signals that regulate food intake and energy homeostasis." Science 280(5368): 1378-1383.

World Health Organisation (2016). *Fact Sheet – Obesity and overweight,* viewed 6th June 2016. Available at: <http://www.who.int/mediacentre/factsheets/fs311/en/>

Wren, A. M., L. J. Seal, M. A. Cohen, A. E. Brynes, G. S. Frost, K. G. Murphy, W. S. Dhillo, M. A. Ghatei and S. R. Bloom (2001). "Ghrelin enhances appetite and increases food intake in humans." J Clin Endocrinol Metab 86(12): 5992.

Wren, A. M., C. J. Small, H. L. Ward, K. G. Murphy, C. L. Dakin, S. Taheri, A. R. Kennedy, G. H. Roberts, D. G. Morgan, M. A. Ghatei and S. R. Bloom (2000). "The novel hypothalamic peptide ghrelin stimulates food intake and growth hormone secretion." Endocrinology 141(11): 4325-4328.

Wu, D., A. B. Molofsky, H. E. Liang, R. R. Ricardo-Gonzalez, H. A. Jouihan, J. K. Bando, A. Chawla and R. M. Locksley (2011). "Eosinophils sustain adipose alternatively activated macrophages associated with glucose homeostasis." Science 332(6026): 243-247.

Wu, N., L. Yin, E. A. Hanniman, S. Joshi and M. A. Lazar (2009). "Negative feedback maintenance of heme homeostasis by its receptor, Rev-erbalpha." Genes Dev 23(18): 2201-2209.

Wynne, K., S. Stanley, B. McGowan and S. Bloom (2005). "Appetite control." J Endocrinol 184(2): 291-318.

Xu, H., G. T. Barnes, Q. Yang, G. Tan, D. Yang, C. J. Chou, J. Sole, A. Nichols, J. S. Ross, L. A. Tartaglia and H. Chen (2003). "Chronic inflammation in fat plays a crucial role in the development of obesity-related insulin resistance." J Clin Invest 112(12): 1821-1830.

Xu, L., G. A. Spinas and M. Niessen (2010). "ER stress in adipocytes inhibits insulin signaling, represses lipolysis, and alters the secretion of adipokines without inhibiting glucose transport." Horm Metab Res 42(9): 643-651.

Xue, B. and B. B. Kahn (2006). "AMPK integrates nutrient and hormonal signals to regulate food intake and energy balance through effects in the hypothalamus and peripheral tissues." J Physiol 574(Pt 1): 73-83.

Yagita, K., F. Tamanini, M. Yasuda, J. H. Hoeijmakers, G. T. van der Horst and H. Okamura (2002). "Nucleocytoplasmic shuttling and mCRY-dependent inhibition of ubiquitylation of the mPER2 clock protein." EMBO J 21(6): 1301-1314.

Yamamoto, T., Y. Nakahata, H. Soma, M. Akashi, T. Mamine and T. Takumi (2004). "Transcriptional oscillation of canonical clock genes in mouse peripheral tissues." BMC Mol Biol 5: 18.

Yamauchi, T., J. Kamon, Y. Minokoshi, Y. Ito, H. Waki, S. Uchida, S. Yamashita, M. Noda, S. Kita, K. Ueki, K. Eto, Y. Akanuma, P. Froguel, F. Foufelle, P. Ferre, D. Carling, S. Kimura, R. Nagai, B. B. Kahn and T. Kadowaki (2002). "Adiponectin stimulates glucose utilization and fatty-acid oxidation by activating AMP-activated protein kinase." Nat Med 8(11): 1288-1295.

Yamauchi, T., J. Kamon, H. Waki, Y. Imai, N. Shimozawa, K. Hioki, S. Uchida, Y. Ito, K. Takakuwa, J. Matsui, M. Takata, K. Eto, Y. Terauchi, K. Komeda, M. Tsunoda, K. Murakami, Y. Ohnishi, T. Naitoh, K. Yamamura, Y. Ueyama, P. Froguel, S. Kimura, R. Nagai and T. Kadowaki (2003). "Globular adiponectin protected ob/ob mice from diabetes and ApoE-deficient mice from atherosclerosis." J Biol Chem 278(4): 2461-2468.

Yamauchi, T., J. Kamon, H. Waki, Y. Terauchi, N. Kubota, K. Hara, Y. Mori, T. Ide, K. Murakami, N. Tsuboyama-Kasaoka, O. Ezaki, Y. Akanuma, O. Gavrilova, C. Vinson, M. L. Reitman, H. Kagechika, K. Shudo, M. Yoda, Y. Nakano, K. Tobe, R. Nagai, S. Kimura, M. Tomita, P. Froguel and T. Kadowaki (2001). "The fat-derived hormone adiponectin reverses insulin resistance associated with both lipoatrophy and obesity." Nat Med 7(8): 941-946.

Yamazaki, S., R. Numano, M. Abe, A. Hida, R. Takahashi, M. Ueda, G. D. Block, Y. Sakaki, M. Menaker and H. Tei (2000). "Resetting central and peripheral circadian oscillators in transgenic rats." Science 288(5466): 682-685.

Yamazaki, S., T. Yoshikawa, E. W. Biscoe, R. Numano, L. M. Gallaspy, S. Soulsby, E. Papadimas, P. Pezuk, S. E. Doyle, H. Tei, Y. Sakaki, G. D. Block and M. Menaker (2009). "Ontogeny of circadian organization in the rat." J Biol Rhythms 24(1): 55-63.

Yanagihara, H., H. Ando, Y. Hayashi, Y. Obi and A. Fujimura (2006). "High-fat feeding exerts minimal effects on rhythmic mRNA expression of clock genes in mouse peripheral tissues." Chronobiol Int 23(5): 905-914.

Yang, J. G., Y. Deng, L. X. Zhou, X. Y. Li, P. R. Sun and N. X. Sun (2013). "Overexpression of CDKN1B inhibits fibroblast proliferation in a rabbit model of experimental glaucoma filtration surgery." Invest Ophthalmol Vis Sci 54(1): 343-352.

Yang, Q., T. E. Graham, N. Mody, F. Preitner, O. D. Peroni, J. M. Zabolotny, K. Kotani, L. Quadro and B. B. Kahn (2005). "Serum retinol binding protein 4 contributes to insulin resistance in obesity and type 2 diabetes." Nature 436(7049): 356-362.

Yang, S., A. Liu, A. Weidenhammer, R. C. Cooksey, D. McClain, M. K. Kim, G. Aguilera, E. D. Abel and J. H. Chung (2009). "The role of mPer2 clock gene in glucocorticoid and feeding rhythms." Endocrinology 150(5): 2153-2160.

Yang, Y. L., Z. L. Shen, Y. Tang, N. Wang and B. Sun (2011). "[Simultaneous telemetric analyzing of the temporal relationship for the changes of the circadian rhythms of brown adipose tissue thermogenesis and core temperature in the rat]." Zhongguo Ying Yong Sheng Li Xue Za Zhi 27(3): 348-352.

Yildiz, B. O., M. A. Suchard, M. L. Wong, S. M. McCann and J. Licinio (2004). "Alterations in the dynamics of circulating ghrelin, adiponectin, and leptin in human obesity." Proc Natl Acad Sci U S A 101(28): 10434-10439.

Yin, L., J. Wang, P. S. Klein and M. A. Lazar (2006). "Nuclear receptor Rev-erbalpha is a critical lithium-sensitive component of the circadian clock." Science 311(5763): 1002-1005.

Yin, L., N. Wu, J. C. Curtin, M. Qatanani, N. R. Szwergold, R. A. Reid, G. M. Waitt, D. J. Parks, K. H. Pearce, G. B. Wisely and M. A. Lazar (2007). "Rev-erbalpha, a heme sensor that coordinates metabolic and circadian pathways." Science 318(5857): 1786-1789.

Yokota, T., K. Oritani, I. Takahashi, J. Ishikawa, A. Matsuyama, N. Ouchi, S. Kihara, T. Funahashi, A. J. Tenner, Y. Tomiyama and Y. Matsuzawa (2000). "Adiponectin, a new member of the family of soluble defense collagens, negatively regulates the growth of myelomonocytic progenitors and the functions of macrophages." Blood 96(5): 1723-1732.

Yoo, S. H., S. Yamazaki, P. L. Lowrey, K. Shimomura, C. H. Ko, E. D. Buhr, S. M. Siepka, H. K. Hong, W. J. Oh, O. J. Yoo, M. Menaker and J. S. Takahashi (2004). "PERIOD2::LUCIFERASE real-time reporting of circadian dynamics reveals persistent circadian oscillations in mouse peripheral tissues." Proc Natl Acad Sci U S A 101(15): 5339-5346.

Yoon, J. C., P. Puigserver, G. Chen, J. Donovan, Z. Wu, J. Rhee, G. Adelmant, J. Stafford, C. R. Kahn, D. K. Granner, C. B. Newgard and B. M. Spiegelman (2001). "Control of hepatic gluconeogenesis through the transcriptional coactivator PGC-1." Nature 413(6852): 131-138.

Yu, J. H. and M. S. Kim (2012). "Molecular mechanisms of appetite regulation." Diabetes Metab J 36(6): 391-398.

Yu, Y. H. and H. N. Ginsberg (2005). "Adipocyte signaling and lipid homeostasis: sequelae of insulin-resistant adipose tissue." Circ Res 96(10): 1042-1052.

Zhang, E. E., Y. Liu, R. Dentin, P. Y. Pongsawakul, A. C. Liu, T. Hirota, D. A. Nusinow, X. Sun, S. Landais, Y. Kodama, D. A. Brenner, M. Montminy and S. A. Kay (2010). "Cryptochrome mediates circadian regulation of cAMP signaling and hepatic gluconeogenesis." Nat Med 16(10): 1152-1156.

Zhang, R., N. F. Lahens, H. I. Ballance, M. E. Hughes and J. B. Hogenesch (2014). "A circadian gene expression atlas in mammals: implications for biology and medicine." Proc Natl Acad Sci U S A 111(45): 16219-16224.

Zhang, W. and S. Bi (2015). "Hypothalamic Regulation of Brown Adipose Tissue Thermogenesis and Energy Homeostasis." Front Endocrinol (Lausanne) 6: 136.

Zhang, Y., R. Proenca, M. Maffei, M. Barone, L. Leopold and J. M. Friedman (1994). "Positional cloning of the mouse obese gene and its human homologue." Nature 372(6505): 425-432.

Zhang, Y. K., G. L. Guo and C. D. Klaassen (2011). "Diurnal variations of mouse plasma and hepatic bile acid concentrations as well as expression of biosynthetic enzymes and transporters." PLoS One 6(2): e16683.

Zhang, Y., B. Fang, M. J. Emmett, M. Damle, Z. Sun, D. Feng, S. M. Armour, J. R. Remsberg, J. Jager, R. E. Soccio, D. J. Steger and M. A. Lazar (2015). "GENE REGULATION. Discrete functions of nuclear receptor Rev-erbalpha couple metabolism to the clock." Science 348(6242): 1488-1492.

Zhao, I., F. Bogossian, S. Song and C. Turner (2011). "The association between shift work and unhealthy weight: a cross-sectional analysis from the Nurses and Midwives' e-cohort Study." J Occup Environ Med 53(2): 153-158.

Zhou, M., J. K. Kim, G. W. Eng, D. B. Forger and D. M. Virshup (2015). "A Period2 Phosphoswitch Regulates and Temperature Compensates Circadian Period." Mol Cell 60(1): 77-88.

Zuo, Y., L. Qiang and S. R. Farmer (2006). "Activation of CCAAT/enhancer-binding protein (C/EBP) alpha expression by C/EBP beta during adipogenesis requires a peroxisome proliferator-activated receptor-gamma-associated repression of HDAC1 at the C/ebp alpha gene promoter." J Biol Chem 281(12): 7960-7967.

Zvonic, S., Z. E. Floyd, R. L. Mynatt and J. M. Gimble (2007). "Circadian rhythms and the regulation of metabolic tissue function and energy homeostasis." Obesity (Silver Spring) 15(3): 539-543.

Zvonic, S., A. A. Ptitsyn, S. A. Conrad, L. K. Scott, Z. E. Floyd, G. Kilroy, X. Wu, B. C. Goh, R. L. Mynatt and J. M. Gimble (2006). "Characterization of peripheral circadian clocks in adipose tissues." Diabetes 55(4): 962-970.

Appendix 1

Chappter 3 statistics

Figure 3.1

Panel A	2-way ANOVA sidak post hoc test		
		F (DFn, DFd)	**P Value**
Growth curve	Interaction	F (16, 1156) = 58.29	P<0.0001
	Diet	F (16, 1156) = 268.5	P<0.0001
	Time	F (1, 1156) = 2954	P<0.0001

Panel A	Unpaired t-test		
	P value	**t, df**	**F,DFn, Dfd**
gWAT weight	0.001	t=6.325 df=58	1.873, 29, 29

Panel B	Unpaired t-test		
	P value	**t, df**	**F,DFn, Dfd**
Activity	0.0122	t=2.947 df=12	1.916, 6, 6
Temperature	0.0006	t=4.592 df=12	1.82, 6, 6

Panel C	2-way ANOVA sidak post hoc test		
		F (DFn, DFd)	**P Value**
Food intake (g/hr)	Interaction	F (11, 120) = 6.929	P<0.0001
	Diet	F (11, 120) = 24.49	P<0.0001
	Time	F (1, 120) = 111.8	P<0.0001
Meal events	Interaction	F (1, 12) = 34.31	P < 0.0001
	Diet	F (1, 12) = 209.3	P < 0.0001
	Time	F (1, 12) = 40.76	P < 0.0001

Panel C	Unpaired t-test		
	P value	**t, df**	**F,DFn, Dfd**
% feeding	0.0002	t=5.281 df=12	1.103, 6, 6

Figure 3.2

Panel A	2-way ANOVA sidak post hoc test		
	Bmal1		
		F (DFn, DFd)	**P Value**
Hypothalamus	Interaction	F (5, 45) = 1.776	P=0.1372
	Time	F (5, 45) = 14.74	P<0.0001
	Diet	F (1, 45) = 0.003026	P=0.9564
Liver	Interaction	F (5, 47) = 4.345	P=0.0025

	Time	F (5, 47) = 121.4	P<0.0001
	Diet	F (1, 47) = 7.576	P=0.0084
Muscle	Interaction	F (5, 46) = 2.776	P=0.0284
	Time	F (5, 46) = 42.57	P<0.0001
	Diet	F (1, 46) = 18.31	P<0.0001
Adrenal Gland	Interaction	F (5, 47) = 13.53	P<0.0001
	Time	F (5, 47) = 77.84	P<0.0001
	Diet	F (1, 47) = 0.009513	P=0.9227
Lymph node	Interaction	F (5, 44) = 0.7934	P=0.5602
	Time	F (5, 44) = 0.5807	P=0.7145
	Diet	F (1, 44) = 0.5838	P=0.4489
Spleen	Interaction	F (5, 48) = 0.3956	P=0.8494
	Time	F (5, 48) = 2.678	P=0.0325
	Diet	F (1, 48) = 3.721	P=0.0597
BAT	Interaction	F (5, 48) = 1.658	P=0.1630
	Time	F (5, 48) = 56.77	P<0.0001
	Diet	F (1, 48) = 2.057	P=0.1580
scWAT	Interaction	F (5, 48) = 1.465	P=0.2189
	Time	F (5, 48) = 64.92	P<0.0001
	Diet	F (1, 48) = 2.433	P=0.1253
gWAT	Interaction	F (5, 44) = 5.801	P=0.0003
	Time	F (5, 44) = 56.18	P<0.0001
	Diet	F (1, 44) = 0.7276	P=0.3983
Per2			
		F (DFn, DFd)	**P Value**
Hypothalamus	Interaction	F (5, 45) = 1.257	P=0.2988
	Time	F (5, 45) = 9.01	P<0.0001
	Diet	F (1, 45) = 0.005844	P=0.9394
Liver	Interaction	F (5, 47) = 4.659	P=0.0016
	Time	F (5, 47) = 35.7	P<0.0001
	Diet	F (1, 47) = 2.52	P=0.1191
Muscle	Interaction	F (5, 46) = 0.4431	P=0.8161
	Time	F (5, 46) = 33.24	P<0.0001
	Diet	F (1, 46) = 19.21	P<0.0001
Adrenal Gland	Interaction	F (5, 47) = 1.332	P=0.2672
	Time	F (5, 47) = 25.48	P<0.0001
	Diet	F (1, 47) = 0.3783	P=0.5415
Lymph node	Interaction	F (5, 44) = 0.4998	P=0.7747
	Time	F (5, 44) = 7.749	P<0.0001
	Diet	F (1, 44) = 1.291	P=0.2620
Spleen	Interaction	F (5, 48) = 2.808	P=0.0265
	Time	F (5, 48) = 14.91	P<0.0001

	Diet	F (1, 48) = 3.271	P=0.0768
BAT	Interaction	F (5, 48) = 2.456	P=0.0464
	Time	F (5, 48) = 26.59	P<0.0001
	Diet	F (1, 48) = 1.561	P=0.2176
scWAT	Interaction	F (5, 48) = 2.644	P=0.0344
	Time	F (5, 48) = 29.47	P<0.0001
	Diet	F (1, 48) = 0.003077	P=0.9560
gWAT	Interaction	F (5, 44) = 2.306	P=0.0605
	Time	F (5, 44) = 21.48	P<0.0001
	Diet	F (1, 44) = 30.54	P<0.0001
Cry1			
		F (DFn, DFd)	**P Value**
Hypothalamus	Interaction	F (5, 45) = 2.689	P=0.0329
	Time	F (5, 45) = 6.863	P<0.0001
	Diet	F (1, 45) = 0.7409	P=0.3939
Liver	Interaction	F (5, 47) = 1.975	P=0.0998
	Time	F (5, 47) = 60.36	P<0.0001
	Diet	F (1, 47) = 0.9906	P=0.3247
Muscle	Interaction	F (5, 46) = 1.492	P=0.2108
	Time	F (5, 46) = 6.198	P=0.0002
	Diet	F (1, 46) = 15.61	P=0.0003
Adrenal Gland	Interaction	F (5, 47) = 6.079	P=0.0002
	Time	F (5, 47) = 32.52	P<0.0001
	Diet	F (1, 47) = 2.919	P=0.0942
Lymph node	Interaction	F (5, 44) = 0.144	P=0.9808
	Time	F (5, 44) = 0.4936	P=0.7793
	Diet	F (1, 44) = 1.055	P=0.3100
Spleen	Interaction	F (5, 48) = 0.6507	P=0.6623
	Time	F (5, 48) = 1.271	P=0.2920
	Diet	F (1, 48) = 1.076	P=0.3049
BAT	Interaction	F (5, 48) = 2.329	P=0.0567
	Time	F (5, 48) = 23.72	P<0.0001
	Diet	F (1, 48) = 0.3267	P=0.5703
scWAT	Interaction	F (5, 48) = 1.446	P=0.2252
	Time	F (5, 48) = 51.57	P<0.0001
	Diet	F (1, 48) = 22.02	P<0.0001
gWAT	Interaction	F (5, 44) = 2.464	P=0.0472
	Time	F (5, 44) = 28.3	P<0.0001
	Diet	F (1, 44) = 9.406	P=0.0037
Rev-erbα			
		F (DFn, DFd)	**P Value**

Hypothalamus	Interaction	F (5, 45) = 1.331	P=0.2683
	Time	F (5, 45) = 13.51	P<0.0001
	Diet	F (1, 45) = 1.342	P=0.2527
Liver	Interaction	F (5, 47) = 5.933	P=0.0002
	Time	F (5, 47) = 27.5	P<0.0001
	Diet	F (1, 47) = 0.06918	P=0.7937
Muscle	Interaction	F (5, 47) = 5.933	P=0.0002
	Time	F (5, 47) = 27.5	P<0.0001
	Diet	F (1, 47) = 0.06918	P=0.7937
Adrenal Gland	Interaction	F (5, 47) = 3.154	P=0.0155
	Time	F (5, 47) = 31.47	P<0.0001
	Diet	F (1, 47) = 12.43	P=0.0010
Lymph node	Interaction	F (5, 43) = 5.786	P=0.0004
	Time	F (5, 43) = 31.16	P<0.0001
	Diet	F (1, 43) = 0.6486	P=0.4250
Spleen	Interaction	F (5, 48) = 5.432	P=0.0005
	Time	F (5, 48) = 23.54	P<0.0001
	Diet	F (1, 48) = 0.0001042	P=0.9919
BAT	Interaction	F (5, 48) = 0.2436	P=0.9410
	Time	F (5, 48) = 14.89	P<0.0001
	Diet	F (1, 48) = 1.316	P=0.2569
scWAT	Interaction	F (5, 48) = 2.453	P=0.0466
	Time	F (5, 48) = 37.83	P<0.0001
	Diet	F (1, 48) = 0.04298	P=0.8366
gWAT	Interaction	F (5, 44) = 11.9	P<0.0001
	Time	F (5, 44) = 43.29	P<0.0001
	Diet	F (1, 44) = 63.07	P<0.0001
*Rev-erb*β			
		F (DFn, DFd)	**P Value**
Hypothalamus	Interaction	F (5, 45) = 0.7631	P=0.5812
	Time	F (5, 45) = 1.752	P=0.1424
	Diet	F (1, 45) = 1.641	P=0.2067
Liver	Interaction	F (5, 47) = 6.903	P<0.0001
	Time	F (5, 47) = 59.07	P<0.0001
	Diet	F (1, 47) = 0.1669	P=0.6848
Muscle	Interaction	F (5, 46) = 0.572	P=0.7210
	Time	F (5, 46) = 2.83	P=0.0261
	Diet	F (1, 46) = 2.538	P=0.1180
Adrenal Gland	Interaction	F (5, 47) = 1.475	P=0.2160
	Time	F (5, 47) = 35.88	P<0.0001
	Diet	F (1, 47) = 2.699	P=0.1071
Lymph node	Interaction	F (5, 44) = 11.9	P<0.0001

	Time	F (5, 44) = 43.29	P<0.0001
	Diet	F (1, 44) = 63.07	P<0.0001
Spleen	Interaction	F (5, 48) = 2.168	P=0.0733
	Time	F (5, 48) = 6.86	P<0.0001
	Diet	F (1, 48) = 0.2612	P=0.6116
BAT	Interaction	F (5, 48) = 0.5721	P=0.7210
	Time	F (5, 48) = 17.65	P<0.0001
	Diet	F (1, 48) = 5.517	P=0.0230
scWAT	Interaction	F (5, 48) = 3.053	P=0.0180
	Time	F (5, 48) = 88.75	P<0.0001
	Diet	F (1, 48) = 23.76	P<0.0001
gWAT	Interaction	F (5, 44) = 2.15	P=0.0770
	Time	F (5, 44) = 27.37	P<0.0001
	Diet	F (1, 44) = 0.08713	P=0.7692
Dbp			
		F (DFn, DFd)	**P Value**
Hypothalamus	Interaction	F (5, 45) = 3.966	P=0.0046
	Time	F (5, 45) = 10.98	P<0.0001
	Diet	F (1, 45) = 0.3647	P=0.5489
Liver	Interaction	F (5, 47) = 10.09	P<0.0001
	Time	F (5, 47) = 95.45	P<0.0001
	Diet	F (1, 47) = 2.251	P=0.1402
Muscle	Interaction	F (5, 46) = 2.412	P=0.0504
	Time	F (5, 46) = 55.99	P<0.0001
	Diet	F (1, 46) = 13.8	P=0.0005
Adrenal Gland	Interaction	F (5, 47) = 8.759	P<0.0001
	Time	F (5, 47) = 46.75	P<0.0001
	Diet	F (1, 47) = 0.794	P=0.3774
Lymph node	Interaction	F (5, 44) = 0.9898	P=0.4349
	Time	F (5, 44) = 17.94	P<0.0001
	Diet	F (1, 44) = 0.08977	P=0.7659
Spleen	Interaction	F (5, 48) = 3.022	P=0.0189
	Time	F (5, 48) = 17.4	P<0.0001
	Diet	F (1, 48) = 0.3966	P=0.5318
BAT	Interaction	F (5, 44) = 2.15	P=0.0770
	Time	F (5, 44) = 27.37	P<0.0001
	Diet	F (1, 44) = 0.08713	P=0.7692
scWAT	Interaction	F (5, 48) = 9.674	P<0.0001
	Time	F (5, 48) = 95.33	P<0.0001
	Diet	F (1, 48) = 5.949	P=0.0185
gWAT	Interaction	F (5, 44) = 5.939	P=0.0003
	Time	F (5, 44) = 31.34	P<0.0001

	Diet	F (1, 44) = 16.35	P=0.0002

Panel B	Unpaired t-test		
	P value	**t, df**	**F,DFn, Dfd**
Amplitude	0.016	t=4.011 df=4	3.316, 2, 2

Figure 3.3

Panel A	2-way ANOVA sidak post hoc test		
Dgat2			
		F (DFn, DFd)	**P Value**
gWAT	Interaction	F (5, 43) = 5.442	P=0.0006
	Time	F (5, 43) = 6.258	P=0.0002
	Diet	F (1, 43) = 59.74	P<0.0001
scWAT	Interaction	F (5, 48) = 2.293	P=0.0601
	Time	F (5, 48) = 6.98	P<0.0001
	Diet	F (1, 48) = 89.67	P<0.0001
Liver	Interaction	F (5, 47) = 0.4529	P=0.8091
	Time	F (5, 47) = 1.624	P=0.1721
	Diet	F (1, 47) = 1.643	P=0.2062
Fasn			
		F (DFn, DFd)	**P Value**
gWAT	Interaction	F (5, 44) = 1.708	P=0.1528
	Time	F (5, 44) = 2.727	P=0.0313
	Diet	F (1, 44) = 127.1	P<0.0001
scWAT	Interaction	F (5, 48) = 1.515	P=0.2030
	Time	F (5, 48) = 2.216	P=0.0679
	Diet	F (1, 48) = 109.3	P<0.0001
Liver	Interaction	F (5, 47) = 3.519	P=0.0088
	Time	F (5, 47) = 1.485	P=0.2128
	Diet	F (1, 47) = 0.3373	P=0.5641
Atgl			
		F (DFn, DFd)	**P Value**
gWAT	Interaction	F (5, 44) = 0.9749	P=0.4437
	Time	F (5, 44) = 1.417	P=0.2369
	Diet	F (1, 44) = 70.98	P<0.0001
scWAT	Interaction	F (5, 47) = 0.9446	P=0.4612
	Time	F (5, 47) = 3.553	P=0.0083
	Diet	F (1, 47) = 0.01993	P=0.8883
Liver	Interaction	F (5, 47) = 1.469	P=0.2178
	Time	F (5, 47) = 6.229	P=0.0002

	Diet	F (1, 47) = 0.9946	P=0.3237
Hsl			
		F (DFn, DFd)	**P Value**
gWAT	Interaction	F (5, 43) = 0.8625	P=0.5140
	Time	F (5, 43) = 2.112	P=0.0823
	Diet	F (1, 43) = 125.5	P<0.0001
scWAT	Interaction	F (5, 48) = 0.4167	P=0.8348
	Time	F (5, 48) = 1.407	P=0.2388
	Diet	F (1, 48) = 46.41	P<0.0001
Liver	Interaction	F (5, 47) = 5.451	P=0.0005
	Time	F (5, 47) = 8.285	P<0.0001
	Diet	F (1, 47) = 18.86	P<0.0001
Lpl			
		F (DFn, DFd)	**P Value**
gWAT	Interaction	F (5, 43) = 1.011	P=0.4232
	Time	F (5, 43) = 1.038	P=0.4076
	Diet	F (1, 43) = 3.835	P=0.0567
scWAT	Interaction	F (5, 48) = 0.8247	P=0.5383
	Time	F (5, 48) = 4.963	P=0.0010
	Diet	F (1, 48) = 95.01	P<0.0001
Liver	Interaction	F (5, 47) = 0.9521	P=0.4566
	Time	F (5, 47) = 1.548	P=0.1933
	Diet	F (1, 47) = 6.764	P=0.0124

Panel B	2-way ANOVA sidak post hoc test		
FASN			
		F (DFn, DFd)	**P Value**
gWAT protein	Interaction	F (1, 8) = 1.576	P=0.2448
	Diet	F (1, 8) = 24.62	P=0.0011
	Time	F (1, 8) = 1.136	P=0.3177

Figure 3.4

Panel A	2-way ANOVA sidak post hoc test		
Pparγ			
		F (DFn, DFd)	**P Value**
Liver	Interaction	F (5, 47) = 1.103	P=0.3714
	Time	F (5, 47) = 1.477	P=0.2152
	Diet	F (1, 47) = 57.1	P<0.0001
Muscle	Interaction	F (5, 46) = 0.7615	P = 0.5822
	Time	F (5, 46) = 0.6894	P = 0.6340

	Diet	F (1, 46) = 5.802	P = 0.0201
scWAT	Interaction	F (5, 46) = 1.591	P=0.1816
	Time	F (5, 46) = 4.959	P=0.0010
	Diet	F (1, 46) = 14.17	P=0.0005
gWAT	Interaction	F (5, 44) = 5.177	P=0.0008
	Time	F (5, 44) = 7.876	P<0.0001
	Diet	F (1, 44) = 55.53	P<0.0001
*Ppar*α			
		F (DFn, DFd)	**P Value**
Liver	Interaction	F (5, 47) = 0.8616	P=0.5139
	Time	F (5, 47) = 5.348	P=0.0006
	Diet	F (1, 47) = 40.57	P<0.0001
Muscle	Interaction	F (5, 46) = 1.218	P = 0.3158
	Time	F (5, 46) = 2.336	P = 0.0569
	Diet	F (1, 46) = 0.4496	P = 0.5059
scWAT	Interaction	F (5, 48) = 1.015	P=0.4195
	Time	F (5, 48) = 2.166	P=0.0735
	Diet	F (1, 48) = 5.009	P=0.0299
gWAT	Interaction	F (5, 44) = 1.902	P=0.1133
	Time	F (5, 44) = 5.994	P=0.0003
	Diet	F (1, 44) = 76.63	P<0.0001
*Pgc1*α			
		F (DFn, DFd)	**P Value**
Liver	Interaction	F (5, 47) = 3.5	P=0.0090
	Time	F (5, 47) = 3.797	P=0.0057
	Diet	F (1, 47) = 2.332	P=0.1334
Muscle	Interaction	F (5, 46) = 0.8315	P = 0.5341
	Time	F (5, 46) = 1.936	P = 0.1065
	Diet	F (1, 46) = 9.149	P = 0.0041
scWAT	Interaction	F (5, 48) = 1.052	P=0.3985
	Time	F (5, 48) = 3.817	P=0.0054
	Diet	F (1, 48) = 15.19	P=0.0003
gWAT	Interaction	F (5, 44) = 2.34	P=0.0573
	Time	F (5, 44) = 1.578	P=0.1860
	Diet	F (1, 44) = 23.77	P<0.0001

Panel B	2-way ANOVA sidak post hoc test		
PPARγ2			
		F (DFn, DFd)	**P Value**
Liver	Interaction	F (1, 8) = 0.6324	P=0.4494
	Time	F (1, 8) = 2.014	P=0.1936
	Diet	F (1, 8) = 119.9	P<0.0001

gWAT	Interaction	F (1, 20) = 0.6094	P=0.4442
	Time	F (1, 20) = 1.921	P=0.1810
	Diet	F (1, 20) = 11.95	P=0.0025
PPARγ1			
		F (DFn, DFd)	**P Value**
Liver	Interaction	F (1, 8) = 1.264	P=0.2936
	Time	F (1, 8) = 0.6669	P=0.4378
	Diet	F (1, 8) = 3.054	P=0.1187
gWAT	Interaction	F (1, 20) = 0.07453	P=0.7877
	Time	F (1, 20) = 0.1796	P=0.6762
	Diet	F (1, 20) = 22.07	P=0.0001

Figure 3.5

Glut4			
		F (DFn, DFd)	**P Value**
Liver	Interaction	F (5, 47) = 2.042	P = 0.0898
	Time	F (5, 47) = 8.273	P < 0.0001
	Diet	F (1, 47) = 1.924	P = 0.1720
Muscle	Interaction	F (5, 46) = 0.8526	P = 0.5200
	Time	F (5, 46) = 0.2000	P = 0.9609
	Diet	F (1, 46) = 55.33	P < 0.0001
gWAT	Interaction	F (5, 44) = 1.616	P=0.1758
	Time	F (5, 44) = 1.517	P=0.2042
	Diet	F (1, 44) = 213.9	P<0.0001
scWAT	Interaction	F (5, 48) = 1.086	P=0.3803
	Time	F (5, 48) = 1.38	P=0.2487
	Diet	F (1, 48) = 31.97	P<0.0001
Glucokinase/Hexokinase			
		F (DFn, DFd)	**P Value**
Liver	Interaction	F (5, 47) = 5.999	P=0.0002
	Time	F (5, 47) = 5.242	P=0.0007
	Diet	F (1, 47) = 5.009	P=0.0300
Muscle	Interaction	F (5, 46) = 0.8898	P = 0.4958
	Time	F (5, 46) = 1.297	P = 0.2818
	Diet	F (1, 46) = 29.86	P < 0.0001
gWAT	Interaction	F (5, 44) = 3.643	P=0.0076
	Time	F (5, 44) = 6.026	P=0.0002
	Diet	F (1, 44) = 184.4	P<0.0001
scWAT	Interaction	F (5, 48) = 3.349	P=0.0113
	Time	F (5, 48) = 5.471	P=0.0005
	Diet	F (1, 48) = 7.461	P=0.0088

Pepck			
		F (DFn, DFd)	**P Value**
Liver	Interaction	F (5, 47) = 1.71	P=0.1508
	Time	F (5, 47) = 5.434	P=0.0005
	Diet	F (1, 47) = 3.468	P=0.0688
Muscle	Interaction	F (5, 46) = 0.7323	P = 0.6030
	Time	F (5, 46) = 0.1384	P = 0.9825
	Diet	F (1, 46) = 0.2451	P = 0.6229
gWAT	Interaction	F (5, 44) = 6.179	P=0.0002
	Time	F (5, 44) = 6.771	P<0.0001
	Diet	F (1, 44) = 117.5	P<0.0001
scWAT	Interaction	F (5, 46) = 1.937	P=0.1063
	Time	F (5, 46) = 5.163	P=0.0008
	Diet	F (1, 46) = 7.565	P=0.0085

Fig 3.6

Panel A	2-way ANOVA sidak post hoc test	
TNFα		
	F (DFn, DFd)	**P Value**
Interaction	F (4, 278) = 79.38	P < 0.0001
Time	F (4, 278) = 92.58	P < 0.0001
Diet	F (1, 278) = 266.4	P < 0.0001
F4/80		
	F (DFn, DFd)	**P Value**
Interaction	F (4, 279) = 164.8	P < 0.0001
Time	F (4, 279) = 171.0	P < 0.0001
Diet	F (1, 279) = 257.5	P < 0.0001

Panel B	2-way ANOVA sidak post hoc test	
TNFα		
	F (DFn, DFd)	**P Value**
Interaction	F (2, 24) = 3.663	P=0.0409
Time	F (2, 24) = 30.51	P<0.0001
Diet	F (1, 24) = 2.156	P=0.1550
F4/80		
	F (DFn, DFd)	**P Value**
Interaction	F (2, 24) = 0.05908	P=0.9428
Time	F (2, 24) = 44.77	P<0.0001
Diet	F (1, 24) = 0.003009	P=0.9567
Bmal1		

	F (DFn, DFd)	P Value
Interaction	F (2, 24) = 20.33	P<0.0001
Time	F (2, 24) = 12.59	P=0.0002
Diet	F (1, 24) = 311.4	P<0.0001
Rev-erbα		
	F (DFn, DFd)	**P Value**
Interaction	F (2, 24) = 33.16	P<0.0001
Time	F (2, 24) = 50.76	P<0.0001
Diet	F (1, 24) = 171.5	P<0.0001
Pparα		
	F (DFn, DFd)	**P Value**
Interaction	F (2, 24) = 3.359	P=0.0517
Time	F (2, 24) = 8.375	P=0.0017
Diet	F (1, 24) = 0.6534	P=0.4269
Pparγ		
	F (DFn, DFd)	**P Value**
Interaction	F (2, 24) = 1.308	P=0.2889
Time	F (2, 24) = 22.3	P<0.0001
Diet	F (1, 24) = 6.424	P=0.0182

Appendix 2

Chapter 4 statistics

Figure 4.1

Panel B	Unpaired t-test		
	P value	**t, df**	**F,DFn, Dfd**
gWAT	<0.0001	t=24.21 df=4	1.474, 2, 2
Liver	0.0186	t=3.83 df=4	2.333, 2, 2

Panel C	2-way ANOVA sidak post hoc test		
		F (DFn, DFd)	**P Value**
Bmal1	Interaction	F (5, 34) = 7.895	P < 0.0001
	Time	F (5, 34) = 11.62	P < 0.0001
	Genotype	F (1, 34) = 38.26	P < 0.0001
Per2	Interaction	F (5, 34) = 3.165	P = 0.0188
	Time	F (5, 34) = 24.25	P < 0.0001
	Genotype	F (1, 34) = 0.7501	P = 0.3925
Dbp	Interaction	F (5, 32) = 2.198	P = 0.0790
	Time	F (5, 32) = 16.07	P < 0.0001
	Genotype	F (1, 32) = 13.13	P = 0.0010

Figure 4.2

Panel A	Unpaired t-test		
	P value	**t, df**	**F,DFn, Dfd**
gWAT weight	0.0019	t=3.385 df=33	4.162, 14, 19

Panel B	2-way ANOVA sidak post hoc test		
		F (DFn, DFd)	**P Value**
Day/Night intake	Interaction	F (1, 10) = 1.547	P=0.2420
	Time	F (1, 10) = 140.2	P<0.0001
	Genotype	F (1, 10) = 1.134	P=0.3119

Panel C	Unpaired t-test		
	P value	**t, df**	**F,DFn, Dfd**
FFA	0.0103	t=3.337 df=8	6.308, 4, 4
Glycerol	0.01	t=3.353 df=8	1.746, 4, 4

Figure 4.3

	2-way ANOVA sidak post hoc test		
		F (DFn, DFd)	**P Value**
VO2	Interaction	F (1, 10) = 1.748	P=0.2155
	Genotype	F (1, 10) = 9.549	P=0.0114
	Time	F (1, 10) = 31.53	P=0.0002
VCO2	Interaction	F (1, 10) = 1.701	P = 0.2214
	Genotype	F (1, 10) = 60.81	P < 0.0001
	Time	F (1, 10) = 18.64	P = 0.0015
kcal/hr	Interaction	F (1, 10) = 5.347	P = 0.0433
	Genotype	F (1, 10) = 78.73	P < 0.0001
	Time	F (1, 10) = 0.06822	P = 0.7992
RER	Interaction	F (1, 10) = 0.1976	P = 0.6661
	Genotype	F (1, 10) = 22.98	P = 0.0007
	Time	F (1, 10) = 7.648	P = 0.0199
COX	Interaction	F (1, 10) = 0.6192	P = 0.4496
	Genotype	F (1, 10) = 68.71	P < 0.0001
	Time	F (1, 10) = 21.34	P = 0.0010
FOX	Interaction	F (1, 10) = 0.006782	P = 0.9360
	Genotype	F (1, 10) = 24.71	P = 0.0006
	Time	F (1, 10) = 7.825	P = 0.0189

Figure 4.4

	Unpaired t-test		
gWAT			
	P value	**t, df**	**F,DFn, Dfd**
Dgat2	0.0342	t=2.246 df=24	2.048, 12, 12
Hsl	0.0166	t=2.675 df=16	3.233, 7, 9
Lpl	0.001	t=4.086 df=15	1.203, 8, 7
Liver			
	P value	**t, df**	**F,DFn, Dfd**
Lpl	0.0007	t=7.654 df=16	t=4.086 df=15

Figure 4.5

Panel A	Unpaired t-test		
	P value	**t, df**	**F,DFn, Dfd**
Body weight loss (%)	0.0002	t=5.773 df=10	1.217, 5, 5

Panel B	2-way ANOVA sidak post hoc test

		F (DFn, DFd)	P Value
TAG	Interaction	F (2, 30) = 5.444	P = 0.0096
	Genotype	F (1, 30) = 3.139	P = 0.0866
	Diet Status	F (2, 30) = 4.031	P = 0.0281
Glycerol	Interaction	F (2, 30) = 0.2288	P = 0.7968
	Genotype	F (1, 30) = 0.6129	P = 0.4398
	Diet Status	F (2, 30) = 3.893	P = 0.0314

Fig 4.6

	Unpaired t-test		
	P value	**t, df**	**F,DFn, Dfd**
VO2	0.0325	t=2.934 df=5	8.120, 3, 2
VCO2	0.0333	t=2.911 df=5	9.494, 3, 2
FOX	0.0308	t=2.981 df=5	5.648, 3, 2

Fig 4.7

	2-way ANOVA sidak post hoc test		
gWAT			
		F (DFn, DFd)	**P Value**
Dgat2	Interaction	F (2, 27) = 0.4463	P=0.6446
	Genotype	F (2, 27) = 32.75	P<0.0001
	Diet Status	F (1, 27) = 5.266	P=0.0297
Fasn	Interaction	F (2, 27) = 3.876	P = 0.0331
	Genotype	F (2, 27) = 35.11	P < 0.0001
	Diet Status	F (1, 27) = 10.60	P = 0.0030
Atgl	Interaction	F (2, 28) = 2.054	P = 0.1471
	Genotype	F (2, 28) = 4.104	P = 0.0274
	Diet Status	F (1, 28) = 2.641	P = 0.1153
Liver			
		F (DFn, DFd)	**P Value**
Dgat2	Interaction	F (2, 25) = 5.924	P = 0.0078
	Genotype	F (2, 25) = 2.590	P = 0.0950
	Diet Status	F (1, 25) = 2.566	P = 0.1218
Fasn	Interaction	F (2, 28) = 1.084	P = 0.3522
	Genotype	F (2, 28) = 18.20	P < 0.0001
	Diet Status	F (1, 28) = 1.052	P = 0.3138
Atgl	Interaction	F (2, 29) = 3.529	P = 0.0425
	Genotype	F (2, 29) = 6.494	P = 0.0047
	Diet Status	F (1, 29) = 3.152	P = 0.0863
Lpl	Interaction	F (2, 30) = 3.965	P = 0.0297

	Genotype	F (2, 30) = 4.974	P = 0.0136
	Diet Status	F (1, 30) = 16.51	P = 0.0003

Fig 4.8

	2-way ANOVA sidak post hoc test		
gWAT			
		F (DFn, DFd)	**P Value**
Hsl	Interaction	F (1, 11) = 0.82	P=0.3846
	Genotype	F (1, 11) = 14.82	P=0.0027
	Treatment	F (1, 11) = 6.986	P=0.0229
Lpl	Interaction	F (1, 10) = 0.01101	P = 0.9185
	Genotype	F (1, 10) = 24.05	P = 0.0006
	Treatment	F (1, 10) = 0.9130	P = 0.3618
scWAT			
		F (DFn, DFd)	**P Value**
Atgl	Interaction	F (1, 9) = 0.6731	P = 0.4332
	Genotype	F (1, 9) = 1.989	P = 0.1921
	Treatment	F (1, 9) = 22.10	P = 0.0011
BAT			
		F (DFn, DFd)	**P Value**
Fasn	Interaction	F (1, 12) = 0.9405	P = 0.3513
	Genotype	F (1, 12) = 4.488	P = 0.0557
	Treatment	F (1, 12) = 7.034	P = 0.0211
Atgl	Interaction	F (1, 9) = 7.036	P = 0.0264
	Genotype	F (1, 9) = 5.573	P = 0.0425
	Treatment	F (1, 9) = 2.644	P = 0.1384

Fig 4.9

	2-way ANOVA sidak post hoc test		
		F (DFn, DFd)	**P Value**
pHSL fold change	Interaction	F (2, 18) = 56.08	P < 0.0001
	Genotype	F (1, 18) = 31.56	P < 0.0001
	Treatment	F (2, 18) = 193.6	P < 0.0001

Fig 4.10

Panel A	2-way ANOVA sidak post hoc test		
		F (DFn, DFd)	**P Value**
gWAT weight	Interaction	F (1, 28) = 0.2046	P = 0.6546
	Diet	F (1, 28) = 39.85	P < 0.0001
	Genotype	F (1, 28) = 5.819	P = 0.0227

scWAT weight	Interaction	F (1, 28) = 23.87	P < 0.0001
	Diet	F (1, 28) = 117.7	P < 0.0001
	Genotype	F (1, 28) = 42.95	P < 0.0001

Panel B	2-way ANOVA sidak post hoc test		
		F (DFn, DFd)	**P Value**
Daily intake	Interaction	F (1, 28) = 1.975	P = 0.1709
	Genotype	F (1, 28) = 5.832	P = 0.0225
	Diet	F (1, 28) = 9.407	P = 0.0048
Food intake - NC	Interaction	F (1, 12) = 1.547	P=0.2420
	Time	F (1, 12) = 140.2	P<0.0001
	Genotype	F (1, 12) = 1.134	P=0.3119
Food intake - HFD	Interaction	F (1, 12) = 28.95	P=0.0002
	Time	F (1, 12) = 66	P<0.0001
	Genotype	F (1, 12) = 18.02	P=0.0011
% light feeding	Interaction	F (1, 28) = 18.54	P = 0.0002
	Diet	F (1, 28) = 0.5339	P = 0.4710
	Genotype	F (1, 28) = 12.42	P = 0.0015

Panel C	2-way ANOVA sidak post hoc test		
		F (DFn, DFd)	**P Value**
TAG	Interaction	F (1, 28) = 2.709	P = 0.1096
	Genotype	F (1, 28) = 1.677	P = 0.2045
	Diet	F (1, 28) = 1.574	P = 0.2187
FFA	Interaction	F (1, 28) = 0.009141	P = 0.9245
	Genotype	F (1, 28) = 7.666	P = 0.0099
	Diet	F (1 ,28) = 24.85	P < 0.0001
Glycerol	Interaction	F (1, 28) = 6.423	P = 0.0164
	Genotype	F (1, 28) = 0.7397	P = 0.3962
	Diet	F (1, 28) = 12.59	P = 0.0012

Fig 4.11

	2-way ANOVA sidak post hoc test		
Liver			
		F (DFn, DFd)	**P Value**
Pparα	Interaction	F (1, 31) = 6.128	P = 0.0190
	Genotype	F (1, 31) = 2.947	P = 0.0960
	Diet	F (1, 31) = 7.678	P = 0.0094

Fig 4.12

	2-way ANOVA sidak post hoc test		
gWAT			
		F (DFn, DFd)	**P Value**
Fasn	Interaction	F (1, 19) = 2.498	P = 0.1305
	Diet	F (1, 19) = 9.500	P = 0.0061
	Genotype	F (1, 19) = 0.8185	P = 0.3769
Atgl	Interaction	F (1, 31) = 4.485	P = 0.0423
	Diet	F (1, 31) = 9.057	P = 0.0052
	Genotype	F (1, 31) = 0.1585	P = 0.6933
Liver			
		F (DFn, DFd)	**P Value**
Fabp4	Interaction	F (1, 30) = 6.158	P = 0.0189
	Diet	F (1, 30) = 11.62	P = 0.0019
	Genotype	F (1, 30) = 11.38	P = 0.0021
Muscle			
		F (DFn, DFd)	**P Value**
Fasn	Interaction	F (1, 31) = 6.099	P = 0.0192
	Diet	F (1, 31) = 15.96	P = 0.0004
	Genotype	F (1, 31) = 5.884	P = 0.0213

Fig 4.13

	2-way ANOVA sidak post hoc test		
		F (DFn, DFd)	**P Value**
FASN	Interaction	F (1, 20) = 0.6688	P=0.4231
	Diet	F (1, 20) = 7.762	P=0.0114
	Genotype	F (1, 20) = 0.3573	P=0.5567
ATGL	Interaction	F (1, 20) = 0.002795	P=0.9584
	Diet	F (1, 20) = 1.287	P=0.2700
	Genotype	F (1, 20) = 0.5446	P=0.4691

Fig 4.14

	2-way ANOVA sidak post hoc test		
gWAT			
		F (DFn, DFd)	**P Value**
Gk/Hk2	Interaction	F (1, 31) = 9.229	P = 0.0048
	Diet	F (1, 31) = 4.620	P = 0.0395
	Genotype	F (1, 31) = 1.740	P = 0.1968
Pepck	Interaction	F (1, 29) = 4.308	P = 0.0469

	Diet	F (1, 29) = 21.45	P < 0.0001
	Genotype	F (1, 29) = 2.813	P = 0.1043
Liver			
		F (DFn, DFd)	**P Value**
Glut2	Interaction	F (1, 31) = 6.916	P = 0.0132
	Diet	F (1, 31) = 0.6021	P = 0.4437
	Genotype	F (1, 31) = 7.401	P = 0.0106
Pepck	Interaction	F (1, 31) = 0.003211	P = 0.9552
	Diet	F (1, 31) = 0.02657	P = 0.8716
	Genotype	F (1, 31) = 18.32	P = 0.0002

Fig 4.15

Panel B	2-way ANOVA sidak post hoc test		
		F (DFn, DFd)	**P Value**
Blood Glucose	Interaction	F (1, 36) = 3.13	P=0.0853
	Genotype	F (1, 36) = 0.4045	P=0.5288
	Treatment	F (1, 36) = 83.66	P<0.0001

Panel C	2-way ANOVA sidak post hoc test		
		F (DFn, DFd)	**P Value**
FFA	Interaction	F (1, 20) = 2.368	P = 0.1395
	Treatment	F (1, 20) = 28.23	P < 0.0001
	Genotype	F (1, 20) = 0.04752	P = 0.8296

Fig 4.16

	2-way ANOVA sidak post hoc test		
Muscle			
		F (DFn, DFd)	**P Value**
Atgl	Interaction	F (1, 13) = 7.599	P=0.0163
	Treatment	F (1, 13) = 8.069	P=0.0139
	Genotype	F (1, 13) = 4.343	P=0.0575
Hsl	Interaction	F (1, 16) = 1.791	P=0.1995
	Treatment	F (1, 16) = 16.85	P=0.0008
	Genotype	F (1, 16) = 1.403	P=0.2536

Fig 4.17

Panel A	2-way ANOVA sidak post hoc test		
		F (DFn, DFd)	**P Value**
NC	Interaction	F (4, 50) = 0.6242	P=0.6474

	Time	F (4, 50) = 18.08	P<0.0001
	Treatment	F (1, 50) = 4.304	P=0.0432
HFD	Interaction	F (4, 50) = 0.8961	P=0.4733
	Time	F (4, 50) = 16.74	P<0.0001
	Treatment	F (1, 50) = 0.7932	P=0.3774

Panel A	Unpaired t-test		
	P value	**t, df**	**F,DFn, Dfd**
NC	0.0459	t=2.279 df=10	13.72, 5, 5

Panel B	2-way ANOVA sidak post hoc test		
		F (DFn, DFd)	**P Value**
NC	Interaction	F (4, 50) = 3.211	P=0.0201
	Time	F (4, 50) = 7.771	P<0.0001
	Treatment	F (1, 50) = 7.917	P=0.0070
HFD	Interaction	F (4, 50) = 0.6336	P=0.6408
	Time	F (4, 50) = 37.75	P<0.0001
	Treatment	F (1, 50) = 4.565	P=0.0376

Panel B	Unpaired t-test		
	P value	**t, df**	**F,DFn, Dfd**
NC	0.0333	t=2.466 df=10	4.014, 5, 5

Fig 4.18

	3-way ANOVA		
		F (DFn, DFd)	**P Value**
Dgat2	Treatment	F (1, 1) = 51.14	P<0.0001
	Genoptype	F (1, 1) = 1.112	P=0.2946
	Diet	F (1, 1) = 5.776	P=0.0183
Fasn	Treatment	F (1, 1) = 28.17	P<0.0001
	Genoptype	F (1, 1) = 2.55	P=0.1138
	Diet	F (1, 1) = 17.2	P<0.0001
Lpl	Treatment	F (1, 1) = 6.949	P=0.0099
	Genoptype	F (1, 1) = 0.002202	P=0.9627
	Diet	F (1, 1) = 0.06347	P=0.8017
Atgl	Treatment	F (1, 1) = 5.321	P=0.0234
	Genoptype	F (1, 1) = 0.0005153	P=0.9819
	Diet	F (1, 1) = 23.41	P<0.0001
Hsl	Treatment	F (1, 1) = 31.94	P<0.0001
	Genoptype	F (1, 1) = 1.46	P=0.2302
	Diet	F (1, 1) = 5.511	P=0.0211
Glut4	Treatment	F (1, 1) = 5.627	P=0.0199

	Genoptype	F (1, 1) = 8.928	P=0.0036
	Diet	F (1, 1) = 23.34	P<0.0001

Appendix 3

Chapter 5 statistics

Figure 5.1

Panel B	2-way ANOVA sidak post hoc test		
Bmal1flox Adipocre			
		F (DFn, DFd)	**P Value**
Bmal1	Interaction	F (4, 35) = 28.66	P<0.0001
	Genotype	F (1, 35) = 88.16	P<0.0001
	Tissue	F (4, 35) = 33.23	P<0.0001
*Rev-erb*α	Interaction	F (4, 34) = 5.222	P=0.0022
	Genotype	F (1, 34) = 9.307	P=0.0044
	Tissue	F (4, 34) = 9.333	P<0.0001
Rev-erbαflox Adipocre			
		F (DFn, DFd)	**P Value**
Bmal1	Interaction	F (4, 39) = 20.08	P<0.0001
	Genotype	F (1, 39) = 60.32	P<0.0001
	Tissue	F (4, 39) = 20.67	P<0.0001
*Rev-erb*α	Interaction	F (4, 39) = 1.4	P=0.2519
	Genotype	F (1, 39) = 24.04	P<0.0001
	Tissue	F (4, 39) = 1.246	P=0.3077

Figure 5.2

	Unpaired t-test		
Males			
	P value	**t, df**	**F,DFn, Dfd**
scWAT weight	0.015	t=3.086 df=8	11.64, 3, 5

Figure 5.3

Panel B	2-way ANOVA sidak post hoc test		
		F (DFn, DFd)	**P Value**
Intake (g)	Interaction	F (1, 12) = 0.8599	P=0.3720
	Time	F (1, 12) = 10.91	P=0.0063
	Genotype	F (1, 12) = 0.7282	P=0.4102
Intake (g/g)	Interaction	F (1, 12) = 1.900	P = 0.1932
	Time	F (1, 12) = 9.608	P = 0.0092
	Genotype	F (1, 12) = 0.9717	P = 0.3437

Fig 5.4

	2-way ANOVA sidak post hoc test		
		F (DFn, DFd)	**P Value**
VO2	Interaction	F (1, 12) = 2.429	P = 0.1451
	Genotype	F (1, 12) = 34.14	P < 0.0001
	Time	F (1, 12) = 2.371	P = 0.1496
VCO2	Interaction	F (1, 12) = 1.755	P=0.2100
	Genotype	F (1, 12) = 40.45	P<0.0001
	Time	F (1, 12) = 2.256	P=0.1589
kcal/hr	Interaction	F (1, 12) = 0.6634	P = 0.4312
	Genotype	F (1, 12) = 17.95	P = 0.0012
	Time	F (1, 12) = 1.212	P = 0.2925
RER	Interaction	F (1, 12) = 0.06407	P=0.8045
	Genotype	F (1, 12) = 31.81	P=0.0001
	Time	F (1, 12) = 1.136	P=0.3074
COX	Interaction	F (1, 12) = 0.9168	P = 0.3572
	Genotype	F (1, 12) = 41.32	P < 0.0001
	Time	F (1, 12) = 1.795	P = 0.2052
FOX	Interaction	F (1, 12) = 0.1266	P = 0.7282
	Genotype	F (1, 12) = 32.39	P = 0.0001
	Time	F (1, 12) = 0.9137	P = 0.3580

Fig 5.5

	Unpaired t-test		
	P value	**t, df**	**F,DFn, Dfd**
Intake (g/g)	0.0028	t=3.93 df=10	3.134, 5, 5

Fig 5.8

	Unpaired t-test		
gWAT			
	P value	**t, df**	**F,DFn, Dfd**
Dgat2	0.0092	t=3.412 df=8	6.185, 4, 4
Fasn	0.0137	t=3.145 df=8	5.533, 4, 4
Lpl	0.0264	t=2.803 df=7	4.388, 3, 4
Atgl	0.0323	t=2.587 df=8	97.32, 4, 4
Hsl	0.01	t=3.358 df=8	15.34, 4, 4

Fig 5.9

	2-way ANOVA sidak post hoc test		
		F (DFn, DFd)	**P Value**
Dgat2	Interaction	F (1, 30) = 1.296	P = 0.2639
	Genotype	F (1, 30) = 3.881	P = 0.0581
	Treatment	F (1, 30) = 5.794	P = 0.0224
Fasn	Interaction	F (1, 31) = 0.6192	P = 0.4373
	Genotype	F (1, 31) = 0.7122	P = 0.4052
	Treatment	F (1, 31) = 12.69	P = 0.0012
Fabp4	Interaction	F (1, 28) = 1.141	P = 0.2946
	Genotype	F (1, 28) = 0.9452	P = 0.3393
	Treatment	F (1, 28) = 9.839	P = 0.0040
Atgl	Interaction	F (1, 29) = 0.2463	P = 0.6234
	Genotype	F (1, 29) = 0.2193	P = 0.6431
	Treatment	F (1, 29) = 12.72	P = 0.0013
Hsl	Interaction	F (1, 27) = 1.379e-005	P = 0.9971
	Genotype	F (1, 27) = 0.7689	P = 0.3883
	Treatment	F (1, 27) = 21.41	P < 0.0001
Lpl	Interaction	F (1, 32) = 0.1618	P = 0.6901
	Genotype	F (1, 32) = 8.419	P = 0.0067
	Treatment	F (1, 32) = 2.820	P = 0.1028
Glut4	Interaction	F (1, 32) = 0.1984	P = 0.6590
	Genotype	F (1, 32) = 4.949	P = 0.0333
	Treatment	F (1, 32) = 0.3016	P = 0.5867

Figure 5.10

	2-way ANOVA sidak post hoc test		
Body Weight			
		F (DFn, DFd)	**P Value**
Male	Interaction	F (1, 14) = 0.2226	P=0.6443
	Genotype	F (1, 14) = 0.6499	P=0.4336
	Diet	F (1, 14) = 170	P<0.0001
Female	Interaction	F (1, 24) = 1.172	P=0.2897
	Genotype	F (1, 24) = 0.07108	P=0.7920
	Diet	F (1, 24) = 42.87	P<0.0001
gWAT			
Male	Interaction	F (1, 14) = 0.001279	P=0.9720
	Genotype	F (1, 14) = 0.1195	P=0.7347
	Diet	F (1, 14) = 52.87	P<0.0001
Female	Interaction	F (1, 22) = 0.01806	P = 0.8943

	Genotype	F (1, 22) = 1.823	P = 0.1907
	Diet	F (1, 22) = 154.3	P < 0.0001
scWAT			
Male	Interaction	F (1, 14) = 2.869	P=0.1124
	Genotype	F (1, 14) = 0.3736	P=0.5508
	Diet	F (1, 14) = 152.4	P<0.0001
Female	Interaction	F (1, 24) = 0.7437	P=0.3970
	Genotype	F (1, 24) = 0.151	P=0.7010
	Diet	F (1, 24) = 116.3	P<0.0001

Fig 5.11

	Unpaired t-test		
Females			
	P value	**t, df**	**F,DFn, Dfd**
Food intake (g)	0.0175	t=2.985 df=8	2.573, 4, 4
Food intake (g/g)	0.0407	t=2.437 df=8	1.189, 4, 4

Fig 5.12

	2-way ANOVA sidak post hoc test		
		F (DFn, DFd)	**P Value**
Body Weight	Interaction	F (1, 12) = 0.1222	P = 0.7327
	Genotype	F (1, 12) = 0.03752	P = 0.8496
	Diet	F (1, 12) = 53.56	P < 0.0001
gWAT	Interaction	F (1, 13) = 0.1023	P=0.7542
	Genotype	F (1, 13) = 0.4683	P=0.5058
	Diet	F (1, 13) = 30.4	P<0.0001
scWAT	Interaction	F (1, 13) = 0.4136	P = 0.5313
	Genotype	F (1, 13) = 1.235	P = 0.2865
	Diet	F (1, 13) = 40.72	P < 0.0001

Fig 5.13

	2-way ANOVA sidak post hoc test		
		F (DFn, DFd)	**P Value**
VO2	Interaction	F (1, 12) = 0.001363	P = 0.9712
	Genotype	F (1, 12) = 49.81	P < 0.0001
	Time	F (1, 12) = 1.380	P = 0.2629
VCO2	Interaction	F (1, 12) = 0.001088	P = 0.9742
	Genotype	F (1, 12) = 65.04	P < 0.0001
	Time	F (1, 12) = 2.139	P = 0.1693

kcal/hr	Interaction	F (1, 12) = 0.01356	P = 0.9092
	Genotype	F (1, 12) = 33.12	P < 0.0001
	Time	F (1, 12) = 0.002110	P = 0.9641
RER	Interaction	F (1, 12) = 0.004998	P=0.9448
	Genotype	F (1, 12) = 17.76	P=0.0012
	Time	F (1, 12) = 1.255	P=0.2846
COX	Interaction	F (1, 12) = 0.05240	P = 0.8228
	Genotype	F (1, 12) = 45.33	P < 0.0001
	Time	F (1, 12) = 0.01694	P = 0.8986
FOX	Interaction	F (1, 12) = 0.03158	P = 0.8619
	Genotype	F (1, 12) = 13.43	P = 0.0032
	Time	F (1, 12) = 0.8546	P = 0.3735